# Safe Human Expeditions Beyond Low Earth Orbit (LEO)

Azita Valinia/NESC
Langley Research Center, Hampton, Virginia

John R. Allen
NASA Headquarters, Washington, DC

David R. Francisco
Johnson Space Center, Houston, Texas

Joseph I. Minow
Marshall Space Flight Center, Huntsville, Alabama

Jonathan A. Pellish
Goddard Space Flight Center, Greenbelt, Maryland

Alonso H. Vera
Ames Research Center, Moffett Field, California

NASA STI Program Report Series

Since its founding, NASA has been dedicated to the advancement of aeronautics and space science. The NASA scientific and technical information (STI) program plays a key part in helping NASA maintain this important role.

The NASA STI program operates under the auspices of the Agency Chief Information Officer. It collects, organizes, provides for archiving, and disseminates NASA's STI. The NASA STI program provides access to the NTRS Registered and its public interface, the NASA Technical Reports Server, thus providing one of the largest collections of aeronautical and space science STI in the world. Results are published in both non-NASA channels and by NASA in the NASA STI Report Series, which includes the following report types:
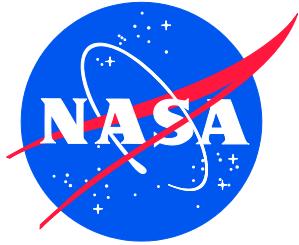
- TECHNICAL PUBLICATION. Reports of completed research or a major significant phase of research that present the results of NASA Programs and include extensive data or theoretical analysis. Includes compilations of significant scientific and technical data and information deemed to be of continuing reference value. NASA counterpart of peer-reviewed formal professional papers but has less stringent limitations on manuscript length and extent of graphic presentations.

- TECHNICAL MEMORANDUM. Scientific and technical findings that are preliminary or of specialized interest, e.g., quick release reports, working papers, and bibliographies that contain minimal annotation. Does not contain extensive analysis.

- CONTRACTOR REPORT. Scientific and technical findings by NASA-sponsored contractors and grantees.

- CONFERENCE PUBLICATION. Collected papers from scientific and technical conferences, symposia, seminars, or other meetings sponsored or co-sponsored by NASA.

- SPECIAL PUBLICATION. Scientific, technical, or historical information from NASA programs, projects, and missions, often concerned with subjects having substantial public interest.

- TECHNICAL TRANSLATION. English-language translations of foreign scientific and technical material pertinent to NASA's mission.

Specialized services also include organizing and publishing research results, distributing specialized research announcements and feeds, providing information desk and personal search support, and enabling data exchange services.

For more information about the NASA STI program, see the following:

- Access the NASA STI program home page at http://www.sti.nasa.gov

- Help desk contact information:

https://www.sti.nasa.gov/sti-contact-form/
and select the "General" help request type.

NASA/TM–20220002905
NESC-RP-20-01589

Safe Human Expeditions Beyond Low Earth Orbit (LEO)

Azita Valinia/NESC
Langley Research Center, Hampton, Virginia

John R. Allen
NASA Headquarters, Washington, DC

David R. Francisco
Johnson Space Center, Houston, Texas

Joseph I. Minow
Marshall Space Flight Center, Huntsville, Alabama

Jonathan A. Pellish
Goddard Space Flight Center, Greenbelt, Maryland

Alonso H. Vera
Ames Research Center, Moffett Field, California

February 2022

Acknowledgments

NASA Engineering and Safety Center
Technical Assessment Report

Safe Human Expeditions Beyond Low Earth Orbit (LEO)

TI-20-01589

Azita Valinia, NESC Lead

January 20, 2022

Report Approval and Revision History

NOTE: This document was approved at the January 20, 2022, NRB.

Approved:	*Digital Signature on PDF Copy – 2/9/22*	
	NESC Director	

Concurred:		
	NASA Chief Health and Medical Officer	

Version	Description of Revision	Office of Primary Responsibility	Effective Date
1.0	Initial Release	Azita Valinia, NESC Chief Scientist, GSFC	1/20/2022

Table of Contents

List of Figures

List of Tables

List of Appendices

Technical Assessment Report

1.0   Notification and Authorization

The NASA Engineering and Safety Center (NESC) has been requested to conduct an interdisciplinary study and workshop focusing on capabilities needed for crew health and safety on long-duration deep space expeditions, in support of the Artemis Program and beyond. The study was focused on integration among four disciplines: 1) space weather monitoring and forecasting, 2) shielding technologies, 3) human health research, and 4) human factors engineering tools. An integrated risk assessment was performed to inform characteristics of mission architecture and capabilities needed for safe, long-duration human expeditions beyond low Earth orbit (LEO).

The key stakeholders for this assessment are the Science Mission Directorate (SMD), the Human Exploration and Operations Mission Directorate (HEOMD), the Space Technology Mission Directorate (STMD), and the Office of the Chief Health and Medical Officer (OCHMO).

Request Submitted	August 24, 2020
Initial Evaluation Approved	September 17, 2020
Assessment Plan Approved	October 8, 2020
Final Report Delivery	January 20, 2022

2.0   Signatures

Submitted by: NESC Lead

Digital Signatures on PDF Copy – 2/9/22

_____

Dr. Azita Valinia

Concurred by:

_____   _____

Dr. John R. Allen   Mr. David R. Francisco

_____   _____

Dr. Joseph I. Minow   Dr. Jonathan A. Pellish

_____

Dr. Alonso H. Vera

This report was co-authored by Azita Valinia, Joseph Minow, Jonathan Pellish, Alonso Vera, John Allen, Nicholas White, Erik Antonsen, Leland Stone, Tony Slaba, Edward Semones, Ryan Norman, James Adams, Ronald Turner, Insoo Jun, Tina Panontin, Kaitlin McTigue, Megan Parisi, Shu-Chieh Wu, David Folta, Noble Hatten, and Kyle Hughes.

Authors declare the findings, observations, and NESC recommendations compiled in the report are factually based from data extracted from program/project documents, contractor reports, and open literature, and/or generated from independently conducted tests, analyses, and inspections.

3.0   Team Members

Name	Discipline	Center/Organization
Core Team		
Azita Valinia	NESC Lead	GSFC
Joe Minow	Space Radiation Environments Lead	MSFC
Jonny Pellish	Technology and Engineering Lead	GSFC
Alonso Vera	Human Systems Integration Lead	ARC
John Allen	Human Health Lead	HQ
Nick White	Integration Lead	Space Science Solutions
Jim Adams	Space Environments	University of Alabama, Huntsville
Claudio Corti	Space Environments	University of Hawaii
Insoo Jun	Space Environments	JPL
Eddie Semones	Space Environments	JSC
Tony Slaba	Space Environments	LaRC
Ron Turner	Space Environments	Analytic Services, Inc.
Mike Xapsos	Space Environments	GSFC
Xiaojing Xu	Space Environments	LaRC
Greg Allen	Technology and Engineering	JPL
Megan Casey	Technology and Engineering	GSFC
Razvan Gaza	Technology and Engineering	JSC
Ruthan Lewis	Technology and Engineering	GSFC
Ryan Norman	Technology and Engineering	LaRC
Kaitlin McTigue	Human Systems Integration	ARC
Jennifer Mindock	Human Systems Integration	JSC/J4 Insights
Tina Panontin	Human Systems Integration	ARC/San Jose State University
Megan Parisi	Human Systems Integration	ARC
Shu-chieh Wu	Human Systems Integration	ARC/San Jose State University
Erik Antonsen	Human Health	JSC/Baylor College of Medicine
Marc Shepanek	Human Health	HQ
Janice Zawaski	Human Health	JSC
Leland Stone	Human Factors	ARC
David Folta	Flight Dynamics	GSFC
Noble Hatten	Flight Dynamics	GSFC
Kyle Hughes	Flight Dynamics	GSFC
Consultants		
J. D. Polk	NASA Chief Health and Medical Officer	HQ
David Francisco	NASA Technical Fellow for Health, Medical, and Performance Flight Standards	JSC
Morgan Abney	NASA Technical Fellow for Environmental Control and Life Support Systems	MSFC
Robert Beil	NESC Systems Engineer	KSC

Name	Discipline	Center/Organization
Nancy Currie-Gregg	Former Astronaut/Human Factors	Texas A&M University
Jennifer Fogarty	Former HRP Chief Scientist	JSC
Bob Hodson	NASA Technical Fellow for Avionics	LaRC
Jon Holladay	NASA Technical Fellow for Systems Engineering	GSFC
Kauser Imtiaz	NASA Technical Fellow for Structures	JSC
Cynthia Null	NASA Technical Fellow for Human Factors	ARC
Kevin Sato	Space Biological and Physical Sciences	ARC
Lisa Simonsen	Radiation Systems Lead, HEOMD	LaRC
Upendra Singh	NASA Technical Fellow for Sensors and Instruments	LaRC
James Spann	Space Weather Lead, SMD	HQ
Michael Stenger	Element Scientist, Research Operations and Integration	JSC
Mary Beth Wusk	NESC Chief Engineer, LaRC	LaRC
Business Management		
Theresa Bardusch	Program Analyst	LaRC/MTSO
Assessment Support		
Linda Burgess	Planning and Control Analyst	LaRC/AMA
Jonay Campbell	Technical Editor	LaRC/KBR
Courtney Hampton	Graphic Artist	LaRC/LAMPS
Kylene Kramer	Project Coordinator	LaRC/AMA

3.1 Acknowledgments

The assessment team is grateful to the following individuals for valuable input, ideas, and helpful discussions that significantly improved the direction and outcome of this assessment: J.D. Polk, David Francisco, Nancy Currie-Gregg, John Allen, Morgan Abney, Robert Hodson, Jon Holladay, Cynthia Null, Leland Stone, Erik Antonsen, Kevin Sato, Lisa Simonsen, James Spann, Michael Stenger, William Paloski, Justin Rowe, James Schier, Julie Robinson, Patrick Troutman, Michelle Rucker, Patrick Chai, Lora Bailey, and Dan Fry.

The assessment team would like to thank the following peer reviewers for their valuable comments and input: Daniel Dorney, Steven Gentz, Robert Hodson, Jon Holladay, Robert Johnson, Jennifer Mindock, Lorraine Prokop, Steven Rickman, James Spann, Michael Xapsos, Janice Zawaski, and Arik Posner.

Furthermore, input from the participants of the NESC/OCHMO "Safe Human Expeditions Beyond LEO" Workshop, held in Houston, Texas, and online on September 14-16, 2021, is acknowledged and greatly appreciated. A list of workshop participants is provided in Appendix A.

4.0   Executive Summary

"Others have said they can go there earlier. Have at it. I want to see that. But when it comes to human life, NASA is going to be very particular, and there are a lot of ifs out there."

NASA Administrator Bill Nelson, during a Washington Post interview July 21, 2021, discussing long-term plans by the Agency to send humans to Mars in the late 2030s.

Planning is underway at NASA for returning humans to the Moon, followed by human missions to Mars. Humans will again venture outside the protective particle radiation shield of the Earth's magnetosphere, this time for durations of months to several years, where they will be vulnerable to long-term exposure from galactic cosmic rays (GCRs) and particles associated with solar storms. Mars missions will leave behind the real-time support of Mission Control and the ability to send spare parts or quickly return crew to Earth in an emergency. Interplanetary mission durations of up to 1000 days in space bring new uncertainties, not only regarding the impact of microgravity and radiation on human health and performance, but also the ability for crew to anticipate and respond to spacecraft system failures.

This NESC assessment is the first of its kind focused on assessing **integrated health risks** to crew on long-duration expeditions beyond low Earth orbit (LEO), **specifically missions to Mars**, and the potential engineering solutions required to minimize those risks. By using a systems approach rather than individual countermeasures, the assessment team has examined the trade space of a subset of human health hazards and the associated risks to identify solutions to mitigate the risks to crew on missions to Mars. As such, this assessment is intended to inform characteristics of those Mars mission architectures that render the lowest integrated human health risks.

Integrated Human Health Risk Assessment

As mission duration and distance from Earth increase, the risk increases that crew capability and the safety net of ground support will degrade over time. This can lead to a decreased ability to perform tasks necessary for mission success and, in the worst cases, negatively impact both the health and safety of the crew during the mission *and* their post-mission long-term health (LTH). It is currently unclear how well crew capability can be maintained in a Mars mission, but it is expected to degrade beyond our historical experience base in any Mars mission scenario. This study primarily focuses on three key hazards and associated risks with long-duration, increasingly Earth-independent missions beyond LEO: radiation exposure, microgravity exposure, and distance from Earth. The latter is also known as inadequate Human Systems Integration Architecture (HSIA).

Radiation risk is expected to increase due to increased time of exposure and loss of the protective effects of Earth's magnetosphere. This primarily affects the risk of radiation carcinogenesis in the LTH domain with suspected contributions to cardiovascular disease (CVD) and central nervous system (CNS) decrements. Increased duration of exposure to altered gravity worsens multiple human system risks and contributes to degradation of crew capability in-mission and for LTH outcomes. Finally, attempting to use the LEO operational paradigm (the current HSIA) with communication and resupply delays on missions to Mars is a high risk. When a spacecraft anomaly situation occurs, a crew of four will be required, in real time, to address problems and maintain operations, as currently achieved by ground-support mission operations center staffed by more than 80 subject matter experts.

In principle, reductions in the LTH risks due to radiation and microgravity exposure can be achieved through decreasing the overall exposure time (via fast transit to Mars). Alternatively, these risks can be reduced by technology investments that enable artificial gravity (AG) and improved radiation monitoring and shielding techniques. Additionally, overall radiation exposure can be reduced by optimizing the mission time during solar maximum (when the overall GCR exposure is the lowest). Furthermore, a radical shift in the operational paradigm, systems design, and human system integration approaches to support crew Earth independence can improve the overall risk posture.

To better understand the combined effects of the risks mentioned above, the NESC team performed an *integrated risk assessment*. Based on the assessment, four themes emerged that could potentially reduce the integrated risks and were further studied: 1) fast Mars transit feasibility, where the round-trip duration of Mars missions is limited to approximately 1 year to minimize the overall flight risks; 2) improved radiation monitoring and shielding techniques, to predict and reduce the harmful impacts of GCRs; 3) optimizing the timing of Mars missions based on the variability of solar cycle and its impact on radiation dose to the crew; and 4) HSIA design requirements to mitigate risks associated with spacecraft management and anomaly resolution during long-duration exploration missions with increased Earth independence.

Fast Mars Transit

The key finding of the fast Mars transit feasibility study is that a round-trip mission duration of approximately 1 year brings many benefits: 1) it reduces cumulative radiation exposure and associated shielding requirements; 2) for the fastest durations, it reduces microgravity exposure and is within bounds of 12 months of microgravity experience on the International Space Station (ISS); 3) it reduces the possible number of time-driven vehicle failures; 4) it eliminates other unknown human health impacts associated with opposition- and conjunction-class 2- to 3-year round-trip scenarios, and 5) it enables *sustainable* deployment of humans and infrastructure to Mars on a regular cadence, allowing steady exploration and colonization of Mars. The study performed in this assessment uses an innovative flight dynamics approach to quantify the minimum total mission Δv (energy) required for a fast Mars transit with total mission duration less than 400 days. The results of this feasibility study show promise for sending humans to Mars and returning them safely with acceptable exposure to microgravity and minimal exposure to radiation using current or near-term technology. Future work is needed to demonstrate that such Δv's are viable and to determine whether such a fast Mars transit is possible without the use of advanced propulsion technologies.

> Fast Mars transit approaches (i.e., round-trip duration of approximately one year) using on-orbit staging with chemical propulsion, or nuclear thermal or electric propulsion (NTP or NEP) technologies should be studied further as a possible baseline mission approach to reduce the integrated risks.

Radiation Monitoring and Shielding

When venturing into cislunar or interplanetary space for long durations, radiation hazards of solar particle events (SPEs) and GCR are encountered. For SPEs originating from solar flares and coronal mass ejections (CMEs), the duration of the events can last from a few hours to several days with an intense fluence of relatively low-energy particles. The greater threat is from SPEs generated by CMEs that can last for a day or two and multiple CMEs over a period of days to a week. GCRs are high-energy, pervasive low-flux particles with much lower fluences, which

for long exposures increase cancer risk and may cause CVD and CNS decrements on long-duration missions. Mitigation strategies (i.e., shielding) are required in both cases to keep crew lifetime exposure below the career NASA exposure limit. Shielding requirements are different for the two cases.

For SPEs, when adequate warning is given, the crew can take shelter for the duration of an event either by reconfiguring cargo in the vehicle or having a dedicated shelter. For the return to the Moon, existing and planned scientific and operational ground- and space-based assets will provide sufficient warning of sporadic eruptions from the Sun. The planned crew shelters will provide adequate protection for the event duration with minimal impact on the completion of mission objectives. For Mars missions, forecasting SPEs that will impact spacecraft and crew in interplanetary space becomes more challenging, and a key finding of this report is that new supporting infrastructure is required to give adequate warnings during crew transit and stay at Mars. It is envisioned that strategic placement of additional monitoring assets in a "solar necklace" formation around the Sun can significantly improve space weather early warning capability.

> Additional space weather monitoring assets (i.e., solar coronagraph and particle detector suites) at Sun-Earth Lagrange point L4 and Sun-Mars L1 and L4/L5 can enable sufficient early warnings for Mars missions during transit and stay. The Sun-Mars L4/L5 assets would also provide a communications relay solution for when the Earth line of sight to Mars is behind or close to the Sun, leading to a 2-week blackout period every 2 years.

It is important to note that for crewed missions on the surface of Mars or in orbit around Mars (when timely communication with Earth is not feasible), it will be necessary to monitor and forecast space weather on location instead of relying on operational instructions based on forecasts generated and transmitted from Earth. Sufficient early warning for the crew at Mars is a requirement that is best met with an Earth-independent capability for space weather forecasting. In this case, development of an Earth-independent space weather forecast capability onboard deep space transit vehicles and on site at Mars to collect and process data and generate space weather forecasts is needed.

Radiation exposure from GCRs becomes an important risk factor for Mars missions and long-duration missions in cislunar space and is challenging to mitigate. The exposure varies depending on the 11-year solar cycle, with the minimum exposure occurring during solar maximum. A key finding of this report is that exposure from GCRs could be reduced by approximately a factor of 2 by timing Mars missions to be during solar maximum. However, special attention needs to be given to solar cycle prediction capability since solar cycles can vary significantly. It is believed that the associated increase in SPE activity during solar maximum can be mitigated with current shield design and optimization strategies. The reduction from solar maximum GCR exposure is worth the effort needed to optimize the timing and duration of Mars missions.[1] Furthermore, GCR shielding standards are needed to impact future crewed spacecraft design for long-duration missions to Mars.

---

[1] In this assessment, the timing of the fast Mars transit feasibility study and solar maximum cycle prediction study actually coincide within the window of 2035-2037.

A standard for GCR shielding for human exploration missions beyond LEO is needed. It is recommended that vehicles and habitat systems provide sufficient protection to reduce exposure from GCR by 15% compared with free space, such that the effective dose from GCR remains below 1.3 millisieverts per day (mSv/day) for systems in space and below 0.8 mSv/day for systems on planetary surfaces. This standard is based on missions during solar minimum (the worst-case scenario). It can be achieved with current aluminum spacecraft structures. For Mars missions *longer than 600 days*, additional GCR mitigation strategies will be required to meet the newly approved 600-mSv crew lifetime exposure limit (except for potentially limited opportunities for missions during solar maximum, when the overall GCR exposure is the lowest).

Other key findings of the radiation shielding assessment are: 1) radiation shielding design needs to be part of the early design process of any vehicle or habitat, to maximize the shielding provided by the required vehicle mass as opposed to the incorporation of additional parasitic shielding mass, and 2) current active shielding concepts are not technologically mature enough for implementation and provide no mass to orbit benefit over passive shielding approaches.

Reducing the Risk of Microgravity Exposure

The ISS has provided a necessary platform for studying the impact of long-duration spaceflight on human health and performance.

This assessment found that there is no overarching NASA strategy for examining the benefits of continuous or intermittent artificial gravity (AG or iAG) for crews on long-duration missions. This is particularly important since *eleven individual health risks* are directly tied to prolonged microgravity exposure. NASA research on the effects of centrifugation after 21 days of bed rest in 2005 and 2006 showed benefits but indicated that continuous exposure of up to 1 hour was not well tolerated, especially by women. European Space Agency (ESA)-led studies have continued this line of research with short-term bed rest combined with AG (BR-AG1) in 2010 and Artificial Gravity Bed Rest – European Space Agency (AGBRESA) in 2019. The latter involved 60 days of head-down bed rest to simulate spaceflight deconditioning and showed benefits from iAG with multiple 30-minute exposures for both men and women. The AGBRESA study showed positive effects on multiple human system microgravity risks with 30 minutes of iAG per day but did not address all concerns and was not able to determine a conclusive AG prescription as a multisystem countermeasure. AGBRESA also noted that iAG appeared to provide superior benefits to continuous AG. Further work is required to confirm the efficacy of particular AG prescriptions as this is the precursor to determining the most promising engineering approaches for reducing the risk of microgravity exposure on long-duration flights.

Human research investigations should be pursued to evaluate more fully the safety and efficacy of an iAG countermeasure for exposure durations (doses) greater than 30 minutes per day, in combination with strict long-duration head-down bed rest deconditioning. Future AG investigations should be supported by current human research efforts to assess lower body negative pressure, as well as plans to use Gateway in combination with surface lunar gravity exposure and explore commercial partnership opportunities to understand in-space centrifugation.

A New Paradigm for Designing Human-Systems Integration Architecture (HSIA)

NASA's mission operations paradigm, which originated with Project Mercury and endured with minimum evolution through Apollo Program, Space Shuttle Program, and ISS missions, has been one of near-complete real-time dependence on experts at Mission Control (MC) to manage the combined state of the mission, vehicle, and crew. MC staff monitor and analyze mission data, identify trends of concern, diagnose and respond to vehicle anomalies, and ensure effective execution of actions. *The current HSIA—where mission safety relies on ground controllers with ready access to resupply—cannot be extrapolated to long-duration exploration missions (LDEMs) beyond LEO.* In addition, regardless of breakthroughs in fast Mars transit, radiation monitoring/shielding, or microgravity exposure, the challenges that emerge from communication delay and resupply constraints demand a radical paradigm shift.

The HSIA key findings for long-duration missions beyond LEO are: 1) the likelihood of high-consequence problems of *uncertain origin* occurring during spaceflight is high (**conservatively, exceeding 50% during Mars transit**) based on historical trends; 2) it is possible to reduce anomaly rates through improved reliability analysis and testing and anomaly impacts through added robustness, but such mitigations address only *known* failure modes and known uncertainties; 3) attempting to use the LEO operational paradigm (i.e., the current HSIA) with communication and resupply delays is high risk; and 4) a radical shift in operational paradigm, systems design, and human/system integration approaches is the only viable approach to improve the risk posture.

> NASA engineering and human health and medical communities should collaborate to develop a strategic plan to address the paradigm shift needed for the operation of long-duration missions beyond LEO. HSIA requirements must be levied at the onset of the design and development cycle for increasingly Earth-independent missions. Research and technology capabilities to focus on include but are not limited to:
> - AI to aid the crew in data monitoring, analysis, and trend identification for vehicle systems.
> - Advanced sensors and sensor fusion to support crew diagnosis and repair of vehicle systems.
> - Virtual/augmented reality for crew execution support.
> - Data integration, data architecture, and data visualization to support crew vehicle diagnostic processes.
> - Asynchronous communication support to mitigate effects of delays and intermittency.
> - Development of simulation capabilities for determining requirements and validating concepts for Earth-independent crew anomaly resolution and complex operation execution.
> - Advanced maintainability standards and sparing approaches (e.g., additive manufacturing) that support crew in both routine operations and conditions requiring critical repairs.

As a final note, this assessment has succeeded in fostering close collaboration between the engineering and human health and medical communities to address the multitude of human health risks using a holistic approach. A key overall finding is that how individual risks

collectively interact to provide an overall integrated risk to crew or mission is not yet well understood. A key overall recommendation is that the engineering and human and medical technical authorities should partner to further refine and explore the integrated human risk trade space to prioritize research and investment into potential game-changing technologies to significantly reduce risk on an initial Mars mission.

5.0   Background, Assessment Plan, and Scope
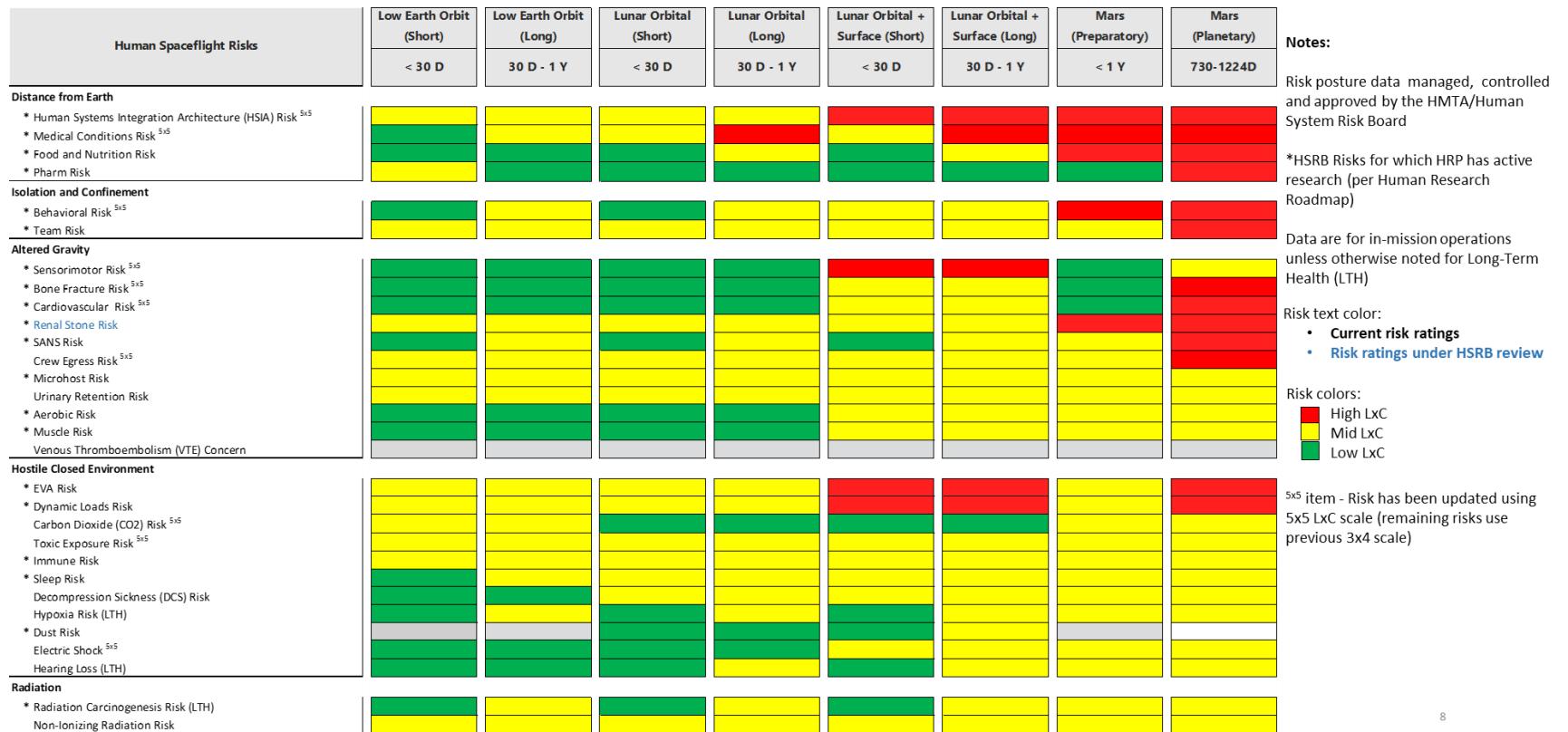
For the past 20 years, NASA's human presence in space has concentrated on activities in LEO, specifically on the ISS. However, a significant body of work was done to lead up to that achievement, from the earliest Mercury missions to the Space Shuttle Program. Behind all of these amazing engineering achievements, concern for the health and safety of the humans transported or resident on these vehicles was paramount.

The NASA Human System Risk Board (HSRB) and the Human Research Program (HRP) have worked with operational medicine and the OCHMO to define and mitigate the human safety, health, and performance risks associated with spaceflight through a countermeasure approach. From those efforts, five hazard categories were identified: 1) Altered Gravity Fields; 2) Distance From Earth; 3) Radiation; 4) Isolation and Confinement, and; 5) Hostile/Closed Environments. Within each of these hazard categories lie a number of associated risks. The HSRB assesses and tracks these risks, assigning a risk score based on the best available evidence for design reference missions (DRMs) ranging from LEO to Mars.

Figure 5.0-1 shows the current state of the known risks associated with the five hazard categories across DRMs that range from LEO to Mars. Twenty-nine of these 30 risks can result in functional impairment that is expected to worsen as mission duration increases. The "30th" risk, the risk of adverse outcomes due to inadequate HSIA, results not in functional impairment but rather the inability to perform complex operations and manage system anomalies with decreased ground support.

Once identified and characterized, these risks are conveyed to the HRP so that studies can be made and countermeasures developed to mitigate their impacts. HRP is focused on understanding and reducing crew health and performance (CHP) degradation; however, broader systems engineering solutions have historically been outside the scope of the program.

The risks identified above present key challenges to the LDEMs NASA is currently planning for extension of human presence beyond LEO. For example, extended exposures to radiation have the potential to cause in-mission health, in-mission performance, and LTH consequences. Similarly, extended durations in microgravity, including one case of an altered gravity field, leads to physiological deconditioning if not appropriately mitigated, with potential impacts to crew health and mission objective performance. Another example is that increased distance from Earth reduces the availability of physical resources from resupply and the availability of information and decision-making resources due to communication delays and architecture challenges, leading to a degradation in a crew's ability to execute complex operations and respond to anomalies.

Human Spaceflight Risks

	Low Earth Orbit (Short) < 30 D	Low Earth Orbit (Long) 30 D - 1 Y	Lunar Orbital (Short) < 30 D	Lunar Orbital (Long) 30 D - 1 Y	Lunar Orbital + Surface (Short) < 30 D	Lunar Orbital + Surface (Long) 30 D - 1 Y	Mars (Preparatory) < 1 Y	Mars (Planetary) 730-1224D

Distance from Earth
* Human Systems Integration Architecture (HSIA) Risk [5x5]
* Medical Conditions Risk [5x5]
* Food and Nutrition Risk
* Pharm Risk

Isolation and Confinement
* Behavioral Risk [5x5]
* Team Risk

Altered Gravity
* Sensorimotor Risk [5x5]
* Bone Fracture Risk [5x5]
* Cardiovascular Risk [5x5]
* Renal Stone Risk
* SANS Risk
Crew Egress Risk [5x5]
* Microhost Risk
Urinary Retention Risk
* Aerobic Risk
* Muscle Risk
Venous Thromboembolism (VTE) Concern

Hostile Closed Environment
* EVA Risk
* Dynamic Loads Risk
Carbon Dioxide (CO2) Risk [5x5]
Toxic Exposure Risk [5x5]
* Immune Risk
* Sleep Risk
Decompression Sickness (DCS) Risk
Hypoxia Risk (LTH)
* Dust Risk
Electric Shock [5x5]
Hearing Loss (LTH)

Radiation
* Radiation Carcinogenesis Risk (LTH)
Non-Ionizing Radiation Risk

Notes:

Risk posture data managed, controlled and approved by the HMTA/Human System Risk Board

*HSRB Risks for which HRP has active research (per Human Research Roadmap)

Data are for in-mission operations unless otherwise noted for Long-Term Health (LTH)

Risk text color:
• **Current risk ratings**
• **Risk ratings under HSRB review**

Risk colors:
 High LxC
 Mid LxC
 Low LxC

[5x5] item - Risk has been updated using 5x5 LxC scale (remaining risks use previous 3x4 scale)

8

Figure 5.0-1. Matrix showing Human System Risks tracked by HSRB and Official High-level Risk Postures for Different DRMs (current as of November 2021)

It was far beyond the scope of this assessment to address each of the risks. Therefore, at the guidance of the NASA Chief Health and Medical Officer, the NESC assessment team was asked to focus its efforts on radiation, altered gravity, and distance from Earth, to identify gaps that might be closed through engineering solutions for DRMs that include long-term lunar orbital and surface activities (i.e., up to 1 year) and Mars missions (i.e., at least 1 year or more). With advice from the assessment steering committee, the team further refined these areas to concentrate on:

- Protection from radiation (e.g., exposure radiation event alerting and active and passive shielding).
- AG.
- Enabling more Earth-independent operations.

The focus of the expeditions was further narrowed to Mars, with Lunar Gateway and surface operations assumed as a proving ground to reduce risks for a Mars mission.

After researching the current state of knowledge and technology (Section 6) supporting the potential engineering solutions in the study scope, the assessment team performed an integrated human health and safety risk assessment (Section 7). The team examined the conceptual interplay among a subset of risks associated with crew, engineered systems, and their integration for Mars mission architectures due to the three hazards in the scope of the assessment. The analysis is intended to inform characteristics of those architectures that render the lowest integrated human health and safety risks. The team followed the analysis with discussion of the potential engineering solutions (Section 8) and developed suggestions (Section 9) for both engineering development and engineering processes to minimize the integrated risks.

6.0 Current State of Knowledge

This section describes the state of the knowledge/art in 1) space radiation environment characterization, 2) radiation mitigation approaches, 3) mitigating space radiation impacts during space operations, 4) human research in AG environments and technology maturity, and 5) HSIAs for long-duration, deep space expeditions beyond LEO.

6.1 Space Radiation Environment Characterization
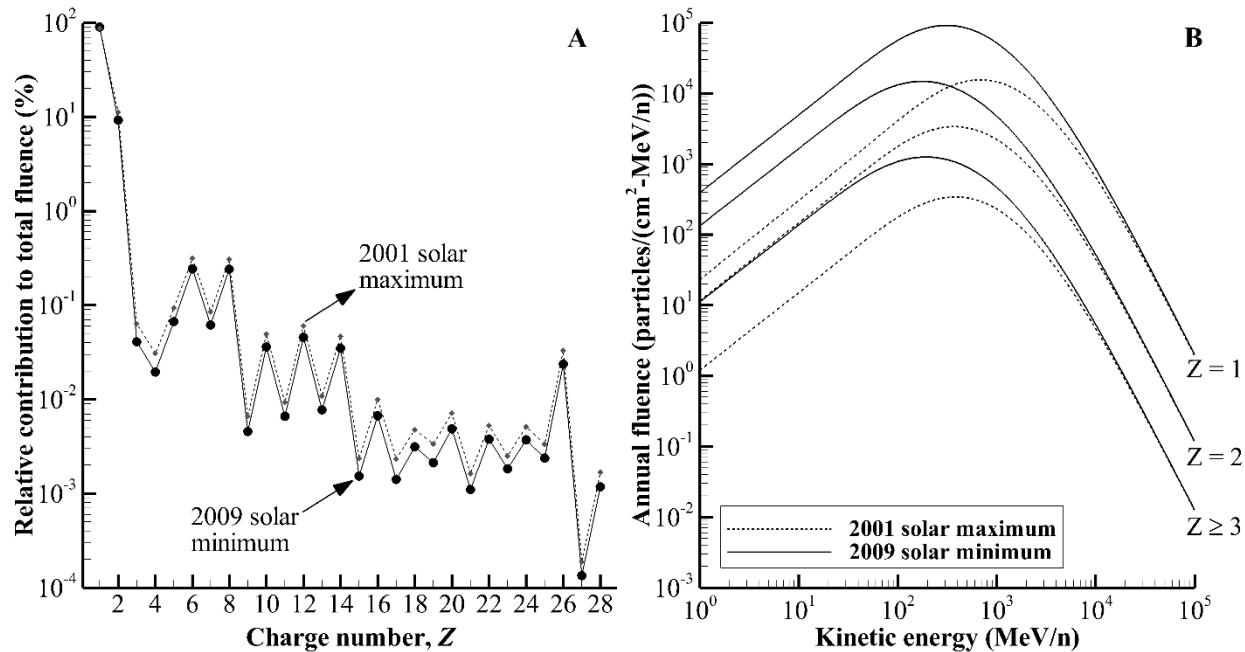
The individual elements of the space environment most relevant for producing radiation dose for crew members during spaceflight are GCR, SPEs, near-Earth trapped radiation environments, albedo environments on or above planetary surfaces, and onboard or nuclear-powered radiation sources. This section describes the characteristics of these environments and compares the total radiation dose flight crews will experience for a variety of reference missions.

6.1.1 Galactic Cosmic Rays (GCRs)

GCRs are believed to originate primarily from supernova explosions and are accelerated to nearly the speed of light in the resulting shockwave. The GCR environment is a complex mixture of highly energetic and fully ionized particles spanning the periodic table of elements. Each ion energy spectrum is modulated by the heliospheric magnetic field (HMF) between solar minimum and maximum on an approximate 11-year cycle. Figure 6.1.1-1 summarizes the particles and energies of relevance to human exposure and risk near 1 astronomical unit (AU). As shown on the left side of Figure 6.1.1-1, protons ($Z = 1$) and helium ($Z = 2$) account for ~89% and ~10% of the total fluence, respectively, while the remaining 1% is represented by particles with $Z \geq 3$.

Although these relative contributions appear largely insensitive to solar modulation, the absolute magnitude and spectral shape of each ion depends greatly on the state of the heliosphere. The HMF intensifies during solar maximum, thereby deflecting a portion of the local interstellar spectrum impinging on the outer boundary of the heliosphere. During solar minimum, the magnetic field is at its weakest point, and the GCR intensity is maximized. Solar modulation effects become increasingly negligible above ~10 GeV/n, as the incoming GCRs are able to propagate through the HMF, and the near-Earth GCR environment appears similar to the local interstellar spectrum found outside the heliosphere. Although overall exposures are reduced by about a factor of 2 during solar maximum compared with solar minimum, it is important to recognize that the GCRs remain highly penetrating at all points in the solar cycle. For example, the range (penetration depth at which a particle comes to rest in matter) of a 1-gigaelectronvolt (GeV) proton in water is over 3 meters (m).

Modern GCR models are sufficiently advanced that they can be reliably used to specify the proton and heavier ions at energies of importance to crew health and single event upsets. For example, error in the current Badhwar-O'Neil (BON) 2020 GCR model is ±15% for spectral flux quantities, a value that is acceptable to physics and biology uncertainties. The end-to-end modeling uncertainty for radiation dose and biological effects can be higher and is due to the combined uncertainties in the environment, radiation transport, and biological effects. Despite the accuracy of current GCR models, there remains a lack of time-resolved, high-precision measurements for heavy ions (Z > 2) that could be important for other health effects (CNS effects in particular) and remain largely unquantified and highly uncertain. The existing GCR models such as BON2020, DLR [Matthia et al. 2013], and other models are currently integrated into tools used by NASA's Space Radiation Analysis Group (SRAG) for operational mission support, shielding design, and radiation dose reduction optimization efforts. These models are also used for both short- and long-term mission planning but are generally not needed to evaluate exposure in flight where dosimetry is used for active monitoring of radiation dose to crew.

Figure 6.1.1-1. Relative Contribution to Total Fluence (%) for Z = 1–28 during 2001 Solar Maximum and 2009 Solar Minimum (left); Energy Spectra for Z = 1, Z = 2, and Combined Z ≥ 3 Ions during Same Time Periods (right)
All calculations were performed with BON2020 model at 1 AU [Slaba and Whitman 2020]

F-1. During solar minimum, the magnetic field is at its weakest point, and the GCR intensity is maximized.

F-2. Although overall exposures are reduced by about a factor of two during solar maximum compared with solar minimum, it is important to recognize that the GCR remain highly penetrating at all points in the solar cycle.

F-3. GCR models are sufficiently advanced that they can be reliably (within ±15%) used to specify the flux of protons and heavier ions of importance to crew health and single event effects (SEEs) if the solar cycle activity is known.

F-4. The ability to predict future GCR environments is limited by the ability to predict future solar activity,[2] including parameters such as sunspot number and the F10.7[3] cm radio flux index, particularly for periods of time beyond the minima in activity between two cycles.

---
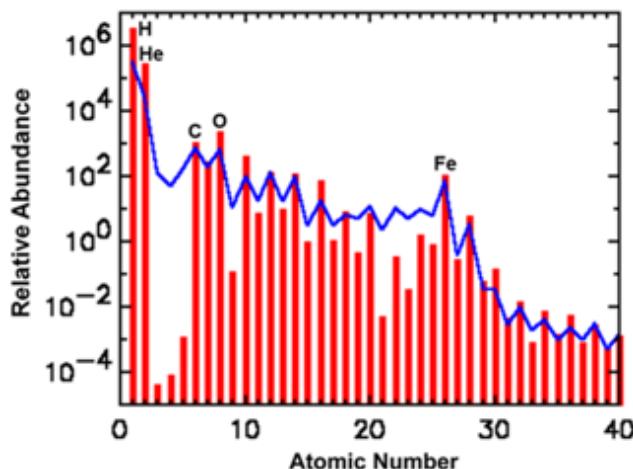
[2] See Section 8.3 for a discussion of solar cycle prediction and GCR environment.

[3] The solar radio flux at 10.7 centimeters (cm) (2800 megahertz (MHz)), often called the F10.7 index, is an indicator of solar activity and is valuable in forecasting space weather.

6.1.2 Solar Particle Events (SPEs)

SPEs are intense bursts of energetic particles from the Sun associated with solar flares and coronal mass ejections. During such storms, protons and heavier ions are propagated along magnetic field lines through the HMF with energies that can extend into the GeV region. Although most SPEs occur during solar maximum, the forecasting of event occurrence, magnitude, spectral characteristics, and duration remains highly uncertain.

Figure 6.1.2-1 shows a comparison of ion solar abundances and GCRs. The two abundance distributions are generally similar. The main differences result from fragmentation of GCR ions from occasional collisions with interstellar hydrogen and helium, which tend to smooth out the GCR distribution relative to solar abundances. All naturally occurring elements in the periodic table are present, although there is a steep dropoff for atomic numbers higher than iron ($Z = 26$). Protons represent the dominant source of acute exposure and risk for astronauts for most SPEs, but moderate $Z \geq 2$ components have been observed for some historical events.
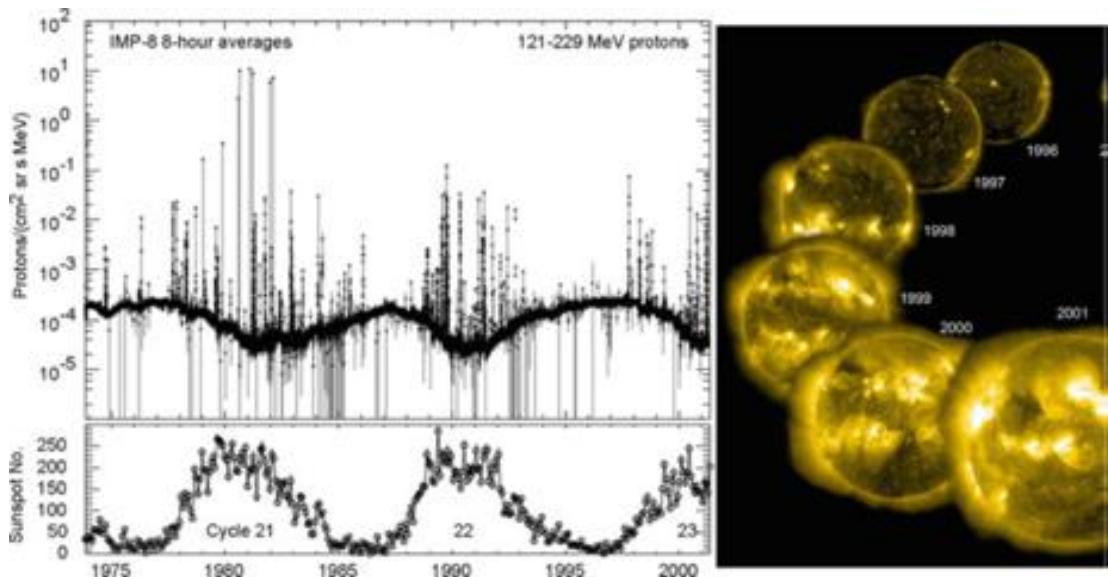
Figure 6.1.2-1. Comparison of Relative Abundances of GCR Ions (blue line) and Solar System Ions (red bars) [NASA 2021]

The energy spectra and heavy-ion content of SPEs vary substantially from event to event. Energy spectra can extend up to ~GeV/n but often do not reach these high energies. The main risk for astronauts comes from protons, as the magnitude and range of the lower energy heavy ions in shielding material is limited. For an extreme event, the total >10 megaelectronvolt (MeV) proton fluence can be on the order of 10^{10} particles/cm^2, while the peak flux can reach on the order of 10^6 particles/(cm^2-sec).

The upper left panel of Figure 6.1.2-2 shows the flux of high-energy (121 to 229 MeV) solar and GCR protons for a 27-year period [Reames 2021]. The spikes in solar proton flux occur more frequently during the solar maximum period and extend orders of magnitude above the GCR proton flux. The lower left panel in the figure shows solar activity levels in terms of the international sunspot number during the same period of time. A mission that is launched during solar maximum will be subject to a higher frequency of SPEs. One that is launched during solar minimum will experience higher intensities of GCRs.
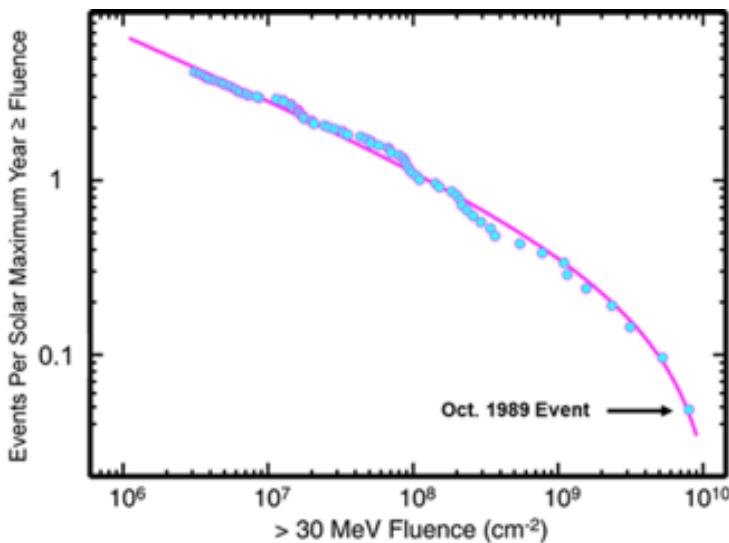
> **F-5.** A mission that is launched during solar maximum will be subject to a higher frequency of SPEs. One that is launched during solar minimum will experience higher intensities of GCRs.

Figure 6.1.2-2. Flux of 121–229 MeV Protons over 27-year Period in 8-hour Averages detected by Goddard Telescope on Interplanetary Monitoring Platform 8 (IMP-8) Spacecraft (upper panel) Monthly international sunspot numbers are shown on lower left for comparison. On right are extreme ultraviolet imaging telescope (EIT) images during rising phase of solar cycle 23 [Reames 2021].

The distribution of solar proton event magnitudes is shown in Figure 6.1.2-3 for the case of >30-MeV proton event fluences [Xapsos 2019]. The smaller event sizes follow a power law, while there is a rapid falloff with increasing event magnitude for very large events. The figure shows the October 1989 event commonly used as a design standard [Townsend et al. 2018]. Its frequency on this plot is once per 20 solar maximum years, or about once every three solar cycles.

The time characteristics of solar proton events and their propagation through the heliosphere are particularly important for human exploration missions. This includes the transit time of solar protons from the Sun to the spacecraft, the time profiles of flux and dose, and the duration of the flux above background level. These characteristics also vary substantially from event to event. A detailed study of the flux and dose versus time profiles is given in Minow et al. [2020]. It was concluded that 10% of all events reach their peak dose rate in 0.75 hours from event onset, while 90% reach their peak in 29.75 hours. Worst-case characteristics of solar proton events observed at 1 AU are listed in Table 6.1.2-1.

Figure 6.1.2-3. Frequency Distribution for Three Solar Cycles of Solar Proton Events during Solar Maximum (line calculated with ESP/PSYCHIC model [Xapsos 2019])

The ability to forecast "all clear" periods when extravehicular activity (EVA) and other critical operations with minimal shielding can be performed is relatively good based on the availability of existing ground- and satellite-based instrumentation for imaging the size and complexity of solar activity regions. Current all-clear forecast techniques are most reliable when there are few or no large active regions on the Sun.

Table 6.1.2-1. Characteristics of Worst-case Solar Proton Events at 1 AU

Energies	Integral Fluence (>10 MeV)	Peak Flux (>10 MeV)	Transit Time[4]	Onset to Peak Dose Rate	Duration
~GeV	~10^{10} cm^{-2}	~10^6 cm^{-2}s^{-1}	<30 min	<30 min	Weeks

F-6. The capability to nowcast (monitor) solar energetic particle events in LEO is sufficient to support crew warnings for onset of radiation events in time to implement radiation mitigation strategies.

F-7. The capability to *predict* the onset of solar energetic particle events in advance is limited.

6.1.3 Near Earth

The near Earth (i.e., within the confines of the geomagnetic field) radiation environment includes attenuated GCRs and belts of intense but comparatively lower energy trapped protons and electrons. The geomagnetic field deflects lower energy GCR ions, especially at equatorial latitudes. Higher energy ions are able to transmit through the Earth's magnetic field and penetrate deep into the atmosphere; these ions may interact with the atmospheric constituents, producing a cascade of secondary particles observable on the ground. Interactions occurring near the top of the atmosphere can eject secondary particles back into the geomagnetic field that

---
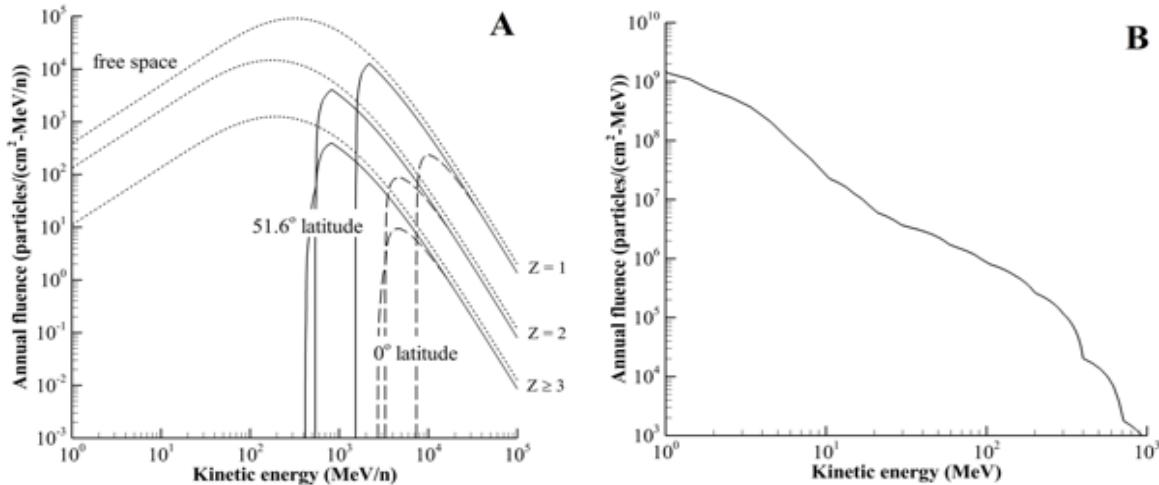
[4] Transit time from the Sun to 1 AU.

become trapped or decay (decay products can also become trapped), thereby providing a continuous source for trapped particle belts. Knowledge of the long-term mean and statistical variations in the charged particle flux trapped in the Earth's magnetic field is sufficiently advanced (error of about 2x for flux and fluence) to support design of crewed spacecraft that transit the belts on their way to and from LEO, the Moon, and Mars.

The ISS operates in LEO at an altitude of ~400 kilometers (km) and an inclination of 51.6°; where it encounters a continuous low dose rate of attenuated GCRs but only crosses the inner Van Allen belt in a confined portion of the trajectory, referred to as the South Atlantic Anomaly (SAA). Both components make important contributions to the total astronaut exposure on ISS. For exploration missions beyond the geomagnetic field, exposures received during transit to free space typically account for a small portion of the total mission exposure, assuming nominal shielding conditions.

The left side of Figure 6.1.3-1 shows the LEO GCR environment at latitudes of 0° and 51.6° N and an altitude of 400 km for the 2009 solar minimum time period [Badavi et al. 2012]; the corresponding free space GCR spectrum is shown for comparison. Above the geomagnetic cutoff energies, the LEO GCR environment is a factor of ~0.68 smaller than the free space spectrum due to terrestrial blockage. At equatorial latitudes, the approximately dipole geomagnetic field is able to reject protons below ~8 GeV and heavier ions below ~4 GeV/n, while at 51.6° N the cutoff energies are reduced for protons and heavier ions to 2 GeV and 1 GeV/n, respectively. GCR dose rates within ISS are about 4.5 times larger at 51.6° N compared with the equator.

The trapped proton spectrum, as calculated with the AP9 model [Ginet et al. 2013], is shown on the right side of Figure 6.1.3-1 for the ISS trajectory (circular orbit at 400 km, 51.6° inclination). The intensity of <100-MeV protons appears quite substantial, and although a majority of these ions are stopped by the mass shielding of ISS, intravehicular exposures can still be noticeably amplified during SAA passes due to thinly shielded regions. Higher energy trapped protons are able to penetrate moderate shielding levels and contribute to total exposure as well.

Figure 6.1.3-1. Energy Spectra for Z = 1, Z = 2, and Combined Z ≥ 3 Ions during 2009 Solar Minimum at Altitude of 400 km and Two Different Latitudes compared with Free Space (left); Trapped Proton Spectrum at an Altitude of 400 km and Circular Orbit Inclination of 51.6° N (right)

F-8.	Knowledge of long-term mean and statistical variations in the trapped radiation belt environments is sufficiently advanced to support design of crewed spacecraft that transit the belts on trajectories between LEO and the Moon and Mars, as long as the time spent in the belts is <24 hours.

F-9.	Knowledge of long-term mean and statistical variations in the trapped radiation belt environments is sufficiently advanced to support design and operations of robotic missions that spend long periods of time in the radiation belts, such as the Gateway Power and Propulsion Element (PPE) and future uncrewed logistics vehicles using solar electric power to operate ion engines for gradual orbit raising through the belts.

F-10.	The ability to forecast the state of the radiation belts for specific short periods of time (i.e., on the order of several weeks) is currently limited due to the lack of nowcast data and predictive models.

6.1.4 Planetary Surface Environments

On the surface of the Moon and Mars, the free space GCR or SPE environments interact with the planetary surface, yielding a back-scattered, or albedo, radiation field. The albedo environment includes all particles that may be produced in nuclear collisions. However, only the neutrons are produced with enough energy and multiplicity to pose a significant additional health risk for astronauts either inside or outside a surface habitat. There have been a limited number of measurements focused on characterizing the radiation environment on the lunar or Martian surfaces, and knowledge of the albedo environments has therefore been guided by modeling and simulation results. Despite the reliability of models in such applications [Matthia et al. 2016, 2017], more data are necessary to fully validate predictions for the broad range of human exploration missions being considered by NASA and other agencies.

6.1.4.1 Moon
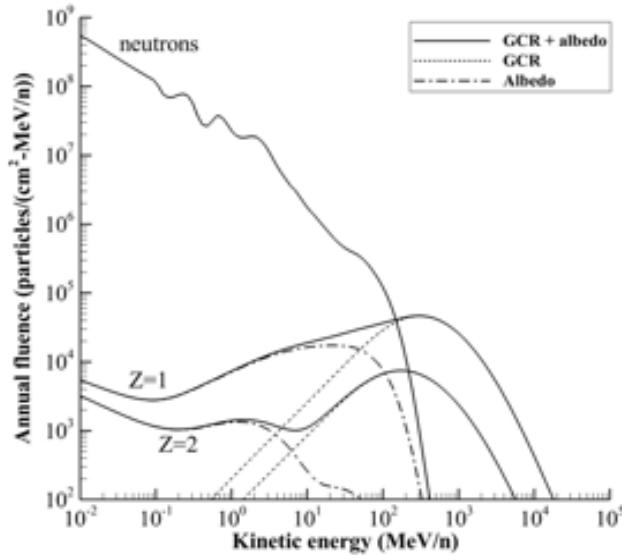
One of the main goals of NASA's Constellation Program was to land humans on the Moon by 2020, and as a result, starting in the mid-2000s several studies were published focused on the lunar radiation environment. McKinney et al. [2006] provided one of the only studies to directly compare simulation results to measurements. The left side of Figure 6.1.4.1-1 shows a comparison of simulation results from MCNPX (Monte Carlo N–Particle Transport Code System Extended) to data from the Apollo 17 Lunar Neutron Density Experiment (LNDE) [Woolum et al. 1975]. The simulated neutron spectrum was further separated into broad energy regions within the lunar subsurface, and as can be seen on the right side of Figure 6.1.4.1-1, epithermal (1 eV to 1 MeV) neutrons are by far the largest component of the flux, especially at depths of ~100 grams per square centimeter (g/cm^2) below the surface. At the surface, however, the epithermal and fast (>1 MeV) components are comparable, and thermal (<1 eV) neutrons appear much smaller. Heilbronn et al. [2015] showed that ~90% of the neutron biological dose in space is attributable to energies between 1 MeV and 1 GeV. The thermal and epithermal neutrons represent a minor fraction of the total biological risk on the lunar surface.

Figure 6.1.4.1-1. Comparison of MCNPX Simulation Results to Data from Apollo 17 LNPE (left); Depth Dependence of Total Neutron Flux in Thermal (<1 eV), Epithermal (1 eV – 1 MeV), and Fast (>1 MeV) Energy Regions at LNPE Site
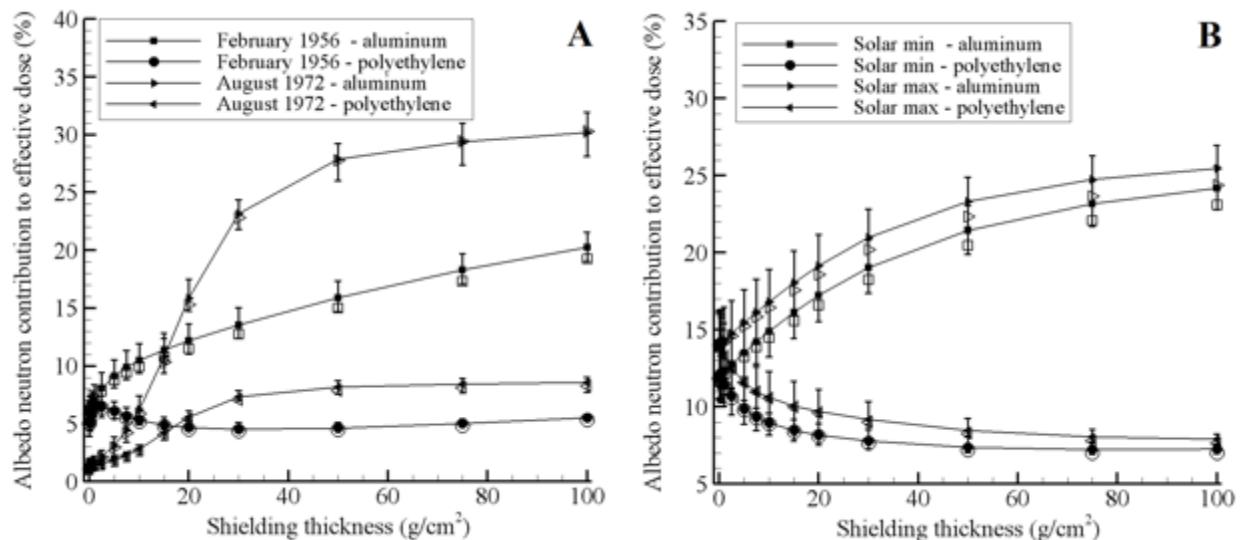
Subsequent studies were published [Wilson et al., 2004; Adams et al., 2007; De Angelis et al., 2007; Hayatsu et al., 2008; Yamashita et al., 2008; Pham and El-Genk 2009; Denisov et al. 2010; Jia and Lin, 2010; Slaba et al., 2011] using various radiation transport codes with a broad range of assumptions pertaining to the ambient environment (SPE or GCR), lunar regolith composition, mass shielding geometry, and local topography. Despite the diverse set of modeling assumptions used in these studies, general agreement can be found in the literature that the albedo neutron contribution to total effective dose (sievert (Sv)) in unshielded conditions was less than 10% for SPE and less than 20% for GCR. Figure 6.1.4.1-2 shows the lunar surface spectra for neutrons and $Z = 1, 2$ ions associated with the 2009 solar minimum GCR environment. The albedo particle energies decline rapidly after ~100 MeV, as would be expected for particles produced from nuclear de-excitation and evaporative processes.

These unshielded estimates are of little value to human missions, where shielding is provided by spacesuits, habitats, and other structures. In that regard, Slaba, Blattnig, and Clowdsley [2011] completed a more comprehensive analysis of the lunar neutron environment accounting for a multitude of factors that affect such calculations. Figure 6.1.4.1-3 shows the albedo neutron contribution to effective dose for SPE and GCR environments as a function of shield thickness for aluminum and polyethylene. The error bars represent bounding values obtained when the neutron component of the effective dose was computed with various biological conversion coefficients and calculation methods. The impact of different regolith compositions was found to be negligible. For SPE, the neutron contribution to effective dose is less than ~15% over the first 20 g/cm^2 of shielding. Although the contribution to total exposure appears as high as 30% for the February 1956 SPE and aluminum shielding, it is important to recognize that the magnitude of the neutron exposure is relatively small in all cases (< 20 mSv). For GCR, there is little difference between the albedo neutron relative contribution during solar minimum or maximum. However, it is clear that polyethylene is more efficient (due to its hydrogen content) than aluminum at attenuating the albedo neutron field.

Figure 6.1.4.1-2. Lunar Surface Radiation Environment for Neutrons and Z = 1 and Z = 2 Ions associated with 2009 Solar Minimum GCR Environment
Results are calculated using BON2020 GCR model [Slaba and Whitman 2020] and HZETRN2020 [Slaba et al. 2020].

Figure 6.1.4.1-3. Percent Contribution to Effective Dose from Albedo Neutrons on Lunar Surface behind Aluminum and Polyethylene Shielding exposed to SPE (left) and GCR (right) Environments Error bars represent minimum and maximum results obtained when neutron component of effective dose was computed with various methods. Closed symbols represent the average of all model results considered. Open symbols correspond to a specific set of models described in detail by Slaba et al. [2011].

Current knowledge of the contribution from albedo neutrons to the total dose that crew members will accumulate on the lunar surface is primarily based on models of the nuclear interactions of GCR and SPE ions with the lunar regolith. Model results are validated against neutron measurements in lunar orbit but only over a limited range of energies. Past efforts to measure lunar albedo neutrons have only extended to energies of 15 or 20 MeV; there is a need to push

these measurements to higher energies in the hundreds of MeV to GeV range to fully characterize the lunar neutron environment in general and to fully evaluate neutron dose contributions for future long-duration exploration of the lunar surface. However, there are technology issues with deploying instruments on the lunar surface to capture the high-energy neutrons. Detector volumes required to measure neutrons of hundreds of MeV to GeV energies are very large, competing with other instrument space and mass on a lunar lander. A dedicated mission may be required to obtain the required neutron measurements. Since the goal is primarily to validate the nuclear interaction models used to simulate the production of neutrons from the GCR source and GCR flux varies slowly over time, a single mission is adequate to characterize the albedo environment. Such measurements are not required for the near-term missions to Gateway and the lunar surface since the current plan is to keep the mission durations sufficiently short such that GCRs and any albedo neutron contributions to crew dose are small compared with the NASA lifetime radiation exposure limit of 600mSv.

The importance of the high-energy neutron measurements is to validate the lunar albedo models so they can be reliably used for design of shielded habits, rovers, and other infrastructure for use on long-duration operations on the lunar surface. It is only when the missions extend for appreciable fractions of a year or longer will radiation dose contributions from GCRs and albedo neutrons begin to exceed program limits, and incorporating additional shielding into infrastructure design becomes an important consideration for mission design. It might be beneficial to obtain in-situ measurements of lunar albedo neutrons (with a neutron detector) on future lunar science missions, with a focus on radiation with high-energy capability to at least hundreds of MeV and few GeV, if possible.

> **F-11.** Past efforts to measure lunar albedo neutrons have only extended to energies of 15 or 20 MeV. In-situ measurements of the secondary neutron environment on the lunar surface extending beyond tens to hundreds of MeV and GeV energies are needed to support dose estimates for long-term lunar exploration.
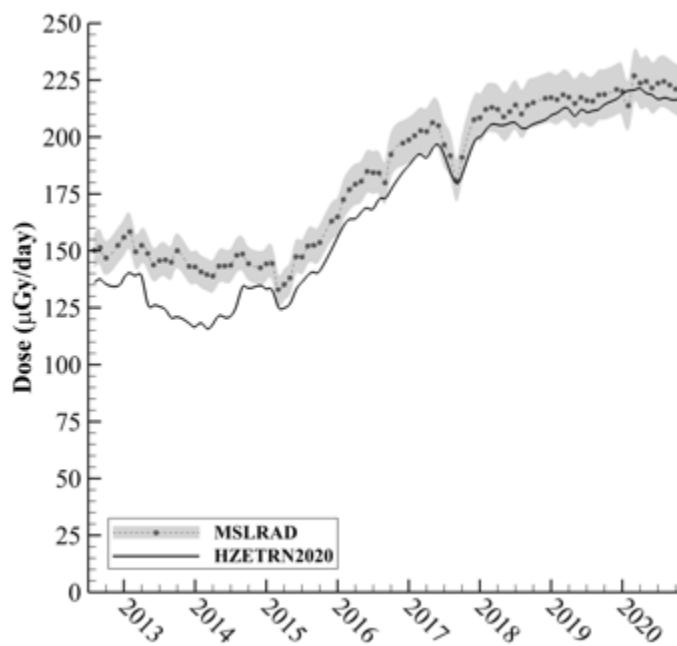
6.1.4.2 Mars

Following the 2009 Augustine Commission [Augustine et al. 2009], exploration was refocused toward Mars, and various studies were published with model-based assessments of the Martian surface radiation environment. More importantly, starting in ~2012, the Mars Science Laboratory Radiation Assessment Detector (MSLRAD) aboard the *Curiosity* rover began operations on the Martian surface. The instrument has provided nearly continuous monitoring of the surface dose rates, as well as spectral information for neutrons and ions in restricted energy bands. The combination of measurements and validated model assessments has led to a reasonable understanding of the Martian surface radiation environment.
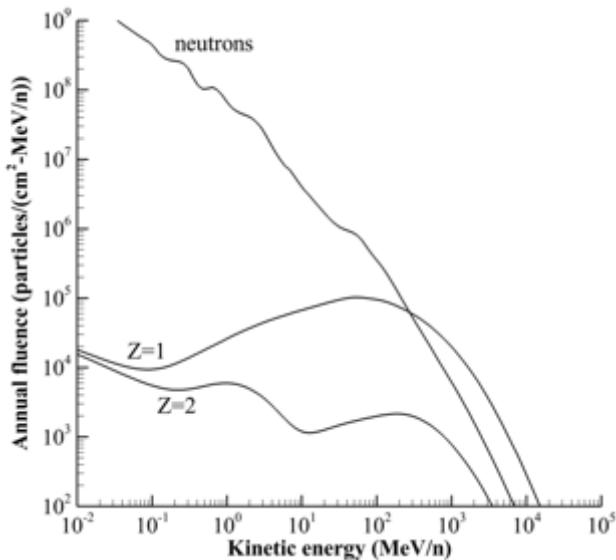
Physical interactions driving the albedo environments on the Moon and Mars are qualitatively similar. However, extra consideration must be given to the CO_2 atmosphere with thicknesses ranging from 15 to 25 g/cm^2. Atmospheric models such as the Mars Climate Database (MCD) [Forget et al. 1999, Millour et al. 2018] and Mars Global Reference Atmospheric Model (Mars-GRAM) [Justh et al. 2019] are able to characterize the total atmospheric thickness and density (g/cm^3) profile, taking into account the elevation dependence as well as seasonal and diurnal pressure variations. The atmospheric models are combined with radiation transport codes to propagate incoming free space radiation environments (SPE or GCR) down to the surface, accounting for interactions in the atmosphere and Martian regolith.

Matthia et al. [2016] published an initial comparison between combined models and MSLRAD data. A more expansive validation effort was subsequently completed in 2017 [Matthia et al. 2017], including various sensitivity tests and detailed model descriptions [Miller et al. 2017]. The models considered were able to reproduce measured dose rates to within 30%, although progress in GCR model development [Slaba and Whitman 2020] and particle transport codes [Slaba et al. 2020] have narrowed this margin, as shown in Figure 6.1.4.2-1. Comparison of individual particle spectra to measurements in restricted energy regions yielded a more complicated picture, especially for light ions. Consistent with gap analysis of Norbury et al. [2012], it was concluded that significant uncertainties remain in the nuclear physics models for light ion production. Ground-based measurements of relevant double-differential cross sections would be needed to close this gap.

Monthly silicon dose rates measured by MSLRAD and calculated with HZETRN2020 are shown in Figure 6.1.4.2-1. The model results are within 7% of measured values on average (–19% and 3% are the bounding differences). Based on the previous studies of Matthia et al. [2016, 2017], similar trends would be expected from Monte Carlo simulation codes despite the use of distinct nuclear interaction models. Figure 6.1.4.2-2 shows the simulated Mars surface spectra for neutrons and $Z = 1, 2$ ions associated with the 2009 solar minimum GCR environment. The neutron spectrum contains a more pronounced high-energy tail associated with forward-directed quasi-elastic production and heavy ion fragmentation within the CO_2 atmosphere. Compared with the lunar surface spectra shown in Figure 6.1.4.1-2, the Mars surface $Z = 1, 2$ ion spectra are somewhat attenuated at high energies and amplified at lower energies. These features are a consequence of atmospheric nuclear interactions.

Figure 6.1.4.2-1. Comparison of HZETRN2020 Model Predictions to Monthly MSLRAD Silicon Dose Rate Data (shaded region is measurement uncertainty about mean values shown as closed symbols)

Figure 6.1.4.2-2. Mars Surface Radiation Environment for Neutrons and Z = 1 and Z = 2 Ions associated with 2009 Solar Minimum GCR Environment (results calculated using BON2020 GCR model [Slaba and Whitman 2020] and HZETRN2020 [Slaba et al. 2020])
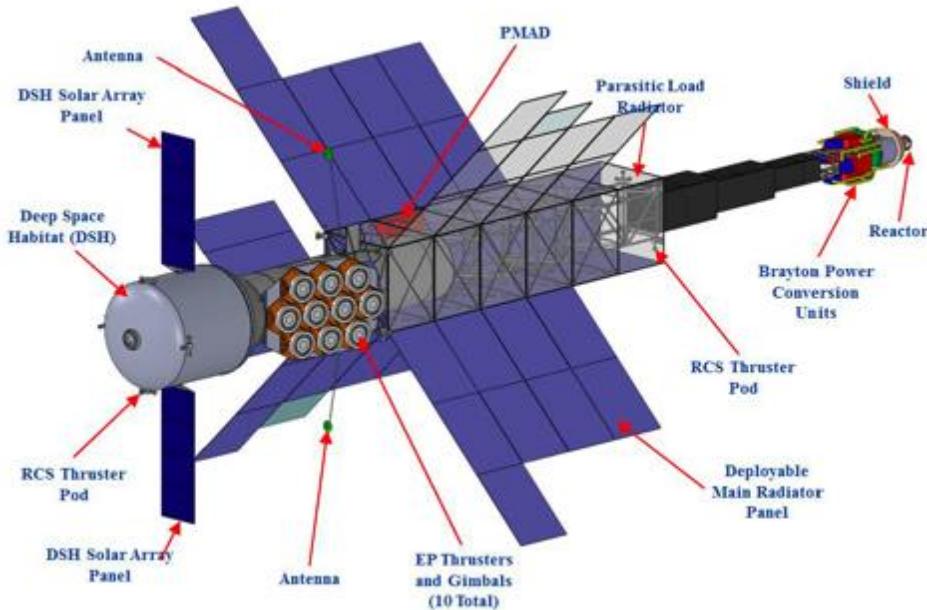
6.1.5   On-board Sources

The use of nuclear fission reactors for future crewed missions to Mars has been, and continues to be, examined by NASA as a potential power source for propulsion (i.e., NTP or NEP) and during surface operations [Gilland et al. 2011, Drake et al. 2014, Oleson et al. 2020, Mason et al. 2021]. While the nuclear reactor offers higher power than conventional methods (e.g., solar cells at >hundreds of kWe versus a few kWe), the effect of reactor radiation has to be mitigated for onboard electronics/materials, as well as for crew members. This is in addition to the natural radiation environments encountered by astronauts during missions beyond near Earth.

Reactor radiation is fundamentally different from space radiation in that they are neutral (neutrons and gammas), and the radiation source is confined in the reactor core rather than omnidirectional. A key challenge to be able to use the nuclear reactor in space missions is to shield the mixed neutron and gamma radiation field. The amount of radiation is dependent on reactor type, thermal power, and operating duration of the reactor. The need for shielding is driven by both electronic and materials tolerance, as well as human dose limits for crewed missions. Low-atomic-number materials (e.g., hydrogen, beryllium, lithium, and boron) provide efficient shielding for the neutron flux, while high-atomic-number materials (e.g., tungsten or depleted uranium) are efficient for shielding the gamma flux [Oleson et al. 2020]. Also, the distance of the electronics and crew from the reactor is an important factor to reduce the radiation dose. Like a point source, the radiation intensity would fall off ~$1/r^2$. A cone-shaped shadow shield covering a small portion of solid angle can be used to effectively attenuate the reactor radiation. Figure 6.1.5-1 illustrates the major components of an example Mars NEP vehicle where the reactor and the shadow shield are shown at the tip of the gigantic vehicle.

Detailed radiation dose computation from various types of nuclear reactors being considered for future crewed missions to Mars is beyond the scope of this study. The important message here is that shielding the reactor radiation is a key challenge. But being the localized source, the reactor radiation can be attenuated by using the distance and material shielding to any practically desired

level. Another important note is that the crew dose limit typically drives the reactor shield design and mass [Oleson et al. 2020].

Figure 6.1.5-1. Major Components of Example Mars NEP Vehicle
[reprinted from Figure 3-53, Drake and Watts, 2009]

> **F-12.** The use of nuclear fission reactors for future crewed missions to Mars has been and continues to be examined by NASA as a potential power source for propulsion (NTP or NEP) or for surface operation. Shielding the reactor radiation is a key challenge for NTP or NEP concepts. The crew dose limit will drive the reactor shield design and mass.

The two types of nuclear propulsion under consideration (NEP and NTP) are described in a National Academies report [National Academies, 2021]. The thermal power produced by the two systems is quite different. NTP requires ~500 megawatts (MW) to be produced by the reactor, while NEP requires only ~3 to 10 MW.

NASA is currently studying a transit vehicle concept that uses NEP. According to the NASA Mars Architecture Team (MAT), the concept is to park the vehicle in a 400 km by 400,000 km elliptical Earth orbit for a long period of testing before departure to Mars. When the vehicle returns from Mars, it will once again be parked in the same orbit. The vehicle's nuclear reactor will be operated during the transit to and from Mars. While parked at Earth, the reactor will also be operated to provide the thrust for orbit maintenance.

In 1975, the Soviet Union began a military ocean surveillance program that employed nuclear-reactor-powered radar satellites named US-A (Upravlyaemy Sputnik-Aktivniy) [Zak, 2021]. Between 1975 and 1988, the USSR orbited 36 of these satellites. They were placed in ~260-km orbits at ~65°°inclination. The nuclear reactors on these satellites produced 100 kW of thermal power [Wikipedia BES-5, 2021]. In 1987, two larger satellites in this series (kosmos 1818 and 1867) were launched into 790-km orbits at ~65°°inclination. These were equipped with Topaz I reactors, which produced 150 kW of thermal power [University of Wisconsin].

In 1980, NASA's Solar Maximum Mission (SMM) was launched. About 6 months after launch, the Gamma Ray Spectrometer (GRS) instrument observed an anomalous signal of 511 keV gamma rays [Share 1989]. These were found to come from positrons striking the SMM. The positrons were from artificial radiation belts created by the US-A satellites. GRS also observed US-A electrons and (when passing within 400 km of a US-A satellite) direct gamma ray emission from the satellite's reactor. The GRS data coming from these reactors often filled the satellite buffer, causing data collection to be suspended until the data could be dumped during a ground station pass.

Because the US-A reactors were designed to operate in space, they were placed on the end of a boom in front of the spacecraft. The reactor core is unshielded except in the direction of the body of the spacecraft. The nuclear fission fragments in the reactor emit gamma rays. These gamma rays escape from the core. Some of them undergo pair production near the surface of the core, and roughly half of the resulting electrons and positrons escape into space. These charged particles can become trapped in the Earth's magnetic field. The production and trapping of these electrons and positrons has been modeled in detail by Hones and Higbie [Hones and Higbie, 1989].

Because all but the last two Russian reactors were in very low Earth orbit, positrons and electrons emitted from the surface of the reactor could only become trapped if they were emitted perpendicular to the local geomagnetic field (i.e., in the local mirror plane for trapped radiation). Even then, most of the trapped electrons and positrons were quickly lost because they were trapped near the edge of the loss cone. Only those emitted when the satellites passed through the SAA region were injected onto complete drift shells, making it possible for them to drift around the Earth, creating a complete radiation belt. Even then, disturbances in the Earth's magnetic field could scatter these trapped particles into the loss cone.

The exceptions were the last two US-A satellites, kosmos 1818 and 1867, which carried Topaz I reactors. They carried a somewhat more powerful reactor, but more importantly, they were in higher altitude orbits. This allowed some of electrons and positrons emitted from the reactor to be injected onto complete drift shells around the entire orbit of the spacecraft. Moreover, many had higher mirror points, which allowed those to remain trapped for much longer. As a result, these two satellites produced much stronger signals in the GRS experiment.

Turning to the reactor in NEP on the Mars transit vehicle, a rough estimate of its ability to create artificial electron and positron radiation belts can be made based on artificial belts created by the US-A satellites. First, the NEP reactor will produce 30 to 100 times more energy than most of the US-A reactors and 20 to 67 times more than the Topaz I reactors. Second, the transit vehicle's orbital inclination will be in the range of +28.4° to –18.4°.This means that a much larger fraction of the electrons and positrons emitted by the reactor (when it is within the Earth's magnetosphere) will become trapped and will remain trapped for much longer than those from the Russian reactors. Also, unlike the US-A satellites, the trapped electrons and positrons from the transit vehicle reactor will fill most of the trapping region within the magnetosphere.

The transit vehicle will, however, spend most of its time outside the part of the magnetosphere where electrons and positrons can become trapped. When the transit vehicle is beyond 12 Earth radii (Re), the emitted electrons and positrons cannot complete a drift around the Earth and will be lost. Only when the transit vehicle is passing through the magnetotail can particles emitted from its reactor reach low altitudes in the polar regions and perhaps be scattered into the outer

radiation belt. The transit vehicle will have an orbital period of 10.81 days and will spend 0.49 days or 4.5% of each orbit inside 12 Re. Therefore, the numbers of electrons and positrons that become trapped in the magnetosphere will be greater than those injected by the US-A satellites, but they will be spread over many L-shells.

Therefore, the intensity of the electron and positron radiation belts created by the NEP reactor operated on the proposed orbit is not known. Since the next generation of gamma ray telescopes will be more sensitive than GRS, a careful assessment is needed to determine the impact the planned transit vehicle's orbit will have on future gamma ray astronomy missions.

> **F-13.** Nuclear reactors operated in the Earth's radiation belts have interfered with gamma ray astronomical observations in the past. It seems likely that a NEP system on the Mars transit vehicle operated within the Earth's magnetosphere will interfere with future gamma ray astronomy missions.

Considering the likelihood that a NEP system operated within the Earth's magnetosphere will interfere with future gamma ray astronomy missions, a careful study should be made of the electron and positron radiation belts this propulsion system can create, followed by an assessment of their impact on gamma ray astronomy. Since the plan is to park the transit vehicle in the same orbit after returning from Mars, the study should include the effects of the increased electron and positron emission due to the fission products that have built up in the reactor's core. The impact may be found to be unacceptable. In this case, NASA may need to explore other modes of operation for nuclear propulsion systems that will not interfere with gamma ray astronomical observations. It should be noted that nuclear thermal rockets have much more powerful reactors and if the concepts of operations (CONOPS) for NEP and NTP DRMs are similar, then NTP would be far more likely to cause interference.

6.1.6 Mission Exposure Summary

Table 6.1.6-1 gives daily exposure rates in terms of dose (milligrays (mGy)), dose equivalent (mSv), and effective dose (mSv) for various thickness of spherical aluminum shielding. Results are given for the 2009 solar minimum and 2001 solar maximum GCR environments in free space and on the surface of the Moon and Mars. These values are scaled by corresponding mission segment durations to yield the total mission exposures provided in Table 6.1.6-2.

Table 6.1.6-1. Daily Exposure within 0, 20, and 40 g/cm^2 Spherical Aluminum Shielding in Free Space and on Surface of Moon and Mars for Solar Minimum (2009) and Solar Maximum (2001) GCR Conditions

		Dose (mGy)[1]			Dose equivalent (mSv)[1,2]			Effective dose (mSv)[3]		
	g/cm^2 →	0	20	40	0	20	40	0	20	40
Solar max.	Free space	0.15	0.21	0.25	1.02	0.69	0.59	0.63	0.51	0.53
	Lunar surf.	0.10	0.12	0.14	0.58	0.39	0.33	0.38	0.31	0.32
	Mars surf.	0.12	0.13	0.15	0.30	0.28	0.30	0.28	0.30	0.32
Solar min.	Free space	0.46	0.52	0.56	2.85	1.50	1.22	1.46	1.09	1.07
	Lunar surf.	0.27	0.28	0.30	1.56	0.82	0.67	0.84	0.64	0.62
	Mars surf.	0.25	0.26	0.28	0.61	0.55	0.56	0.54	0.56	0.59

[1]Values have been calculated without the influence of any human tissue shielding and would be directly comparable to an area dosimeter placed at the center of the spherical shield.
[2]Dose equivalent is calculated using the ICRP 60 quality factor [ICRP 1991].
[3]Effective dose is calculated using the ICRP 60 quality factor [ICRP 1991] and ICRP 103 [ICRP 2007] tissue weights for a female astronaut [Slaba et al. 2010].

Table 6.1.6-2. Mission Exposures derived by Scaling Daily Values from Table 6.1.6-1 by Corresponding Mission Segment Durations

	Mission	Duration[4] (days)	Dose (mGy)[1]			Dose equivalent (mSv)[1,2]			Effective dose (mSv)[3]		
			0	20	40	0	20	40	0	20	40
Solar max.	Artemis II	10	1.5	2.1	2.5	10.2	6.9	5.9	6.3	5.1	5.3
	Artemis III	30	4.6	6.4	7.6	30.5	20.7	17.6	19.0	15.4	15.8
	Artemis III (surf)	23.5/6.5	4.2	5.8	6.9	27.7	18.7	16.0	17.4	14.1	14.4
	Gateway – 6 mo.	183	28	39	46	186	126	108	116	94	96
	Gateway – 12 mo.	365	56	78	92	372	252	215	232	188	192
	Mars DRM	621/40	99	137	163	644	440	377	405	331	339
	Mars DRM	840	128	178	213	855	580	494	533	432	442
Solar min.	Artemis II	10	4.6	5.2	5.6	28.5	15.0	12.2	14.6	10.9	10.7
	Artemis III	30	13.8	15.5	16.7	85.5	44.9	36.5	43.8	32.8	32.1
	Artemis III (surf)	23.5/6.5	12.6	14.0	15.0	77.1	40.5	33.0	39.8	29.9	29.2
	Gateway – 6 mo.	183	84	95	102	522	274	223	267	200	196
	Gateway – 12 mo.	365	168	189	203	1040	546	445	533	399	391
	Mars DRM	621/40	295	332	356	1795	950	779	929	702	688
	Mars DRM	840	386	434	466	2395	1256	1023	1228	918	899

[1]Values have been calculated without the influence of any human tissue shielding and would be directly comparable to an area dosimeter placed at the center of the spherical shield.
[2]Dose equivalent is calculated using the ICRP 60 quality factor [ICRP 1991].
[3]Effective dose is calculated using the ICRP 60 quality factor [ICRP 1991] and ICRP 103 [ICRP 2007] tissue weights for a female astronaut [Slaba et al. 2010].
[4]X/Y format denotes X days in free space and Y days on the surface.

The following summary statements can be made in the context of the old NASA radiation limit of 3% risk of exposure-induced death (REID) evaluated at a 95% confidence level (CL). Table 6.1.6-2 indicates that for solar maximum, assuming that the assigned crew has had no flight experience:

- All crew would qualify for Artemis missions.
- All crew would qualify for 6-month Gateway missions.
- Some crew would qualify for 12-month Gateway missions depending on age and sex.
- Some older male crew members may qualify for the Mars DRMs.

For solar minimum, assuming that the assigned crew has had no flight experience:

- All crew would qualify for Artemis missions.
- A majority of crew would qualify for 6-month Gateway missions (younger females would cross the risk limit).
- Some older male crew members may qualify for 12-month Gateway missions.
- No astronauts would qualify for the Mars DRMs.

With the newly proposed NASA permissible exposure limit (PEL) of 600-mSv, all crew without prior flight experience will qualify for all missions listed in the table, with the exception of Mars DRMs during solar minimum.

| F-14. | Radiation exposure on the lunar surface is about twice that of ISS. Lunar surface exposures depend more heavily on the exposure quantity (dose equivalent versus effective dose) and shielding. Taking these factors into account, Table 6.1.6-2 shows that the exposures range from 1.56 mSv/day (dose equivalent with no shielding at solar minimum) to 0.31 mSv/day (effective dose with 20 g/cm^2 shielding at solar maximum). |

| F-15. | Exposures during solar minimum are higher by roughly a factor of two than during solar maximum, depending on shielding. |

| F-16. | Mitigating the exposure from a reactor can be achieved by employing combinations of passive material shielding and distance. However, such mitigation strategies may lead to challenging and possibly unrealistic launch and in-flight requirements. |

| F-17. | During solar minimum, astronauts' radiation exposure during Mars DRMs will exceed lifetime allowed radiation exposure limits even if that limit is raised to 600 mSv as recommended by the National Academies study. |

6.2 Radiation Mitigation

6.2.1 Passive Shielding for Electronics/Materials from GCR and SPE

Spacecraft electronics and materials are also affected by radiation and need to be shielded accordingly, depending on their tolerance level to the space radiation. Long-term cumulative radiation effects that need to be considered are total ionizing dose (TID) and displacement

damage dose (DDD). For some active electronics parts, single event effects (SEEs) are another class of mechanisms, which can be destructive (e.g., single event burnout) or transient (e.g., single event upset).

Most of the TID and DDD on missions that are long enough to experience one or more SPEs will be from the SPE protons (the electrons and the heavier elements in SPEs do not make a significant contribution). Typical TID and DDD tolerance levels for commonly used spacecraft electronics and materials are much higher than the typical exposure requirement level for astronauts (e.g., >a few tens of grays (Gy) versus ~cGy); the shielding requirement tends to be much more lenient compared with the shielding requirement for humans. Furthermore, note the radiation effects on electronics and materials do not have to include radiation quality effects, which means the dose is strictly based on energy deposition in materials. Therefore, doses from GCR and solar energetic particle electrons and heavy ions are ignored in most cases for electronics/materials because of their low flux levels. Only the SPE protons have been included in the dose estimates for spacecraft electronics/materials, typically using conventional aluminum shielding. Work on developing innovative shielding approaches for solar protons has been limited (Atwell et al. 2013).

For SEEs, it depends on the linear energy transfer (LET) threshold that must be exceeded to cause the effect. SEEs can be induced by GCR or SPE. For human missions with a reasonably well-shielded spacecraft, the mass required to obtain a significant reduction in SEE rate in an internally situated component is usually unfeasibly large. Therefore, mitigation of SEEs relies primarily on strategies other than additional shielding (e.g., part selection, part design to improve hardness, etc.). On the other hand, the HZE (high atomic number, high energy) particles (especially for GCR heavy ions) cannot be shielded easily, and it has been common practice in the spacecraft design community not to worry about shielding them for SEEs. However, the SPE heavy ion spectra are softer than the GCR heavy ion spectra, and the shielding can be efficient.

F-18.	Only limited work has been done on innovative electronics radiation shielding for human exploration vehicles for solar protons for TID and DDD outcomes.

F-19.	For human-rated vehicles and habitats, the mass required to significantly reduce SEEs in electronics is typically unfeasibly large.

F-20.	SEE mitigations for human-rated missions are typically accomplished through means other than shielding, including but not limited to part selection and part design to improve hardness.

6.2.2   Crew Radiation Shielding

A significant component of the NASA strategy for mitigating radiation risks to crew is levying radiation requirements. The ionizing radiation requirements are covered by the OCHMO Level 1 requirements in NASA-STD-3001, Space Flight Human System Standards, Volume 1, "Crew Health," and Volume 2, "Human Factors, Habitability, and Environmental Health" [NASA-STD-3001, 2015, 2019]. Per the NASA standards requirements framework, detailed program-level ionizing radiation requirements were applied to the Orion Multi-Purpose Crew Vehicle (MPCV), Gateway, and Human Landing System (HLS) as follows:

- For the MPCV, 14 detailed radiation requirements are covered under the Human-Systems Integration Requirements (HSIR) for both intravehicular activity (IVA) and EVA operations.

- For Gateway (Level 2), the requirements were separated into four top-level requirements covered under the "GP Human System Requirements (HSR)" and 10 subsystem specification requirements covered under the "GP Subsystem Specification for Crew Health and Performance (CHP)."

- For the HLS (Level 3), four top-level requirements covered under the "HLS Program System Requirements Document (PSRD)." The PSRD requirements are considered as baseline for development of the commercial company specific requirements (e.g., "PaSRD Technical Authority Agreements SpaceX"). In addition, the HLS team has been tasked to add further fidelity to the HLS sustained phase requirements in preparation for a requirement study period following Option A. Therefore, the original four HLS ionizing radiation requirements have been consolidated in three detailed "HLS Program Sustained System Requirements," with two approved and one in the review process.

The Orion, Gateway, and HLS requirements are listed in full in Appendix B.

Table 6.2.2-1 shows the NASA PELs for non-cancer effects [NASA-STD-3001, 2015]. Of special note for the protection against acute radiation syndrome (ARS) is the 30-day limit for blood forming organs (BFO), which is meant to protect against depletion of the hematopoietic system. The limits on the lens of the eye are intended to prevent early onset of severe cataracts [NCRP 2000]. To limit the effects of late skin conditions (e.g., dermal atrophy, necrosis and fibrosis), the 30-day limit of 1,500 mGy-Eq has been set. This short-term limit for the skin is also considered protective of erythema and other acute skin effects.

Table 6.2.2-1. NASA PELs for Short-term and Career Non-cancer Effects

ORGAN	30 days (mGy-Eq)	1 year (mGy-Eq)	Career (mGy-Eq)
Lens	1000	2000	4000
Skin	1500	3000	6000
BFO	250	500	–
Heart	250	500	1000
CNS	500 mGy	1000 mGy	1500 mGy
CNS (Z ≥ 10)	–	100 mGy	250 mGy

6.2.2.1 SPE Shielding

NASA's strategy for crew protection from an SPE is to provide storm shelters (i.e., specific regions in the habitable volume of the vehicle to be preferentially shielded). Architectures with permanent shelters and reconfigurable shelters, where mass available within the vehicle or habitat is moved to create the shelter, have been considered. The repurposing of onboard supplies and consumables has been shown to be a viable strategy for both permanent and reconfigurable options and is the preferred design implementation compared with adding parasitic passive shielding (e.g., water). This is the approach used for Artemis.

This approach was based on four SPE protection requirements for storm shelters [Townsend et al. 2018]: (1) establish a blood-forming-organ limit of 250 mGy-Eq; (2) doses should be equivalent to the sum of the proton spectra during the October 1989 event series; (3) any necessary assembly of the protection system must be completed within 30 minutes of event

onset; and (4) astronaut radiation exposures must follow the ALARA (As Low As Reasonably Achievable) principle. Proposed requirement (1) was chosen because, of the acute PELs shown in Table 6.2.2-1, it is expected to drive shielding design. The choice of the October 1989 SPE spectrum was due to the high-energy nature of that model of the event. The radiation exposure to astronauts is dominated by the more penetrating high-energy particles, and this event is known to be the most intense set of events occurring within 30 days during the satellite era of measurements. The requirement that any protection system must be completed within 30 minutes of event onset is based on analysis showing that the probability of exceeding the 250 mGy-Eq to BFOs during that first 30 minutes is low [Townsend et al. 2018]. The requirement for ALARA traces back to NASA-STD-3001 (Volume 1) [NASA-STD-3001, 2015]. ALARA minimized the risk of stochastic effects (e.g., cancer) for which there is no threshold dose.

An SPE storm shelter design by Simon et al. [2014] considered two designs for an SPE storm shelter: 1) an option where water could be diverted to shield the crew within the quarters, and 2) a reconfigurable option where stowage within the vehicle could be reconfigured to build a shelter. The addition of water shielding was also investigated to determine the amount of shielding needed to lower crew exposure by 50%. For a small amount of additional water mass (1.308 tonne), the exposure from an SPE could be lowered by 50% at a 68% confidence level for the configuration considered, depending on the spectrum and size of the SPE. Simon et al. noted that there was significant room for improvement in optimization of onboard materials to lower the exposure further, and zero additional mass solutions may exist for the 50% reduction in exposure.

SPE storm shelter design should be considered early in the design lifecycle to optimize available mass for the shelter and ensure minimal (or ideally zero) additional mass solutions.

F-21. SPEs are considered mitigated as a health risk with adequate shielding.

F-22. Zero additional mass solutions are possible for SPE storm shelters within a vehicle or habitat.

F-23. While shielding mass and geometrical distribution are the primary drivers of protection, preferential use of hydrogen-rich, low-atomic-charge materials in the design of storm shelters improves shielding properties.

6.2.2.2 GCR Shielding

As discussed in Section 6.1.1, GCRs are a low-intensity, high-energy radiation source of charged particles. Therefore, GCRs are not typically a concern for the short-term PELs discussed above. GCRs, however, are a concern for the LTH of crew on long-duration missions to Mars that last many years. NASA has a PEL that limits the career exposure of astronauts, *"Planned career exposure to ionizing radiation shall not exceed 3 percent Risk of Exposure-Induced Death (REID) for cancer mortality at a 95 percent confidence level to limit the cumulative effective dose (in units of Sievert) received by an astronaut throughout his or her career."* This PEL is the limiting factor for crew exposure during long-term exploration missions. Shielding is the only viable strategy for crew protection from GCR, and this must be an integral part of the spacecraft design from the beginning for at least the crew habitat areas where the crew spend the majority of their time.

Recreating the GCR environment on Earth is extremely difficult due to constraints on particle accelerators [Simonsen et al. 2020, Wilson et al. 1991]. As an alternate, NASA has invested in models of the GCR space radiation environment, its interaction with spacecraft and the crew [Wilson et al. 1995; Slaba et al. 2010; Norman et al. 2013; Wilson et al. 2014]. The radiation transport models are validated and verified where possible, with many benchmarks against Monte Carlo codes, which have been extensively validated against experimental data [Heinbockel et al. 2011; Slaba et al. 2011; Slaba et al. 2013; Norman et al. 2013; Slaba et al. 2017; Warner et al. 2018].

Aluminum and its alloys are a typical choice used in the construction of spacecraft and has been the first choice to provide radiation shielding material. However, due to the high energies and composite nature of the ions comprising the GCRs, material shielding at spacecraft thicknesses is of limited utility in reducing crew exposure. The production of secondary nuclear fragments from the target nuclei in the shielding material is an important factor. Slaba et al. [2017] showed that for aluminum shields a local minimum may exist in the dose equivalent versus shielding thickness curve for the GCR environment.

For the same areal density of material, materials that contain less complex nuclei (smaller atomic number and mass number) are better at attenuating the GCR environment [Wilson et al. 1991]. Materials with high hydrogen content are superior shielding materials because the number of electrons per unit mass is the largest for hydrogen. For hydrogenous materials, Slaba et al. [2017] considered polyethylene and, contrary to the aluminum case, found flattening of the dose equivalent versus shielding thickness curve with enough polyethylene shielding thickness. These two results, when considered together, indicate that for a complex space vehicle, given the multitude of different materials it contains, there may be a shielding thickness beyond which either the dose equivalent increases or adding more mass does not provide any added benefit. This implies that there may be a practical limit to what traditional, passive GCR shielding can achieve for an exploration vehicle. Inclusion of radiation protection considerations in early spacecraft architecture trades and throughtout the design is required to optimize radiation protection without other system constraints.

F-24.	For a real vehicle, taking into account all the mass and varied materials, improvements in human exposure within the vehicle are typically in the region of diminishing returns where very large additional thickness of shielding are needed to make moderate improvements in reducing exposure.

F-25.	Hydrogen-rich, low-atomic-charge materials are the shielding material of choice to reduce crew exposure to GCRs to manageable levels.

F-26.	The amount of shielding mass required to provide a given benefit in exposure reduction is highly dependent on assumed spacecraft and shield architecture.

6.2.3 Active Shielding

Active shielding deflects high-energy particles through electrostatic, magnetic, or combined electrostatic/magnetic fields generated on the spacecraft and redirects the incoming GCR away from the crew habitat. There have been several concepts for space vehicles with magnetic shielding. NASA Institute for Advanced Concepts (NIAC) studies include two configurations in

"Active Radiation Shield for Space Exploration Missions" by Battiston et al. [2011] and one configuration with excursions in "Magnet Architectures and Active Radiation Shielding" by Westover et al. [2020]. A review paper examining each, along with a modified version of ESA concepts, was published by Ambroglini et al. [2016]. There have been periodic reviews of the status of technologies for active shielding (e.g., [Townsend 2005]).

There are many technological challenges common to both electrostatic and magnetic shielding approaches. The omnidirectional nature of the space environment means active shielding concepts must provide nearly spherical coverage to deflect GCR particles with energies in the GeV/nucleon range. Structural components of the spacecraft and shield generator must be able to withstand large forces, particularly against loss of field symmetry to balance the forces (e.g., in the startup and shutdown or when individual elements degrade or fail).

Power is a significant challenge for electrostatic concepts to maintain high positive voltage (or electric field) to repel/deflect high-energy ions in the presence of the space plasma electrons. The same field that repels positive charged ions will continuously attract the plasma electrons, which will work against the potential. Therefore, electrostatic systems will require a continuous MV-class power source to maintain the positive voltage. There are no estimates of the system mass for a configuration employing electrostatic systems to reduce exposure inside a shielded habitat.

Many magnetic shielding approaches rely on currents in superconducting coils to produce the large fields with minimal power to maintain the current. However, the fields contain stored energy that has to be applied initially and when the system unexpectedly shuts down or is turned off. The energy density of a magnetic field is $B^2/2\mu_0$. For B in tesla, and with $\mu_0 = 4\pi \times 10^{-7}$ H/m, the energy density is $0.4\,B^2$ megajoules per cubic meter (MJ/m^3). The energy contained inside cylindrical superconducting solenoids of vehicle sizes ranges from a few to several tens of gigajoules (GJ). If the superconductor "quenches" or loses its superconducting character, then the system must be designed to manage the sudden thermal load from resistive heating.

The general properties of two magnetic shielding concepts are summarized in Table 6.2.3-1.

Table 6.2.3-1. Comparison of Two Magnetic Shielding Concepts

Concept	Estimated Mass of Active Shielding Components (metric ton)	Magnetic Field Strength Times Field Thickness (Tm)	Shielded Habitat Dimensions (m)
Westover Multiple solenoid coils surrounding a central habitat (6-1 solenoid design)	a) 36[*] b) 72	a) 8 Tm b) 20 Tm	Cylindrical 10 m long by 6 m diameter
Ambroglini SR2S continuous coil toroid**	a) 96[#] b) 137[#]	a) 8 Tm b) 23 Tm	Cylindrical 6 m long by 4.5 m diameter

* Extracting this mass from the report is difficult, as different sections written independently have various mass estimates, ranging up to 53 Mt when including a 35% mass margin and compensation coils to reduce the magnetic field in the habitat. Similar fidelity for the 20 Tm is not readily apparent. It is not clear which elements or mass margins are included in the Ambroglini mass estimates.

** Space Radiation Superconducting Shield (SR2S)

The reported shield masses refer to the mass in the Geant4 simulation. Actual mass for engineering design will likely be larger.

The dose reduction provided by active shielding is configuration specific and difficult to quantify from the available publications. The studies cited above generally applied Monte Carlo particle tracking techniques (e.g., Geant3/Geant4) with the flux of representative ions and energies converted to dose measures. Significantly, the habitats are modeled as thin-walled hollow cylinders, without internal structure. This simplification in particular makes it difficult to assess the dose reduction with/without active shielding. When comparing doses of similar configurations, Ambroglini found dose reductions (field on versus field off) from ~20% at 8 Tesla-meters (Tm) (96 *metric tons* of magnetic shielding components) to 45% at 23 Tm (137 *metric tons* of magnetic shielding) in their SR2S continuous-coil toroid study; 23 Tm represents the technological limit of the present-day high-temperature superconductors (HTSC) and potentially tens of GJ of stored energy.

The Westover study concluded that *"the configuration studied here does not offer dramatic improvements over passive shielding"* and *"further development of enabling technologies such as superconductor current densities and lighter weight structural materials are needed to allow configurations that would offer significant improvements over passive shielding."*

F-27. In principle, sufficiently intense magnetic shielding or electrostatic shielding concepts could reduce radiation exposure on long-duration missions by deflecting high-energy GCR particles away from a crewed vehicle.

F-28. Active shielding concepts studied to date within the limits of current technology do not offer dramatic improvement over passive shielding in terms of mass and power requirements and bring new risks in the case of system failure.

F-29. There is no mature electrostatic shielding design available to estimate even a rough comparison with passive shielding.

O-1. With the present-day HTSC technology, dose reduction from magnetic shielding can be up to ~45% with 23 Tm (field on versus field off). The total shield mass in the simulation is 137 metric tons, and the stored energy in the shield exceeds 15 GJ. The actual engineering design mass can be (much) larger.

O-2. Magnetic shielding concepts encounter many operational, technical, and design challenges, to include managing the thermal energy release of potential quenching of the superconducting coils and restoring the magnetic fields after a shutdown of the current (planned or otherwise).

6.3 Mitigating Space Radiation Impacts on Space Operations

Mitigating harmful effects of the space radiation environment on the health of flight crews is a multifaced process. NASA typically starts by establishing radiation exposure requirements for flight crews and then designs vehicle shielding and mission operations that will keep crew exposure levels below the required limits. Multiple space weather parameters are monitored by NASA in support of mission operations to determine the current state of the space radiation environment and for use as inputs to dose projection models to forecast changes in the radiation environments that could impact crew health and mission operations.

This section describes two important aspects of the radiation mitigation process. Section 6.3.1 summarizes the radiation mitigation CONOPS developed by NASA establishing the data sources and instrumentation used to characterize the space environment during flight operations. The section also describes methods for using the data as input to flight rules and operational procedures used to protect crew from harmful effects of radiation during periods when the space radiation environment is enhanced above nominal background levels. Section 6.3.2 describes the spacecraft and instrumentation that provide general space environment data and, in particular, the space radiation data required to protect flight crews from the space radiation environment. Modeling of the space radiation environment is increasingly being used to more fully utilize the measurements and improve the nowcast capabilities for specifying the state of the radiation environment of importance to crew health and to forecast the future state of the radiation environment. Current models and tools and potential future developments to improve forecast techniques are also discussed in Section 6.3.2.

6.3.1 From ISS to Artemis Operations

As NASA's space exploration goals extend from support of operations at the ISS in LEO to include new programs with orbital and surface operations on the Moon and Mars, the operational paradigm must also transition to meet the needs of crew health and safety in the new environments. In the case of the space radiation environment, the impact of both the persistent GCR background and the episodic SPEs must be monitored to effectively maintain crew radiation exposure to levels as low as reasonably achievable.

NASA operational experience in protecting crews from space radiation hazards started with the earliest manned spaceflight missions and continued through the Apollo, Space Shuttle, and ISS Programs. SRAG at Johnson Space Center (JSC) is NASA's organization responsible for ensuring that the radiation exposure received by astronauts remains below established safety limits. To fulfill this responsibility, SRAG provides radiological support during missions, preflight and EVA crew exposure protections, evaluation of radiological safety with respect to

crew exposure to radioisotopes onboard spacecraft, comprehensive crew exposure modeling, and development and operation of radiation instruments to characterize and quantify the radiation environment inside and outside the spacecraft. In addition, the long history of the space program has been a benefit to mission planning, influencing advancements in space weather modeling methods, monitoring capabilities, and vehicle shielding concepts. These technologies have been applied to the next generation of space travel through the development of new instrumentation, updated vehicle design, and innovative tools for console operations.

Through application of these combined assets, SRAG developed an updated concept of operations for radiation protection of crews that will be used by NASA's Artemis Program during upcoming exploration missions to the Moon, including the Earth/Moon transit environments and the orbital and surface environments in cislunar space. Details of this plan are described in Appendix C. This appendix describes how the new Artemis radiation protection plans are based on the operational experience in protecting ISS crews from the LEO radiation environment and how LEO radiation mitigation techniques have been evolved and improved for use in protecting crews on Artemis lunar missions and the impacts of the radiation constraints on operations. The Artemis radiation mitigation concept of operations is the current state of the art in protecting flight crews from potential health risks due to the space radiation environment.

The human/system ionizing radiation requirements for Artemis mission elements include a number of requirements for measurements needed to protect the crew from radiation. The more challenging requirements are:

- **Charged-particle monitoring:** The external fluence of particles with $Z < 3$ with energies between 30 and 300 MeV/nuc, particles with $3 \leq Z \leq 26$ with energies between 100 and 400 MeV/nuc, and the integral fluence of these particles at higher energies should be continuously measured and recorded as a function of energy and time with a free space full-angle field of view of 65 degrees or greater.

- **Radiation Flux Monitoring in Space Suits:** An omnidirectional detector must continuously measure and record the flux from charged particles with an LET of 0.2 to 300 keV/micrometer, as a function of time, at two shielding depths: <0.5 g cm^2 water equivalent and 3.0 g cm^{-2} water equivalent. The reason for the smaller depth is that any SPEs have intense fluxes at low energies that are capable of penetrating the suit and delivering a dose to the skin or eyes that exceeds the crew exposure limits.

The procedures for radiation protection of space crews have not yet been written for the lunar or Mars missions. Based on the procedures used for missions to the ISS, some expectations can be developed for the instrumentation needed for crew safety on future deep space missions. Knowledge (and forecasts) will be required for the occurrence of low SPEs (LSPEs) that deliver flux that is >10 protons/cm2.s-1.ster-1 (called a particle flux unit or PFU) at energies >10 MeV and energetic SPEs (ESPEs) that deliver >1 PFU of protons at energies >100 MeV. This is because proton flux data from LSPEs and ESPEs will be used to forecast the total crew dose and will play a role in the decisions to move the crew to a shielded location during the more intense parts of the event to minimize the crew dose. It will take at least 30 minutes to get the crew into a shielded location. Moreover, estimating the crew dose from an event will require a forecast of the duration of the event and the time-intensity profile of the event. Most of the relevant observational gaps arise from sparse spatial/temporal/spectral coverage rather than lack of measurement capability. They can be addressed with current technology and capabilities.

While the Artemis radiation mitigation CONOPS were developed for the near-term lunar missions, the same GCR and SPE environments will be present during Mars missions. In a similar manner to how the radiation protection procedures developed for protecting ISS crews have been used as the basis for developing the new Artemis radiation mitigation CONOPS, the Artemis CONOPS can be used as the basis for developing space radiation mitigation techniques for use during future Mars exploration programs. Mars exploration programs will benefit from testing the Artemis radiation mitigation techniques during the lunar exploration missions with near-term opportunities to demonstrate which strategies work and identify areas where improvements are necessary before taking on the commitment of long-duration missions to Mars.

6.3.2 Space Environment Measurements and Modeling

This section focuses on the measurements (including the instrumentation and missions needed to provide the measurements) and the forecasting models needed to manage the radiation exposure of space crews on missions beyond LEO. While there are many missions and instruments producing relevant measurements, the focus here is mainly on instrumentation and missions that provide data on a time scale that can be used to manage crew radiation exposure.

Section 6.3.2 is organized as follows. Section 6.3.2.1 discusses existing or planned missions and instruments, and the measurements taken to characterize the state of the space radiation environment. Recommendations for missions, instrumentation, measurements, and forecast models that are relevant to missions beyond LEO have been provided in recent studies. This section references the relevant findings, observations, and recommendations from these studies (listed in Appendix E) and identifies any gaps that must be addressed for human missions to Mars. Section 6.3.2.2 discusses forecast models.

6.3.2.1 Missions, Instruments, and Measurements

A number of existing missions and instruments currently provide space environment data to the US and international space weather systems. Many of these systems will continue to contribute to the protection of space crews on missions beyond LEO; these systems are discussed in the studies listed in Appendix E.

Of the instruments on existing missions that produce the data used in real time to manage the radiation exposures of space crews, all provide sufficiently accurate data. Some space weather nowcast and forecast systems use both real-time and archival data from the Solar and Galactic Proton Sensor (SGPS) detectors on the Geostationary Operational Environmental Satellite (GOES)-R series satellites. The detectors on GOES-16 have been shown to give inconsistent measurements. Some of the inconsistencies are quite large. The National Oceanic and Atmospheric Administration (NOAA) has completed final validation of the SGPS suites on GOES-16, but only one of the known instrumental issues has been corrected. Another does not need correction, and a third cannot be corrected due to a lack of solar proton data >100 MeV because there have been no large SPEs since these satellites were launched. The archival data in the National Centers for Environmental Information (NCEI) since October 2020 have been corrected for the first issue. When sufficient high energy solar proton data have been collected, the remaining GOES-16 issue will be corrected, and the same corrections will be found and applied to GOES-17, allowing it to reach final validation.

6.3.2.1.1 *Missions and Instruments Planned or in Development to Support Missions Beyond LEO*

Several new space environment missions and instrument systems are currently in the planning phase or are being actively developed for upcoming flights; these will be useful for characterizing aspects of the space environment of relevance to the space radiation problem for flight crews:

- **Space Weather Follow-On (SWFO) L1 Mission:** NOAA's SWFO-L1 mission will be launched to L1 in February 2025. It will use a suite of instruments to make in-situ measurements of the solar wind thermal plasma and magnetic field and will carry a Compact Coronagraph (CCOR) instrument to detect CMEs and provide data on their size, mass, speed and direction. As with the Solar and Heliospheric Observatory (SOHO) satellite's Large Angle and Spectrometric Coronagraph (LASCO), CCOR will provide essential data for running the WSA-Enlil solar wind model, which has been operational at the Space Weather Prediction Center (SWPC) since 2011. The in-situ measurements of the solar wind speed and interplanetary magnetic field provide 15- to 60-minute warnings of a possible enhancement in solar energetic particle flux associated with the arrival of an interplanetary CME (ICME). Low-latency data will be generated for operational use.

- **L5 Space Weather Mission:** The ESA Space Situational Awareness (SSA) Lagrange mission to L5 is to be launched in 2027. L5 is the fifth Sun-Earth Lagrange point located at 1 AU and trailing Earth by 60 degrees. Eight months after launch, it will be commissioned while it is still near L1. Thirty-eight months later it will be placed in orbit of L5, where it is expected to be operational for at least 5 years. This mission will carry a CCOR, a heliospheric imager (HI), an extreme ultraviolet (EUV) imager, an X-ray monitor, a vector magnetograph, and a particle spectrometer. From its location at L5, it can observe active regions that have not yet rotated onto the solar disk, as seen from Earth, thus providing advanced warning of the potential for severe space weather. Its CCOR, together with those on SWFO-L1 and GOES U, will provide a stereo view of CMEs. Low-latency data will be generated for operational use.

- **Interstellar Mapping and Acceleration Probe (IMAP):** NASA's IMAP mission will be co-manifested with SWFO-L1 on a launch in February 2025. . It will carry instruments to measure the solar wind, suprathermal ions, relativistic electrons, and a three-axis magnetometer. Low-latency data will be generated for space weather research and operational use

- **Aditya at L1:** The Indian Space Research Organization (ISRO)'s Aditya spacecraft is projected for launch in January 2022. It is an operational mission with a planned 3-year lifetime. It will carry a coronagraph, an ultraviolet (UV) imager, X-ray spectrometers, and a magnetometer. It will also make solar wind measurements. SWPC plans to use data from Aditya. Low-latency data will not be generated.

- **Heliophysics Environmental and Radiation Measurement Experiment Suite (HERMES) on Gateway:** NASA's HERMES will measure electrons up to 9 MeV and ions up to 190 MeV. The data from HERMES will be returned only with a high latency so the data will not be useful for managing the radiation exposure of the crew, but it may be used after a radiation exposure has occurred to estimate organ doses. Low-latency data will not be generated.

- **European Radiation Sensor Array (ERSA) on Gateway:** ESA's ERSA will measure energetic particles from the Sun, GCRs, neutrons, and ions around the Gateway. ERSA also carries the European Active Dosimeter, which measures the energy that would be deposited by radiation in living tissue in order to understand human radiation exposure. Like HERMES, the ERSA data will be returned only with a high latency, but the data may be used for post-exposure assessments.

- **Polarimeter to Unify the Corona and Heliosphere (PUNCH) in Sun-synchronous LEO:** This NASA mission (projected for a 2023 launch) consists of a constellation of four small satellites. It will produce three-dimensional images of the solar corona through its transition into the solar wind. NOAA is expecting it to have significant operational benefits. Low-latency data will be generated for operational use.

Instruments that are operationally useful (in contrast to basic science measurements that do not support flight operations) for measuring parameters of relevance to protect flight crews from the space environment, in general, and space radiation in particular, are listed in Table 6.3.2.1-1. The table includes instruments that are currently deployed and returning data as well as planned instruments for future deployments.

Table 6.3.2.1-1. Instruments for Measuring Parameters of Relevance to Protect Flight Crews from Space Environments, in Particular Space Radiation

Measurement	Instrument	Existing instruments					Planned Instruments						Purpose
		GOES-R	SOHO	ACE	DSCOVR	SDO	GOES-U	Lagrange	SWFO-L1	IMAP	Aditya	Punch	
In Situ magnetic field	Magnetometer			MAG						magnetometer	magnetometer		ICME Detection
Photospheric magnetic field	Magnetograph					HMI		Magnetograph					All-Clear Forecast
Type II and III noise	Radio detector												Particle Acceleraton
UV Imager	UV imager	SUVI	EIT			AIA	SUVI	EUV Imager			UV imager		Flare Locaton
EUV monior	EUV Sensor	EXIS					EXIS						Flare Detection
x-ray flux	X-ray Sensor	EXIS				STIX	EXIS	X-ray Monitor			x-ray spec.		Flare Detection
Solar Electron Flux	Electron Telescope		EPHIN	EPAM						HIT			SPE Warning
suprathermal protons	Electrostatic Analysers+TOF		CELIAS	EPAM						SWAPI, CODICE			Warning of Shock Arrival
Proton Flux	Proton Telescope	SGPS	ERNE + EPHIN				SGPS						SPE Onset
Alpha Particle Flux	Helium Telescope	EHIS	ERNE + EPHIN				EHIS						Dose Computation
Heavy Ion Flux	Heavy Ion Telescope	EHIS	ERNE				EHIS						Dose Computation
Solar Wind density and speed	Electrostatic Analysers+TOF+ Plasma Probe		CELIAS/ MTOF	SWEPAM	PlasMag				SWiPS	SW instrument			ICME Cetection
CME images	Coronagraph		LASCO + UVCS				CCOR	CCOR	CCOR		coronagraph		CME Imaging
Helosphereic Imager								HI					ICME Imaging
Solar Corona Imager												Solar Corona Imager	Imaging SW Structures

Note: The SOHO spacecraft is not a reliable source of operationally useful low latency data

HMI (Helioseismic And Magnetic Imager); SUVI (Solar Ultraviolet Imager); EIT (Extreme Ultraviolet Imaging Telescope); EXIS (Extreme Ultraviolet and X-ray Irradiance Sensor); ERNE (Energetic and Relativistic Nuclei and Electron); EPHIN (Electron, Proton, and Helium Instrument); SGPS (Solar and Galactic Proton Sensor); EHIS (Energetic Heavy Ion Sensor);; CELIAS (Charge, Element, and Isotope Analysis System); MTOF (Mass Time Of Flight); MAG (MAGnetic field experiment); HIT (High-energy Ion Telescope); AIA (Atmospheric Imaging Assembly); STIX (Spectrometer Telescope for Imaging X-rays); SWEPAM (Solar Wind Electron Proton Alpha Monitor); EPAM (Electron, Proton, and Alpha Monitor); SWAPI (Solar Wind and Pickup Ion); CoDICE (Compact Dual Ion Composition Experiment); PlasMag (Plasma Magnetometer); SWiPS (Solar Wind Plasma Sensor); LASCO (Large Angle Spectroscopic Coronagraph); UVCS (Ultraviolet Coronograph Spectrometer); CCOR (Compact Coronagraph); HI (Heliospheric Imager)
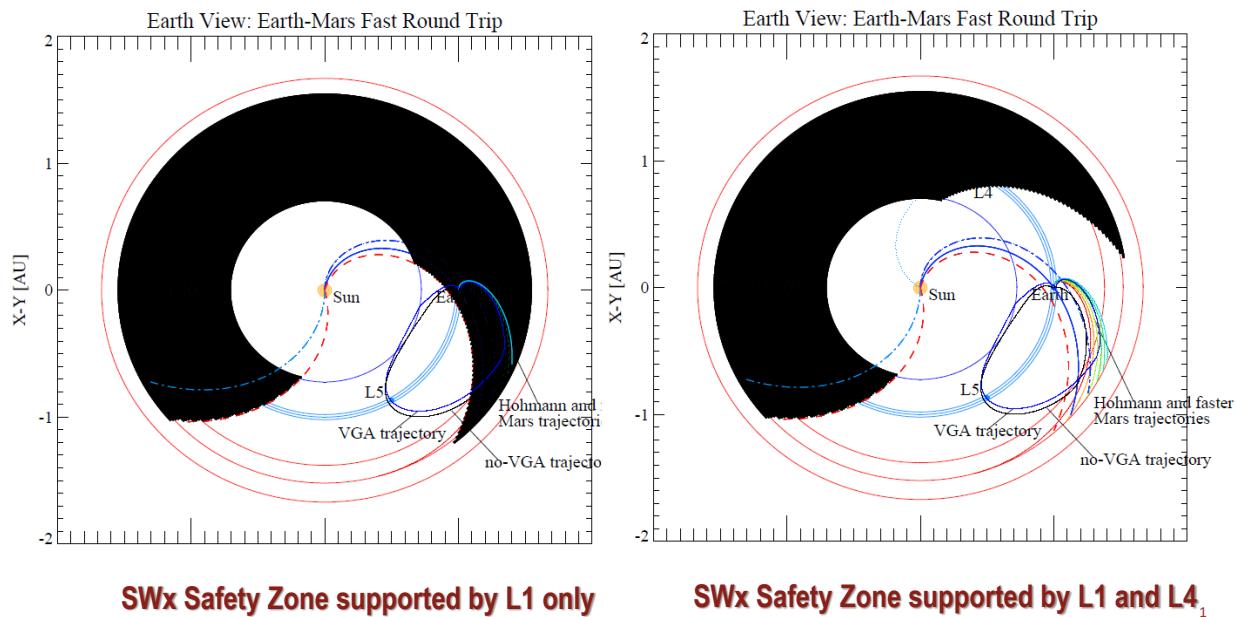
6.3.2.1.2   Recommendations for future Space Weather Missions and Instruments

NASA and other federal agencies have recently completed several studies that describe the relevant space weather parameters that must be measured to protect flight crews from the space radiation environment, as well as the assets in terms of missions and instrumentation required to obtain the necessary data. Rather than repeating the work in this assessment that is already documented in existing reports, the assessment team chose to review the studies and summarize the findings and recommendations relevant to this work. The summaries are given in Appendix E, with only the most important findings and recommendations included there. Appendix F lists all the documents reviewed by the team. The recommendations therein enhance the foundational knowledge base to better understand the space radiation environment.

After reviewing these previous studies, it is generally agreed that increased capabilities for space weather monitoring and modeling are required to give sufficient early warning for explorations beyond LEO and especially for Mars missions both in transit and at Mars. This study envisions that strategic placement of additional monitoring assets in a "solar necklace" formation around the Sun (measuring solar activity and the upstream solar wind) can significantly improve space weather early warning capability. The highest priority for placement of such assets are proposed to be at the Sun-Earth L1, L4, and L5 Lagrange points.

As discussed in the previous section, NOAA's SWFO-L1 mission to L1 is planned for launch in 2025, and ESA's L5 Space Weather mission is planned for launch in 2027 . Another important radiation monitoring asset would be a mission located at Sun-Earth L4. A magnetograph on a satellite located at Sun-Earth L4 would provide magnetic field data within 30 degrees of the west limb of the Sun on the side visible from Earth and extending 30 degrees behind the west limb as well. This information is essential for making all-clear forecasts of potential eruptive solar activity, including CMEs and SPEs based on magnetic field proxy measurements as active regions move between 60 and 120 degrees west solar longitude. All-clear and event probability forecasts for flares, CME, and SPEs provide adequate warnings for managing crew activities that are particularly exposed to the radiation environment (e.g., EVAs). A Sun-Earth L4 platform will also provide observations of flares that occur behind the west limb. Without such a mission, a flare occurring behind the west limb may go undetected, and the resulting SPE will arrive without warning in cislunar space. There would be no advance warning for the crew, so they would be exposed to radiation from the SPE, accumulating radiation dose during the time required to take shelter. If the flare spawns a CME, it will be observed by SWFO-L1. This will allow the crew to be alerted of a probable impending SPE, albeit with some delay. Figure 6.3.2.1.2-1 shows the area in the ecliptic plane to which an all-clear forecast applies with respect to observations solely from L1 or from L1 and L4 combined. Detailed assumptions that were the basis for the calculations in the figure are given in Posner [2021] and Posner et al. [2021].

Fast Mars Round Trips and SWx Safety Zones

Figure 6.3.2.1.2-1. SWx Safety Zone based on Earthbound Observations (left) and Extended SWx Safety Zone (right) (Figure courtesy of Noble Hatten, NASA Goddard Space Flight Center (GSFC)) Most SPE forecasting models depend on direct flare observations and/or magnetograph observations. Such models face limitations concerning solar activity at or behind the W limb of the Sun that may cause significant threat of SPE exposure for astronauts in the Earth/Moon system [Posner et al. 2021]. The SWx Safety Zone based on Earthbound observations is shown on the left-hand side as the unshaded region. The region can be extended by placement of a suitable Earth-Sun L4 mission that extends observations of the Sun far beyond the W limb as seen from Earth [Posner 2021]. This extended SWx safety zone is shown on the right and includes much of the short-term Earth-Mars round trip trajectory (trajectory information courtesy of Noble Hatten, NASA GSFC).

Furthermore, this assessment identified an additional capability gap in space weather monitoring and modeling that if filled in the near future could reduce the risk to crews on long-duration missions to Mars (both in transit and at Mars). Placing monitoring assets at Sun-Mars L1 [Posner and Strauss 2020] and Sun-Mars L4 and/or L5 will enable advanced early warning forecasting capabilities for Mars missions. The Sun-Mars L4/L5 will also serve the dual purpose of filling the 2-week communication blackout period with the crew on the surface of Mars (or in orbit around Mars) when the Earth line of sight to Mars is behind or close to the Sun, a phenomenon that occurs every 2 years.

> **S-1.** Additional space weather monitoring assets (i.e., solar coronagraph and particle detector suites) at Sun-Earth Lagrange point L4 and Sun-Mars L1 and L4/L5 can enable sufficient early warnings for Mars missions during transit and stay. The Sun-Mars L4/L5 assets would also provide a communications relay solution for when the Earth line of sight to Mars is behind or close to the Sun, leading to a 2-week blackout period every 2 years.

6.3.2.2 Forecast Models

6.3.2.2.1 *Existing Forecasting Capabilities*

The NOAA SWPC forecast model uses deterministic formulas and human judgment. The input parameters for this model are time-integrated soft X-ray flux, peak soft X-ray flux, occurrence or nonoccurrence of metric radio Type II and Type IV sweeps, and the location of the associated flare. The X-ray event parameters are derived from 1-minute averages of soft X-ray flux using the GOES Extreme Ultraviolet and X-ray Irradiance Sensors (EXIS). The solar flare location is derived either from ground-based solar observatories using hydrogen-alpha telescopes or from spaced-based instruments such as the GOES Solar Ultraviolet Imager (SUVI) or the SOHO EIT. Based on the statistical information, the model provides forecasters with a probability for a proton event, a prediction for the maximum flux at 10 MeV, and the time of maximum of the proton event. SWPC does not use information about CMEs because of the latency of the LASCO data coming from SOHO (i.e. by the time the CME images are available for analysis, the SPE onset has occurred or is imminent). Sheeley et al. [1983] have shown a clear relationship between the duration of an X-ray event and the likelihood for a CME.

Unlike LEO missions, deep space missions will have no protection from the Earth's geomagnetic field, and there will be limited communication capability between the crew and the ground. Continuous monitoring and prediction of the space weather environment will be needed so NASA can take corrective action to minimize crew dose. SRAG's CONOPS for these missions will transition from one based on nowcasting to one based on forecasts that provide the flight control team the time and information needed for responding to a space weather event.

SRAG and the Community Coordinated Modeling Center (CCMC) have partnered to create the Integrated Solar Energetic Proton Event Alert/Warning System (ISEP) at GSFC to bring state-of-the-art space weather models from research and development to operational use at NASA. These models will have a user interface that will allow the SRAG console operator to view and compare the results from several different models simultaneously and provide feedback to the CCMC that can be used to improve the models. The forecast models, as they exist today, do not meet SRAG's needs. Much work will be needed to develop models that provide accurate forecasts with the lead-time SRAG needs to act on them.

The models for predicting solar energetic particles that are currently being transitioned to operations by ISEP include HESPERIA REleASE, UMASEP-10 & 100, HESPERIA UMASEP-500, SEPSTER, and STAT. HESPERIA REleASE model currently uses real-time electron flux measurements from the Advanced Composition Explorer (ACE)/Electron Proton Alpha Monitor (EPAM) and SOHO's Electron Proton Helium Instrument (EPHIN). UMASEP-10 & 100 and HESPERIA UMASEP-500 use soft X-ray flux and differential proton flux measurements, as well as measurements of the integral proton flux >10 MeV and >100 MeV. SEPSTER uses coronagraph data to obtain CME width, speed, and connection angle and also uses solar radio burst data.

> **F-30.** The HESPERIA REleASE model will benefit from an instrument that will provide real-time electron fluxes 24/7 in the energy range of 1 to a few MeV.

STAT makes use of two other models, CORHEL and EMMREM. CORHEL uses data on coronal base plasma temperature and density and the radial component of the solar magnetic field from synoptic magnetograms for selected Carrington rotations of the solar surface (obtained

from Kitt Peak Observatory). Presumably, this could be modified to use magnetograph images instead. EMMREM provides time-dependent radiation exposure data based on a database of observed events and time series.

These models fall into the following categories: empirical models; empirical or semi-empirical probabilistic models, physics-based models, first-principles plasma transport models, and models based on machine learning. Many of these models will improve with better and more comprehensive measurements.

O-3.	There are at least 40 short-term forecast models (new models under development and currently available models), many of which are being refined.

6.3.2.2.2 *Observation on Forecast Models*

It is important to note that for crewed missions on the surface of Mars or in orbit around Mars (when timely communication with Earth is not practical), it will be necessary to monitor and forecast space weather on location instead of relying on operational instructions based on forecasts generated and transmitted from Earth. Sufficient early warning for the crew is a requirement that is best met with an Earth-independent capability for space weather forecasting. This capability must include timely access to appropriate solar observations and upstream solar wind particle measurements, with sufficient on-site computing power to analyze and model data to generate timely and actionable space weather forecasts.
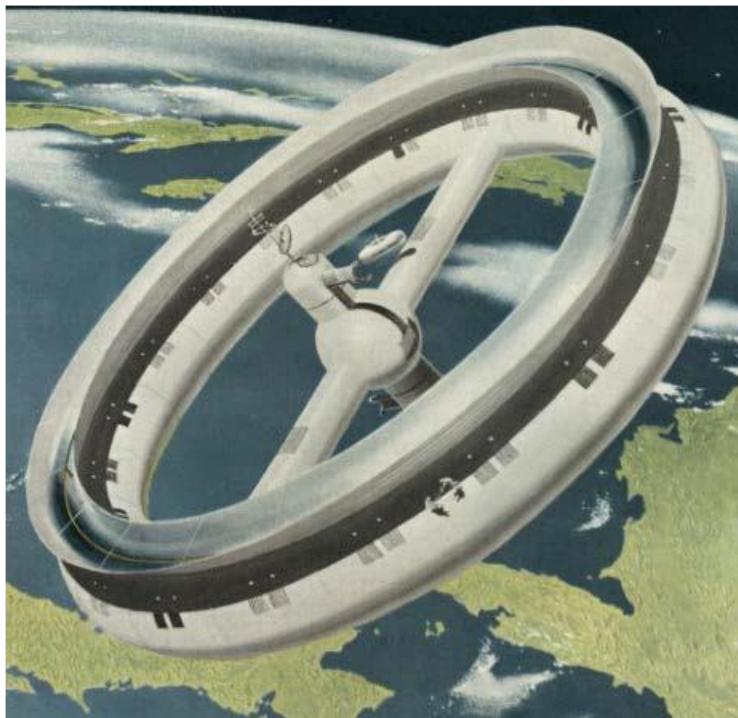
O-4.	To protect crews in deep space (and at Mars) when near real-time communications with Earth is not feasible, increased on-location capability to generate timely and actionable space weather forecasts is required. Development of an Earth-independent space weather forecasting capability (i.e., onboard transit vehicles or on site at Mars) is needed such that the system collects and processes data and generates space weather forecasts autonomously. This will require on-site computational and modeling capabilities, as well as retrieval and processing of data from solar observatories at various locations in the solar system.

6.4   Artificial Gravity (AG)

Buckley et al. [2007] define AG as the simulation of gravitational forces aboard a space vehicle that is in orbit (i.e., free fall) or in transit to another planet. The term *artificial gravity*, or *AG*, is reserved for a spinning spacecraft or a centrifuge within the spacecraft such that a gravity-like force is produced. It is not gravity as experienced on Earth, rather it is an indistinguishable inertial force in terms of its action on any mass [Buckley et al. 2007].

AG has been in popular science literature for decades. Wernher von Braun, in his *Collier's Weekly* series entitled "Man Will Conquer Space Soon!" described plans for manned spaceflight. One of those articles depicted a rotating space station that is shown in Figure 6.4-1 [von Braun, 1952]. In that article, titled "Crossing the Last Frontier," von Braun wrote, "However, there can be no doubt that permanent weightlessness might often prove inconvenient. What we require, therefore, is a 'synthetic' gravity within the space station. And we can produce centrifugal force—which acts as a substitute for gravity—by making the "wheel" slowly spin about its hub (a part of which can be made stationary)." Based on other references, AG was conceived of all

the way back in 1883, when Konstantin Tsiolkovsky described centrifugation as a means of creating AG in space in his manuscript entitled "Free Space" [Paloski and Charles 2014].

Figure 6.4-1. Space Station Concept envisioned by Wernher von Braun in his 1950s Collier's Weekly Article Series
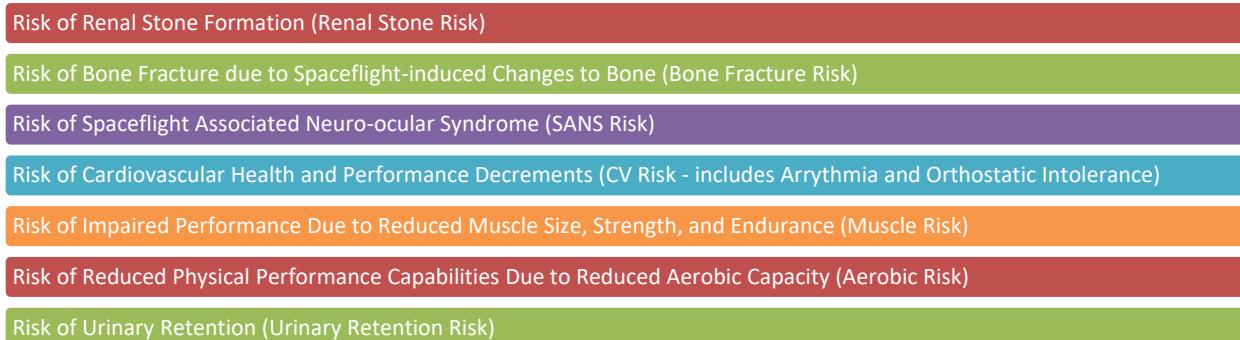
While there are technically several ways to generate a force that simulates gravity (e.g., linear acceleration, mass, and centripetal acceleration), all but centripetal acceleration are impractical for orbital or interplanetary transit implementations. That said, rotating a whole vehicle, part of a vehicle, or providing a rotating apparatus internal to a vehicle in space are not trivial from an engineering point of view. Since the beginning of human spaceflight, organizations have chosen to use countermeasures other than AG as the primary mitigation for the deleterious effects of sustained altered gravity fields (i.e., anything other than 1 g, including microgravity, lunar gravity (0.167 g), and Martian gravity (0.379 g)) on the body. Research on ground- and space-based approaches to understand microgravity's effects on the human body have continued through present day.

6.4.1 Human Research to Date

Crew members are subjected to the aspects of the space environment in spaceflight. This environment is characterized by hazards that are unchangeable aspects of spaceflight harmful to humans [Human System Risk Management Plan 2020]. Those hazards include altered gravity, radiation, isolation and confinement, hostile closed environment, and distance from Earth. For altered gravity, exposure to a gravity environment that is less than Earth-normal begins a process of adaptation. Some of these adaptations create issues for human bodies that developed to function in a 1-g environment.

Altered gravity is a significant cross-cutting hazard for human system risks when considering factors for safe exploration beyond LEO, especially for Mars missions where long-duration exposure to microgravity significantly exceeds our current baseline experiences and possible

countermeasure applicability. As shown in Figure 6.4.1-1, NASA's HSRB defines no fewer than seven primary risks tied to the altered gravity hazard. Since CHP are critical to successful human exploration beyond LEO, NASA developed the HRP to investigate and mitigate the highest risks to human health and performance by providing essential countermeasures and technologies for human space exploration.

Risk of Renal Stone Formation (Renal Stone Risk)

Risk of Bone Fracture due to Spaceflight-induced Changes to Bone (Bone Fracture Risk)

Risk of Spaceflight Associated Neuro-ocular Syndrome (SANS Risk)

Risk of Cardiovascular Health and Performance Decrements (CV Risk - includes Arrythmia and Orthostatic Intolerance)

Risk of Impaired Performance Due to Reduced Muscle Size, Strength, and Endurance (Muscle Risk)

Risk of Reduced Physical Performance Capabilities Due to Reduced Aerobic Capacity (Aerobic Risk)

Risk of Urinary Retention (Urinary Retention Risk)

Figure 6.4.1-1. NASA Human System Risk Board Primary Risks associated with Altered Gravity Hazard (risks are listed in descending order based on score rank, current as of publication of this report)

Altered gravity risks can impact in-mission operational performance as well as long-term human health, although in-mission performance impacts are likely a higher priority. At present, NASA mitigates altered gravity risks through a range of countermeasures, including but not limited to:

- Diet
- Fluid loading
- In-flight exercise
- Pharmaceuticals
- Preflight conditioning
- Selection standards
- Task design

Some altered gravity risks (e.g., spaceflight associated neuro-ocular syndrome (SANS)), are unique and currently lack broadly accepted countermeasures [Laurie et al. 2020; Mader et al. 2011, 2013]. Additionally, there are limited countermeasures for neuro-vestibular system adaptation to microgravity other than AG. These impacts affect standing without assistance; walking, including risk of falling; climbing; vehicle or telerobotic control; spatial orientation; and monitoring displays. On return to Earth, the effects of altered gravity recover over 2 to 7 days, depending on specific actions. Current altered gravity hazard mitigations appear to work for times up to approximately 1 year, but more data are required to build trends for longer duration uses or applications.
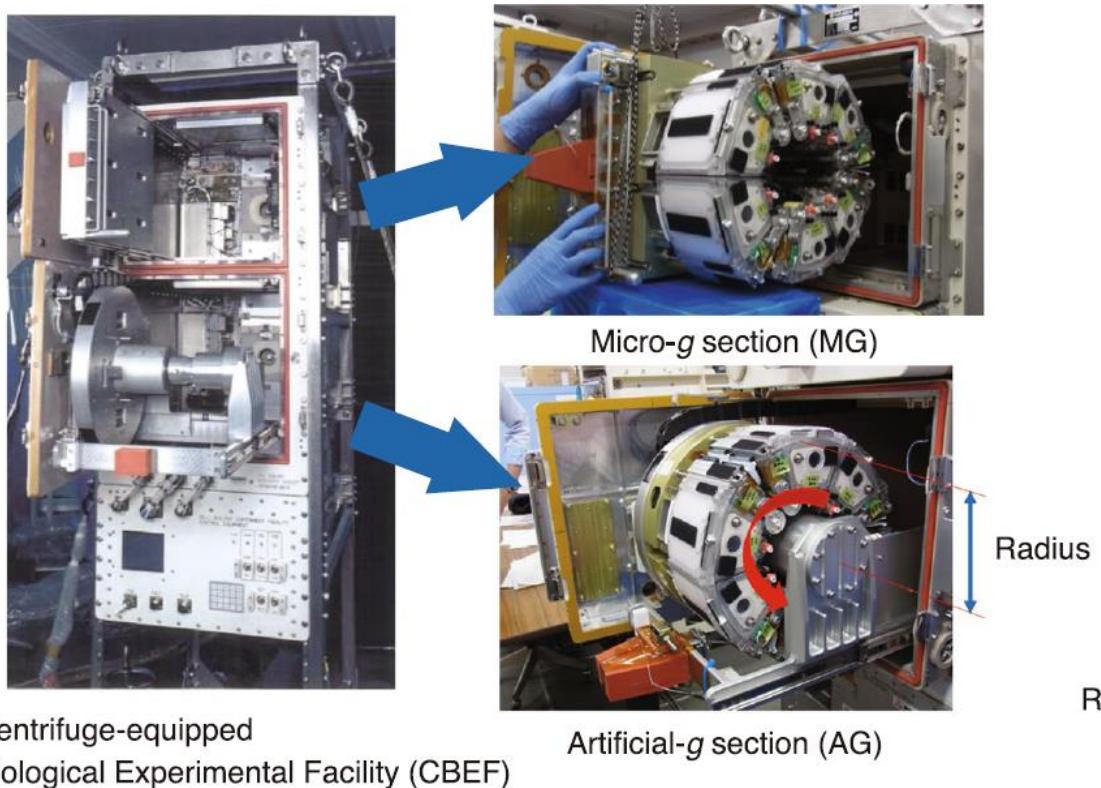
AG has the unique feature—in contrast to the countermeasures listed above—of protecting all physiological systems in all individuals against the effects of an altered gravity hazard because throughout evolution all creatures on the surface of the Earth adapted to the same 1-g level [Paloski and Charles 2014; Paloski and Young 1999]. Implementing AG for long-duration (>1 Earth year) missions could mitigate many risks, reduce countermeasure complexity,

eliminate countermeasure side effects, and increase human performance [Clément et al. 2015]. However, to potentially reap the benefits of AG, an appropriate dose-response function must be determined. Is the gravity dose continuous or intermittent? What is the duration of application? Answers to these questions have both human and engineering implications.

At the first AG workshop in 1999, Paloski and Young wrote, *"More than 30 years of sporadic activity in artificial gravity research has not elucidated the fundamental operating parameters for an artificial gravity countermeasure. For this reason, we do not advise NASA to discontinue support of countermeasures under development. Instead, we recommend that NASA allocate the resources – primarily deploying and funding a peer-review research program – necessary to initiate artificial gravity parametric studies on the ground and in flight"* [Paloski and Young 1999]. These statements were repeated as valid at a similar 2014 AG workshop, although an additional 15 years had elapsed [Paloski and Charles 2014].

In the past decades, there have been more than 100 publications globally on AG, especially pertaining to human research. Many of these articles have been documented in several key references [*Artificial Gravity*, 2007; Clément 2015, 2017; Clément & Bukley, 2008; Paloski and Charles 2014; Paloski and Young 1999] and are not reiterated here.

Since 2017, several significant AG advances have been reported in the literature that are applicable to the human research focus. A Japan Aerospace Exploration Agency (JAXA) project called Multiple Artificial-gravity Research System (MARS) focused on elucidating the impacts of partial gravity (partial-*g*) and microgravity (μg) on mice using newly developed mouse habitat cage units that were installed in the Centrifuge-equipped Biological Experiment Facility (CBEF) in the ISS [Shiba et al., 2017]. A picture of the CBEF and mouse habitats is shown in Figure 6.4.1-2. MARS followed in the footsteps of other microgravity experiments on mice that were performed on the Space Shuttle, robotic spacecraft, and the ISS. The use of the CBEF and centrifugation provided additional insights on how to prevent muscle and bone atrophy in humans undergoing long-term space voyages [Furukawa et al. 2021].

Figure 6.4.1-2. CBEF
CBEF has two compartments: micro-g section and artificial-g section with a centrifuge; centrifuge
accommodates six habitat cage units, and rotation radius where it contacts floor is 0.15 m
[Shiba et al. 2017]

In the past 20 years, there have been several comprehensive AG studies on humans, focused on the use of short-radius centrifugation. From 2006 to 2007, work was conducted at the University of Texas Medical Branch as part of the International Multidisciplinary Artificial Gravity (IMAG) collaboration. The study used 21 days of head-down bed rest (HDBR) combined with 1 hour daily of 1 *g* at the heart and 2.5 *g* at the feet. HDBR has been used for at least 50 years as a ground-based analog for microgravity-induced physiologic changes [Pavy-Le Traon et al. 2007]. The ESA conducted a similar study in 2010 called BR-AG1 [Linnarsson et al. 2015].

The AGBRESA study is the most recent attempt to study the effects of continuous and intermittent AG on participants spending 60 consecutive days in strict 6° HDBR performed at the :envihab at the German Aerospace Center in Cologne, Germany (see Figure 6.4.1-3). However, research on the effects of AG countermeasures during HDBR is scarce, with only a few additional studies to cite [Moore et al. 2010; Seaton et al. 2007].

Figure 6.4.1-3. AGBRESA Participants' Beds tilted 6 degrees downward at Head End to allow Negative Effects of Weightlessness in Space to be induced on Earth [Braun 2019]

The AGBRESA study is the first investigation on the effects on cognitive performance of a continuous and iAG countermeasure during and after a 60-day HDBR period. The study's work led to a number of important findings on the viability of strict HDBR to simulate in-space deconditioning adaptations, but it found no evidence for an effect of either continuous or iAG on either cognitive performance or subjective responses. This conclusion suggests that more efforts are needed to establish a useable dose-response relationship for application of AG as a sufficient countermeasure for risks associated with the altered gravity hazard. While HDBR appears to be suitable ground-based analog in many cases, NASA still lacks human-based in-space AG research for comparison. Earth gravity contamination and other factors could limit the efficacy of ground-based centrifugation.

Additionally, the AGBRESA study was used to support further examination of HDBR's ability to induce SANS [Laurie et al. 2021]. It was also the first attempt to test AG as a potential SANS countermeasure by using a daily exposure to centrifugation. In this instance, AG was unable to mitigate the development of SANS-associated ocular changes. As stated previously, in the case of ground-based experiments, future altered gravity countermeasure investigations should target a longer duration and/or greater magnitude of exposure. Such studies could also be extended into the space environment assuming the availability of acceptable AG production techniques.

F-31.	Altered gravity is a significant cross-cutting hazard for human system risks when considering factors for safe exploration beyond LEO, especially for Mars missions where long-duration exposure to microgravity significantly exceeds our current baseline experiences and possible countermeasure applicability.

F-32.	Upon return to Earth, the effects of altered gravity recover over periods approaching 1 week, depending on specific actions. Current altered gravity hazard mitigations appear to work for times up to ~1 year, but more data are required to build trends for longer duration uses or applications.

F-33.	AG has the unique feature of potentially protecting all physiological systems in all individuals against the effects of an altered gravity hazard, because throughout evolution all creatures on the surface of the Earth adapted to the same 1-g level.

O-5.	Some altered gravity human health and performance risks, like SANS, are unique and currently lack broadly accepted countermeasures.

S-2.	Human research investigations should be pursued to evaluate more fully the safety and efficacy of an iAG countermeasure for exposure durations (doses) greater than 30 minutes per day, in combination with strict long-duration head-down bed rest deconditioning. Future AG investigations should be supported by current human research efforts to assess lower body negative pressure, as well as plans to use Gateway in combination with surface lunar gravity exposure and explore commercial partnership opportunities to understand in-space centrifugation.

6.4.2   State of AG Technology

There are several ways to generate a force that can approximate the gravitational force experienced on Earth. However, programmatic and technical limitations reduce the trade space to linear and centripetal acceleration [Artificial Gravity 2007]. Linear acceleration would require specialized spacecraft propulsion systems to produce useful levels of AG over long periods of time—near-constant acceleration for the first portion of the journey and then near-constant deceleration for the second portion of the journey, each achieving significant fractions of or near 1 g performance. At present, spacecraft engine technology cannot achieve useful levels of thrust for long enough durations to be useful from the standpoint of AG production. That leaves rotational motion to produce centripetal acceleration as the only viable source of AG currently available for use on the ground or in space.

Centripetal acceleration can be realized in three ways that produce AG for spaceflight applications:

- Spin a spacecraft about its own axis (usually assumed to also be the center of mass).
- Rotate two spacecraft connected by a tether about the system's center of mass.
- Use a short-radius centrifuge aboard a spacecraft.

In the first two cases, everything in the spacecraft system is exposed to AG, and the radius of rotation is generally "large." In the last case, only the objects on the short-radius centrifuge are exposed to AG. On the ground, most human AG experiments have been conducted using short-radius centrifugation, although globally there are a few large-radius centrifuges that have been used for human research (e.g., the 1958 Pensacola studies at the Naval Medical Research Laboratory). As discussed here, large-radius rotational systems (the first two examples) have tended to be dismissed for spaceflight use based on a variety of factors, which means that most AG centrifugation research has focused on short-radius systems.

Many AG designs were thoroughly researched in the 1960s, starting with large toroidal designs and moving to rigid boom structures and finally to deployable tethered designs as the practicalities of space exploration required designs to become cheaper and easier to develop. During the design stages for Skylab and later the ISS, both had competing or complementary

designs that offered AG for research purposes, but both programs ultimately decided there was more to be gained with microgravity research in the near term. With Artemis and Moon-to-Mars efforts underway, it is worth reviewing that decision once again to determine whether AG has sufficient benefits to earn a supporting role.

Ground-based AG research on humans and other biological systems has been conducted for decades. In space, AG studies have focused on cell and animal models, like plants and mice. However, there has been very little in-space AG research on humans. In 1966, the Gemini XI mission performed the only attempt at an AG space station by rotating the spacecraft connected to an Agena rocket casing using a tether. The rotating system obtained 0.15 revolutions per minute and only induced 1.5×10^{-4} g for 4 hours. This is shown in Figure 6.4.2-1. There has not been an in-space demonstration of a spacecraft spinning about its center of mass for the purpose of generating AG. As detailed by Paloski and Charles et al. [2014], the only other attempts to induce AG in space on humans occurred on Spacelab-1 in 1985 using an ESA-developed short-track linear sled, on the International Microgravity Laboratory (IML)-1 in 1992 with rotating chairs, and on the Neurolab mission on STS-90 in 1998 with an off-axis rotator [Paloski and Charles 2014]. The rotating systems all had short radii.

Figure 6.4.2-1. Gemini XI Spacecraft tethered to an Agena Rocket Casing on September 14, 1966 (Gemini XI command pilot Charles "Pete" Conrad and pilot Dick Gordon maneuvered the craft to keep the tether taut between the two; by firing the side thrusters to slowly rotate the combined spacecraft, they were able to use centrifugal force to generate about 1.5×10^{-4} g of AG for about 4 hours; Image credit: NASA)
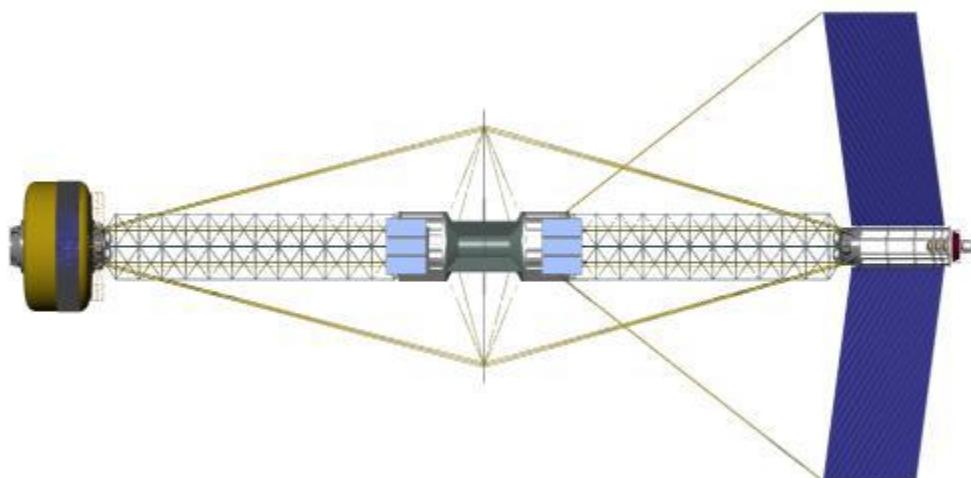
Before discussing other in-space centrifugation concepts, it is important to mention the Artificial Gravity with Ergometric Exercise (AGREE) project. AGREE was born out of a 2009 International Life Science Research announcement and would have evaluated the effectiveness of short-radius centrifugation in space by attaching an experiment to the ISS. AGREE was to have been built by ESA but was cancelled by NASA when engineers determined that mechanical loads would compromise ISS. More details on AGREE are available in references that have already been discussed [Paloski and Charles 2014].

Joosten, Borowski, and Zipay wrote an excellent section in the 2014 Artificial Gravity Workshop White Paper [Paloski and Charles 2014] in which they detailed a range of factors that likely prevented available AG concepts from receiving more serious engineering assessments:

- Lack of definitive design requirements, especially acceptable AG levels and rotation rates.
- Perception of high vehicle mass and performance penalties.
- Incompatibility of resulting vehicle configurations with space propulsion options.
- Perception of complications associated with de-spun components (e.g., antennae and photovoltaic arrays).
- Expectation of effective crew microgravity countermeasures other than AG.

Their assessment from 2014 appears to remain valid even in the case where some of the apprehensions could be overstated. In 2002, one of the first detailed vehicle design AG impact studies was carried out by Joosten [2007]. It was aimed at whole-vehicle AG, with a primary focus on resulting mass penalties and other sources of mission performance degradation.

The 2002 study focused on three different whole-vehicle AG implementations and ended up advocating a "fire baton" design for its feasibility, which included compatibility with nuclear propulsion systems. This design concept is shown in Figure 6.4.2-2. For this design, the study anticipated continuous AG at a level of 1 g, requiring a greater than 56-m radius habitat to spin at a rate of less than four revolutions per minute. By replicating a continuous near 1 g environment, this vehicle design would in principle avoid the need for substantial human research to determine an appropriate dose-response relationship for other AG scenarios using short-arm centrifugation, levels less than 1 g, and/or intermittent application of gravity generation.

Figure 6.4.2-2. "Fire Baton" Vehicle Concept considered as Part of 2002 Vehicle Design Engineering Analysis focused on Whole-vehicle AG Generation Concepts [Joosten 2007]

Full-vehicle AG appears to offer the widest array of microgravity mitigation opportunities, but there have always been concerns with the practicality of implementation [Rowe 2020]. Large toroidal craft like those popularized in the early days of the space race would take a huge investment in time and capital to complete and would be unreasonable for missions to Mars or beyond due to the fuel requirements to move. Smaller rigid structures like booms can be used to separate habitable volumes from a center of rotation, but these require either advancements with in-space assembly or in-space manufacturing to complete and, once completed, fix the number of

variable gravity environments that can be generated. Commonly, the lightest option, tethered systems, can be designed for a wide variety of environments since the length of the habitable volume from the center of rotation is adjustable, but generating rotation with a flexible tether system while thrusting causes a variety of issues that makes their use during the actual Mars transfers complicated at best.

While small component-level AG mitigation research is deservedly getting a lot of attention at present, there should still be ongoing research into addressing the concerns for full-vehicle AG within the Artemis and Moon-to-Mars planned CONOPS. Based on recent work [Rowe 2020], there seems to be some promise for using a tethered system adapter between a transfer stage and a Mars transfer vehicle, which could provide full-vehicle AG with minimal mass and launch requirements if interfaces are scabbed for in advance; one recent concept design claims that the full AG adapter system could even be designed to fit within a single commercial launch vehicle. The advantages of an Earth-like or Mars-like environment at all times for an extended duration either during transit, prior to crew descent, or even as just an analogue during a shakedown mission in Earth's vicinity could offer significant advantages over the smaller rotational systems currently being researched.

This report section is focused on AG technology since it may offer the broadest countermeasure benefits for altered gravity hazard-associated risks. However, it bears mentioning that lower-body negative pressure (LBNP) can be used as a partial altered gravity countermeasure to prevent cardiovascular deconditioning and to reduce orthostatic intolerance from the microgravity environment of spaceflight [Goswami et al. 2019]. This reference contains an excellent reference section of its own that spans at least 40 years of literature and can be consulted for more detailed information on LBNP [Arbeille et al. 1992; Gazenko et al. 1981; Hargens et al. 1991; Lee et al. 2007]. By itself, LBNP cannot address all in-scope risks, but its implementation and application may be less fraught than continuous or intermittent human centrifugation when considering all space system programmatic and technical factors.

F-34.	There are several ways to generate a force that simulates gravity (e.g., linear acceleration or centripetal acceleration), although all but centripetal acceleration appear to be impractical for orbital or interplanetary transit implementations, leading to a focus on short- and large-radius centrifugation systems.

F-35.	In recent studies, intermittent ground-based short-radius centrifugation AG appeared to have a positive effect on deconditioning responses induced by strict HDBR, suggesting that future efforts target longer duration and/or greater magnitudes of exposure to iAG.

F-36.	The engineering trade space for in-space options to produce continuous and iAG exposure (e.g., internal short-arm centrifuges, tethers, and other rotating systems) contains several point designs with various levels of detail but is not as sophisticated as the current state of the art for ground-based AG investigations. This is largely driven by the lack of a consensus dose-response model for an AG countermeasure.

O-6. To date, there have only been four documented instances of in-space human-based AG research: 1) during Gemini XI in 1966, 2) on Spacelab-1 in 1985, 3) on IML-1 in 1992, and 4) during the Neurolab mission on STS-90 in 1998.

6.5 Human-Systems Integration Architecture (HSIA)

The reliance on real-time communications has been a key part of crewed spaceflight missions from their inception. Since the Mercury missions in the 1960s, in-flight operations have had a large ground component working in real time with the crew and vehicles. Problem solving and decision making have been almost entirely carried out by Mission Control. Similarly, execution of complex or safety-critical procedures in space has been largely done with ground oversight. Mission Control, composed of hundreds of highly trained experts, has served as the safety net for crewed spaceflight missions. How this is done has changed little over the past 60 years. The overall capability to resolve urgent anomalies remains very much in the expertise of the human controllers on the ground. One of the most important findings of this study is with respect to just how much time the ground team spends monitoring vehicle data, as well as working on anomaly resolution—hundreds of person hours per day.

One can think of the whole system—including the crew, the engineered systems supporting the mission, human experts on the ground, data systems, screens, communication devices, and physical spaces—as being a HSIA that enables execution of complex operations and resolution of safety-critical issues. An HSIA is the instantiation of communication, coordination, and collaboration between humans and systems.

The HSIA currently in place is the result of a slow evolution over a series of orbital and lunar missions. It is not really state of the art; for example, some designs and implementations lag behind more recent technological advances (e.g., integrated data systems). The current HSIA for ISS has been adequate for mission success because of the advantages of LEO and real-time access to the expertise of Mission Control. A key challenge with safe exploration beyond LEO is that the HSIA currently in use will no longer work, as communication delays and resupply challenges increase with distance. The HSRB frames this as a "Risk of Adverse Outcomes Due to Inadequate Human Systems Integration (HSI) Architecture."
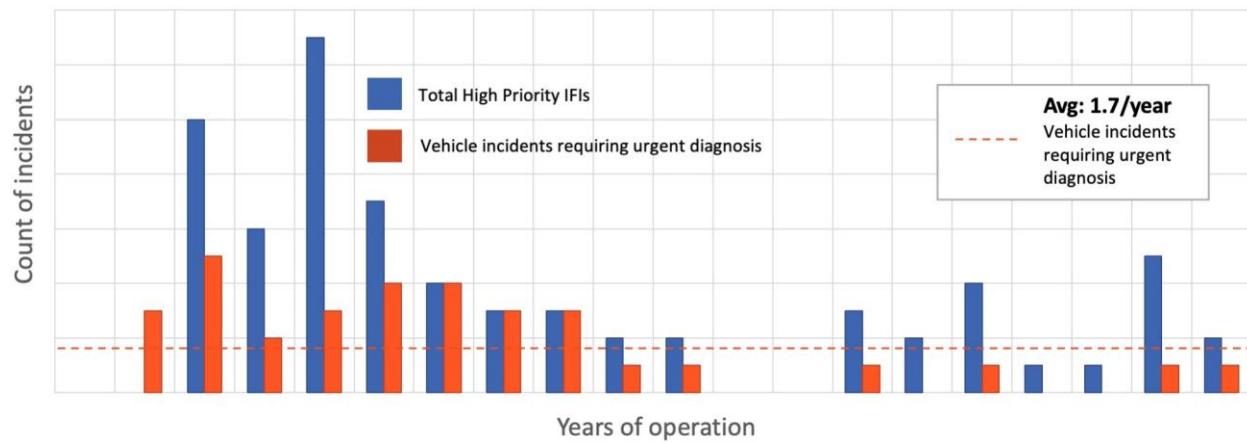
There are very few, if any, analogs on Earth for safe exploration beyond LEO that can help characterize what is needed for a small group of humans to perform independently as part of a complex technological system for extended periods of time. If, as in nuclear submarines, long periods of no communication are required by the mission, then many crew members (i.e., 50 to 100) with relevant expertise are used. If, as in summiting Mount Everest, an intermittently isolated group with limited expertise (e.g., first aid only) must achieve the goal, then the duration of the mission as a whole is relatively short. Most examples on Earth are mitigated by either real-time communication, a large crew, or a short-duration mission. There is no evidence base, within or outside NASA, for how a small group of humans on an extended expedition dependent on the proper functioning of equipment can survive without real-time operational and engineering support.

The discussion here begins with an assessment of the risk of in-mission anomalies and the capability on the ground to mitigate that risk. Specifically, the focus will be on unanticipated anomalies of unknown origin requiring immediate response and how frequently these occur. Case studies charactering in detail two such anomalies experienced on ISS are then presented.
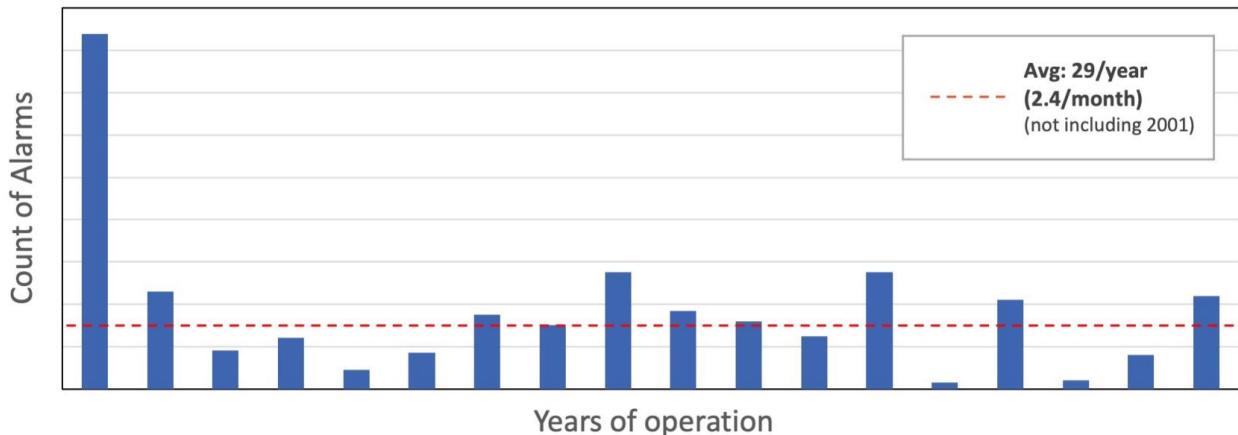
(In Section 8, these two case studies are described in terms of how they would transpire if they were to occur during Mars transit or during Mars surface operations.) The remainder of this section focuses on the state of knowledge of current risk mitigation capabilities: communications, data systems, maintainability/repairability, and intelligent systems.

6.5.1 Historical Anomaly Rates

Analyses of unanticipated, critical malfunctions occurring during crewed spaceflight missions indicate that such anomalies are typical occurrences. Despite the unparalleled preparation and expertise that goes into every NASA mission, the ISS experienced 67 high-priority anomalies from 2002 to 2019, 33 of which were vehicle subsystem-related incidents requiring urgent diagnosis [Panontin et al. 2021]. The distribution of these anomalies over the life of the ISS is shown in Figure 6.5.1-1. During the "burn-in" phase of ISS (i.e., the first 6 years), the average number of anomalies requiring urgent diagnosis was ~3 to 4 times per year; a 2- to 3-year Mars mission would effectively take place entirely within the burn-in phase of the equipment, and a similar rate of major vehicle malfunctions might be expected. Alarms informing the crew there is a critical malfunction occur, on average, more than twice per month on ISS (Figure 6.5.1-2). During the Apollo era, the 11 crewed missions accumulated a total of 362 anomalies, with 35 of those incidents considered urgent and significant [Panontin et al. 2021].

Figure 6.5.1-1. High-priority Anomalies for ISS
(red bars show highest priority items requiring urgent response, and blue bars show total high
priority items for investigation (IFIs) that were of unknown initial urgency)

Figure 6.5.1-2. Total Number of Class 2 Alarms by Year
(Class 2 alarms (or warnings) indicate that crew or ground must take immediate action to avoid
injury or death of crew or damage to ISS; there are an average 29 Class 2 alarms per year on ISS
(excluding data from 2001))
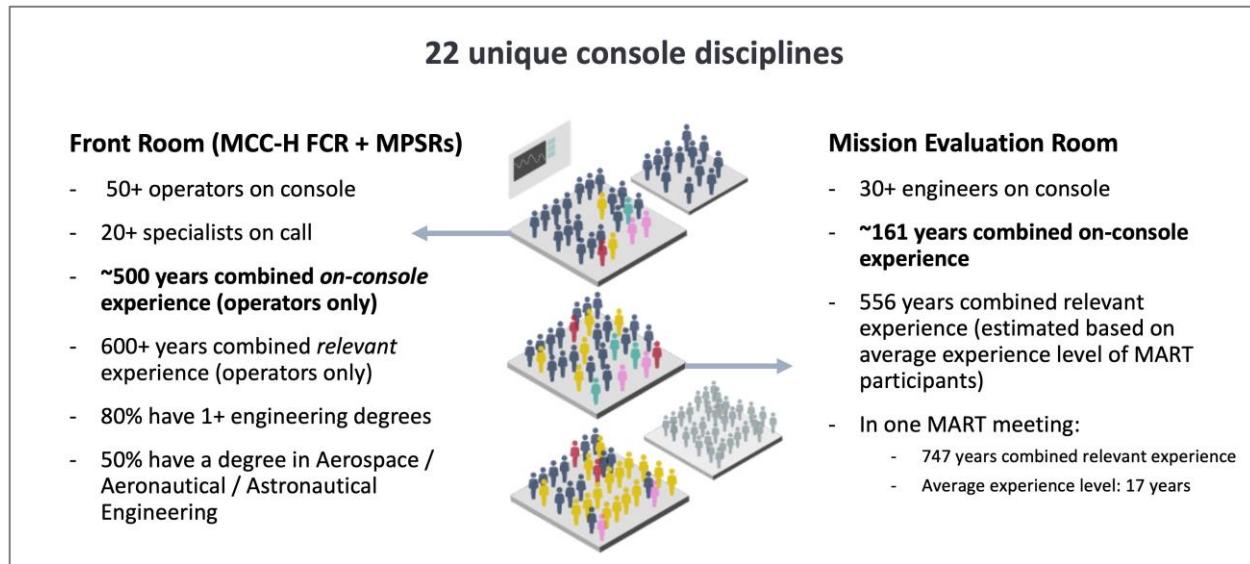
Here, the term *anomaly* refers to unintended or off-nominal function of vehicle systems with consequences that can range from benign to life-threatening. Anomalies that require urgent response are those that affect critical subsystems, deplete essential resources, and/or involve uncertainty, meaning there is no set procedure in place for response, causal analysis is required, and short-times-to-effect for unwanted consequences are possible. Even with the best engineering processes in place, vehicle anomalies will continue to occur throughout the duration of a mission. Anomalies continue to occur throughout any given mission (and therefore the total number of anomalies may increase with mission length), and the rate of anomalies is higher during the burn-in phase of a vehicle and increases with the complexity of mission operations.

F-37.	The likelihood of high-consequence problems of uncertain origin occurring during spaceflight is high (conservatively, exceeding 50% during Mars transit) based on historical trends.

6.5.2 Current HSIA in Support of In-flight Anomaly Resolution

6.5.2.1 ISS Team Expertise

Despite these anomaly rates, NASA crewed spaceflight missions continue to succeed largely due to an HSIA that is ground based and labor intensive. This current HSIA relies on the extraordinary capabilities of Mission Control and Mission Evaluation Room (MER) teams to respond to anomalies quickly and effectively. ISS missions are supported by 80+ experts on the ground at any given time, with a combined 600+ years of system-specific experience across 22 unique console disciplines (Figure 6.5.2.1-1) [McTigue et al. 2021].

***Figure 6.5.2.1-1. Level of Mission Control Expertise supporting ISS Missions
("Front Room" estimates include flight controllers in Mission Control Center Houston (MCC-H)
Flight Control Room (FCR) and back rooms (or multi-purpose support rooms (MPSRs)). "Mission
Evaluation Room" estimates include engineers on console during a nominal shift and,
separately, engineers present during a multilateral anomaly response team meeting (MART).)***

This level of expertise is contrasted with that expected for a four-person crew in Table 6.5.2.1-1.
A small crew will face the unprecedented challenge of independently responding to anomalies
that have historically been handled by a team 20 times their size. Unlike the experts in Mission
Control who specialize in mastering a single system, these crew members are likely to be
generalists with a broader understanding of a wide range of systems [Hadfield 2018].

Table 6.5.2.1-1. Comparison of Expertise available to ISS from Mission Control with Notional Astronaut Crew for a Mars Mission

"The Ground Team": 85+ System Experts in MCC-H Front Rooms, Back Rooms, and Mission Evaluation Room	Four Crew Members (estimated based on all current active astronauts eligible for flight assignment and current ISS training practices as of April 2021)
~660 years combined specific systems experience	~91 years combined relevant work experience
~2 years to operator certification	2 years astronaut candidate training
Additional years to specialist certification	~2 years flight-assigned training
In-depth understanding of a single system	Trained on inventory and stowage, communications and tracking, electrical power system, external thermal control system (ETCS), environmental control and life support systems (ECLSS), internal thermal control system (ITCS), emergency, motion control system, on-orbit maintenance, structures and mechanics, crew systems, visiting vehicle, orbital mechanics, crew medical officer, medical operations, EVA, robotics, operations local area network, photo/television (See Dempsey [2018] for a list of ISS systems and consoles)
Training builds academic engineering background	Academic background varies
Constantly using skills and studying flight rules	Time gap between training and flight; degradation of knowledge may be significant

> **F-38.** For human spaceflight missions, monitoring of mission system data and diagnosis/mitigation of unanticipated critical malfunctions have been done from the ground by 80+ highly experienced engineers with deep systems expertise. Some of this data monitoring and problem-solving capability will need to be on board to support the crew when ground intervention is unavailable or delayed.

6.5.2.2 Current In-flight Anomaly Resolution Processes

To characterize current in-flight anomaly resolution capabilities, detailed timelines were reconstructed for past ISS anomaly resolution processes. Based on analyses of the ISS IFIs database, two anomalies were selected that met the criteria of being high priority (i.e., affecting a safety-critical system) and requiring urgent response. The team selected a 2013 Cooling Loop anomaly to characterize a critical troubleshooting event and a 2010 Oxygen Generation Assembly (OGA) anomaly to characterize a critical maintenance/repair event. OGA anomaly timelines will not appear in this version of this report due to data sensitivity; for more information, see Valinia et al. [2022].

Relevant MER artifacts were reviewed for each anomaly. Artifacts included Anomaly Resolution Team (ART) and Flight Investigation Team (FIT) meeting PowerPoint presentations, ART and FIT meeting summaries, and ISS daily summaries, among others. These artifacts contained the historical telemetry data, manufacturing data, schematics, fault trees, and other data sources used to diagnose and resolve these events. Available articles detailing the events of interest were also reviewed [Dempsey 2018; JSC SM&A Flight Safety Office 2014; Jones 2016; Takada et al.

2015]. In total, over 90 artifacts from the Cooling Loop anomaly and over 75 artifacts from the OGA anomaly were reviewed. System status information, crew actions, MCC actions, and MER actions were captured to map the sequence of events. The data, analyses, and interactions that informed key decision points throughout the anomaly resolution process were noted. Using these data points, timelines were created detailing ground actions and in-orbit events for the anomalies as they occurred. This version of this report contains only publicly available details on these anomalies.
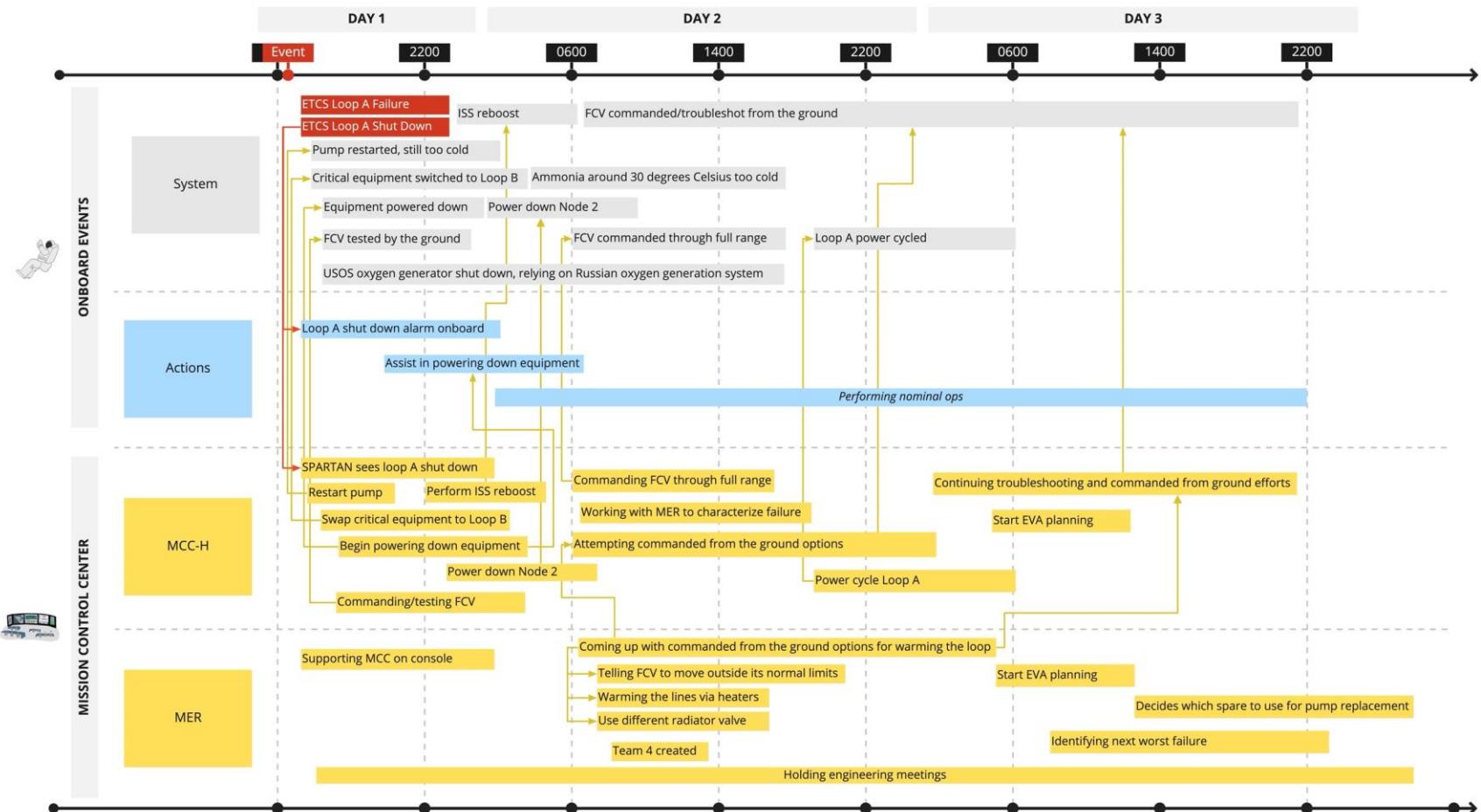
As demonstrated by these examples, anomaly resolution is an iterative process involving hypothesis generation and testing. Depending on the outcome of testing, usually achieved by executing a procedure, new hypotheses and tests are generated. If this is happening in LEO, the iterative process can be carried out by the ground with a real-time cadence.

6.5.2.2.1   Cooling Loop Anomaly, 2013

The first anomaly investigated took place in December 2013: the "Loop A Flow Control Valve Bias" incident (see Figure 6.5.2.2.1-1). The anomaly began when the fault detection, isolation, and recovery (FDIR) software automatically shut down Cooling Loop A after the loop became too cold to operate safely. Suddenly, half of the systems on the ISS were in danger of overheating, as the pump was no longer circulating fluid. When the first alarms sounded, the crew was immediately informed that the ground was aware and responding. The ground team (including people in MCC-H, MPSRs, and the MER) had to move quickly, as this fault required urgent response.

The ground team determined which critical systems needed to be moved to contingency cooling and which systems should be safely powered down using existing documentation on system thermal constraints. Simultaneously, the ground team began procedures to recover the pump. Pump recovery procedures were time-constrained and had to be completed within the first few hours of the incident, meaning that procedures had to be initiated almost immediately. During the first few hours of the incident, the ground team also proceeded to execute various workarounds in an attempt to get the cooling loop to a safe temperature. At the same time, the ground was shedding heat loads and performing tests to characterize the failure. The crew assisted in powering down certain equipment onboard the ISS at the end of their day but otherwise maintained nominal operations.

Over the next several days, the ground attempted many commanded-from-the-ground options, but ultimately an EVA was required to remove and replace the pump module. Prior to EVA preparation, the crew primarily proceeded with nominal operations, as most of the troubleshooting and safing activities were conducted from the ground. This team focused on investigating the immediate anomaly response; therefore, only the first two days of the event are included in the timeline.
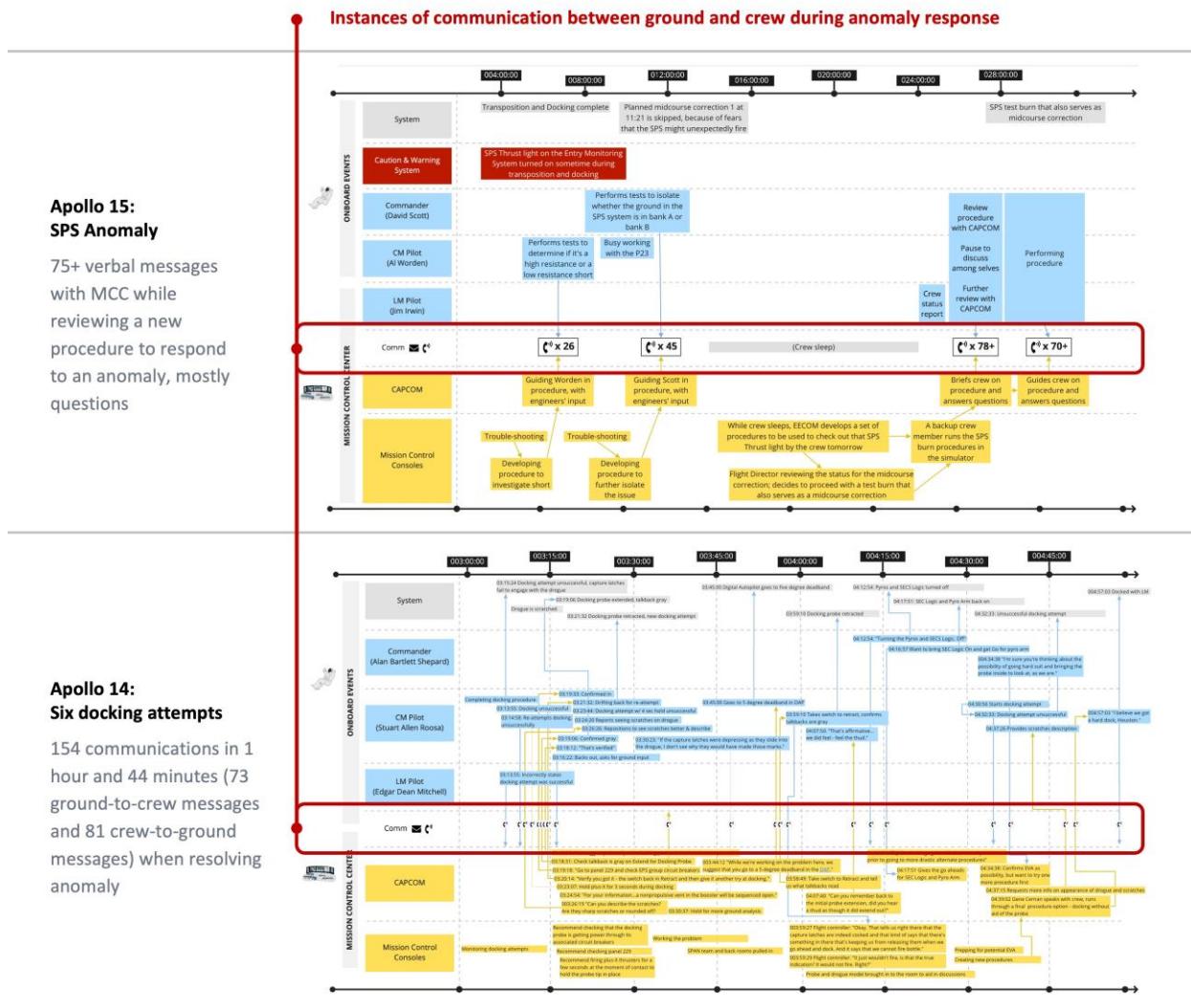
Figure 6.5.2.2.1-1. Cooling Loop Anomaly: Mapping of Actual Events as they unfolded in December 2013

6.5.2.2.2 OGA Anomaly, 2010

The second anomaly investigated involved an OGA repair task. In 2010, the OGA Hydrogen Dome Orbital Replacement Unit's (ORU's) cell stack had a high voltage failure, causing the OGA to shut down. Teams on the ground immediately began considering the possibility of removing the Hydrogen Dome ORU and replacing it with a spare unit already onboard the ISS. Simultaneously, investigations into past OGA water samples revealed a lower pH than expected, and the ground suggested remediation of the recirculation loop to address this issue. Two days after the initial failure, the decision was made on the ground to move ahead with the Hydrogen Dome ORU removal and replacement (R&R) and the remediation of the recirculation loop. The failed ORU was later returned to Earth for in-depth failure investigation.
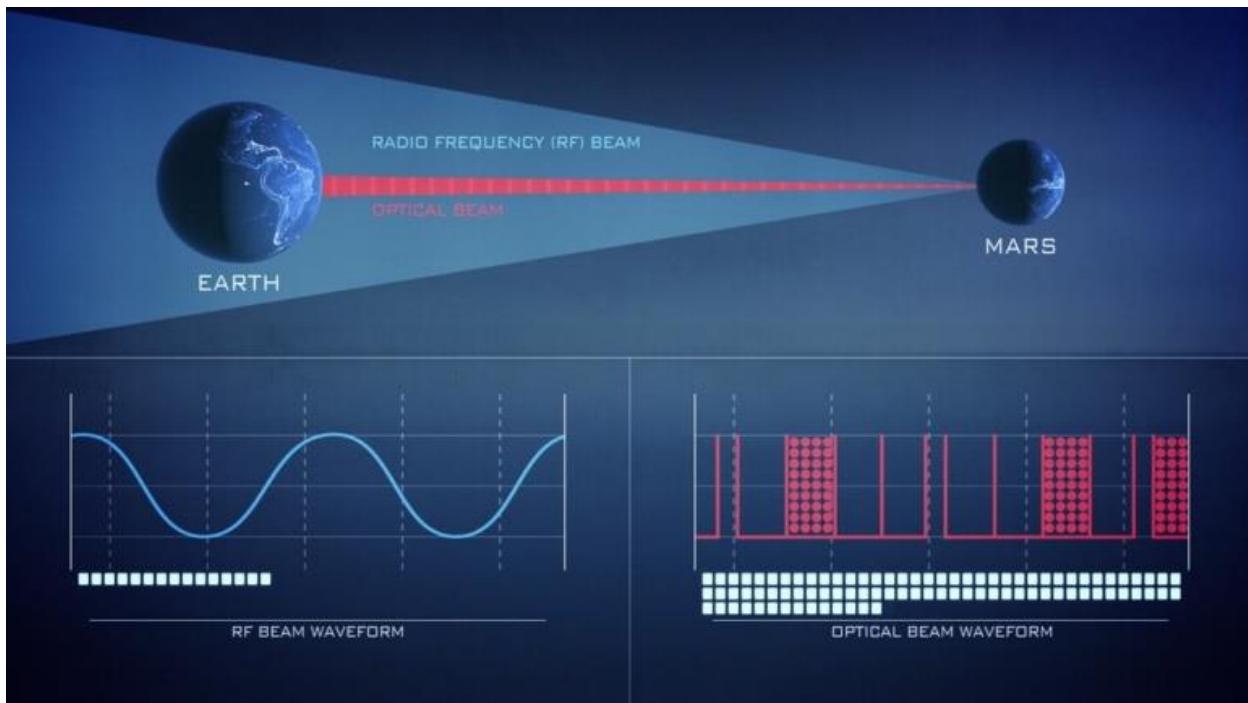
6.5.2.3 Current Space Communications

The constant, real-time support of the vast pool of expertise in ground-based MCCs and MERs have provided the safety net for past and current missions during critical events and anomalies. The extent of real-time communications is significant, as shown in Figure 6.5.2.3-1. For example, during an Apollo 15 Service Propulsion System anomaly, over 75 verbal messages were exchanged during the approximately 1 hour the crew spent reviewing a procedure, and during an Apollo 14 docking anomaly, 154 communications were exchanged in 1 hour and 44 minutes as the crew attempted to dock [Apollo Lunar Surface Journal 2018]. For exploration beyond LEO, however, this safety net may be compromised; communication with Earth-bound resources may be intermittent, delayed, or data limited as the crew travels to the Moon and beyond.

Figure 6.5.2.3-1. Quantification of Communication between Ground and Crew during Anomaly Response

Signals to and from spacecraft are line of sight. Currently, crewed and robotic missions rely primarily on radio frequency (RF) waves for communications. As future missions require greater data streams at greater distances, communication systems with higher frequency infrared waves—optical or laser communications—are being developed. The beams of laser transmitters, at wavelengths ~10^4 times shorter than RF waves, spread out less over distance and provide more concentrated communications power at the receiver with lower required transmitted power. *Transmission rate* is independent of frequency, whether RF or optical. Waves move at the same speed but have higher data content, so the data bandwidth is higher. Higher bandwidths can carry more data per second, allowing spacecraft to downlink data more quickly (see Figure 6.5.2.3-2).
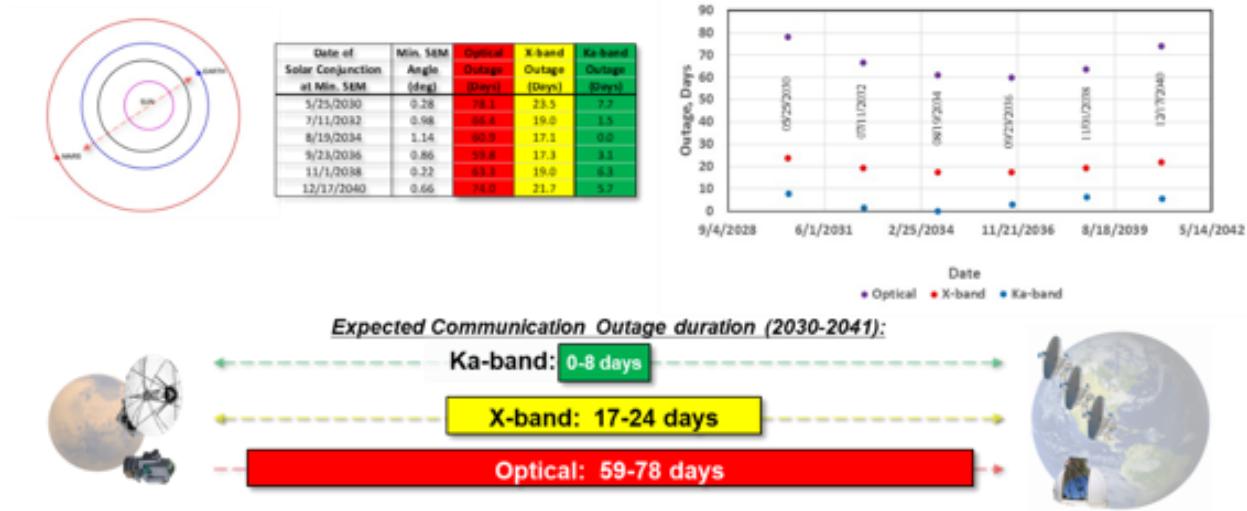
Figure 6.5.2.3-2. Graphic Representation of Difference in Data Rates between Radio and Laser Communications (source: NASA)

However, all communications speeds, even optical communications, are bound by the speed of light (~186,000 miles per second), and far from Earth, latency can become a challenge. For example, the distance between Mars and the Earth ranges from 35 million to 250 million miles. Corresponding communications delays to and from Mars, then, will range from 4 to ~24 minutes, respectively.

Another important factor that will affect communications between exploration crews and Earth-based support is link availability. Link availability describes the amount of time that mission elements can connect to Earth stations to flow data and is a function of lines of sight and sources of interference. Communication between Earth and deep space mission elements are not normally possible with a single radio or optical link, so relays will be needed between surface, orbiting, and Earth elements. Figure 6.5.2.3-3 shows link availability issues associated with superior solar conjunction. This issue can be anticipated and accommodated with relay satellites. Weather on Earth may also affect reception of optical communications; for example, the likelihood of cloud cover impeding communications at any Earth station is estimated to be 30%.

While the exact magnitude of this risk varies with specifics of season and location, it is an important concern for link availability.

Expected Communication Outage duration (2030-2041):

Ka-band: 0-8 days

X-band: 17-24 days

Optical: 59-78 days
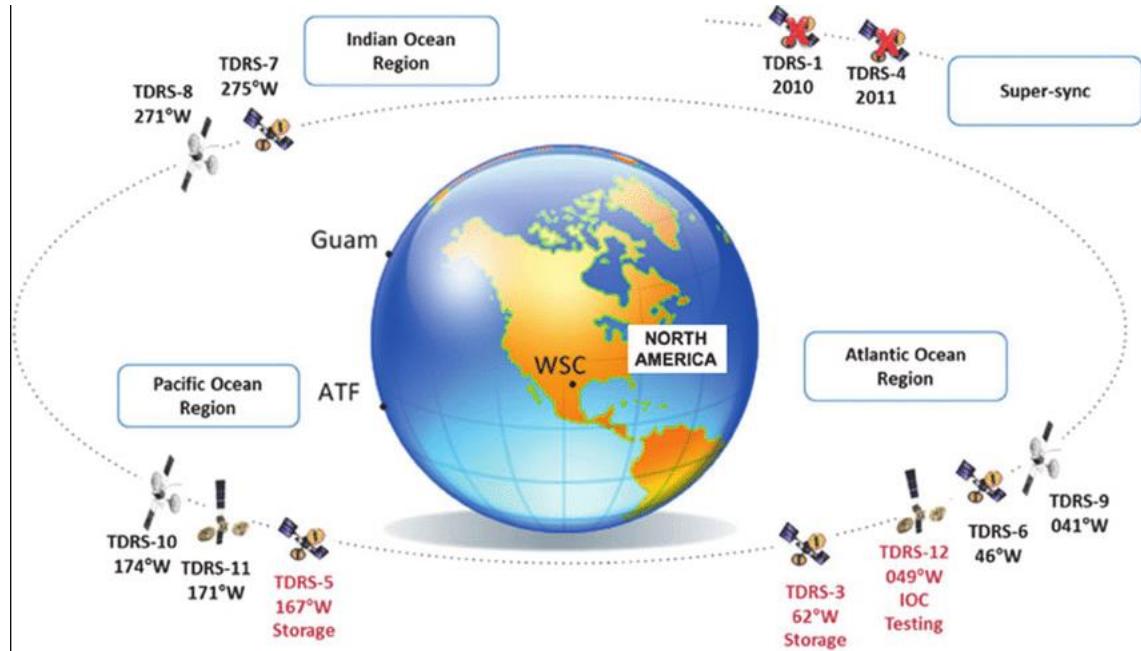
Figure 6.5.2.3-3. Superior Solar Conjunction can result in Anticipated Loss of Communications without Additional Satellite Relays (source: NASA Space Communication and Navigation (SCaN) team)

6.5.2.3.1 Crewed Space Communications (ISS)

The ISS primarily uses S-band RF frequencies to communicate with ground control centers. It is used to send commands to the ISS and telemetry data from the ISS to the ground. More than 30,000 data points that monitor conditions onboard the ISS (e.g., temperatures, flow rates, etc.) can be radioed to the ground via S-band every 10 seconds. However, this represents only a subset of the data available on the ISS, with more than 300,000 sensors generating data. The rest of the data can be retrieved directly from the onboard computer memory when needed for troubleshooting, without constantly taxing the available bandwidth.

Data rates for the ISS S-band system have improved significantly over time. In as late as 2017, the forward (up) link (i.e., transmission to the ISS) had the capability to transmit only 72 kilobits per second (kbps), while the return (down) link (i.e., transmission from the ISS) could transmit 192 kbps. Currently, the uplink capability is 20 megabits per second (Mbps) and the downlink is 300 Mbps. For comparison, smartphones transmit data at ~ 10 Mbps, TV streaming at ~25 Mbps for HDR.

The main communication path between the ISS and ground control centers is the Tracking and Data Relay Satellite (TDRS) system (Figure 6.5.2.3.1-1). The TDRS system consists of satellites in geosynchronous orbit at three different regions above Earth that provide global coverage and near-continuous communications. Rather than waiting to pass over a ground station, the ISS can relay data 24 hours a day, 7 days a week.
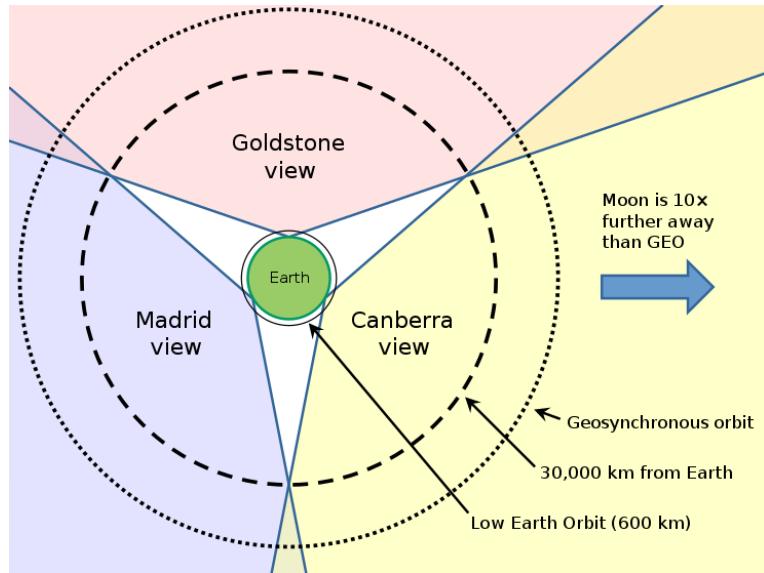
Figure 6.5.2.3.1-1. Current TDRS Constellation (note that satellite locations are approximate and vary from year to year (source: NASA))

> **F-39.** Every 10 seconds, ISS generates 300,000 individual pieces of data but only sends 30,000 to the ground. The rest are pulled down by the ground as needed to solve problems.

6.5.2.3.2   *Robotic Mission Deep Space Communications*

Communications from deep space can be extremely difficult to receive on Earth, as the received power drops by the square of the distance traveled. Solar system background noise, interference from Earth's or another planet's atmosphere, and noise introduced by the receiving system may also degrade signals from deep space.
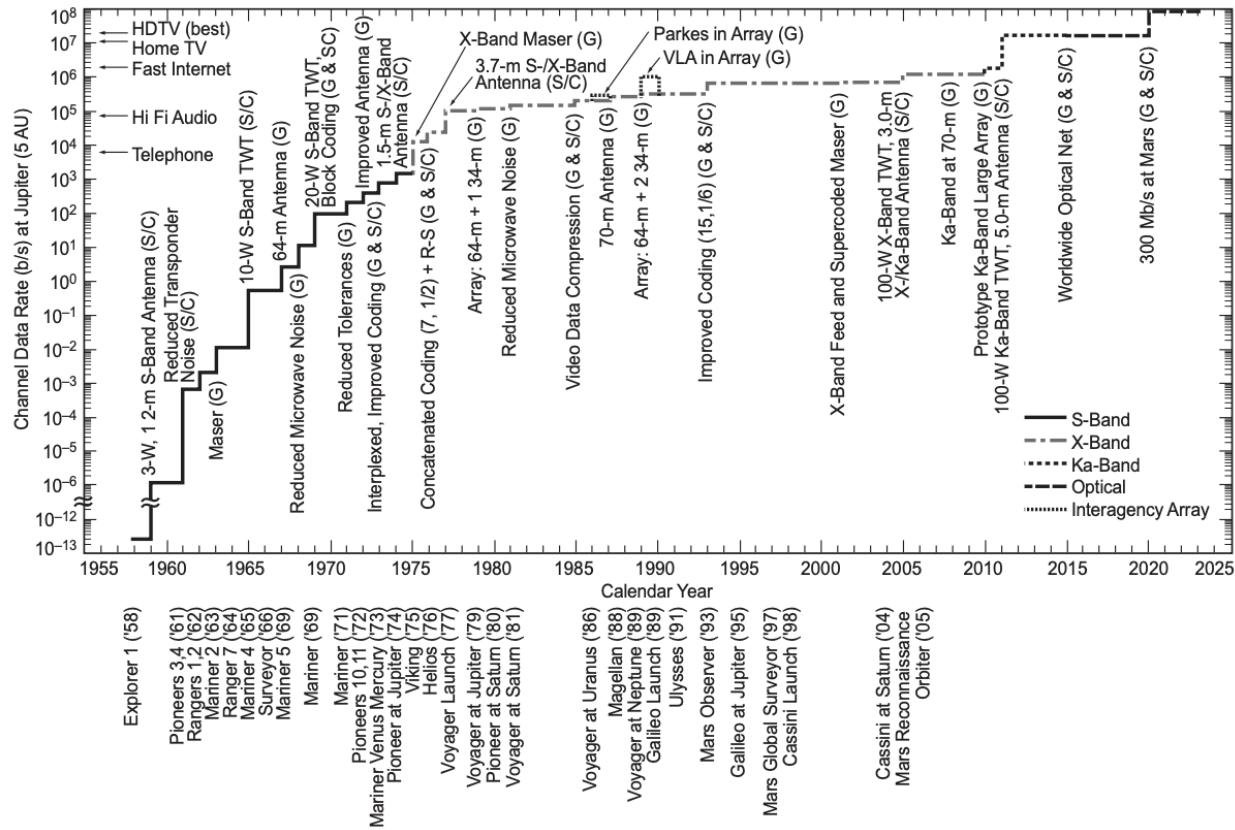
The current communication path for interplanetary spacecraft is the Deep Space Network (DSN). An array of giant radio antennas using high-power transmitters to provide uplink and sensitive receivers to detect downlink, the DSN acquires telemetry data, transmits commands, uploads software modifications, and tracks spacecraft positions. It consists of three facilities spaced equidistant from each other (120 degrees apart longitudinally) around the world, permitting constant communication with spacecraft. Before a distant spacecraft sinks below the horizon at one DSN site, another site can pick up the signal and carry on communication. These facilities are at Goldstone near Barstow, California; near Madrid, Spain; and near Canberra, Australia. To provide consistent two station coverage for lunar and deep space coverage, DSN station coverage overlaps beyond 30,000 km (19,000 miles) and gives 8-14 hours of daily view (see Figure 6.5.2.3.2-1).

Figure 6.5.2.3.2-1. View from Earth's North Pole, showing Field of View of Main DSN Antenna Locations
Once a mission gets more than 30,000 km (19,000 miles) from Earth, it is always in view of at least one station [reprinted from: Wikimedia Commons Free Media Depository, https://commons.wikimedia.org/wiki/File:DSNantenna.svg].

DSN radio frequencies include S band (2–4 gigahertz (GHz)), X band (8–12 GHz) and Ka band (27–40 GHz). The data rate through DSN has increased 10 orders of magnitude since 1955, mainly due to different parts of the RF spectrum being used. Comparisons to commercial RF product (e.g., phone) data rates are also shown in Figure 6.5.2.3.2-2. In the future, the DSN will support optical communication in the infrared frequency band, increasing rates even further.
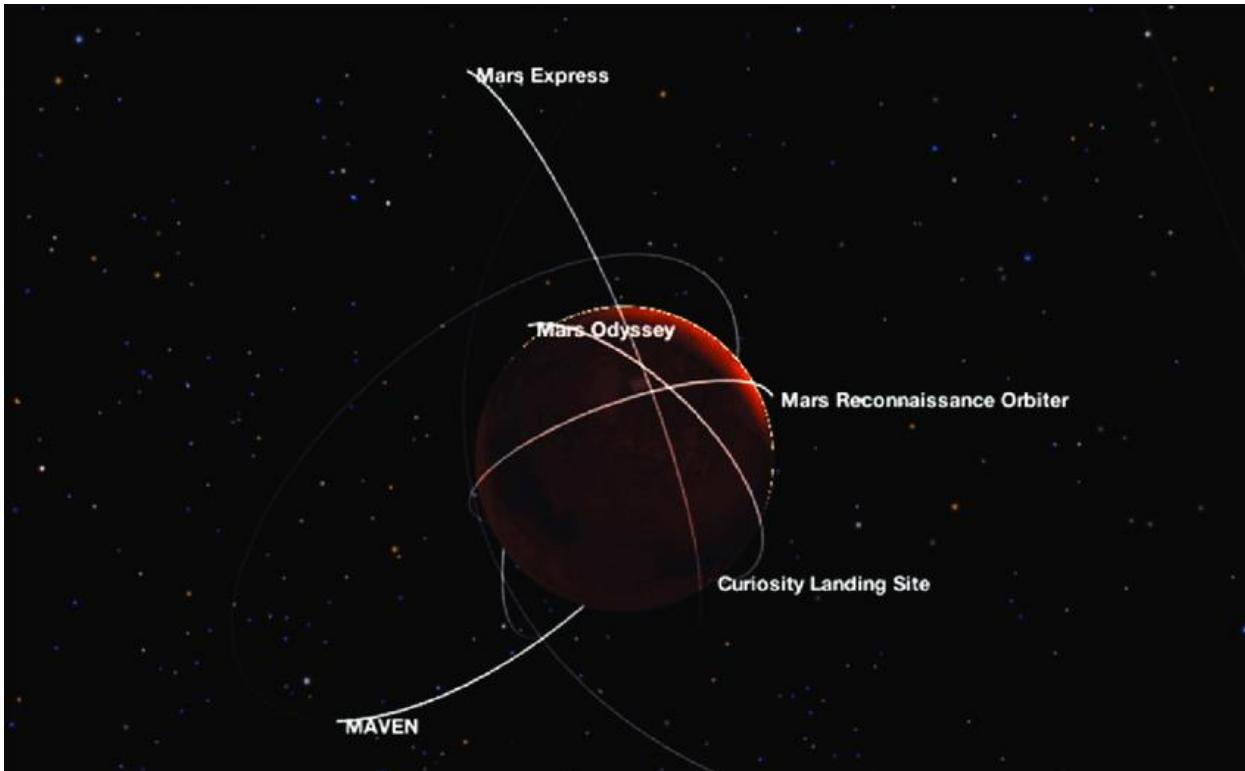
Figure 6.5.2.3.2-2. Deep Space Optical Communications (source: Hamid Hemmati, California Institute of Technology, Jet Propulsion Laboratory)

6.5.2.3.3   Mars Deep Space Communications

The network of relays at Mars evolved gradually over time. The original relay infrastructure was developed to support the Mars Exploration Rovers. The relay capabilities of science oribiters were designed in anticipation of future missions [Edward et al., 2006]; however, these relays operate in low-Mars orbits and transit quickly so that their link availability is brief [Vuong and Vuong, 1997] (see Figure 6.5.2.3.3-1). For example, today's Mars surface rovers operate with 8 to 10 minutes per sol (Martian solar day) of link availability.

Surface element to relay data rates are no more than 6 Mbps. Data rates to Earth can be 1 to 5 Mbps. With these rates, the Mars Reconnaissance Orbiter requires 7.5 hours to transmit all the data stored in its onboard recorder, and 1.5 hours to send a single high-resolution image. However, only about 125 kbps can be returned per surface element by the limited relay opportunities [Chamberlain et al. 2015; Lock et al. 2016]. The forward (up) link to Mars is currently limited to 40 to 256 kbps.

***Figure 6.5.2.3.3-1. Combined NASA-ESA Current Mars Relay Infrastructure, 2018
(source: https://eyes.nasa.gov)***

F-40.	Currently, Earth/Mars communications have far lower data rates and link availability than those used to support crewed missions in LEO.

6.5.2.4   Onboard versus Ground Trend Analysis and Knowledge Base Access

Broadly speaking, NASA has two kinds of data in the context of human space exploration: telemetry data from vehicle sensors and engineering data from human-conducted analyses before and during mission operations. Both kinds of data are critical to anomaly resolution, as carried out by the ground for the past 60 years of human space exploration. Nevertheless, on current vehicles such as the ISS, much of the data collected from sensors, often at a rate of multiple times per second, are left onboard. Specific data are pulled down to Earth as needed to diagnose a specific problem. Similarly, for the Mars rover missions, a small subset of the onboard telemetry captured by the rover is radiated back to Earth. When there is a problem with the rover, ground controllers can run diagnostic tests and pull more specific data. As of 2017, the volume of telemetry generated by complex space vehicles was very large compared with the communication pipeline back to Earth, even for vehicles in LEO (see Section 6.5.2.3). Machine learning techniques have been used to determine what data are important to downlink in bandwidth constrained environments. This poses some degree of risk in situations where an anomaly is unanticipated and the machine learning algorithms have not been trained for the specific contingency. Nevertheless, it can be expected that such capabilities will continue to improve over the coming years and that, in combination with bandwidth improvements (as discussed in Section 8.5.2.1), will provide critical data for time-delayed ground support functions.

Aggregating and integrating engineering data (e.g., parts lists, system drawings, testing history, problem history, etc.) is challenging. Although the set of NASA spaceflight engineering data is not "big data" by current standards, it is still not managed in an integrated manner. For example, the total number of PRACA reports generated by the Space Shuttle Program was just under one million. A large number, to be sure, and more than any one ground controller or mission engineer could have in their head, but not a sufficient amount nor the right kind of data for machine learning or discovery technologies (see Section 8.5.2.4).

The Columbia Accident Investigation Board (CAIB) report attributed some causality to what they termed "dysfunctional databases" [Columbia Accident Investigation Board 2003]. The CAIB found that there were about 50 separate PRACA systems for shuttle, each with its own nomenclature and process flow. It was not possible to see patterns across the PRACA systems. To this day, there are hundreds of processes and engineering data analysis repositories for other data, such as Hazards Analyses and Failure Modes Effects Analyses, and for each type of data, there are many independent repositories. People misattribute accidents to *unknown unknowns*, but, if one examines the history of such events across complex engineered systems, it becomes clear that the source is most often *unknown knowns*: the information is in our data systems but we simply cannot see the relationships.

The Constellation Program began an effort to integrate data systems by data type and across data types. All PRACA reports were to be in one system using the same nomenclature and process, across all elements of the program. In addition, PRACA reports would be associated with other data types, such as Parts, so that an analyst troubleshooting a vehicle issue might be able to see all previous problems associated with a given physical part. With the cancellation of the program, much of this effort was stopped or delayed.

> **F-41.** Current databases supporting ISS operations are not well integrated on the ground nor are they accessible to the crew.

6.5.2.5 Current Maintainability, Diagnosability, Repairability Approaches
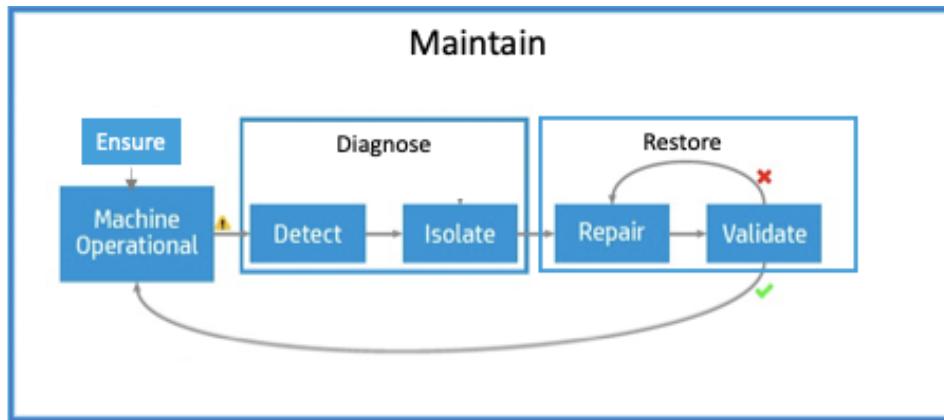
Maintainability, diagnosability, and repairability are several (among many) nonfunctional requirements that specify quality characteristics or attributes of a system. In this case, the attributes are related to avoiding and/or mitigating consequences of equipment or system failure. Maintainability, diagnosability, and repairability have a significant human/systems integration element (in contrast to reliability, for instance, which is predominantly physics-based). Nonfunctional requirements, as performance or functional requirements, must be addressed during the design cycle. For deep space exploration, vehicles, habitats, or other elements need to possess the attributes of maintainability, diagnosability, and repairability so that crew can support nominal system operations and address off-nominal behavior with on-board resources with reasonable effort.

Maintainability is the ease with which hardware and software systems can be preserved against failure or decline to operate as needed. It can also be expressed as the probability that an item will be retained in, or restored to, a specified condition within a given period of time. Diagnosability is the ease with which the nature of a problem can be determined or distinguished. In engineered systems, it is expressed as the ease of fault detection and isolation. Repairability is the ease with which a system can be restored to a sound condition. This should include validation of the restoration.

In some cases, the attributes of diagnosability and repairability can be subsumed under that of maintainability. As shown in Figure 6.5.2.5-1, the act of maintenance can include the acts of diagnosis and repair, as well as preventative measures to ensure operation.

Figure 6.5.2.5-1. Attributes of Diagnosability and Repairability Subsumed Under Maintainability [Adapted from Girbau 2020]

6.5.2.5.1 *ISS Maintenance Approach*

On ISS, crews generally execute three categories of in-flight maintenance including: preventive, corrective, and diagnostic. *Preventive maintenance* includes regular inspections, lubrications, cleanings, etc., that are performed to ensure continued proper operation of a system. *Corrective maintenance* involves repairing or replacing components that have stopped working either because of end-of-life conditions or because failures have occurred unexpectedly. When equipment ceases to operate correctly and it is not obvious what has occurred, *diagnostic maintenance* is required first to determine where faults might be located to help establish the best way to remedy the hardware or situation.

ISS logistics practices, including maintenance planning, spare/line replaceable unit (LRU) manifesting, stowage, inventory tracking, etc., were examined in a 2006 study [Evans et al. 2006]. The goal of the study was to inform future crewed exploration architectures. The study found that current practices have positive aspects and have successfully supported the ISS. However, the study also identified several shortcomings, including a high-level of excess complexity, redundancy of information/lack of a common database, and a large human-in-the-loop (HITL) component. The overall process (circa 2006) is depicted in Figure 6.5.2.5.1-1.
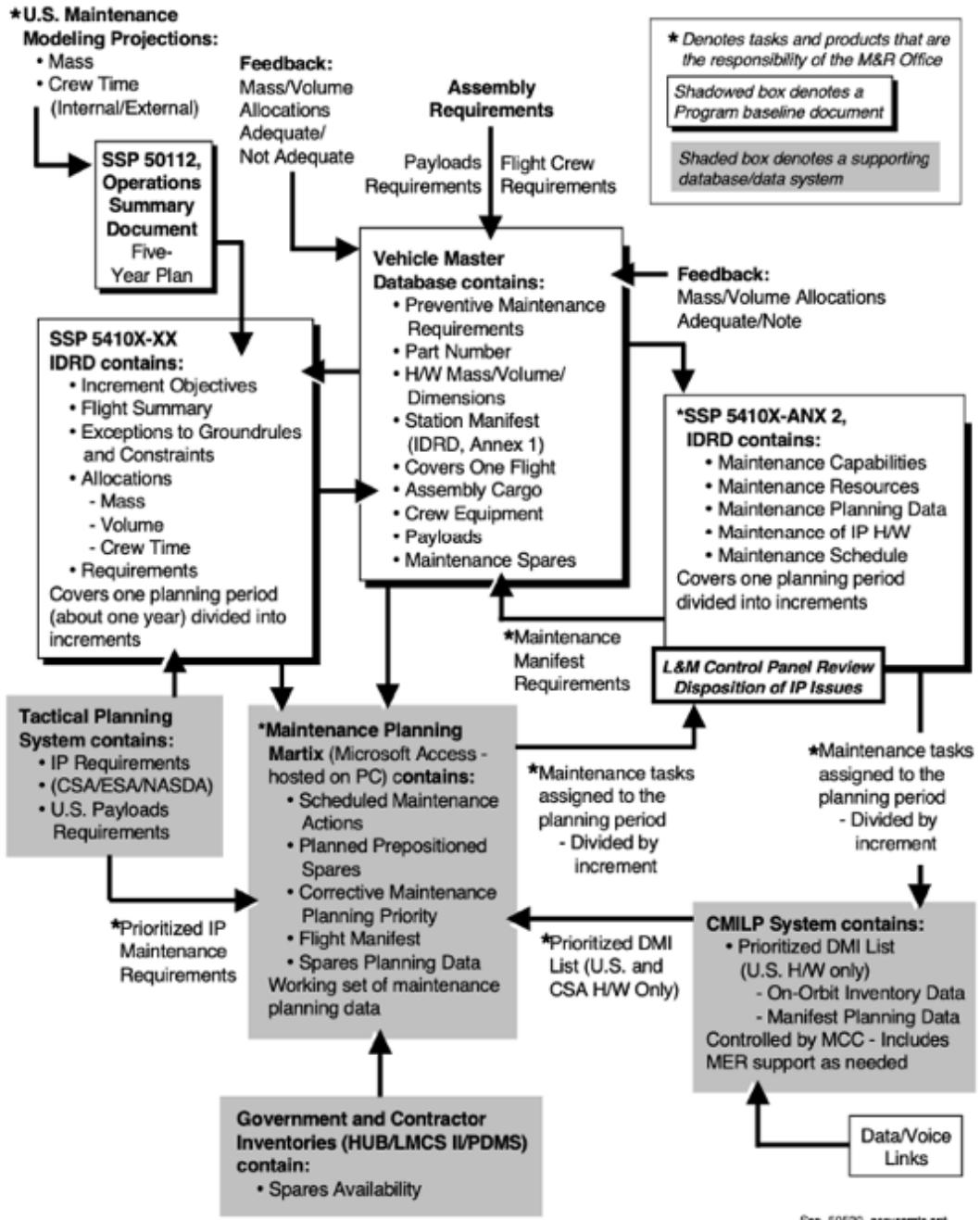
Figure 6.5.2.5.1-1. ISS Support Planning Process [reprinted from Evans et al. 2006]
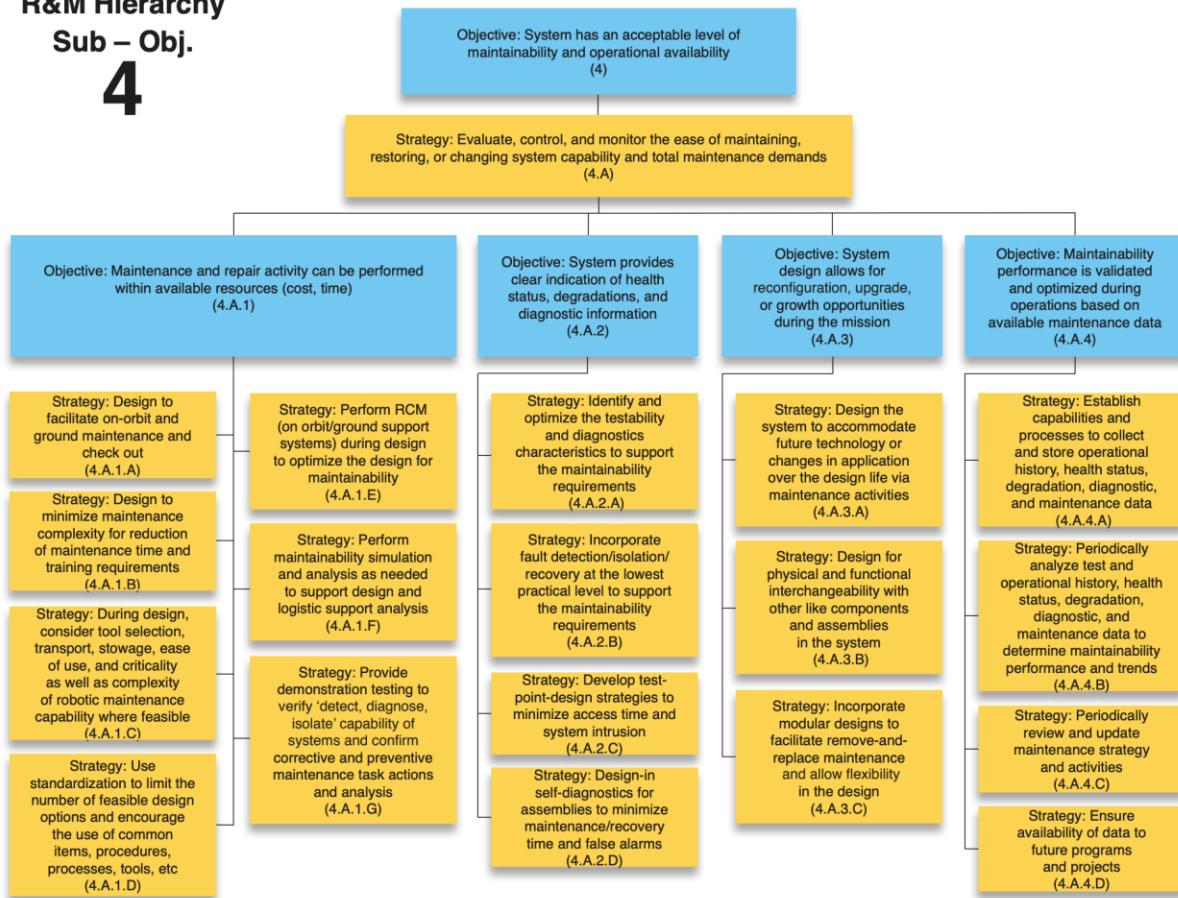
6.5.2.5.2   Maintainability Standards

The NASA standard for reliability and maintainability (R&M) for spaceflight and support systems is NASA-STD-8729.1A. Rather than specifying a fixed set of requirements and processes, NASA-STD-8729.1A provides only the key R&M objectives. This allows the flexibility to determine requirements and tailor approaches based on risk tolerance. The objectives specified for maintainability are shown in Figure 6.5.2.5.2-1. Note that these include objectives related to diagnosability and repairability.

R&M Hierarchy Sub – Obj. 4

Objective: System has an acceptable level of maintainability and operational availability (4)

Strategy: Evaluate, control, and monitor the ease of maintaining, restoring, or changing system capability and total maintenance demands (4.A)

Objective: Maintenance and repair activity can be performed within available resources (cost, time) (4.A.1)

Objective: System provides clear indication of health status, degradations, and diagnostic information (4.A.2)

Objective: System design allows for reconfiguration, upgrade, or growth opportunities during the mission (4.A.3)

Objective: Maintainability performance is validated and optimized during operations based on available maintenance data (4.A.4)

Strategy: Design to facilitate on-orbit and ground maintenance and check out (4.A.1.A)

Strategy: Design to minimize maintenance complexity for reduction of maintenance time and training requirements (4.A.1.B)

Strategy: During design, consider tool selection, transport, stowage, ease of use, and criticality as well as complexity of robotic maintenance capability where feasible (4.A.1.C)

Strategy: Use standardization to limit the number of feasible design options and encourage the use of common items, procedures, processes, tools, etc (4.A.1.D)

Strategy: Perform RCM (on orbit/ground support systems) during design to optimize the design for maintainability (4.A.1.E)

Strategy: Perform maintainability simulation and analysis as needed to support design and logistic support analysis (4.A.1.F)

Strategy: Provide demonstration testing to verify 'detect, diagnose, isolate' capability of systems and confirm corrective and preventive maintenance task actions and analysis (4.A.1.G)

Strategy: Identify and optimize the testability and diagnostics characteristics to support the maintainability requirements (4.A.2.A)

Strategy: Incorporate fault detection/isolation/recovery at the lowest practical level to support the maintainability requirements (4.A.2.B)

Strategy: Develop test-point-design strategies to minimize access time and system intrusion (4.A.2.C)

Strategy: Design-in self-diagnostics for assemblies to minimize maintenance/recovery time and false alarms (4.A.2.D)

Strategy: Design the system to accommodate future technology or changes in application over the design life via maintenance activities (4.A.3.A)

Strategy: Design for physical and functional interchangeability with other like components and assemblies in the system (4.A.3.B)

Strategy: Incorporate modular designs to facilitate remove-and-replace maintenance and allow flexibility in the design (4.A.3.C)

Strategy: Establish capabilities and processes to collect and store operational history, health status, degradation, diagnostic, and maintenance data (4.A.4.A)

Strategy: Periodically analyze test and operational history, health status, degradation, diagnostic, and maintenance data to determine maintainability performance and trends (4.A.4.B)

Strategy: Periodically review and update maintenance strategy and activities (4.A.4.C)

Strategy: Ensure availability of data to future programs and projects (4.A.4.D)

Figure 6.5.2.5.2-1. Assessing Acceptability of Level of Maintainability and Operational Availability in a System [reprinted from NASA Standard 8729.1A 2017]

NASA-STD-3001, Volume 2, "Human Factors, Habitability, and Environmental Health" [2019], contains additional, specific requirements related to maintainability, diagnosability, and repairability. These 17 requirements are categorized under:

- General (3)
- Maintenance efficiency (6)
- Accessibility (6)
- Failure notification (2)

NASA STD-3001 superseded NASA-STD-3000 [1995], the man/system integration standard that was created to provide a single, comprehensive document defining all requirements for space facilities and related equipment that directly interface with crewmembers. NASA-STD-3000 contained considerably more, and more highly specified, requirements related to maintainability than NASA STD-3001.

In addition to these standards and requirements, designing for maintainability, diagnosability, and repairability should consider the following approaches:

- Simplicity – minimize maintenance complexity.

- Standardization – minimize variety of components that meet hardware requirements.
- Interchangeability – maximize ability to exchange parts or assemblies between like equipment without modification.
- Modularization – structure equipment to facilitate separation and recombination.
- Functional packaging – kit all required elements for standard maintenance tasks.
- Accessibility – maximize visibility and safety, in addition to proximity.
- Fault annunciation and isolation – maximize fault information provided by system.
- Identification – maximize consistency and ability to distinguish among components, procedures, etc.
- Spares – optimize level (box, component, etc.) and number.

Diagnosability approaches should address complications, such as:
- Hidden faults
- Cannot duplicate (CND)
- Retest OK (RTOK)
- Fault isolation ambiguity
- False remedies
- False alarm

Due to the constraints of long-duration exploration missions that would render the current approaches impractical, and informed by relevant content coming from multiple NASA standard documents, an effort to develop cohesive and comprehensive standards for Earth-independent maintainability, diagnosability, and repairability of vehicle systems is recommended.

F-42.	NASA STD 8729.1A and NASA-STD-3001 are based on evidence that comes primarily from LEO and could be incomplete for the full suite of beyond Earth orbit mission objectives (e.g., human lunar return segment, sustained lunar presence segment, and humans to Mars segment).

O-7.	Current approaches to system robustness (e.g., carrying and/or upmassing many ORUs) may not be feasible for extended missions beyond LEO.

O-8.	Safe and cost-effective beyond-LEO operations will require a new approach to flight-like systems testing and HITL simulation during development.

7.0   Integrated Human Health Risk Assessment for Missions to Mars

All exploration programs, projects, and missions navigate their way through the challenges of balancing multiple types of risks, opportunities, and constraints (e.g., technical, cost, schedule, personnel, and political). When human crewmembers are part of the operating system, the risks to their safety, health, and performance must be included in the trade studies.

The human side of this balancing act can be described as follows. As mission duration increases, the risk that crew capability will degrade over time increases. This can lead to a decreased ability

to perform tasks necessary for mission success and, in the worst cases, negatively impact the health and safety of the crew both in mission and in their LTH. Engineering solutions (e.g., fast transit, AG, space weather monitoring and radiation mitigation) are intended to minimize this degradation of crew capability throughout the mission, keep the likelihood of successful task performance high, and minimize the LTH risks to the crews. Each of these engineering solutions carries system trades and challenges that make successful implementation uncertain in exploration missions. It is currently unclear how well crew capability can be maintained in a Mars mission. However, crew capability is expected to degrade beyond our historical experience base in any Mars mission scenario. Both the extent of degradation and our ability to mitigate the resulting risk are dependent on the effective design and implementation of vehicle, suit, and habitat systems that support the human crew throughout the mission. This leads to consideration of the vehicle side of the balancing act.

As the distance from Earth increases, the operational challenges that the mission experiences also change beyond our historical experience base. At the same time crew capability is decreasing due to degradation from other hazards, the mass, power, volume, and data bandwidth allocations are shrinking for the spacecraft as the distance from Earth increases. And, when far enough from Earth, the small crew is asked to do far more than they have historically been asked to do when real-time communication with Mission Control was possible. These changing realities must be acknowledged and considered as they lead to increasingly difficult challenges in HSIA for long-duration missions beyond LEO.

Consider the following: LEO missions have access to real-time support from MCC engineers and flight surgeons. In contrast, deep space crewed missions will be confronted with high-latency communications that prohibit real-time operational and medical support, infrequent resupply, an inability to evacuate or be rescued, and exposure to greater solar and galactic cosmic radiation. These differences carry the risk that the operational paradigm successfully used in LEO is insufficient to ensure mission success in exploration spaceflight. In a Mars mission, communications can be delayed up to 48 minutes for a round-trip message. In the current paradigm, maintenance and repair for ISS rely heavily on real-time communications with Mission Control to identify, diagnose, and resolve anomalies that occur in the spacecraft or medical issues with crew. Successful resolution of anomalies relies on teaming the knowledge and experience base in the MCC (diagnosing issues and recommending interventions) with the performance capability of the astronaut crew (physically conducting repairs or treating ill/injured crew). In the case of emergency repairs or health issues, real-time communication ensures that the crew has access to the knowledge of ~80 experts at MCC to troubleshoot issues. A Mars crew loses real-time communications early in the mission. This changes the distribution of responsibility between the crew and MCC and requires increasing crew autonomy to successfully respond to urgent issues. While crew autonomy clearly must increase to make up for the loss of real-time communications, several other factors are converging that make actual crew autonomy more difficult to achieve:
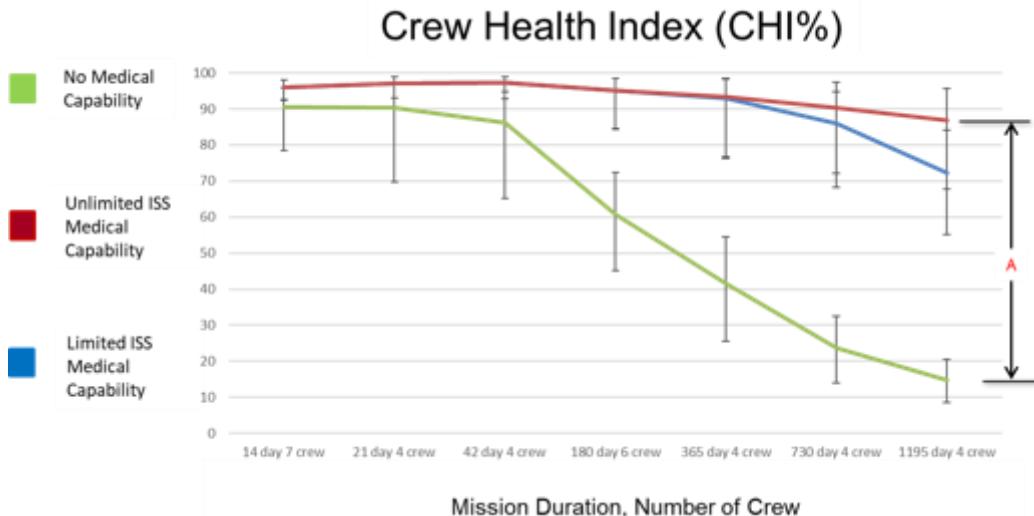
- Mass, power, volume, and data bandwidth for the vehicle become more limited as distance from Earth increases [Antonsen et al. 2016; Human System Risk Management Plan 2020; Ball and Evans 2001; Hamilton et al. 2008; Davis et al. 2021].
- Resupply logistics become more challenging and affect access to spares for repairs, effective medications that can degrade over time, and varieties of food and nutrition that underlie crew health and resilience [Blue et al. 2019a, 2019b; Cooper et al. 2011; Douglas et al. 2020].

- Rapid Earth-return evacuation options change, increasing evacuation times from hours to days for lunar missions and removing evacuation options completely in a Mars mission [Ball and Evans 2001; Antonsen et al. 2016].

- Radiation protection from Earth's magnetosphere is removed potentially contributing to central nervous system and cardiovascular health issues as well as long term cancer risks for crews [Huff et al. 2016; Nelson et al. 2016; Chancellor et al. 2018; Cucinotta and Cacao 2020].

- Communication access to families and support from home decreases, potentially affecting crew resilience [Slack et al. 2016; Palinkas et al. 2000; Hughlett et al. 2020; Landon et al. 2018].

At a time when the cognitive and physical performance of the crew must improve to meet the added mission responsibility that loss of real-time communications presents, the limitations brought by increasing distance from Earth and mission duration actually serve to decondition and degrade the crew. This is a challenging problem to solve without the vehicle, suit, and habitat systems evolving to effectively support the crew in the state they will experience throughout the mission. This is in part an information and data problem and in part a systems engineering and integration problem. Vehicle, suit, and habitat systems must make up for two losses: the loss of the knowledge and expertise from Mission Control in specific cases and the expected degradation of performance the crew will experience throughout a long mission.

To be explicit, the recommendations regarding fast transit, AG, and space radiation protection seek to minimize the degradation in CHP expected throughout these missions and in LTH impacts. The HSIA risk discussed in this and other sections seeks to address the loss of knowledge and expertise from Mission Control and ensure that the systems designed and implemented in the mission architecture effectively make up for the remaining degradation in crew capability.

Establishing how much crew capability will be degraded during exploration missions will determine how mission systems will need to accommodate that degradation. Figure 7.0-1 shows an estimate of how the Crew Health Index (CHI) changes with mission duration [Antonsen et al. 2021]. CHI is a calculated result of the Integrated Medical Model (IMM) used by NASA for estimating medical risk. As a reflection of Quality Adjusted Mission Time Lost, it is not perfect, but it is the only evidence-based quantitative assessment available to inform mission planners about the magnitude of degradation of crew capability during these mission types. Here 100% CHI indicates a fully functional crew and 0% CHI indicates a completely incapacitated crew. For reference missions, there are durations and crew complement for the Space Shuttle (14 days, 7 crew) and a typical ISS mission (180 days, 6 crew). The three curves show the calculated degradation of CHI as a function of medical capability provided: Unlimited ISS Medical Capability (resupply available), Limited ISS Medical Capability (no resupply available), and No Medical Capability (also represents ineffective medical capability).

**Figure 7.0-1. Estimate of how Crew Health Effects on Performance (Crew Health Index or CHI) is expected to Change over Different Mission Durations
("A" shows the potential curves for CHI depending on type and effectiveness of medical capability provided in mission [Antonsen et al., 2021])**

The marker "A" in Figure 7.0-1 shows the potential range of CHI depending on the medical capabilities in the CHP system designed into the mission. There are two important takeaways. First, crew capability degradation will occur, and the dependence on mission duration is only partially dependent on altered gravity and radiation. Second, the degree to which the impacts manifest in overall crew capability, mission success, and LTH can be influenced greatly by how effectively the mission architecture, HSIA, and systems support the crew throughout the mission. Figure 7.0-1 illustrates how one system, the CHP system, can either succeed or fail in supporting the crew based on how it is designed and implemented into the larger mission architecture. In the case of a Mars mission, all of the vehicle systems contribute to crew health, performance, safety, and, by extension, crew capability. The CHP system is described in detail in Appendix D.

The rest of this section explores the current understanding of the multidimensional risk space associated with microgravity exposure, radiation exposure, and HSIA. To examine risk trends, each risk is depicted as a function of mission duration with a second dimension (one of the groups of candidate engineering solutions) viewed parametrically. For this study, risk is defined as the probability of a selected outcome measure. These can include loss of crew (LOC)/loss of mission (LOM), loss of mission objectives (LOMO) due to inadequate crew performance, or LTH[5] outcomes (e.g., medical conditions and quality-of-life impacts). These include estimations

---

[5] LTH does not represent a mission risk per se but raises significant ethical concerns as the health of returning astronauts after the mission must be taken into account. The Institute of Medicine [Kahn et al. 2014], at NASA's request, suggested an ethics-based decision framework for exploration spaceflight that includes ethical principles of avoiding harm, beneficence, acceptable risk/benefit balance, fidelity, fairness, transparency in decision making, and a commitment to continuous learning, as well as risk decision levels: health standards (including waivers), mission-specific, and individual informed consent. To this end, the TREAT Astronauts Act (To Research, Evaluate, Assess, and Treat Astronauts Act) authorizes NASA to 1) expand on current medical monitoring services and, 2) begin providing diagnostic and treatment services for conditions that are associated with spaceflight, which will be provided without any cost-sharing obligation for the astronaut (e.g., deductible or copayment). Additionally, this

of risk due to: 1) known threats/hazards and 2) incomplete characterization of the magnitude of identified threats/hazards and of unknown threats/hazards. Mission duration is used to describe trends as durations increase and for comparison to the ISS experience base. In cases where quantitative metrics for risk are available, they are discussed. When quantitative metrics for risk are not available, a qualitative discussion is included. These sections seek to provide insight into the trade-space options that are likely to result in effective risk mitigation at the mission level.

F-43.	As mission duration increases, crew capability is expected to degrade and the likelihood of LTH impacts is expected to increase. Estimates of expected crew capability degradation are limited.

F-44.	A radical shift in operational paradigm, systems design, and human/system integration approaches is the only viable approach to improve the risk posture.
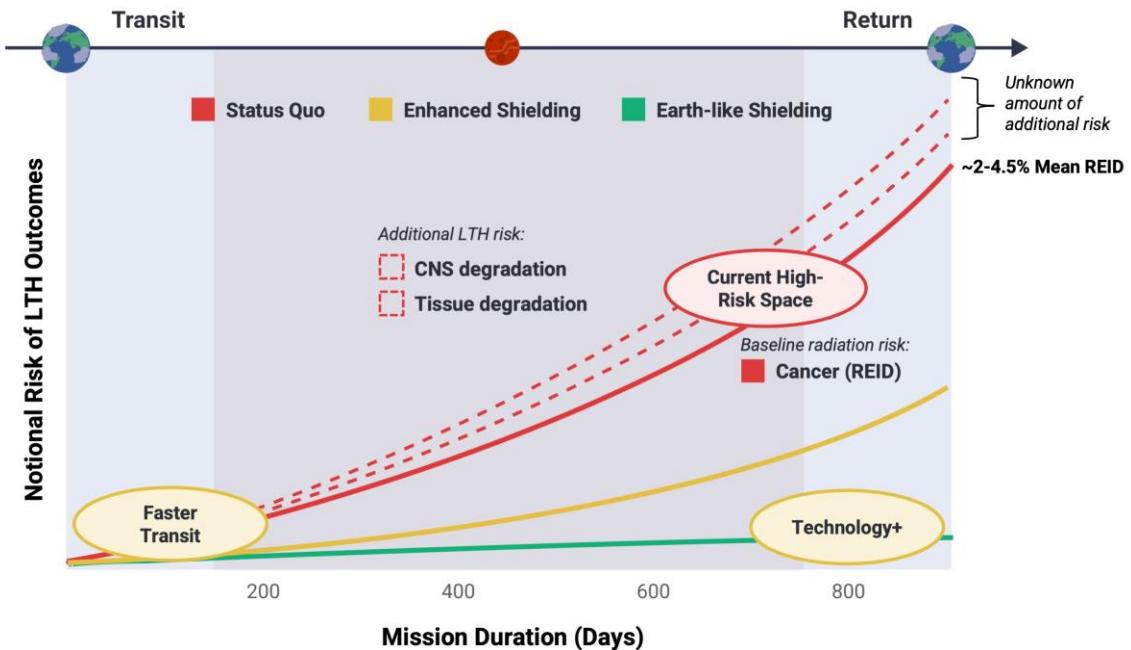
O-9.	Interventions such as fast transit, AG, and radiation mitigations are intended to limit the extent of crew capability degradation and LTH impacts.

7.1 Slice 1: Radiation Exposure Risk

Description: As mission duration increases beyond LEO, radiation risk is expected to increase due to increased time of exposure and loss of the protective effects of Earth's magnetosphere. This primarily affects the risk of radiation carcinogenesis in the LTH domain with suspected contributions to CVD and CNS disease still being characterized [Nelson and Huff 2016; Patel et al. 2016]. In mission risk due to acute radiation syndrome is considered low with spacecraft shielding that has been flown in the past and current recommendations for shielding [Blue et al. 2019c]. Figure 7.1-1 shows the current high-risk space (red line) when considering the upper 95% confidence interval (CI) for the REID due to carcinogenesis. The yellow line illustrates decreased risk through improved shielding or a decrease in our estimate of risk that may be achieved with an improved knowledge base. As estimates of risk improve, the uncertainty is expected to narrow, which may also improve our perception of the risk; this improvement may also be illustrated by the yellow line. Finally, the green line shows the bounding case where advanced shielding technologies or other interventions that may someday approach Earth-like shielding could further improve the risk.

---

health surveillance supports ongoing evaluation of health standards, improves mission safety, and reduces risks for current and future astronauts. While the TREAT Astronauts Act may mitigate some of the consequences of the LTH risk, it does not reduce the increased risk of adverse health incidences due to spaceflight, so it remains critical to assess LTH when choosing between mission designs.

Figure 7.1-1. Notional Radiation Risk Trends showing Current Risk Space and Domains that illustrate Potential Improvements in LTH Outcomes from Radiation Exposure
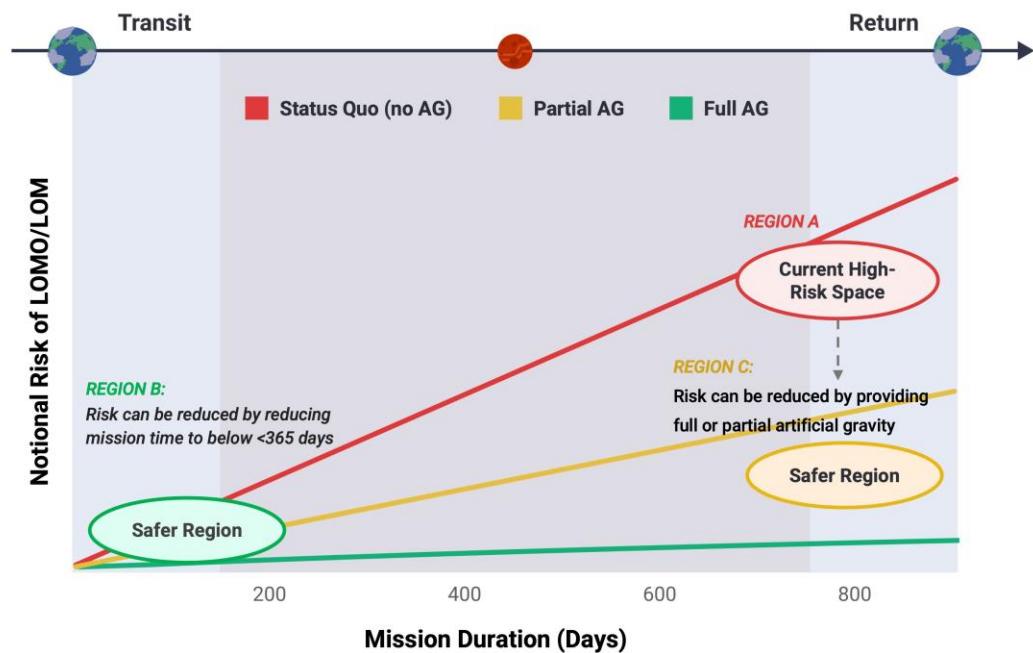
F-45.	Reductions in the radiation-associated LTH risk can be achieved through decreasing exposure time (fast transit) and/or decreasing exposure magnitude (shielding improvements).

O-10.	Improving the knowledge base that frames our understanding of mechanisms and consequences of radiation carcinogenesis, CVD, and CNS impacts may serve to decrease our estimate of risk associated with a Mars mission.

7.2   Slice 2: Altered Gravity Exposure Risk

Description: Long exposures to an altered gravity field serve to degrade crew capability. While historically the bulk of spaceflight exposure has been to microgravity, the potential magnitude of beneficial impacts from lunar or Mars gravity levels that may be experienced by crew is currently unknown. Fifteen of the 30 Human System Risks are in large part a consequence of altered gravity exposure and are significant contributors to degradation of crew capability over time. In the current high-risk space, astronauts will be exposed to a gravity environment characterized by either microgravity or Mars gravity (3/8 g) depending on the mission phase. The longer mission duration, the more severe crew capability impacts become. These impacts will be a mission reality unless one of two interventions occur. First, fast transit can serve to decrease exposure time and thus decrease cumulative degradation of crew capability in mission. This is illustrated by the green Region B in Figure 7.2-1. Second, if some form of AG is implemented in mission, then the cumulative effects of altered gravity will be reduced. In the case of full 1 g, it may move toward the yellow Region B shown in Figure 7.2-1. Partial AG from a short arm centrifuge is suspected to have some mitigating impact on the risk if implemented. A dose-response curve is not available for partial gravity, and as such, the

magnitude of possible mitigation is not well characterized. The yellow line shows a notional illustration of this expected effect. Effectiveness of countermeasures during a mission that does not implement some level of AG is dependent on sufficient mass and volume allocations to provide ISS-level exercise capabilities and sufficient crew motivation to implement these countermeasures. These can become ineffective if crew do not use them as intended or if, through poor human systems integration and systems engineering processes, inadequate exercise capability is ultimately provided in mission.

Figure 7.2-1. Notional Risk Trends showing Current Risk Space and Domains that illustrate Potential Improvements in In-mission Risks due to Altered Gravity Exposure

The human system risks that have an in-mission dependence on altered gravity (primary and secondary) include:

- SANS
- Sensorimotor alterations
- Bone fracture
- Cardiovascular
- Aerobic capacity
- Muscle strength
- Venous thromboembolism
- Urinary retention
- Renal stone
- MicroHost
- Immune
- Sleep

- Dynamic loads
- EVA injury
- Crew egress

The human system risks that have a known LTH dependence on altered gravity exposure include:

- SANS
- Bone fracture

F-46.	Increased duration of exposure to altered gravity worsens multiple human system risks and contributes to degradation of crew capability in mission and for LTH outcomes.

F-47.	Improvements in fast transit or AG can serve to improve risk by reducing exposure time or reducing exposure magnitude.

O-11.	Implementation of fast transit faces engineering hurdles, some outside the scope of this report. These include increases in system complexity that can worsen HSIA risk. In the case of NTP or NEP, risks include development uncertainty and additional radiation considerations for astronauts.

O-12.	Implementation of AG solutions faces developmental hurdles and increases to system complexity that can worsen HSIA risk.

O-13.	Status quo approaches rely on adequate exercise capability to be accepted and fielded by programs during the systems trades and design phases. Historically, this has been a challenge for NASA programs.

7.3   Slice 3: Reduced Ground Support Risk

Description: Figure 7.3-1 shows the notional risk of LOMO/LOM due to inadequate HSIA. Although the HSIA risk is a *function of distance from Earth* rather than mission duration, it is plotted here against mission duration for consistency assuming a ~ 900 day Mars mission. The blue dotted line shows the cumulative probability of a significant anomaly occurring increasing throughout the mission duration (based on the average ISS 1.7/year rate (see Section 6.5.1, Figure 6.5.1-1). Such anomalies bear consequences ranging to LOM, loss of vehicle, and LOC. The red solid line shows the notional cumulative probability of an unresolved anomaly occurring (i.e., an anomaly that the crew-vehicle system is unable to resolve with the onboard HSIA). This trend is affected by the change in one-way communications delay throughout the notional mission as depicted by the yellow line. Because the largest communications delay is experienced near the middle of a Mars mission (e.g., peak distance from Earth), the darker grey box shows a notional representation of the domain where round-trip communication delay is expected to move the crew to a more autonomous operational paradigm than has been experienced before in human spaceflight. Reduction of the risk associated with unresolved anomalies that is mitigated by effective onboard support is shown by the dotted red line.
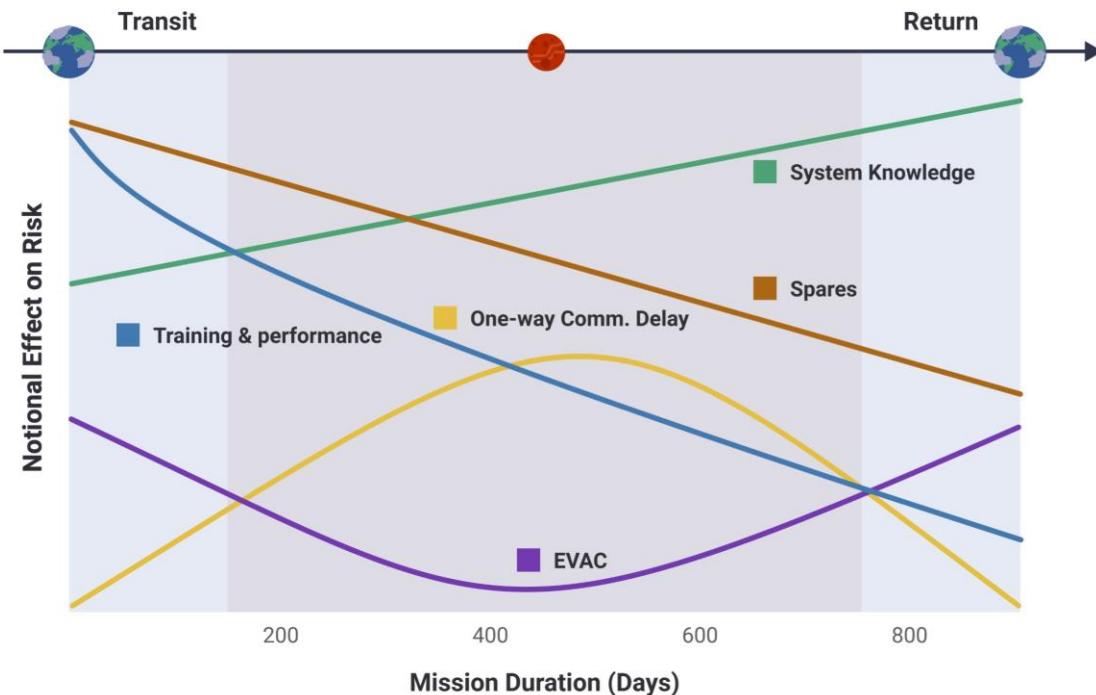
Figure 7.3-1. Notional Risk Trends Due to Inadequate HSIA (these are dependent on factors shown in Figure 7.3-2)

As described here, the trend of the solid red line indicating unresolved anomalies is associated with the communications delay variation throughout the mission. It is also due in part to crew health deterioration and in part to another set of variables that affect crew capability, including:

- **System knowledge:** Crew knowledge and confidence in the vehicle systems are likely to increase throughout the mission as they encounter and deal with anomalies.

- **Evacuation (EVAC):** Options for evacuation in the case of a vehicle failure or health issues decrease as the distance from Earth increases and improve with Earth proximity.

- **Spares and consumables:** Spare parts, including possibly three-dimensional printed parts, for maintaining and repairing critical systems and consumables are used as the mission progresses. If spares are not available or cannot be made, the options for mitigating anomalies decrease.

- **Training and performance:** These show a similar trend to spares; as time continues, the effectiveness of pre-mission training wanes. If in-mission training is realized as part of vehicle systems, then this risk can be mitigated.

Figure 7.3-2 shows this set of variables and their expected variation with mission duration. These trends currently can only be described qualitatively.

Figure 7.3-2. Notional Variables that exert Influence on Ability of Earth-independent Crew to Resolve Anomalies, with the Expected Influence Curves

Assumptions: The notional HSIA risk analysis uses ISS operational experience in LEO. Over its 20-year operational history, the ISS has experienced, on average, 1.7 system anomalies per year that were categorized as high priority or required urgent diagnosis/intervention (see Section 6.5). Such anomalies, if unsuccessfully resolved, have the potential to result in LOC/LOM. In the ISS operational paradigm, real-time support from Mission Control (~80 experts) is responsible for nearly all diagnoses and recommendations for intervention. This constant, real-time support is a primary risk mitigation for ISS and a major reason that adverse outcomes have not been realized during ISS operations. It can be postulated that the loss of real-time communications will have a significant effect on the ability of crews to detect, diagnose, and intervene on vehicle/system anomalies. This assumes that Mars Mission Control will still have 80+ experts and that anomalies will occur that have a time-to-consequence of 40 to 50 minutes or evolve in a way that challenges asynchronous assistance. However, there is significant uncertainty associated with extrapolating anomaly rates and resolution capabilities to the Mars mission operational paradigm, especially considering the unquantified interplay of variables that can affect crew performance.

F-48.	Attempting to use the LEO operational paradigm (the current HSIA) with communication and resupply delays is high risk.
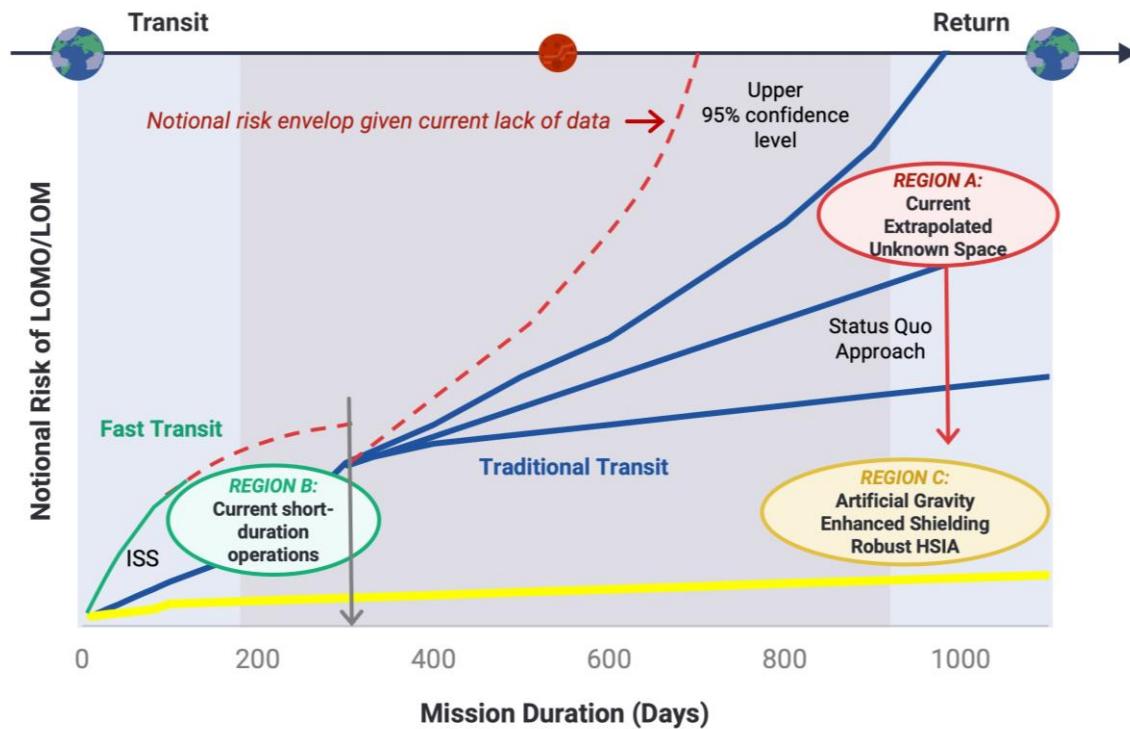
F-49.	A trade space exists between the benefits and increased complexity of new engineering solutions (e.g., fast transit, AG, active shielding, and advanced AI) which affects the HSIA risk.

> **O-14.** NASA has not adequately characterized the magnitude of the HSIA risk and the set of countermeasures needed to ensure mission success.

7.4 Regions of Interest

Within the depiction of these three risks, it becomes clear there are three regions of particular interest that are consistent among slices; these are shown in Figure 7.4-1 to illustrate integrated risk as well as possible risk:

- The "status quo" long-duration mission (>2 years) with current countermeasures, identified as Region A.

- The short-duration "fast transit" scenario(s) with current countermeasures (<1 year), identified as Region B.

- A long-duration "Earth equivalent" mission (>2 years) with more complete mitigation of the three hazards in the scope of this report, identified as Region C. Note there is indeed a continuum between Regions A and C.

Figure 7.4-1. Current Best Illustration of Qualitative Notional Integrated Risk of LOMO/LOM associated with Described Risk Areas

Figure 7.4-1 highlights these three regions, with salient qualitative features. First, note that fast transit associated with Region B does not have the same level of risk currently associated with LEO missions. This is because, regardless of the mission timeframe, the communications delays and limitations on evacuation still apply as distance from Earth increases. Second, the three blue lines marked as traditional transit show a range of possibilities within Region A that are dependent on the success or inadequacy of human/system integration processes that determine vehicle design and operation. The presence or absence of countermeasures and systems

capabilities that address crew capability degradation and make up for the loss of real-time support will determine the level of risk in Region A faced by a traditional mission model. The dotted red line illustrates the upper envelope of risk at a notional 95% CI that currently cannot be calculated. Finally, Region C shows the hypothetical domain that may be achieved by implementation of one or more game-changing approaches, including AG, enhanced radiation countermeasures, and robust HSIA. These are all discussed here in further detail.

7.4.1 LOC/LOM Risks

Region A

Region A includes the current DRM Point of Departure (PoD 2020), Alternative Short Stay (2020), and Basis of Comparison (BoC 2019), lasting between a total of 771 and 1224 days [HEO-DM-1002]. Here, mission risks and challenges are extrapolated in time and carry considerable uncertainty. This region represents the status quo in terms of engineering solutions with associated lower costs and smaller technology risks; however, the cumulative uncertainty across the identified human/systems challenges propagates such that there is a *high likelihood of serious adverse outcomes (e.g., LOC/LOM).* Future research results from extended Artemis lunar missions that involve crew performing on the lunar surface will provide data on the effects of partial gravity exposures during long-duration missions and progressively more Earth-independent operational experience to help reduce this uncertainty.

> **F-50.** The risks of microgravity exposure, radiation exposure, and reduced ground support (inadequate HSIA) increase with Mars mission duration/distance from Earth such that there is a high likelihood of serious adverse outcomes (e.g., LOC/LOM) for 3-year missions (if unmitigated).

Region B

Within Region B, mission risk and challenges are clearer and at least partially understood given the wealth of experience with ISS and in Earth-based analogs of the same duration. In the ISS operational paradigm, a myriad of countermeasures and mitigations have allowed for missions with a reasonably high degree of resilience and effectiveness (although not risk free).

For microgravity exposure, a Mars mission of this shorter (1-year) duration would be able to leverage some of the knowledge and experience from ISS to mitigate the health and performance challenges that accompany crew deterioration over time.

For radiation concerns, there is additional unquantified radiation contribution in operating beyond the Earth's magnetosphere, specifically in cardiovascular and CNS effects. However, given the overall exposure levels and known mitigation strategies, the LOMO/LOM risk from radiation is deemed small and is classified by the HSRB as an accepted risk ($L \times C = 1 \times 1$) [Blue et al. 2019c].

For the HSIA risk, the total number of anomalies expected to occur in a 1-year mission would be reduced from that of a 3-year mission. However, the HSIA challenges (e.g., reduced ground support, lack of resupply, and the effects of a smaller crew) would remain and would be expected to scale with system complexity. Many of the new technologies that would enable fast transit face significant technical hurdles and may increase system complexity and thus increase the notional risk due to inadequate HSIA [[National Academies of Sciences, Engineering, and Medicine, 2021].

Much could be learned about these operational scenarios using Artemis as a test bed, but this would require a considerable increased investment in research over the next decade and, given that the missing data would require 2- to 3-year studies for data collection, it would also take a significant amount of time to fill this key knowledge gap (i.e., the current absence of any human/system data associated with a 2- to 3-year mission).

> **F-51.** A 1-year Mars mission duration significantly reduces the risks of microgravity exposure and radiation exposure. Some benefits would be gained for the risk associated with reduced ground support (inadequate HSIA), but these may be offset by the increased system complexity needed to shorten mission duration.

Region C

Within Region C, mission risk is well identified given that any engineering solution that succeeds in approximating Earth-like or other known low-risk conditions (i.e., Earth gravity, radiation, and largely unlimited decision/operations support and resupply) could at least theoretically succeed in keeping the risks due to microgravity, radiation, and inadequate HSIA relatively low. While getting into this region would require surmounting new and significant engineering challenges (e.g., spinning vehicles, enhanced shielding, breakthrough AI decision support) and may not be fully feasible, being in this region would *de facto* dramatically reduce the hazards associated with deep space missions and reduce the uncertainty.

Full AG (restoration of 1 Earth g) is expected to substantially mitigate approximately 15 of the 30 human/system risks tracked by the HSRB[6] (and partial AG may partially mitigate these individual risks) by moving the mission into an environmental regime where the gravity-associated hazards are relatively well known and understood. Thus, integrated LOMO/LOM and LTH risks would be much lower. Lesser versions of this AG scenario (e.g., lower continuous g levels, intermittent short-armed centrifugation) might also be fully or significantly effective, but there is currently insufficient scientific evidence to determine what minimum g-restoration regime would be necessary to provide meaningful improvement over currently contemplated Region A countermeasures.

For Region C, there is currently no feasible approach for reducing space radiation exposure to Earth-like levels. Passive shielding solutions lead to enormous and impractical mass requirements and costs. Active shielding concepts continue to be investigated but are not yet able to appreciably reduce exposure from high-energy GCR. Pharmaceutical solutions remain theoretical and bear unwanted side effects that could worsen risk [Blue et al., 2019a]. Incremental improvements in shielding and other countermeasures may lower risk, but no concrete path forward currently exists to achieve Region C for the radiation challenge.

Similarly, there is no concrete forward path to achieve Region C for the HSIA challenge. If a vehicle could be built that would carry 100+ crew members with the necessary expertise, if there were a Newton-level breakthrough in AI such that machines could do adaptive problem solving, or if there were space communications that overcame light-time delay, then this risk could be fully mitigated into a Region C. This assumes ongoing access to experts on the ground and that

---

[6] The Human System Risks with expected mitigation due to full AG include SANS, bone fracture, cardiovascular aerobic capacity, muscle strength, urinary retention, crew egress, venous thromboembolism, sensorimotor alterations, renal stone, microhost, immune, sleep, dynamic loads, and EVA injury.

these experts may catch some but not all problems before they become critical. Analyses of MCC support presented in this report indicate that much of MCC's current mitigation functionality depends on real-time communications. Barring such breakthroughs, to achieve some risk reduction it will be necessary to rethink how we design vehicles and habitats such that they are more maintainable, diagnosable, and repairable by the crew than they have been in the past. Further, the selection and preparation of crew will likely differ [Landon et al. 2017, 2018]. Mission systems will need to be wrapped around crew capabilities rather than dependent on ground mitigation. Systematic improvements in HSIA to support Earth-independent operations are critical.

The additional system complexity introduced by unprecedented engineering designs and new technologies to provide AG and advanced radiation shielding is likely to increase the overall risk by increasing the number of potential anomalies in a mission and putting additional requirements on the crew to effectively respond to this new set of possible anomalies in mission. As it stands, the likelihood of finding adequate engineering solutions that move the notional risk into Region C is unlikely when considering the planning timelines for Mars missions.

F-52.	Significant investments in research and technology advancement are needed to reduce the risks of microgravity exposure, radiation exposure, and reduced ground support (inadequate HSIA) to acceptable levels for long Mars mission durations.

O-15.	Apart from AG, Newton-level breakthroughs needed for radiation protection and HSI are unlikely to move a Mars mission toward LEO-like risk levels.

7.4.2 Post-mission LTH Risks

Among the spaceflight LTH risks, radiation-induced carcinogenesis, CVD, and CNS decrements present serious potential long-term consequences with open research gaps needing to be addressed [Human Research Program 2021]. NASA has set career PELs to manage the risk of these LTH effects [NASA-STD-3001, 2019]. The cancer PEL is specified such that an astronaut's career exposure does not exceed a 3% added REID evaluated at a 95% CL to conservatively protect against uncertainties in the risk projection. REID is used to quantify the excess lifetime risk of cancer mortality attributable to radiation exposure and includes sex and age dependencies. Over the range of exposures of interest to human spaceflight, REID is nearly proportional to exposure and decreases with increasing age. For the same exposure, REID for females is larger than for males due to increased radio sensitivity in the lung and additional risk from reproductive organs [Cucinotta et al. 2013]. NASA is currently in the process of updating the standards to a dose-based standard that will likely take place within a year of this writing [National Academies of Sciences, Engineering, and Medicine, 2021].

Regions A and C

Long-duration missions to Mars will lead to exposures beyond the current PEL for all crew with the associated significant post-mission LTH risks. Depending on mission parameters and time in solar cycle, crew exposures can reach ~1 Sv, or physical doses of 0.5 Gy. For NASA astronauts, assumptions regarding smoking status and other health factors are applied when calculating REID. For this reason, astronauts are estimated to have a lower baseline cancer risk than the general US population. At these levels, excess cancer mortality risks (i.e., above baseline risks in an unexposed population) evaluated at the upper 95% confidence level can approach rates seen

in the average US population [Simonsen and Slaba 2021], depending on the underlying epidemiological and radiobiology data and models considered. Thresholds for CVD and CNS effects may also be crossed, thereby increasing the total risk to crew. At this time, there are no viable strategies that are able to mitigate (beyond the known uncertainties) the risk due to radiation exposures. However, NASA undertook an ethical review in 2014 that provided a framework for assessing the risk-benefit balance to the Agency and crews. This framework from the National Academies provides a pathway for responsible exceptions to the current PELs in the domain of Mars missions [Kahn et al. 2014].

The LTH effects of many of the human system risks have significant uncertainty. Despite collecting post-career data through the Lifetime Surveillance of Astronaut Health (LSAH), the population reflects astronauts who have primarily flown in LEO, and those that have flown on ISS have not aged sufficiently to create a significant cohort. Despite this, there is emerging evidence that long-duration astronauts are more susceptible to bone fracture than expected had they not flown. There is no signal of increased radiogenic cancers in the astronaut population to date. The long-term consequences of SANS beyond vision changes remain uncertain, but there have been no clinical signs of additional neurologic or psychiatric issues from the LSAH population. There has been increased risk of injuries from the dynamic loads experienced in the Soyuz landing environment. Data on 70 ISS United States Operational Segment crew members showed that the Brinkley model underpredicted landing injuries in all categories, including four moderate injuries that resulted in pain or functional impairment for crew members for months to years following their mission. The important takeaway is that the uncertainties are high across multiple human system risks when extrapolated in the LTH domain.
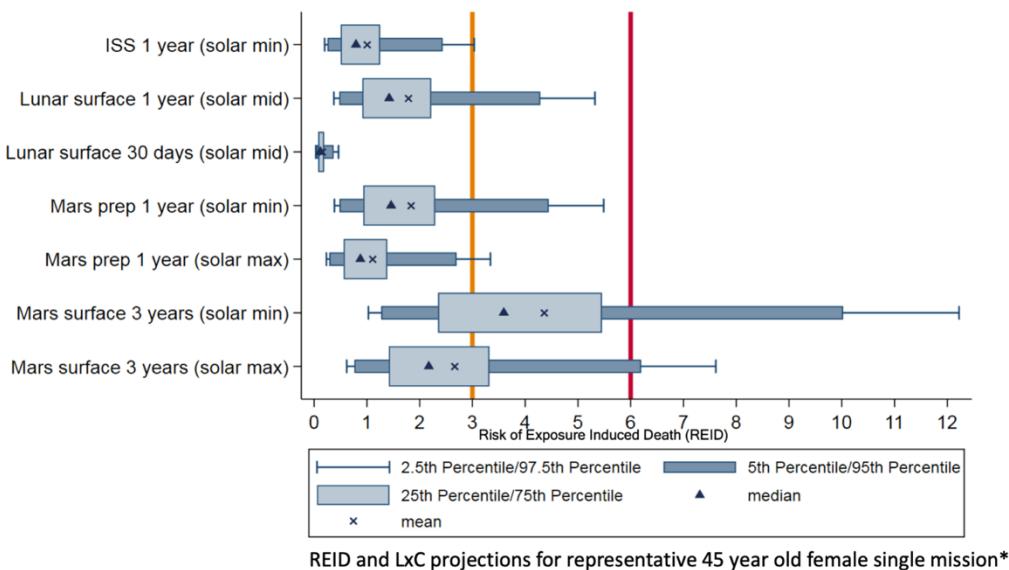
Region B

Space radiation cancer risk projections carry an uncertainty of a factor of ~3.6 (or ~260%) [Simonsen and Slaba 2021]. Quantifying the risk of radiation-induced CVD is even more uncertain due to insufficient epidemiological data to provide a basis from which space radiation effects can be estimated. Ground-based experimental data also exhibit possible dose thresholds and nonlinear dose-response relationships that confound risk projections. At this point, CNS decrements are the least well characterized of the three health risks. Ground-based experiments in rodent models are limited in number, often yield complex dose-response relationships, and have yet to elucidate basic mechanisms or biological targets as has been done for space radiation-induced cancer. Methods for translating animal experimental data to humans also remain elusive. Despite these uncertainties and the critical need for further research in these areas, it is believed that the current cancer PEL is sufficiently conservative to adequately protect against the risk of CVD and CNS decrements. Nuclear propulsion technologies employed to reduce transit time could introduce an additional radiation exposure. However, it would be anticipated that adequate shielding of the reactor would be inherent to such concepts to fully justify their use in space exploration.

For nominal shielding conditions, astronauts participating in short-duration missions of 30 days or less will receive exposures below ~50 mSv with corresponding risk estimates well below current NASA limits for lifetime cancer mortality. On the other hand, a 1-year mission will lead to exposures between 200 and 400 mSv depending on time in solar cycle. Assuming no prior flight experience or other significant terrestrial exposures, such doses may lead to REID projections beyond the current PELs for some crew, depending on age and sex. For example, the

NASA cancer risk model estimates that all astronauts receiving less than 185 mSv will satisfy the PEL, while all astronauts receiving more than 325 mSv will exceed it.

Figure 7.4.2-1 shows the results of a comparison for %REID between several possible missions, including ISS, lunar surface, Mars preparatory, and Mars surface missions. The mean and median values are shown, as well as several CIs for clarity. Calculations are done for solar maximum (lowest radiation dose) and solar minimum (highest radiation dose) for an exemplar case of a 45-year-old female with no prior flights.

Figure 7.4.2-1. Visualization of Estimated REID calculated at Median and Mean and showing Associated Quartile, 90% and 95% CIs for Missions ranging from 1 year ISS at Solar Minimum to Mars Surface 3 years at both Solar Maximum and Solar Minimum (orange line highlights 3% REID, exposures where upper 95% CIs exceed the current NASA standards) [Source: SRAG, NASA JSC]

Current NASA standards protect to less than 3% excess risk at the upper 95% CI. Any extension of the CIs beyond the red line exceeds current NASA standards. These results are calculated by the NASA Space Radiation Cancer model [National Research Council 2012]. Additional work comparing accelerated Mars mission (426 days) with standard Mars mission (890 days) timeframes has been performed. Those results show the difference in the mean REID during solar maximum conditions and suggest a 1.5-2× increased likelihood of the lifetime risk of radiation exposure-induced death from cancer for the longer mission duration [Antonsen et al. 2021]. Note that REID is a measure of the radiation-induced excess risk above what is observed in an un-irradiated, or background, population. For Americans, the lifetime risk of dying from any cancer is 21% for males and 18% for females [American Cancer Society 2022]. Lower numbers are typically used for comparison for astronauts based on smoking status and other health assumptions. Recent updates on astronaut mortality have not found an association between radiation exposures and cancer or cardiovascular mortality in the astronaut cohort to date [Elgart et al. 2018]. However, this must be understood in the context of limited numbers, shorter flight durations, and lower radiation exposures in historical missions.

The LTH risk due to the cumulative microgravity exposure of a 1-year Mars mission is largely equivalent to that on the ISS, assuming that the appropriate level of countermeasures are

included in the vehicle and CHP system design. This largely refers to exercise countermeasures that are of similar efficacy to the full suite available on the ISS. Because of the challenges associated with mass and volume allocations that depend on the mission distance from Earth, this assumption is not a given.

There is, by definition, no post-mission LTH risk associated with HSIA.

8.0   Approaches for Human Health Risk Mitigation

8.1   Fast Transit to Mars

This case study focuses on mitigating human health and performance risks associated with three of the hazards as discussed in Section 7.0. As discussed earlier, extended mission duration compounds the integrated risks. Therefore, engineering solutions to expedite fast transit to deep exploration targets (in this case Mars) are considered. Shortening the time for staging/phasing, the out-bound transit, the Mars surface stay, and/or the Earth return transit would have a direct impact on reducing many human health and performance risks factors for in-mission and post-mission phases. Reduced mission durations primarily benefit altered gravity and radiation human health and performance risk factors. Other benefits of Mars fast transit include avoiding the need for reliance on *in-situ* resource utilization or resupply missions for initial exploration, and reducing the new capability needs and technological and logistical burdens associated with more traditional 900- to 1200-day architectures. Fast transit to Mars will also lay the foundation for sustained missions to Mars and will enable rapid building of infrastructure on the surface of Mars so that humans can live and explore the planet on a long-term basis once they arrive.

Mars fast transit is consistent with the core principles laid out in HEODM-007, including prioritization of reduced Mars mission duration and pursuit of the minimum possible Mars mission architecture for humanity's first expedition to the surface. Fast transit architectures can help inform and round out the portfolio of additional architecture options among the studies in work for the 2030s. Fast transit can also accelerate progress overall in space exploration by advancing a narrower set of universally needed technologies and capabilities.

Fast transit candidate technologies, including NTP and NEP, were recently evaluated by the National Academy of Science. The findings suggest that engineering and developmental realities likely preclude an NEP solution as a technology candidate for Mars missions in the 2030s [Space Nuclear Propulsion Technologies Committee 2021]. They did conclude that NASA could invest in an aggressive development program that may enable an NTP option for a Mars mission launching in 2039 [Space Nuclear Propulsion Technologies Committee 2021]. However, given that mature NEP or NTP systems qualified to carry humans to Mars may be decades away, this case study focuses only on Mars fast transit feasibility from a flight dynamics perspective.

For this case study, "fast transit" is defined as a total Mars mission duration around 400 days or less. The benefits expected of an alternative short mission such as described here have been approximated in prior IMM and NASA Space Cancer Risk (NSCR) model predictions [Antonsen and Van Baalen 2021; Cucinotta et al. 2013]. As compared with a 426-day accelerated Mars mission, a 923-day "standard" Mars mission carries:

- Approximately **2.9** times increased likelihood of experiencing loss of crew life (LOCL) event.

- Approximately **4.7** times increased likelihood that a serious medical condition would occur that would warrant medical EVAC were it available.

- Approximately **19%** worse CHI that contributes to performance decrements across the duration of the mission.

- Between **1.5** and **2** times increased likelihood of the lifetime risk of REID from cancer.

8.1.1 Reference Mission Scenarios

HEO-DM-1002 provides interim guidance on general crewed phase duration assumptions for three conceptual human Mars reference missions; these are shown in Table 8.1.1-1. As outlined in HEO-DM-1002, the Point of Departure (PoD 2020) reference should be used for near-term analysis, research, or technology objectives, which represents a total mission duration between 2.1 and 2.4 Earth years. For longer-term analysis, research, or technology development, the longer stay Basis of Comparison (BoC 2019) reference represents upper bounds for *durations of subsequent expeditions* beyond the first-crew PoD 2020 mission and represents a total mission duration of no more than 3.4 Earth years. An intermediate mission is also included in Table 8.1.1-1, which uses a short-stay concept to fill the niche for a mission with modest surface infrastructure paired with a more efficient in-space transportation system and represents a total mission duration of no more than 2.8 Earth years. These mission concepts may be deprecated or revised when the change request for HEOMD-007 is formally accepted by the Directorate Program Management Council and HEO-DM-1002 is rescinded.

Table 8.1.1-1. Crewed Mars Mission Phase Durations for Research and Analysis Purposes [adapted from HEO-DM-1002]

Reference Mission	Mars Crewed Phase Duration Time (Earth Days)				Interplanetary Time and Total Crew Time Away from Earth
	Crewed Cis Lunar Staging / Phasing	Out-Bound Transit	Mars Surface Stay	Mars Orbit Loiter + Earth Return Transit	
	Microgravity	Microgravity	0.376 g	Microgravity	
Point of Departure (PoD 2020)	**90-day** initial Earth launch window + **40 days** after return (4 crew)	**305 days** (all 4 crew)	**30 days** (only 2 of 4 crew)	**50-day** Mars orbit loiter (2 of 4 crew on surface for 30 of 50 days) then **375 days** return transit (all 4 crew)	**730 days** interplanetary. **Total at least 771 but no more than 860 days**
Alternative Short Stay (2020)	**90-day** initial Earth launch window + **40 days** after return (4 crew)	**Up to 200 days** (all 4 crew)	**30 days** (only 2 of 4 crew)	**Up to 500-day** Mars orbit loiter (2 of 4 crew on surface for 30 of 500 days) then **up to 200 days** return transit (all 4 crew)	**Up to 900 days** interplanetary. **Total no more than 1030 days**
Basis of Comparison (BoC 2019)	**90-day** initial Earth launch window + **40 days** after return (4 crew)	**429 days** (all 4 crew)	**Up to 300 days** (all 4 crew)	**365 days** (all 4 crew)	***1094 days** interplanetary. **Total no more than 1,224 days**

*Durations shown for this concept assume the 2039 departure opportunity; durations vary by opportunity year, but 2039 is generally a bounding case.

Within the context of this case study, another conceptual mission architecture was considered for research and analysis purposes, and high-level details are shown in Table 8.1.1-2. In particular, the Fast Transit (FT 2021) mission concept theoretically meets the objective of targeting a mission duration significantly less than 730 days. A preliminary investigation of trajectories for such a mission architecture is presented in the following section, which describes results of trajectory optimizations performed using GSFC's Evolutionary Mission Trajectory Generator (EMTG) with the goal of minimizing the total mission Δv.

Table 8.1.1-2. Alternative Crewed Mars Mission Phase Durations for Research and Analysis Purposes

Reference Mission	Mars Crewed Phase Duration Time (Earth Days)				Interplanetary Time and Total Crew Time Away from Earth
	Crewed Cis Lunar Staging / Phasing	Out-Bound Transit	Mars Surface Stay	Mars Orbit Loiter + Earth Return Transit	
	Microgravity	Microgravity	0.376 g	Microgravity	
Fast Transit 2021 (FT 2021)	TBD	**130 days** (all crew) [TBR]	**5-15 days** (TBD crew) [TBR]	**270 days** (all crew) [TBR]	**380-390 days** interplanetary. **Total ~400 days**

This feasibility study is discussed in the next section.

8.1.2 Fast Mars Transfer Feasibility Study

8.1.2.1 Introduction

This study describes trajectory feasibility analysis performed by NASA GSFC's Navigation and Mission Design Branch to examine trajectory options for a fast (≤400 day roundtrip) crewed mission to Mars. This analysis builds on and specifically aims to optimize and address key concerns with assumptions made in Bailey et al. [Bailey et al. 2013; Folta et al. 2005, 2013]. This analysis was performed subsequent to a technical interchange meeting with members of the MAT in which the study team for this work attempted to gain a better understanding of realistic values for relevant parameters that could be applied to this study. The current study team fully acknowledges that the work of the MAT encompasses a broader scope than trajectory design alone, and the information presented in this document is not intended to represent a direct competition to the MAT study. Rather, the analysis discussed here is intended to provide a basis for discussion and a groundwork for future analyses into fast Mars transfer options.

With that in mind, the remainder of this feasibility study describes in more detail the scenario under consideration and the tools used to construct trajectory options for this scenario. Preliminary trade study results are presented. Finally, avenues for future work to advance the meaningfulness of this analysis are discussed.

8.1.2.2 Methods

For this study, the software tool Evolutionary Mission Trajectory Generator (EMTG), developed at GSFC, was used for trajectory optimization [Ellison et al. 2018; Englander and Conway 2017; Vavrina et al. 2016]. EMTG was chosen because of its suitability for broad, early-phase trade studies. The scenario was modeled as described in the following bullets. The trade parameters are summarized in Table 8.1.2.2-1.

- The spacecraft departs Earth using a zero-sphere-of-influence (ZSOI), patched-conic launch assumption.

- The spacecraft cruises to Mars. During the Earth-to-Mars cruise, the spacecraft is allowed to perform one deep space maneuver (DSM). The cruise flight time is either unconstrained or constrained to be ≤60 days, ≤90 days, or ≤120 days. The motivation to trade constraints on the Earth-to-Mars flight time in addition to the overall 400-day mission-duration maximum is that, all other factors equal, it is preferable to minimize the Earth-to-Mars transfer time rather than the Mars-to-Earth transfer time. Doing so helps minimize crew risk by placing larger amounts of crew time in deep space later during the mission (i.e., closer to Earth return and Earth-based aid) rather than earlier during the mission.

- At Mars arrival, the spacecraft performs a maneuver at periapse to capture into a 2.5-sol or 5-sol period orbit at Mars with a periapse altitude of 250 km. The capture orbit is constrained to have an inclination of 35 deg relative to the true-of-date Mars equatorial frame to allow the crew to reach a landing site with a latitude up to 35 deg. The orbit size and inclination were selected to be consistent with the assumptions made by the MAT.

- The spacecraft is required to remain in Mars orbit for approximately 10, 15, or 20 sols (i.e., an integer multiple of the period of the capture orbit). The orbit of the spacecraft at Mars is modeled explicitly, as opposed to the ZSOI, patched-conic modeling of Earth departure. In other words, the central body used for the two-body gravity model switches from the Sun to Mars once the spacecraft enters Mars' sphere of influence (SOI). Once at Mars, Mars is modeled as a gravitating body that the spacecraft orbits, not a point in space that the spacecraft intercepts (as was done in Bailey et al. [2013] and Folta et al. [2013]). The spacecraft is allowed to perform one maneuver while in Mars orbit to align the spacecraft for its eventual Mars departure maneuver. Once departed, the central body switches back from Mars to the Sun when the spacecraft exits Mars' SOI. The modeling of additional elements of a full CONOPS was beyond the scope of the work performed thus far. Examples of such elements include rendezvous with pre-placed assets in Mars orbit and the maneuvers of the crew vehicle to move to and from the surface of Mars.

- After staying in Mars orbit for the required amount of time, the spacecraft performs a maneuver near periapse (between –5 deg and 5 deg true anomaly) to place it on a trajectory back to Earth.

- The spacecraft cruises to Earth. During the Mars-to-Earth cruise, cases were modeled in which the spacecraft performs no gravity assists (GAs) or one Venus gravity assist (VGA). The spacecraft is allowed to perform one DSM between each body encounter. The inclusion of a VGA as a trade parameter for the Mars-to-Earth journey was based on the results of a lower-fidelity trade study, which suggested that a VGA during the Mars-to-Earth journey could reduce overall Δv requirements for missions launched during portions of the launch period considered by this trade study. Conversely, the lower-fidelity study suggested that a VGA during the Earth-to-Mars journey would *not* reduce overall Δv requirements, so a VGA during the Earth-to-Mars journey was not included as a trade parameter in the study used to produce the results presented here.

- Earth arrival is modeled as a ZSOI patched conic intercept with the Earth. However, an analytic approximation of a maneuver required to capture the spacecraft into a highly elliptical Earth orbit (periapse altitude = 300 km, apoapse altitude = 318,622 km) is added to the overall Δv total for the mission to approximate the Δv required for Earth capture. From there, the mission may go a few different directions that were not investigated explicitly in this study. For example, after Earth capture, the crew may enter directly into Earth's

atmosphere via an entry capsule (e.g., Orion), or perform additional maneuvers to rendezvous with other assets (e.g., Gateway) before returning to Earth, possibly using a new vehicle obtained at the rendezvous point.

- All trajectory segments are modeled as conics (i.e., two-body, point-mass gravity) for computational speed.
- All propulsive maneuvers (i.e., launch, DSMs, capture/departure maneuvers) are modeled as instantaneous Δv maneuvers.
- The beginning-to-end duration of the mission is constrained to be 400 days or less.

Table 8.1.2.2-1. Trade Parameters

Trade Parameter	Value(s)
Launch date	January 1, 2035 – December 31, 2037
Mars orbit period	2.5 sols, 5 sols
Time in Mars orbit (sols)	10, 15, 20
Total mission duration (days)	≤ 400
Earth-to-Mars flight time (days)	≤ 60, ≤ 90, ≤ 120, unconstrained
GAs	None or VGA during Mars-to-Earth journey

O-16. The analyses described in this assessment report are based on assumptions and constraints developed after consultation with the MAT.

O-17. The trajectory characteristics, including Δv requirements, described in this assessment report represent values obtained for the specific set of assumptions and constraints described in the Fast Mars Transfer study document. Additional analysis would be required to draw conclusions for different sets of assumptions and constraints.

O-18. The analyses described in this assessment report focus on overall Δv minimization. However, further study of the Fast Mars Transfer scenario will necessarily take into account additional, possibly competing, objectives. Additionally, Δv requirements must also be translated into fuel requirements based on architectural development (e.g., propulsion system selection, staging selection, etc.).

An important point to clarify is that the time spent in Mars orbit is not the same as useful crew time spent on the surface of Mars. In general, the more time spent in Mars orbit, the more time the crew can spend on the surface, but the precise correlation depends on multiple factors, including Mars parking orbit period (2.5 sols or 5 sols for this study), surface arrival/departure CONOPS, and overall risk posture. For example, one possible CONOPS involves capturing into Mars orbit at periapse, then having the crew depart the interplanetary vehicle at the first Martian apoapse to then land on the surface near the periapse of the parking orbit. In this CONOPS, a full orbit period passes before the astronauts land on the surface. If the process is reversed to depart the surface (i.e., the ascent vehicle departs the surface when the interplanetary vehicle is near periapse to rendezvous near apoapse, followed by a Mars departure burn at the next periapse), then another full orbit period is required to depart the Mars system *after* the crew has left the surface of Mars. Thus, if this CONOPS were to be used, 10 sols spent by the interplanetary vehicle in Mars orbit does not actually provide any surface time for the astronauts if the orbit

period is 5 sols, and a more aggressive CONOPS is required to make possible crew surface time. Another option is to decrease the size of the Mars parking orbit, thereby providing additional periapses and apoapses in the same absolute amount of time. However, as discussed later when comparing the Δv requirements for the 2.5-sol and 5-sol Mars orbit cases, this comes with the drawback of requiring additional Δv to capture/escape at Mars with the interplanetary vehicle. Direct entry and/or departure to/from the Martian surface are alternative CONOPS elements that could increase time on the surface.

To summarize, when interpreting the results presented here:

- For a 5-sol capture/parking orbit:
  - A 10-sol stay in Mars orbit requires a CONOPS different from the "traditional" CONOPS described in the previous paragraph or a smaller Mars parking orbit to allow non-trivial crew surface time.
  - A 15-sol stay in Mars orbit results in 5 sols of crew surface time, assuming the CONOPS described in the previous paragraph.
  - A 20-sol stay in Mars orbit results in 10 sols of crew surface time, assuming the CONOPS described in the previous paragraph.
- For a 2.5-sol capture/parking orbit:
  - A 10-sol stay in Mars orbit results in 5 sols of crew surface time, assuming the CONOPS described in the previous paragraph.
  - A 15-sol stay in Mars orbit results in 10 sols of crew surface time, assuming the CONOPS described in the previous paragraph.
  - A 20-sol stay in Mars orbit results in 15 sols of crew surface time, assuming the CONOPS described in the previous paragraph.
- For all cases, depending on risk posture, a smaller Mars parking orbit may also be required to yield appropriate crew surface time.
- For a given Mars orbit stay time, the amount of crew surface time could be increased by decreasing the size of the Mars parking orbit, at the cost of increasing the Δv required to capture/escape at Mars and possibly increasing the Δv required to reorient the orbit at Mars.

O-19.	For a Mars orbit stay time of 20 sols or less, a 5-sol Mars parking orbit may be too large to allow for an acceptable amount of time for the crew on the Martian surface.

O-20.	The analyses described in this feasibility study provide only a cursory overview of possible operational concepts for a crewed Mars mission with a total duration of less than 400 days.

O-21.	Further work is needed to develop additional mission architecture elements of a fast crewed Mars mission to provide context for the described Δv trade study.

O-22.	Further work is needed to investigate the implications of current technology and near-term technology development on the feasibility of a fast crewed Mars mission architecture based on the described trajectories.

8.1.2.3   Preliminary Results

8.1.2.3.1   *Unconstrained Earth-to-Mars Flight Time*

This section describes candidate trajectories whose Earth-to-Mars flight time is not specifically constrained (although the total mission flight time is constrained to be less than 400 days) and represent the minimum Δv cases found in this study. Figures 8.1.2.3.1-1 and 8.1.2.3.1-2 show Δv as a function of launch date for the launch period investigated for the 5-sol and 2.5-sol parking orbit cases, respectively. The different marker types in the figures represent different Mars orbit stay times and whether or not a Mars-to-Earth VGA is used.

Figure 8.1.2.3.1-1. Δv as Function of Launch Date for 5-sol Mars Parking Orbit, with and without VGA

Figure 8.1.2.3.1-2. Δv as Function of Launch Date for 2.5-sol Mars Parking Orbit, with and without VGA

When examining Figures 8.1.2.3.1-1 and 8.1.2.3.1-2, it is clear that the automated trade study procedure used to generate the trajectories did not "finish" in the time available to perform the work. This is the cause of the "stray" markers that do not conform to the broader trends present in the figures. Nevertheless, several comments can be made about the data.

- There are multiple local minima in the figures: there is a local minimum in June/July 2035 for the no-VGA and the Mars-to-Earth VGA cases, there is a local minimum in December 2036 for the no-VGA case, and there is a local minimum in September 2037 for the no-VGA case (one Earth-Mars synodic period after the June/July 2035 opportunity).

- The overall lowest-Δv cases found are for the Mars-to-Earth VGA scenario using a June/July 2035 launch. The smallest Δv values are given in Table 8.1.2.3.1-1.

- If no VGA is allowed, then the overall lowest-Δv cases are found during the December 2036 launch opportunity. The smallest Δv values are given in Table 8.1.2.3.1-2.

- Thus, for the launch period considered, allowing the Mars-to-Earth VGA saves on the order of 1 kilometers per second (km/s) Δv versus the minimum Δv value found for a trajectory with no GAs.

- As expected, increasing the Mars orbit stay time from 10 to 20 sols increases the Δv requirement. The "penalty" for increasing the stay time by 5 sols varies but is on the order of several hundred meters per second (m/s).

- Also as expected, a shorter Mars parking orbit period increases the Δv requirement. The 2.5-sol period case requires several hundred m/s additional Δv compared with the 5-sol period case.

Table 8.1.2.3.1-1. Minimum-Δv Trajectories, VGA during Mars-to-Earth Transfer

Mars Orbit Stay Time	Mars Parking Orbit Period	Launch Date	Earth-to-Mars Flight Time	Total Δv
10 sols	5 sols	6/25/2035	132 days	13.67 km/s
15 sols	5 sols	7/3/2035	128 days	14.26 km/s[7]
20 sols	5 sols	6/18/2035	129 days	14.76 km/s[8]
10 sols	2.5 sols	6/25/2035	131 days	13.87 km/s
15 sols	2.5 sols	6/25/2035	130 days	14.27 km/s
20 sols	2.5 sols	6/24/2035	128 days	14.70 km/s

Table 8.1.2.3.1-2. Minimum-Δv Trajectories, no VGA

Mars Orbit Stay Time	Mars Parking Orbit Period	Launch Date	Earth-to-Mars Flight Time	Total Δv
10 sols	5 sols	12/3/2036	260 days	15.02 km/s
15 sols	5 sols	12/4/2036	259 days	15.37 km/s
20 sols	5 sols	12/3/2036	253 days	15.74 km/s
10 sols	2.5 sols	12/4/2036	261 days	15.24 km/s
15 sols	2.5 sols	12/3/2036	256 days	15.56 km/s
20 sols	2.5 sols	12/3/2036	252 days	15.94 km/s

F-53.	For the scenario and launch period analyzed in this study, minimum roundtrip Earth-Mars-Earth Δv requirements are found to be approximately 14 km/s when a VGA is used during the Mars-to-Earth journey and approximately 15 km/s when no VGA is used.

F-54.	During the 2035 to 2037 launch period analyzed in this study, a VGA during the Mars-to-Earth journey is found to reduce Δv requirements by more than 1 km/s. A VGA requires the geometry of Earth, Mars, and Venus to align properly, so the geometry for a beneficial VGA does not repeat as frequently as the geometry for an Earth-Mars-Earth trajectory without a VGA.

F-55.	For the scenario analyzed in this study, placing the spacecraft in a 2.5-sol Mars parking orbit increases Δv requirements by approximately 200 m/s compared with placing the spacecraft in a 5-sol orbit.

F-56.	For the scenario analyzed in this study, increasing the Mars orbit stay time from 10 sols to 15 sols increases Δv requirements by 300 to 600 m/s. Increasing the Mars orbit stay time from 15 to 20 sols increases Δv requirements by a further 300 to 600 m/s.

---

[7] It is almost certain that a lower-Δv trajectory exists for this case because of the comparable-Δv trajectory found for the 2.5-sol parking orbit case.

[8] It is almost certain that a lower-Δv trajectory exists for this case because of the lower-Δv trajectory found for the 2.5-sol parking orbit case.

F-57.	The minimum-Δv trajectories without a VGA use a >2km/s DSM during the Earth-to-Mars journey.

O-23.	Further analysis on Mars parking orbits smaller than 5 sols (e.g., 2.5 sols) is needed because the benefits of a smaller orbit are likely to outweigh the Δv penalty for a Mars orbit stay time of 20 sols or less.

O-24.	Additional trade studies are needed to further understand specific elements of the fast Mars trajectory trade space, such as the >2 km/s DSM during the Earth-to-Mars journey for the minimum-Δv trajectory without a VGA.

F-58.	The minimum-Δv trajectories found in this study result in minimum solar distances approximately equal to Venus's orbital distance, regardless of whether a VGA is used. Solar distances less than Earth's orbital distance are driven by the short flight-time requirement.
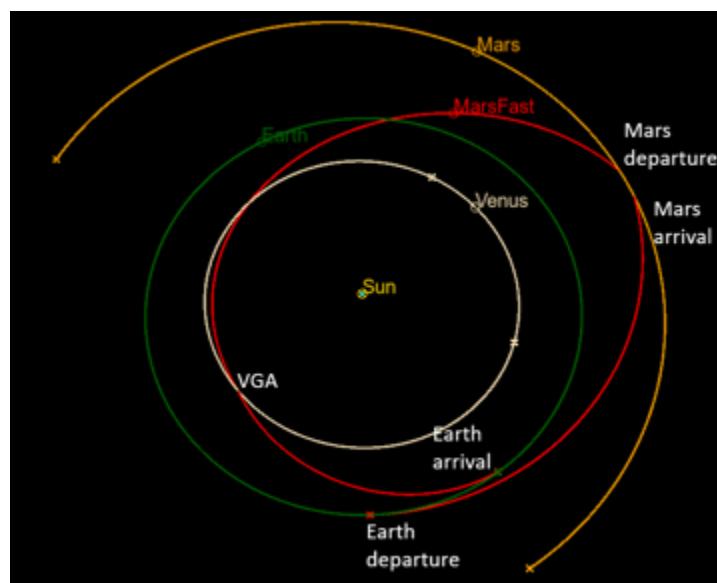
F-59.	The minimum-Δv trajectories found in this study result in maximum solar distances approximately equal to Mars's orbital distance. Solar distances greater than Mars' orbit distance are generally incompatible with the short flight-time requirement.

Tables 8.1.2.3.1-1 and 8.1.2.3.1-2 show the overall minimum-Δv trajectories found for the cases with and without a VGA, respectively. For 10-sol Mars orbit stay times, additional details are given for the minimum-Δv cases in Table 8.1.2.3.1-3. These trajectories are also plotted in Figures 8.1.2.3.1-3 and 8.1.2.3.1-4, respectively.
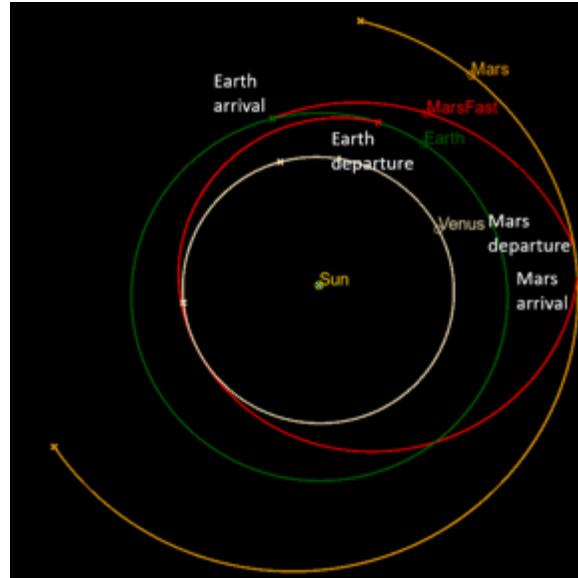
Table 8.1.2.3.1-3. Trajectory Characteristics for Minimum-Δv Cases for 10-sol Mars Orbit Stay Times

Trajectory Characteristic	With VGA, 5-sol orbit	With VGA, 2.5-sol orbit	Without VGA, 5-sol orbit	Without VGA, 2.5-sol orbit
Dates				
Earth departure date	6/25/2035	6/25/2035	12/3/2036	12/4/2036
Mars orbit capture date	11/4/2035	11/3/2035	8/20/2037	8/22/2037
Mars orbit departure date	11/14/2035	11/13/2035	8/30/2037	9/1/2037
Earth arrival date	7/29/2036	7/29/2036	1/7/2038	1/8/2038
Timespans				
Earth to Mars SOI	130 days	129 days	258 days	259 days
In Mars orbit	10 sols	10 sols	10 sols	10 sols
Mars SOI to Earth	256 days	257 days	128 days	127 days
Total mission duration	400 days	400 days	400 days	400 days
Maneuvers				
Earth departure	3.972 km/s	3.992 km/s	3.637 km/s	3.601 km/s
Earth-to-Mars DSM	0.000 km/s	0.000 km/s	2.760 km/s	2.761 km/s
Mars capture	2.609 km/s	2.692 km/s	3.215 km/s	3.211 km/s

Trajectory Characteristic	With VGA, 5-sol orbit	With VGA, 2.5-sol orbit	Without VGA, 5-sol orbit	Without VGA, 2.5-sol orbit
Mars orbit reorientation	0.340 km/s	0.475 km/s	0.494 km/s	0.600 km/s
Mars departure	5.660 km/s	5.620 km/s	3.583 km/s	3.714 km/s
Mars-to-Earth DSM (no VGA)	N/A	N/A	0.000 km/s	0.000 km/s
Pre-VGA DSM	0.000 km/s	0.000 km/s	N/A	N/A
Post-VGA DSM	0.000 km/s	0.000 km/s	N/A	N/A
Earth capture	1.089 km/s	1.087 km/s	1.333 km/s	1.319 km/s
Total Δv, including Earth departure	13.669 km/s	13.867 km/s	15.023 km/s	15.207 km/s
VGA				
Date	5/13/2036	5/13/2036	N/A	N/A
Altitude	1004 km	1068 km	N/A	N/A
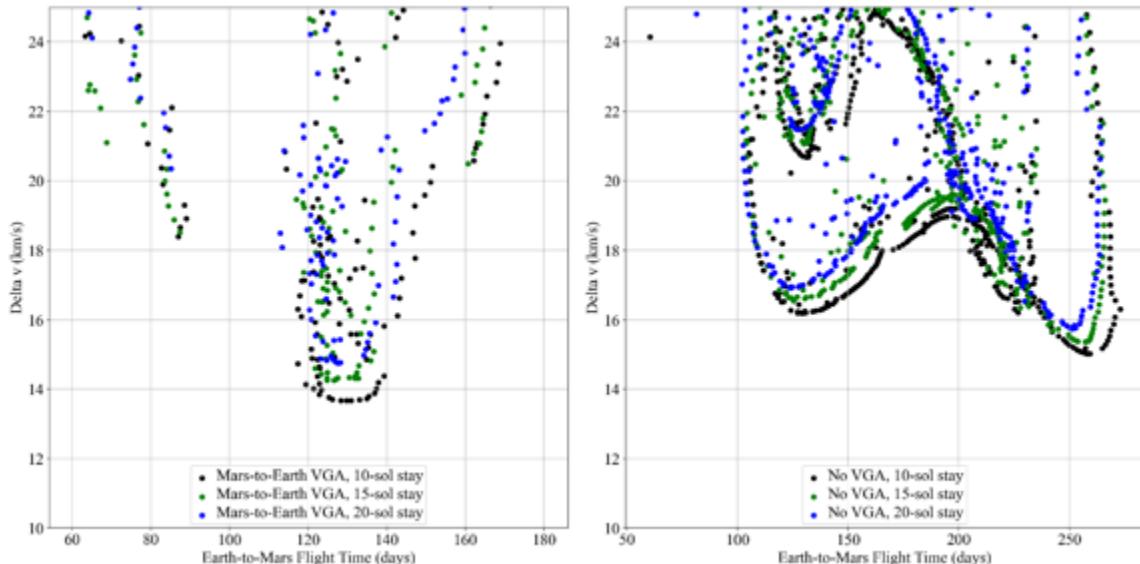
Figure 8.1.2.3.1-3. Overall Minimum-Δv Solution found with VGA (13.67 km/s)
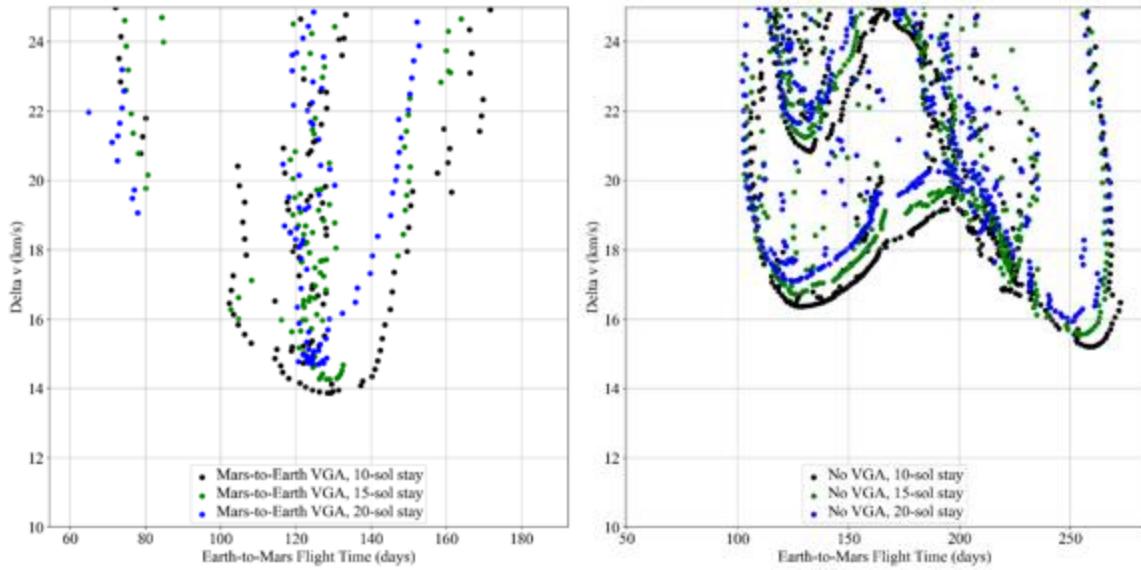
Figure 8.1.2.3.1-4. Overall Minimum-Δv Solution found without VGA (15.02 km/s)

Figures 8.1.2.3.1-5 and 8.1.2.3.1-6 show total Δv as a function of Earth-to-Mars flight time. In addition to the stray data points providing further verification that additional optimization is possible for some cases, it is clear that all local minima previously described have an Earth-to-Mars flight time well over 100 days (approximately 125 days for the minimum-Δv VGA case).

Figure 8.1.2.3.1-5. Δv as function of Earth-to-Mars Flight Time for 5-sol Mars Parking Orbit with (left) and without (right) VGA; Unconstrained Earth-to-Mars Flight Time

Figure 8.1.2.3.1-6. Δv as Function of Earth-to-Mars Flight Time for 2.5-sol Mars Parking Orbit with (left) and without (right) VGA; Unconstrained Earth-to-Mars Flight Time

8.1.2.3.1.1   Alternative Option: Minimum Time in Deep Space with Longer Time Spent at Mars

An alternative option to strictly enforcing a 400-day total mission duration is to focus on minimizing crew time in space rather than minimizing end-to-end mission duration. This option is worth considering because time spent on Mars is likely to be better on the human body and mind than time spent in a spacecraft in interplanetary space. Additionally, trajectory options that prioritize minimizing cruise time could yield both reduced total cruise time and reduced Δv requirements compared with the solutions presented in more detail here. The cost would be an increase in the total mission duration; specifically, an increase in the amount of time the crew spends at Mars. Potential advantages and disadvantages of this option are described in Table 8.1.2.3.1-4.

Table 8.1.2.3.1-4. Potential Advantages and Disadvantages of minimizing Crew Time in Deep Space while increasing Time Spent at Mars

Advantages	Disadvantages
Shorter time in microgravity	Longer total mission duration
More time available for *in situ* study of Mars	More resources required at Mars
Fewer resources required in transit	Increased reliability/maintenance requirements on assets at Mars
Lower total Δv requirement for crew's trajectory to/from Mars	
Longer time at Mars allows for increased mission schedule flexibility and margin for activities at Mars	

An example trajectory of this type can be pieced together from the Earth-to-Mars leg of the "With VGA" column and the Mars-to-Earth leg of the "Without VGA" column in Table 8.1.2.3.1-3. This option would result in the crew staying at Mars from the "With VGA" Mars arrival date until the "Without VGA" Mars departure date. The details of a trajectory option of this type are given in Table 8.1.2.3.1-5. The Mars orbit reorientation maneuver magnitude is approximated as the maximum of the reorientation maneuver magnitudes given in

Table 8.1.2.3.1-3. The total time spent in cruise is reduced by more than 100 days, from more than 380 days to less than 260 days. The total mission duration, however, is increased from 400 days to nearly 930 days, with about 660 days available to spend on the Martian surface. The total Δv is reduced by more than 1 km/s and does not require a VGA, compared with the best case presented in Table 8.1.2.3.1-3, which does require a VGA.

Table 8.1.2.3.1-5. Trajectory Characteristics for Sample Short In-space Time, long at-Mars Time Case; no VGA

Trajectory Characteristic	5-sol orbit	2.5-sol orbit
Dates		
Earth departure date	6/25/2035	6/25/2035
Mars orbit capture date	11/4/2035	11/3/2035
Mars orbit departure date	8/30/2037	9/1/2037
Earth arrival date	1/7/2038	1/8/2038
Earth to Mars SOI	130 days	129 days
In Mars orbit	665 days	558 days
Mars SOI to Earth	128 days	127 days
Total cruise duration	258 days	256 days
Total mission duration	927 days	928 days
Maneuvers		
Earth departure	3.972 km/s	3.992 km/s
Earth-to-Mars DSM	0.000 km/s	0.000 km/s
Mars capture	2.609 km/s	2.692 km/s
Mars orbit reorientation	~0.600 km/s	~0.600 km/s
Mars departure	3.583 km/s	3.714 km/s
Mars-to-Earth DSM (no VGA)	0.000 km/s	0.000 km/s
Earth capture	1.333 km/s	1.319 km/s
Total Δv, including Earth departure	~12.097 km/s	~12.317 km/s

F-60. If the total mission duration for a crewed mission to Mars is allowed to be significantly greater than 400 days, then the crew time in interplanetary cruise can be significantly reduced compared with the case in which the total mission duration is limited to 400 days. The additional total mission duration is spent at Mars.

O-25. It would be beneficial to examine in more depth the implication of trajectory options that produce short total cruise times (less than 300 days) but long Mars stay times (greater than 600 days).
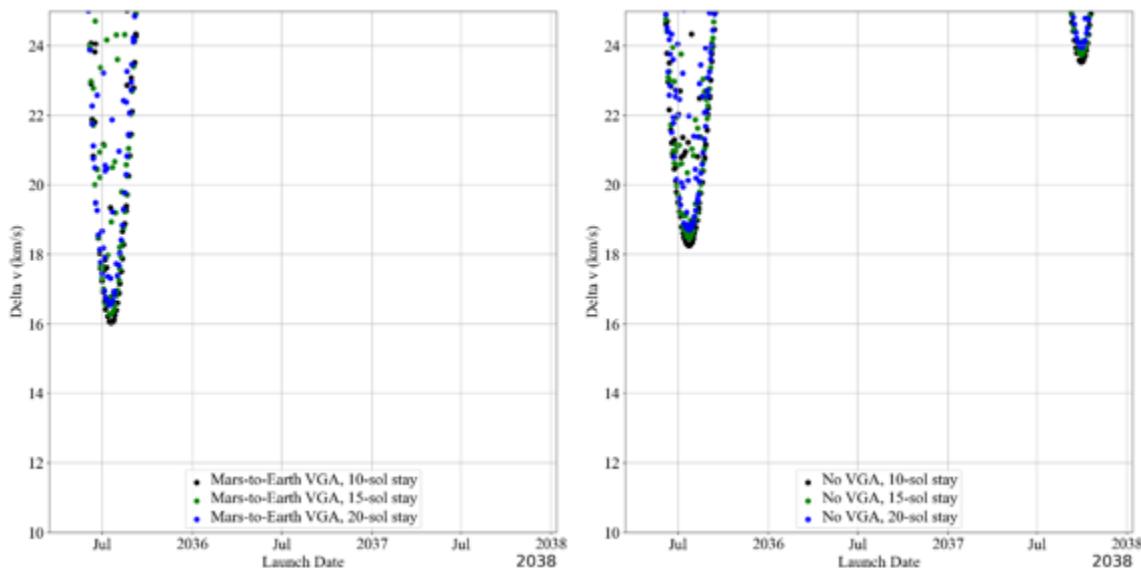
8.1.2.3.2 *Constrained Earth-to-Mars Flight Time*

In addition to limiting total mission duration to under 400 days, there are benefits of having a shorter trip time for the cruise to Mars than for the return cruise to Earth. For example, if a crew emergency were to occur during cruise, it is preferable that the crew be on their way to Earth—and ground-based assistance—rather than to Mars. Decreasing the Earth-to-Mars cruise time reduces the likelihood of a crew emergency happening during this time. Thus, in addition to the unconstrained Earth-to-Mars flight time results presented in the previous section, this section describes trajectories resulting from constraining the Earth-to-Mars flight time to be no greater than 60, 90, or 120 days. As expected based on Figures 8.1.2.3.1-3 and 8.1.2.3.1-4, the Δv values
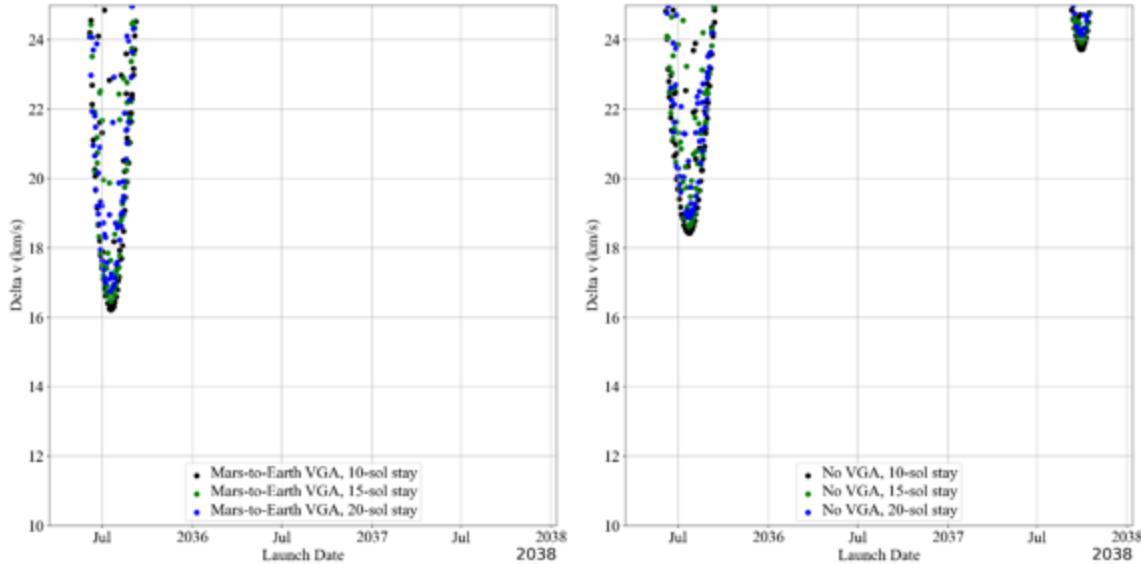
are greater than for the unconstrained case. For a 60-day Earth-to-Mars flight time, no solutions have been found with a total Δv less than 25 km/s, and no further details of 60-day cases are discussed here. On the other end of the spectrum, the Δv penalty for restricting the Earth-to-Mars flight time to no greater than 120 days is relatively small (on the order of 100 m/s) for the summer 2035 launch opportunity because the Earth-to-Mars flight time for the Δv-optimal case is only marginally greater than 120 days even when the Earth-to-Mars flight time is unconstrained. However, the Δv penalty on the December 2036 launch opportunity is much larger because of the ~260-day Earth-to-Mars flight time for the Δv-optimal case when the Earth-to-Mars flight time is not constrained.

For a 90-day Earth-to-Mars flight time, the Δv penalty grows to greater than 2 km/s for the summer 2035 launch opportunity, with or without a VGA during the Mars-to-Earth leg. The lowest-Δv trajectory found (with a VGA) requires more than 16 km/s of Δv. The 90-day limited case is shown in Figures 8.1.2.3.2-1 and 8.1.2.3.2-2.

F-61.	The minimum-Δv trajectories found in this study have Earth-to-Mars flight times of approximately 130 days. Restricting the Earth-to-Mars flight time to 90 days or fewer results in a Δv increase of more than 2 km/s.

Figure 8.1.2.3.2-1. Δv as Function of Launch Date for 5-sol Mars Parking Orbit with Earth-to-Mars Time of Flight no Greater than 90 days, with and without a VGA

Figure 8.1.2.3.2-2. Δv as Function of Launch Date for 2.5-sol Mars Parking Orbit with Earth-to-Mars Time of Flight no Greater than 90 days, with and without a VGA

8.1.2.4   Comments on Concept Feasibility and Recommendations for Future Work

This feasibility study represents an initial investigation to update and improve upon the fast Mars mission architecture presented in Bailey et al. [2013] and Folta et al. [2013]. Specifically, this study presents trajectories obtained by minimizing the Δv required for a crewed mission to Mars with a total flight time no greater than 400 days, with 10 to 20 sols spent in a Mars parking orbit, with orbit periods of 2.5 or 5 sols. A subset of this time would be used for operations on the Martian surface.The analysis techniques and assumptions used here address some potential concerns with the assumptions made in the 2013 study, such as:

- **Stay time at Mars:** This analysis increases the Mars stay time, examining cases with stay times of up to 20 sols in Mars' SOI. In addition, this analysis examines Mars parking periods of 2.5 sols and 5 sols, providing insight into the trade between Δv and parking orbit size.

- **Earth return:** This analysis does not assume direct entry to Earth upon return and includes Δv for capture into a highly elliptical Earth orbit in the overall Δv budget.

Nevertheless, additional design elements discussed in Bailey et al. [2013] must be evaluated in future work to assess mission architecture feasibility. This list includes:

- Distribution of staging and propellent resources (e.g., propellant depots in cislunar space and/or at Mars) and prepositioning of assets. These elements were integral to the architecture proposed by the 2013 study and make feasible larger end-to-end Δv requirements when compared with architectures that do not use staging or prepositioning.

- Prepositioning of assets.

- Propulsion system selection and design.

- Crew asset design, including interplanetary vehicle/habitat, Mars landing and ascent vehicles, and Mars surface habitat.

- Food and water requirements and distribution.

This list forms part of the multitude of directions in which future work could proceed to increase the realism of the preliminary results presented here and/or further explore the trade space of possibilities for a fast Mars transfer. Some of these activities could be performed by the current study team, while others would benefit greatly from increased collaboration with the MAT and potentially other experts. Possible work includes:

- Exploration of additional launch dates. This work examined a 3-year launch period (2035-2037), which covers slightly more than one Earth-Mars synodic period. However, there are differences in Δv requirements from one synodic period to the next, as well as other time-dependent effects, ranging from the physical (e.g., solar cycle, availability of VGAs) to the programmatic (e.g., launch vehicle availability, funding profiles) that necessitate the investigation of a longer time period for launches.

- Investigation of launch-period duration requirements for the fast Mars transfer option and comparison with the launch-period duration requirements of alternative architectures.

- Investigation of the risks and benefits of using prepositioned propellant assets (e.g., in Mars orbit) versus bringing all resources to Mars at once to determine whether currently available chemical propulsion systems are viable to perform the maneuvers required by a fast Mars transfer.

- Investigation of mission duration constraints between the 400-day value studied in this report and durations of greater than 800 days proposed in alternate architectures.

- Investigation of the effects of different propulsion systems on the trajectories. The work presented here assumes Δv impulses for all maneuvers to simplify the optimization problems. In reality, of course, these maneuvers are finite burns that do not occur instantaneously. Modeling the maneuvers more realistically allows for (1) the estimation of fuel requirements for different propulsion systems and (2) the estimation of the effects of "finite burn losses" (e.g., the reduction in the efficiency of a maneuver because it does not occur instantaneously at the optimal time).

- Further inclusion of realistic CONOPS constraints. The work presented in this study attempts to approximate some CONOPS constraints (e.g., the inclination of the Mars orbit to allow the astronauts to achieve a desired landing site). However, there are many potential CONOPS constraints that were not considered in this study. Further refinement of a realistic CONOPS and inclusion of derived requirements on the trajectory are needed to make results directly comparable with those produced by previous studies that *were* based on a fully developed CONOPS. To give one example, this work did not examine the requirements for a crew "taxi" vehicle at Mars to take the astronauts from the primary interplanetary vehicle to the Mars surface and back.

- Investigation of the implications of using the Lunar Gateway and possible Mars Gateway as staging areas.

- Investigation of the implications of the trajectory options on the overall mission architecture. Perhaps mostly importantly, this work has not attempted to address how many launches would be required to preposition assets in the Earth-Moon system and/or at Mars to accomplish a fast crewed Mars mission.

- Investigation of the risks and beneifts of using Earth-Mars cycler trajectories. One of the key trades is that, while cycler trajectories potentially enable multiple missions to Mars using currently available propultion systems with significant propellant savings, these architectures

require hyperbolic rendezvous of the crew with an interplanetary vehicle that has been prepositioned on the cycler trajectory. Such a rendezvous is required both at Earth departure and Mars departure, and may require the ability to abort the rendezvous to produce an acceptable risk level.

- Additional investigation of minimizing total flight time in interplanetary space rather than minimizing the total mission duration. This report presents a sample trajectory of this type, but the assessment team did not perform significant analyses to fully characterize this trajectory trade space. In addition to trajectory optimization, this work requires a trade of crew time spent in interplanetary space versus time spent at Mars versus total mission duration, and the impact of the three on the crew's physical and mental health.

- Increase the modeling fidelity. In particular, the Earth departure and Earth arrival events are modeled using ZSOI patched-conic events and therefore do not represent true flyable trajectories. At the same time, changing the modeling fidelity is unlikely to result in a large change in Δv requirements unless other assumptions also change (e.g., the size of the Earth-return capture orbit).

- Investigation of additional factors that were not the focus of this study but that may drive aspects of the trajectory design. For example, the mental health of the crew in isolation may play a role in the maximum allowable curise flight time to and from Mars (in addition to restrictions based on exposure to microgravity and radiation). Mental health in isolation may also play a role in crew size—which drives vehicle mass and resource needs in space and at Mars—and how many crew members venture to the Martian surface versus stay in Mars orbit. These factors could have direct impacts on the trajectory requirements and therefore the feasibility of the mission.

S-3.	Fast Mars transit approaches (i.e., round-trip duration of approximately one year) using on-orbit staging with chemical propulsion, or nuclear thermal or electric propulsion (NTP or NEP) technologies should be studied further as a possible baseline mission approach to reduce the integrated risks.

8.2   Passive Shielding for Mars Mission GCR Protection

8.2.1   Background
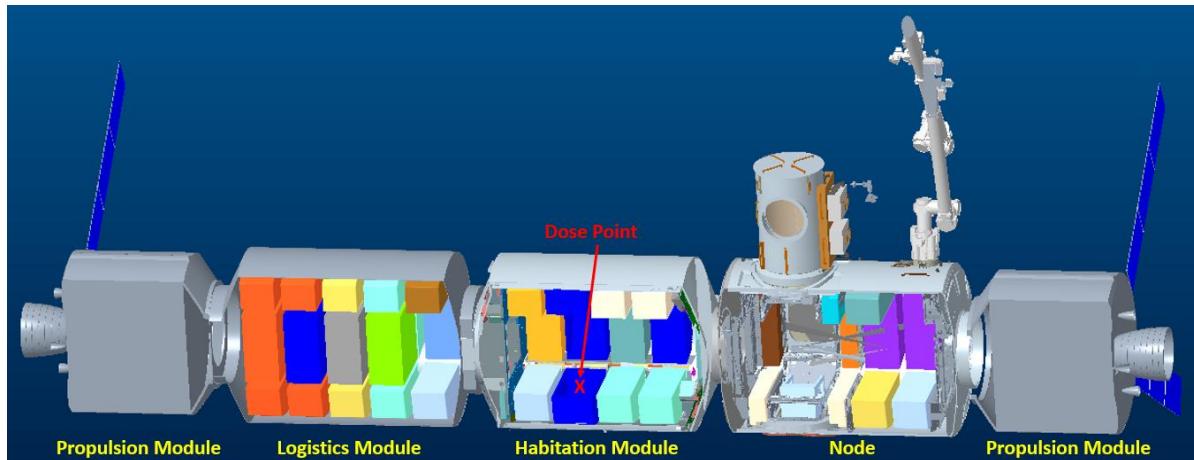
Numerous analyses have been performed examining the effectiveness of material mass shielding for space radiation [Townsend et al. 1989; Simonsen et al. 1990; Wilson et al. 1991, 2001]. As the radiation environment of space is dominated by high-energy ions with charges ranging from $Z = 1$ to $Z = 26$ and higher, any material encountered by the environment will induce both atomic and nuclear interactions. The space radiation environment is typically defined by the source of the radiation, with two main sources considered: solar and galactic. SPEs originate from the Sun, and GCRs originate from within the galaxy but outside the solar system. In general, it has been shown that passive spacecraft shielding is highly effective in shielding SPEs, while shielding GCRs with traditional mass shielding is more difficult due to the high energy and complex nature of GCRs.

The secondary environment induced from the primary particles is a combination of primary particles that have not changed through nuclear interactions and secondary particles produced through nuclear interactions. The analysis of shielding material in simple slabs has generally shown that the smaller the average charge of a shielding material, the better the shielding

efficacy of the material [Wilson et al. 1991]. This is especially true for materials that have high hydrogen content. The charge to mass ratio of hydrogen means that it is particularly good at slowing particles through elastic collisions. Additionally, the simple nucleus of hydrogen consisting of a single proton means that target fragmentation is not an issue for hydrogen. Note that the largest driver of shielding effectiveness is the mass of material, and the material composition is secondary to that consideration.

8.2.2 Examination of Passive Shielding for Mars Mission GCR Protection Analysis Assumptions
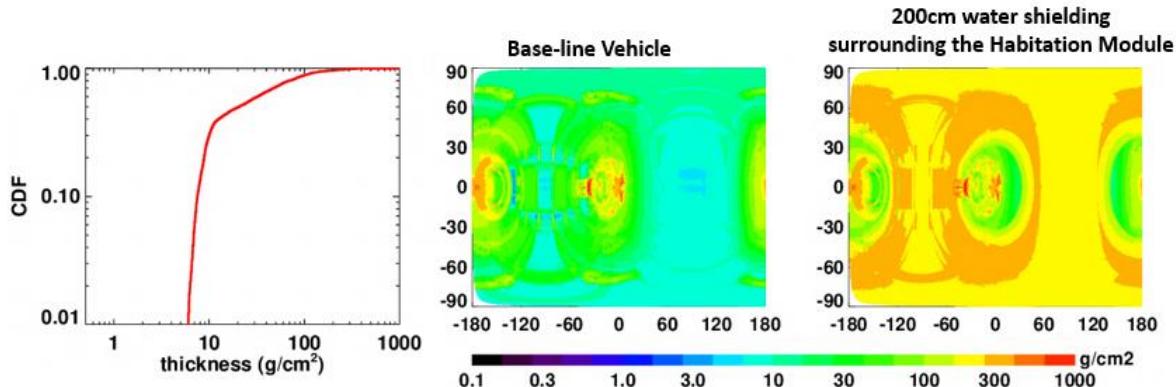
A set of calculations has been performed for one specific long-duration vehicle model to better understand the likely impact on astronaut GCR exposure of adding passive shielding material to an already heavily shielded spacecraft. The vehicle chosen for this analysis, which is shown in Figure 8.2.2-1, was originally developed for a SPE shielding study [Ewert et al. 2017]. This model was designed to represent one possible version of a vehicle to transport astronauts to Mars. An effort was made to ensure that it contains approximately appropriate masses for vehicle structures, vehicle systems, food, water, and other supplies for a Mars mission, but this model does not represent NASA's current plan for the Mars transit vehicle. These calculations were performed for one location in the vehicle model, shown with the red "X" in Figure 8.2.2-1, at the center of one of the crew quarters in the Habitation Module. A water sphere with a radius of 15 cm was used to roughly approximate the shielding human tissue provides to points within the body. Dose equivalent at the center of the sphere placed at the dose point within the crew quarters was calculated.

Figure 8.2.2-1. Long-duration Vehicle Model used for this Study
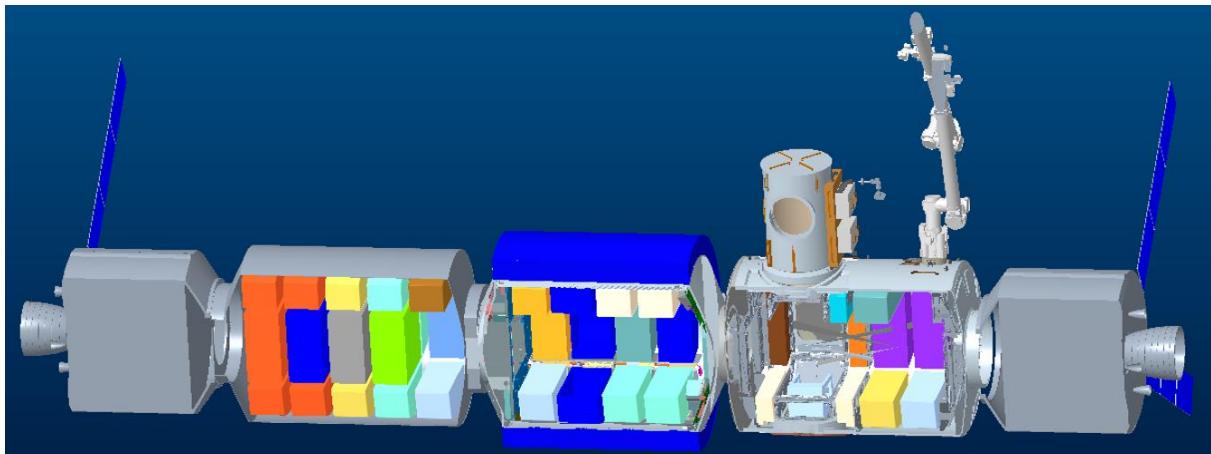
For these calculations, the external GCR environment was modeled using BON2020 model [Slaba and Whitman 2020]. The solar minimum environment used in these calculations represents the average daily fluence spectra that occurred between January 1, 1976, and December 31, 1976. For comparison purposes, one solar maximum calculation was also performed. The solar maximum environment used represents the average daily fluence spectra for 1981. The transport of the external environment through the spacecraft and the water sphere was calculated using the three-dimensional version of the HZETRN space radiation transport code [Slaba et al. 2020], and dose equivalent was evaluated using the ICRP60 quality factor [ICRP 1991]. The dose equivalent at the center of the 15-cm water sphere without any vehicle shielding was found to be 1.18 mSv/day for solar minimum conditions.

To facilitate the transport calculations, the vehicle model was ray traced. To ensure that the mass surrounding the dose point was accurately represented, 61,954 rays were included in the ray-trace distribution. The distribution of the vehicle shielding mass is shown in Figure 8.2.2-2. The cumulative distribution plot shows that the areal density of the shielding provided by the vehicle varies from a few g/cm^2 in some directions to hundreds of g/cm^2 in other directions.

Figure 8.2.2-2. Distribution of Vehicle Shielding Mass
(cumulative distribution plot (left), base-line vehicle (middle), and vehicle with 200 cm
water wall surrounding Habitation Module (right))

To evaluate the protection provided by water shields of various thicknesses, water shields were added around the Habitation Module, as shown in Figure 8.2.2-3, and calculated dose equivalent was compared with that of the baseline vehicle. The shielding distributions of the vehicle and with a 200-cm water wall are shown in the middle and right panels of Figure 8.2.2-2.

Figure 8.2.2-3. Long-duration Vehicle Model with Water Wall surrounding Habitation Module

8.2.3   Analysis Results

Initially, the dose equivalent was calculated for the baseline vehicle for both solar minimum (i.e., 1.08 mSv/day) and solar maximum (i.e., 0.55 mSv/day) environments. This shows that traveling during solar maximum with adequate solar storm shielding, if that were possible, might reduce astronaut exposure by ~50% as compared with solar minimum. Additionally, the fact that SPEs are more easily shielded by passive measures implies that there is likely a net benefit from missions during solar maximum when SPEs are more likely to occur. Section 8.3 contains a

discussion of solar cycle effects on exposure. A series of calculations was performed for the solar minimum environment with water walls of various thicknesses surrounding the Habitation Module. The results are given in Table 8.2.3-1. This table contains mass values for the various water-wall thicknesses. It should be noted, however, that the mass of the water wall is highly dependent on the geometry. A vehicle with a larger radius would have larger water-wall masses, and the mass would be larger if the water wall extended further in either direction. The mass values are presented here only to demonstrate how very large the masses could be; Table 8.2.3-1 shows that it would take an exceptionally large water wall (i.e., ~1000 cm) to reduce astronaut exposure by 50% and that that water wall would have a very large mass.

The lack of decreasing dose equivalent with increasing water shield shown in Table 8.2.3-1 is not a surprise. The phenomenon is related to the findings detailed in Slaba et al. [2017], where a rise in dose equivalent was found for increasing thickness of spherical aluminum shielding. Slaba et al. also found a flattening out of dose equivalent with increasing thickness of polyethylene spheres. The vehicle considered in this analysis was more complex from both a geometry and material standpoint compared with the analysis done in Slaba et al. [2017], but the findings in this work still generalize: the initial thickness of shielding material attenuates the GCR environment, but increasing values from approximately 20 to 100 g/cm^2 of material either showed increasing exposure (aluminum) or flattening out of the response (polyethylene). While Slaba et al. [2017] only considered material thickness up to 100 g/cm^2, it is known from conservation of energy and experiments throughout the atmosphere [Wilson et al. 1991] that there will be an eventual decrease in the radiation exposure with sufficient mass. The results of Table 8.2.3-1 are consistent with that understanding.

Table 8.2.3-1. Calculated Dose Equivalent Values for Various Water-Wall Thicknesses

Water-Wall Thickness (cm)	Dose Equivalent (mSv/day)	Reduction in Dose Equivalent (%)	Water-Wall Mass (Tonne)
0	1.08	0	0.0
20	1.06	1.9	1.9
50	1.10	-1.9	4.7
100	1.10	-1.9	9.3
200	0.96	10.7	18.7
300	0.83	23.6	28.0
400	0.72	33.7	37.3
500	0.65	40.0	46.7
1000	0.55	49.0	93.0

The difference between adding water inside versus outside the vehicle was examined. The dose equivalent inside the water sphere was evaluated for the baseline vehicle with 20 or 50 cm of water added inside the crew quarters, next to the water sphere; those results were compared with the results for 20- or 50-cm external water walls, as shown in Table 8.2.3-2. Adding water closer to the astronauts will probably provide better protection, and this approach could reduce the mass needed. However, the amount of water shielding that can be incorporated inside the spacecraft may be limited by the vehicle design. For this baseline vehicle, no more than 50 cm of water would fit, but a larger diameter module might have more room for shielding materials. As spacecraft for long-duration human missions are designed, further investigation of interior shielding may be needed. Performing trade studies examining multiple possible interior shield designs early in the design process may lead to lower-mass shielding solutions.

Table 8.2.3-2. Comparison of Dose Equivalent Values for Internal Water Walls with Those for External Water Wall

Water-Wall Thickness (cm)	Dose Equivalent for Internal Water Walls (mSv/day)	Dose Equivalent for External Water Walls (mSv/day)
0	1.08	1.08
20	1.01	1.06
50	1.05	1.10

8.2.4   Summary

The addition of water shielding was considered for a sample Mars vehicle design. Water was considered as an additional shielding material due to the better shielding qualities of water compared with typical spacecraft structural materials (i.e., aluminum). It was shown that increasing the water shielding had an impact on the dose equivalent within the vehicle only for thicknesses of water greater than 100 g/cm^2. During GCR solar minimum conditions, it took an additional 1000 g/cm^2 of water, equaling 93 tonnes, to reduce the dose equivalent to the value of only the vehicle (no additional shielding) during GCR solar maximum conditions (0.55 mSv/day). Mass savings could be found with integrated design of the vehicle shielding. Even with the large masses of parasitic water shielding, these masses were still comparable or smaller than the active shielding approaches considered. A major finding was that the active shielding concepts considered did not provide dramatic improvements compared with passive shielding.

F-62.	Human exposures during solar maximum can be as much as 50% lower than during solar minimum when all other variables are constant.

F-63.	The increased probability of an SPE during solar maximum may not result in an increase in radiation risk since the SPE exposure can be minimized with reasonable design of a storm shelter.

F-64.	Large values of additional water mass for shielding, on the order of 1000 cm, may be needed to reduce the exposure of solar minimum GCR environment to the exposure level for solar maximum GCR.

F-65.	The uncertainty in transport codes used to study the shielding efficacy is largely unquantified at material thicknesses greater than 100 g/cm^2.

O-26.	Additional work needs to be done to quantify the uncertainty in radiation transport codes at large material thicknesses (greater than 100 g/cm^2).

F-66.	Adding shielding to the interior of a vehicle, as opposed to the outside of the vehicle, creates a more optimal solution because less mass is required to optimize shield thickness and mass located closer to the astronaut is a more efficient shield.

8.3 Timing of Mars Missions As a Radiation Mitigation Strategy: Solar Cycle Variability Impacts on Crew Radiation Dose

8.3.1 Introduction

The mitigation of health risks from GCR presents a significant challenge for human exploration due to the large biological uncertainties associated with exposure and the lack of physical mitigation strategies. Mars mission dose varies significantly with solar cycle. Within our solar system, the solar wind modulates the flux of GCRs over an approximate 11-year cycle with an intensity that is inversely correlated with solar activity. During phases of higher solar activity, the GCR intensity is at a minimum, whereas at solar minimum, the GCR intensity is maximal. At solar maximum, the cosmic ray flux is decreased by a factor of three to four compared with solar minimum, whereas exposure estimates behind typical spacecraft shielding are reduced by roughly a factor of two. Large amounts of shielding would be required to provide an equivalent reduction in dose. Major SPEs during solar active periods could reduce the variability by increasing mission dose during solar active periods, but since SPE exposure is significantly reduced by nominal spacecraft shielding and further reduced by internal storm shelters, the largest exposure would still likely occur on missions occurring over solar minimum.

The previous and current solar cycles 24 and 25 have been a period of historically low solar activity, with a correspondingly high GCR throughout the entire cycle. Continuation of extremely low solar activity could both decrease the probability of solar storms and increase the contribution from GCR. Thus, the opportunity is that a mission launched during solar active periods could substantially reduce the crew dose. Understanding the intensity of solar activities for future missions thus supports key mitigation strategies for both GCR and SPE forecasting and sheltering requirements.

Efforts to improve the ability to forecast solar cycle length would be beneficial to long-range Mars mission planning. Under conditions modeled here to estimate the benefit, it was found that reducing the uncertainty in solar cycle duration by half (from 2.8 years to 1.4 years) increases the length of the launch window to meet a 600-mSv exposure limit, from 6 months to 2 years. However, the dates of favorable launch depend on the average forecast duration. Most of the research effort today is focused on predicting solar cycle intensity: peak at solar maximum and depth at solar minimum. However, solar cycle length variation will have a significant impact on estimates of solar activity if the projection is for 20 years out:

- Two consecutive short cycles (9.6 years) will be at solar minimum in 2039.
- Two nominal solar cycles (11 years) will be at solar minimum in 2042, while in the declining active phase in 2039.
- Two long cycles (12.4 years) will be at minimum in 2045 and will be near solar maximum in 2039.

Note that this extreme variability (whether projected solar activity during a mission is high or low) is significantly reduced when looking out only 10 years, or one solar cycle. Five years out, when some launch window flexibility is still possible, may make it increasingly possible to launch during solar active periods.

This review is intended to bound the impact of solar cycle variability on the total exposure that astronauts would experience in a 2- to 3-year Mars mission and identify how further

improvements in solar cycle forecasting could support radiation risk reduction. The upcoming sections address the following:

- Review the range of exposures for the last several solar cycles under nominal shielding.
- Characterize radiation exposure consistent with observed solar cycle variability.
- Estimate the variability of the mission dose of nominal Mars missions with respect to solar cycle intensities and durations.
- Consider the contribution of periodic SPEs (which occur during solar active periods) on the exposure totals.

8.3.2 Radiation Exposure Variability within a Solar Cycle

There are two sources of natural radiation that contribute to the dose of a deep space mission: the slowly varying but highly energetic GCRs, and lower-energy, but potentially intense, periodic SPEs. These two radiation sources vary out of phase with one another: the GCR peaks at solar minimum, while SPEs are rare near solar minimum, with higher probability during solar active periods, particularly the years before and after solar maximum.

The NASA tool OLTARIS [OLTARIS] was used to quantify the radiation exposure for this assessment. OLTARIS has several built-in GCR environments representing historic solar maxima and minima. Note that approximations were made to focus on solar cycle variability. More thorough analyses of detailed spacecraft configurations were prepared in other parts of the assessment. This assessment used the following configurations:
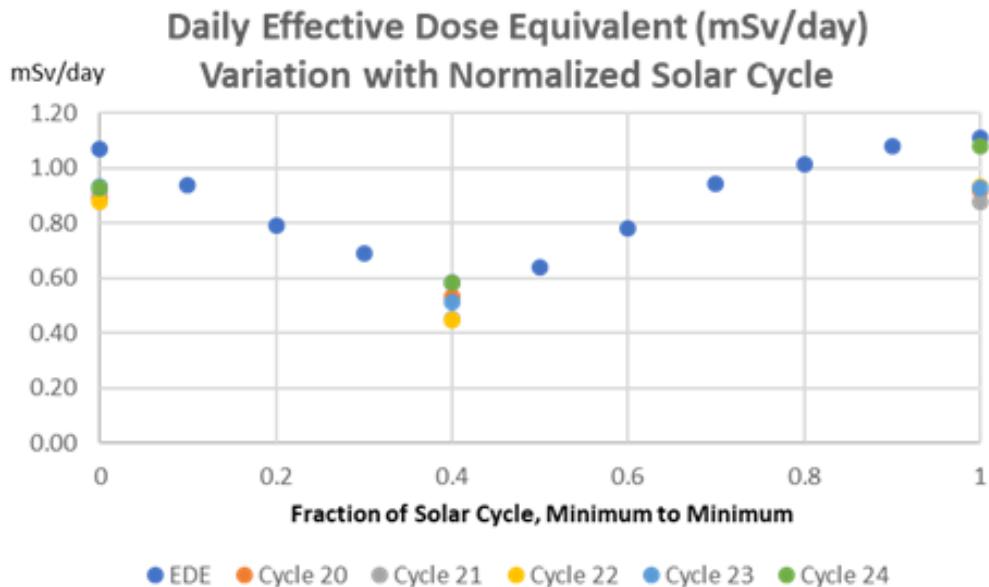
- Nominal 30-g/cm^2 spherical aluminum shielding.
- BON2020 Deep Space 1-AU GCR.
- Whole-body effective dose equivalent (EDE) computerized anatomical male (CAM), never-smoker.

Table 8.3.2-1 shows the results for historical solar minima/maxima, where the exposure was calculated for daily EDE. Other considerations (e.g., shielding depth and geometry, gender, etc.) yield slightly different quantitative results, but the trends found here are representative of more general configurations.

Table 8.3.2-1. Daily EDE (mSv/day) as calculated by OLTARIS assuming 30 g/cm² Aluminum Sphere, Male Human Avatar (CAM), and BON2020 GCR Model for Various Historical Solar Minima and Maxima

Effective Dose Equivalent (mSv/day)	
1965 Solar Minimum	**0.89**
1977 Solar Minimum	**0.92**
1987 Solar Minimum	**0.88**
1997 Solar Minimum	**0.93**
2010 Solar Minimum	**0.93**
2019 Approaching Minimum	**1.08**
1970 Solar Maximum	**0.53**
1982 Solar Maximum	**0.45**
1991 Solar Maximum	**0.44**
2001 Solar Maximum	**0.51**

In addition to historical solar minima/maxima, OLTARIS allows specific dates. This study used 10 dates distributed from 2010 to 2020 to represent variability through the most recent solar cycle. The results are shown in Figure 8.3.2-1, with historic solar minima and maxima exposures added.
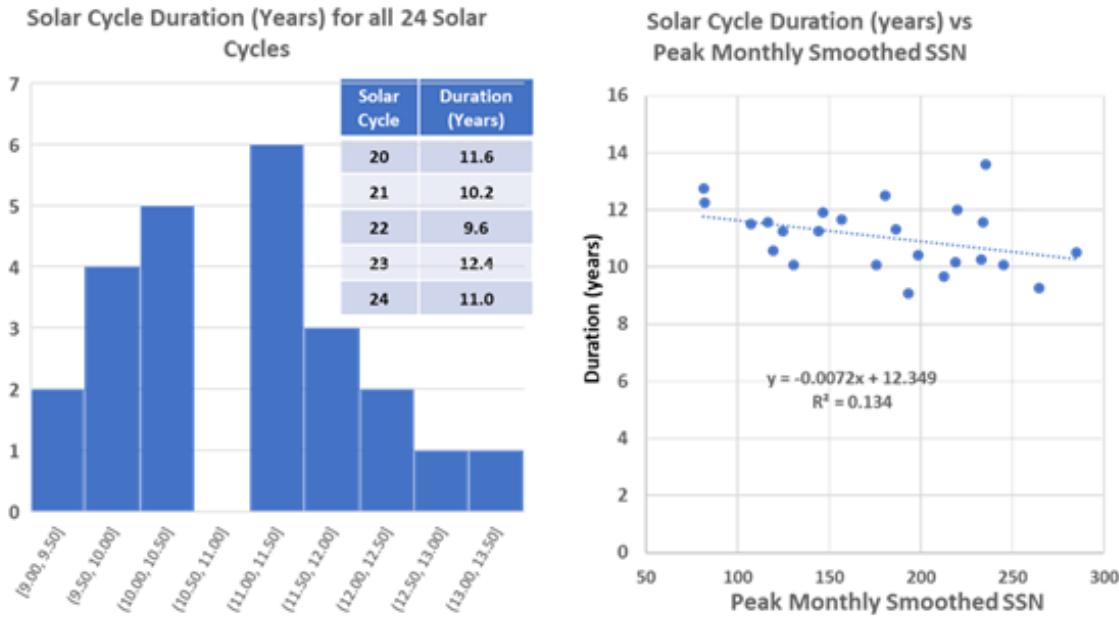
Figure 8.3.2-1. Daily EDE for 2010 to 2020 (axis is elapsed fraction of solar cycle) as calculated by OLTARIS assuming 30 g/cm² Aluminum Sphere, Male Human Avatar (CAM), and BON2020 GCR Model
Also shown are various historical solar minima and maxima (From Table 8.3.2-1) to illustrate variability within cycle.

Note that the variation is typically close to a factor of two within most cycles (with a low of 1.6 and a high of 2.1), and nearly a factor of 2.5 when comparing extreme minima with extreme maxima. The EDE, which includes body self-shielding, does not vary significantly between 20 and 40 g/cm² (less than 5%).

8.3.3 Solar Cycle Variability

Solar activity varies roughly over an 11-year cycle. Sunspot numbers have been tracked since 1750 for 24 cycles [Van Driel-Gesztelyi and Owens 2020; Clette et al. 2014]. The cycle duration (minimum to minimum) has varied from 9 to over 13.5 years. The most recent cycles, for which there are estimates of radiation exposure, have varied from 9.6 to 12.4 years (Figure 8.3.3-1).

Figure 8.3.3-1. Solar Cycle Duration over Past 24 Solar Cycles
Histogram on left shows distribution of 24 solar cycle durations (years). Insert is duration of cycles 20 through 24, used for this assessment. Graph on right shows variation of solar cycle duration with peak monthly smoothed sunspot number. Linear fit shows only a weak correlation of duration and amplitude.
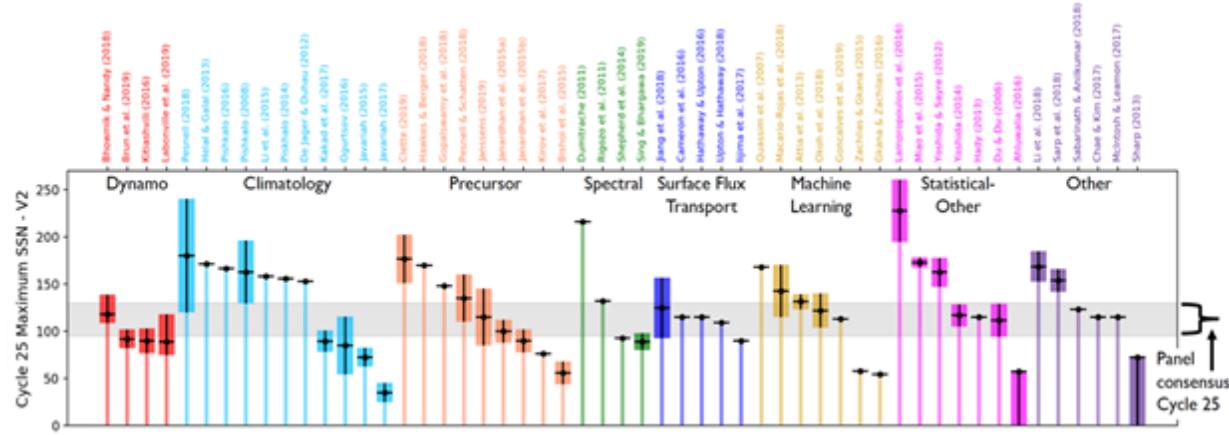
The heliophysics community has been studying the underlying physics of the solar cycle and attempting to forecast the magnitude of future cycles for decades. Note that forecasting the duration of the cycles has not been a research focus. Hathaway [2010] provided an overview of solar cycle prediction techniques for cycle 24; an update to the cycle 24 predictions was provided by Pesnell [2016], and a more recent review encompassing cycle 25 was produced by Dibyendu Nandy [2020].

Community workshops have been held since 1979 (beginning of solar cycle 21) to provide forecasts of pending solar cycles [Biesecker 2008]. Solar cycle forecasting was addressed in Solar-Terrestrial Predictions workshops in Meudon, France, in 1984 [NOAA 1986], Leura, Australia, in 1989 [NOAA 1990], and Hitachi, Japan, in 1996 [Hiraiso Solar Terrestrial Research Center 1997]. The first "official" forecast, for cycle 22, was in 1989 [Wu 1989], driven in part by a need to forecast satellite drag to support planning for the Hubble Space Telescope repair. It was followed in 1997 by the second "official" prediction panel, a NOAA panel predicting cycle 23 [Joselyn et al. 1997]. More recently, NOAA hosted a committee to provide consensus forecasts of solar cycles prior to solar cycles 24 [Biesecker] and 25 [Upton 2020].

In December 2018, NOAA put out a call for cycle 25 predictions. Predictions were accepted through February 1, 2019. NOAA also conducted a literature review for published predictions.

The Consensus Prediction was announced at the 2019 Fall American Geophysical Union meeting (see Figure 8.3.3-2). NOAA considered about 60 predictions in the following categories for Cycle 25:
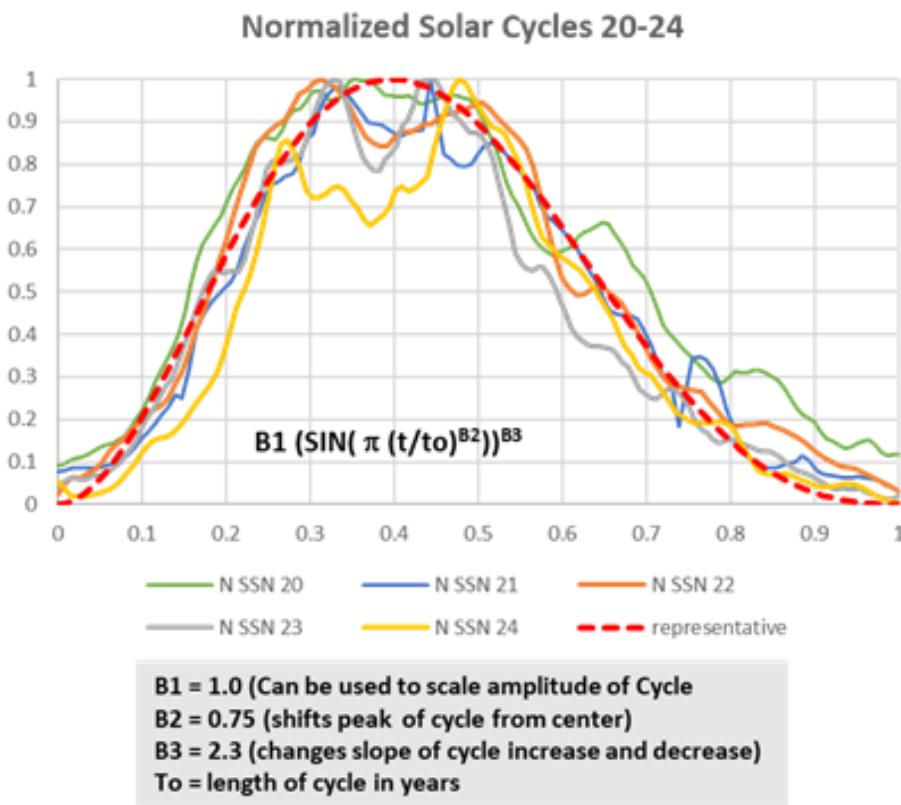
- Numerical methods
  - Climatology (~12)
  - Spectral/statistical (~12)
  - Machine learning/neural networks (~6)
- Physics-based methods
  - Precursor (~12)
  - Surface flux transport (~5)
  - Dynamo (~4)
- Other (~10)

Figure 8.3.3-2. Sixty-one Forecasts for Solar Cycle Maximum Sunspot Number and Associated Uncertainties, as reviewed by Solar Cycle 25 Consensus Workshop
[Figure courtesy of the Solar Cycle Consensus Committee]

For this assessment, a normalized fit to the most recent cycles was prepared, shown in Figure 8.3.3-3. Note that for this fit, solar maximum is about 4 years into a 10-year cycle.

Note that the cycle length variation will have a significant impact on estimates of mission dose if the projection is for 20 years out: two consecutive short cycles will be at solar minimum in 2039; two nominal solar cycles will be at solar minimum in 2042 and in the declining active phase in 2039; and two long cycles will be at minimum in 2045 and near solar maximum in 2039.

Normalized Solar Cycles 20-24

$B1 (SIN(\pi (t/to)^{B2}))^{B3}$

Legend: N SSN 20, N SSN 21, N SSN 22, N SSN 23, N SSN 24, representative

B1 = 1.0 (Can be used to scale amplitude of Cycle
B2 = 0.75 (shifts peak of cycle from center)
B3 = 2.3 (changes slope of cycle increase and decrease)
To = length of cycle in years

***Figure 8.3.3-3. Smoothed Solar Cycles 20-24 normalized to Maximum of 1.0 and
Effective Length of 1.0***
Superimposed on cycles is representation used in this assessment of normalized solar cycle.
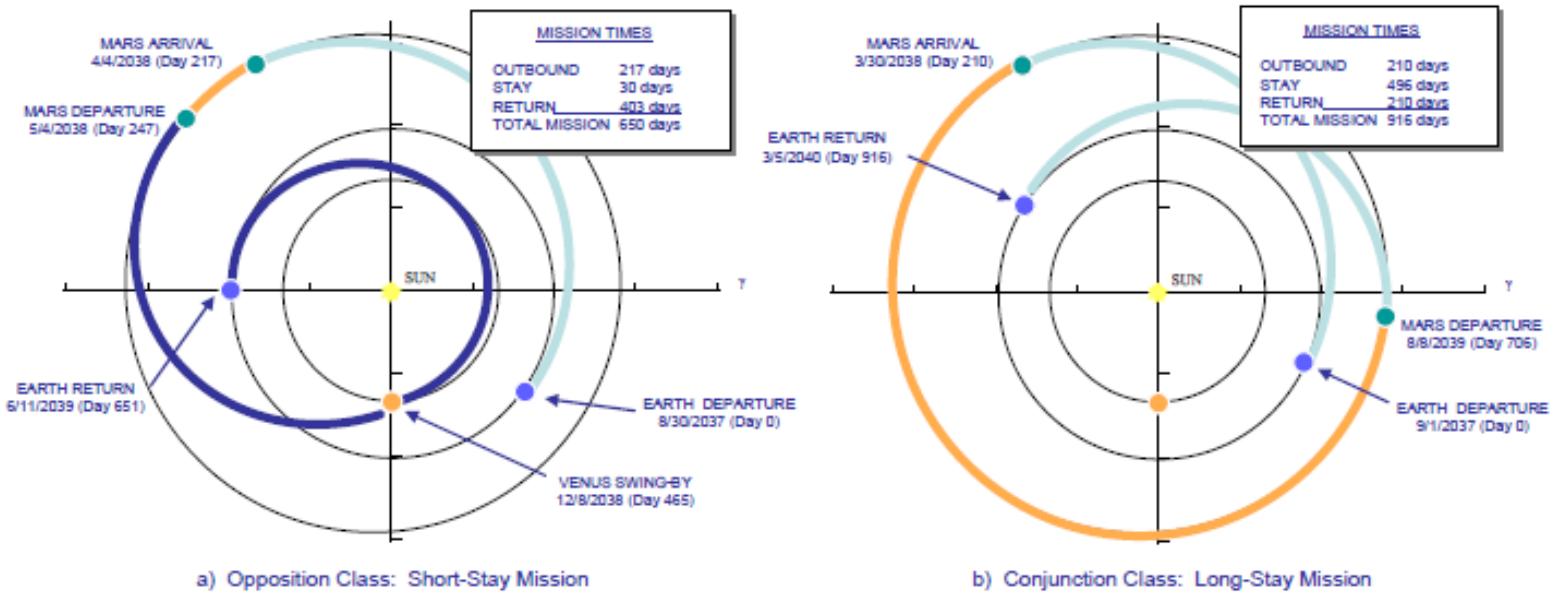
8.3.4 Mission Assumptions

To estimate a mission dose, information is needed about the mission launch date and duration. Figure 8.3.4-1 shows the two broad classes of Mars missions: *conjunction* (long stay, most energy efficient) and *opposition* (short stay, requires more energetic propulsion but overall significantly shorter mission duration). For both classes of missions, launch windows occur about every 26 months, determined by the relative positions of the Earth and Mars. Total mission energy requirements vary between mission opportunities and within a narrow launch window. Shown are nominal characteristics of a mission in 2039. This section will focus on short-stay missions with durations from 770 to 1030 days but will consider impacts on mission durations as short as 600 days.

Launch opportunities for 2030 to 2040 and associated mission durations are shown in Figure 8.3.4-2, as presented in Figure 3-13 in NASA/SP-2009-566-ADD [Drake 2009b]. The solar activity bar in that figure is the assumption used for that study, not this assessment, which looks at variations in the solar cycle duration.
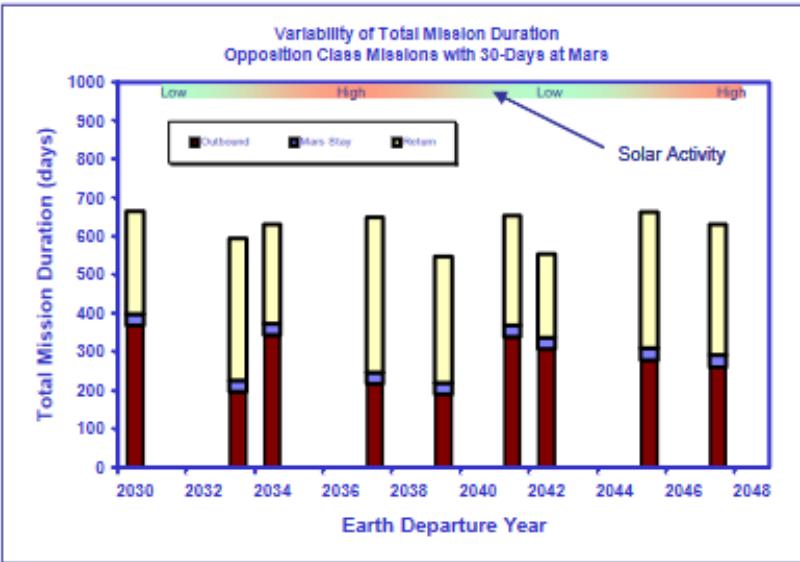
This assessment further used information provided in Table 1 of HEO-DM-1002 [HEO-DM-1002], which was produced to "provide updates on likely crewed Mars mission durations for use in assessments of human systems risk, human research studies to reduce those risks, and duration-dependent technology development." Figures 8.3.4-3 and 8.3.4-4 are reproduced from that document.

Figure 8.3.4-1. Trajectories for Typical Opposition Class (short-stay, left) and Conjunction Class (long-stay, right) Missions [National Academies of Sciences, Engineering, and Medicine 2021; Drake 2009a, p. 48]
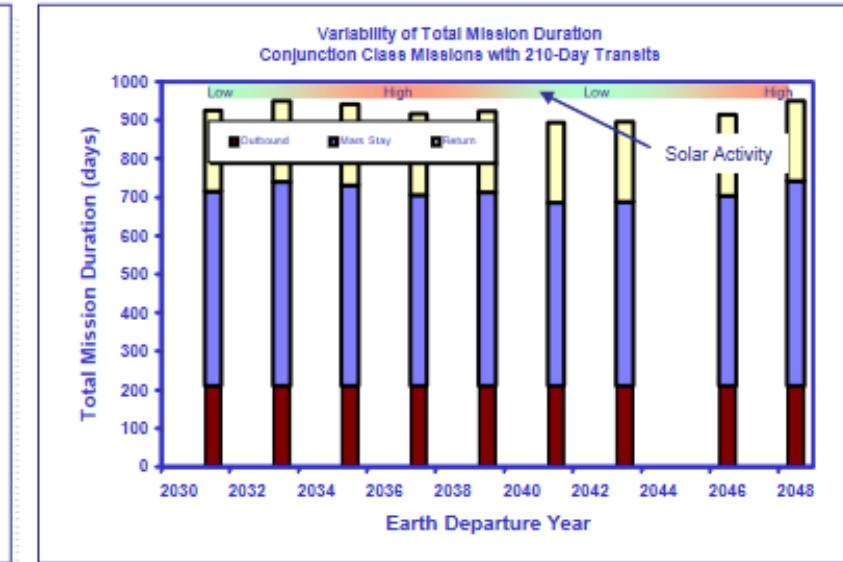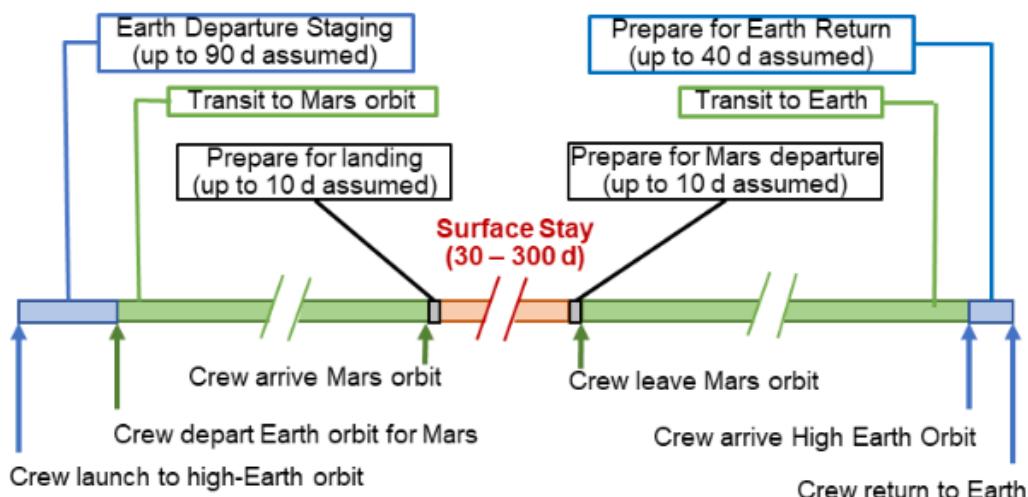
Figure 8.3.4-2. Mars Mission Launch Opportunities as presented in [Drake 2009b]
Solar activity bar is assumption used for that study.

Ref. Mission	Mars Crewed Phase Duration Time (Earth days)				Inter-planetary Time and Total Crew Time Away from Earth	Total (for all crew) Mars Surface EVA Hours
	Crewed Cis Lunar Staging/ Phasing	Out-bound Transit	Mars Surface Stay	Mars Orbit Loiter + Earth Return Transit Earth		
	Microgravity	*Micro-gravity*	*0.376 g*	*Microgravity*		
Point of Departure (PoD 2020)	**90-day** initial Earth launch window **+ 40 days** after return (4 crew)	**305 days** (all 4 crew)	**30 days** (only 2 of 4 crew)	**50-day** Mars orbit loiter (2 of 4 crew on surface for 30 of 50 days) then **375 days** return transit (all 4 crew)	**730 days** inter-planetary. **Total at least 771 but no more than 860 Days**	Up to **320 crew-hours**[2] (among 2 crew)
Alternative Short Stay (2020)	**90-day** initial Earth launch window **+ 40 days** after return (4 crew)	Up to **200 days** (all 4 crew)	**30 days** (only 2 of 4 crew)	Up to **500-day** Mars orbit loiter (2 of 4 crew on surface for 30 of 500 days) then Up to **200 days** return transit (all 4 crew)	Up to **900 days** inter-planetary. **Total no more than 1030 Days**	Up to **320 crew-hours** (among 2 crew)
Basis of Comparison (BoC 2019)	**90-day** initial Earth launch window **+ 40 days** after return (4 crew)	**429 days** (4 crew)	Up to **300 days** (all 4 crew)	**365 days** (4 crew)	[3]**1094 days** inter-planetary. **Total no more than 1,224 Days**	No more than **3000 crew-hours**[4] (among 4 crew)

Human Exploration and Operations (HEO) Systems Engineering and Integration (SE&I) Decision Memorandum Mars Mission Duration Guidance for Human Risk Assessment and Research Planning Purposes HEO-DM-1002

Figure 8.3.4-3. NASA Guidance on Mission Duration for Short- and Long-stay Missions
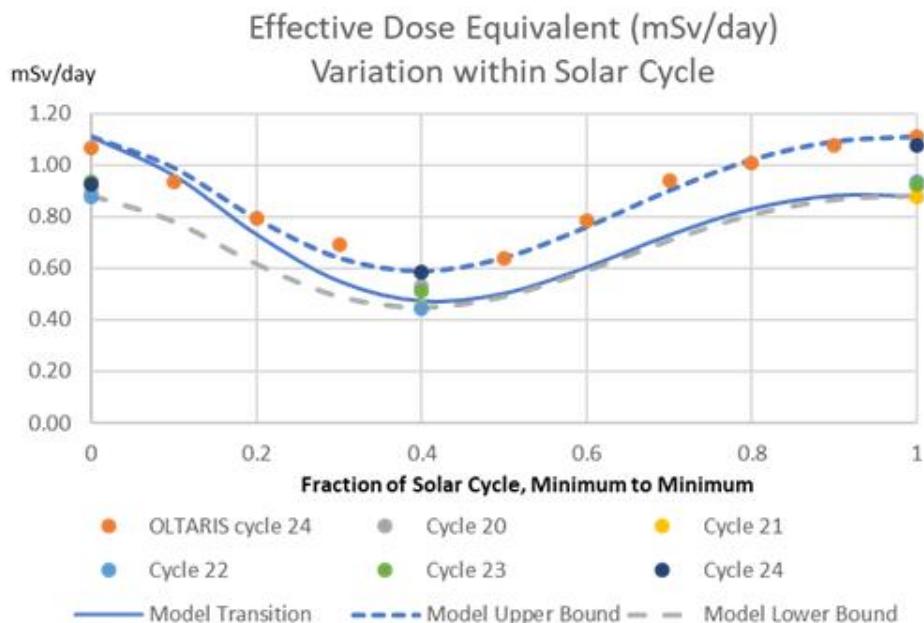
Figure 8.3.4-4. Illustrated Mission Timeline Overview from HEO-DM-1002

For this assessment, the dose on the Martian surface is not treated differently from the dose in deep space. This is because it is harder to get a nominal Mars surface dose, but it should result in a conservative bound. Also, from HEO-DM-1002, some of the crew may stay in orbit during a short-stay mission. Note also that time on the surface for a short stay is a small fraction of the mission (30 days out of 771 to 1030 days). This is a more significant compromise for the long-stay missions, with a surface stay of up to 300 days out of 1094 to 1224 days. However, it is not as likely that the first mission will be a nearly year-long surface stay; therefore, this assessment is focused on short-stay missions.

8.3.5 Model Setup

A numerical representation of the daily EDE was prepared using the variation of exposure and the shape of a nominal solar cycle (Figure 8.3.5-1).

Figure 8.3.5-1. Same as Figure 8.3.2-1, but showing Daily EDE Model for Nominal Cycle: Upper Bound, Lower Bound, and Transition from Upper to Lower Bound
Model equation is described in text.

The equation developed for this analysis has two components: a linear fit from the start of the cycle to the end of the cycle, minus a scaled version of the solar cycle variation:

Linear fit:

A1 + (A2-A1)*t/to

A1 = EDE/day at start of cycle (0.88 to 1.11 mSv/day)

A2 = EDE/day at end of cycle (0.88 to 1.11 mSv/day)

t = time in cycle in years

 to = cycle length in years (9.6 to 12.4 years)

Curved fit:

B1 (SIN (π (t/to)^{B2}))^{B3}

B1 the amplitude of decrement, is Bo + dB
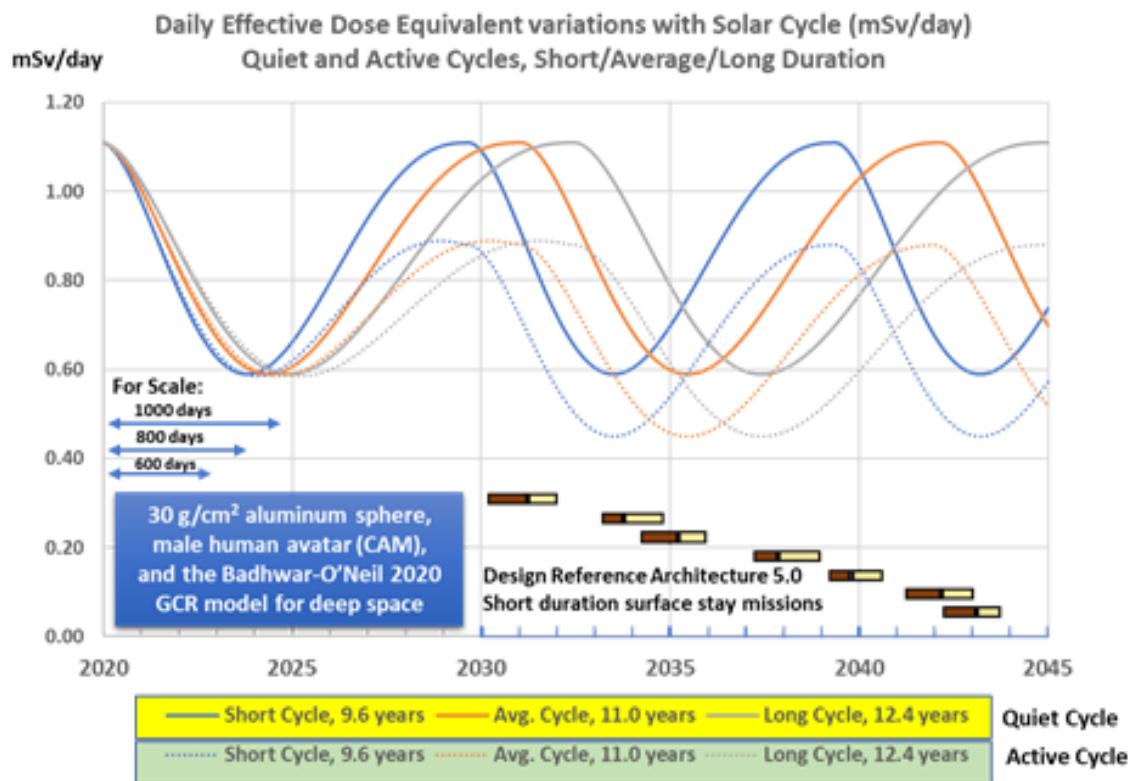
Bo is the (minimum of A1 and A2) – 0.59

dB varies from 0 to 0.14, to adjust the depth of the EDE

B2 scales the shape to move peak from the center of the time range (0.75 is used)

B3 scales the rise and fall of the shape (2.3 is used)

The final representation of the fit for a range of solar conditions is shown in Figure 8.3.5-2.

Figure 8.3.5-2. Deep Space EDE Variations with Solar Cycle (mSv/day) for Quiet and Active Cycles, and Short/Average/Long Solar Cycles for Indicated Shielding
Each cycle is assumed to start at estimated daily dose in 2020. Scale lengths are included to show possible mission integration times. Mission timelines for short-duration surface stay are included from Drake [2009b].
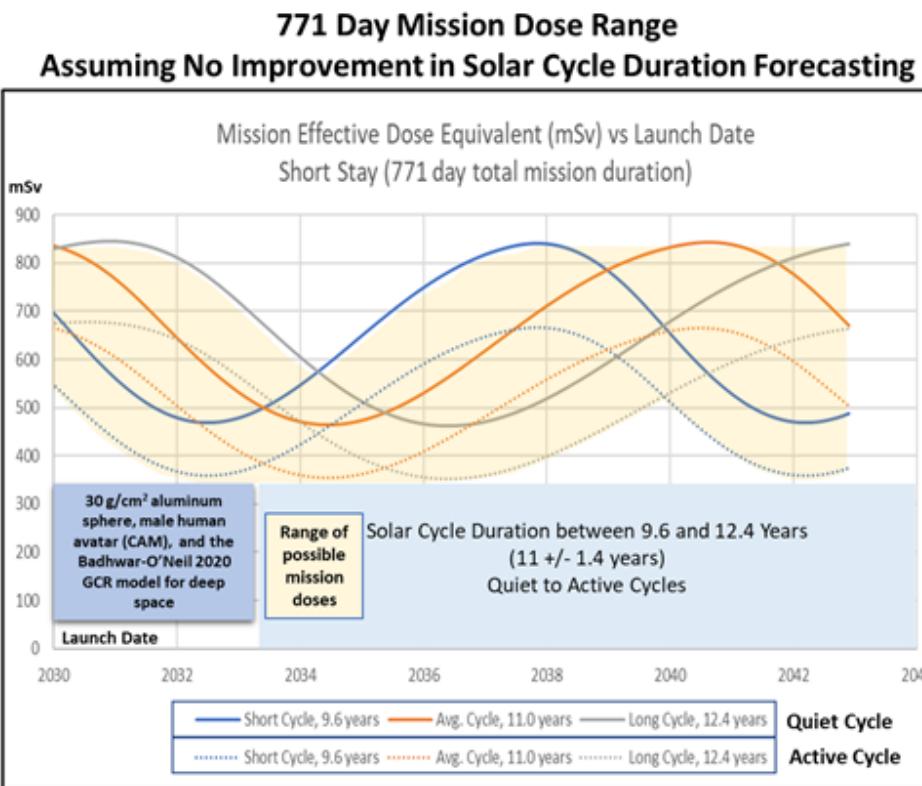
The total mission dose for a mission that launches in a given year is the integral of the daily dose over the full mission. The mission dose will depend significantly on:

- Launch date
- Mission duration
- Solar cycle progress over the mission duration
- Solar cycle intensity over the mission duration

It is important to note that in any case, the schedule for a Mars mission is likely to be driven by factors other than expectations of solar activity levels. The schedule will be driven by policy considerations, including cost and hardware development and political considerations. Launch windows constrained by orbital mechanics will be a major design driver. A schedule delay due to hardware delays could force a launch delay of 26 months to the next available launch window.

8.3.6 Model Results with No Improvement in Solar Cycle Duration Forecasting
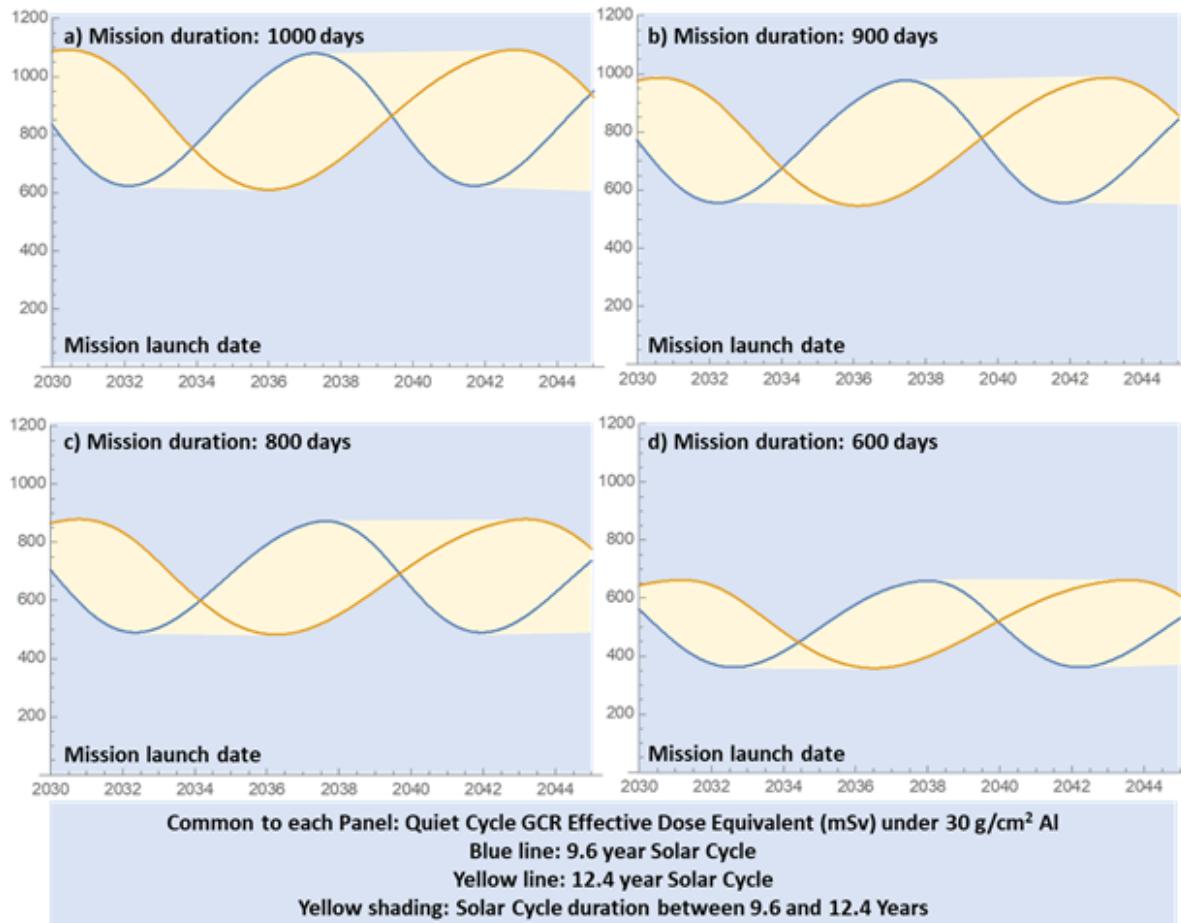
Solar cycle duration forecasts today are limited to the climatologically observed range. Based on recent cycles, that range is from 9.6 to 12.4 years. Figure 8.3.6-1 shows the mission exposure variation for a short-duration (771-day) mission versus launch date for active and quiet solar cycles with duration ranging from 9.6 to 12.4 years. The launch date is treated as continuous to show the dependence on time, but recall that mission duration for a given launch date is dictated by orbital mechanics and the mission architecture.

Figure 8.3.6-1. Variation in Mission Dose for a 771-day, Short-stay Mars Mission, assuming No Improvement in Solar Cycle Forecasting, with Cycle Duration Ranging from 9.6 to 12.4 Years

The mission dose ranges from 360 mSv for a mission during solar maximum of an active cycle (reduced GCR flux) to 845 mSv for a mission during solar minimum for a quiet solar cycle (enhanced GCR flux). If the mission dose limit is 600 mSv, as proposed in NASA's recommended change to exposure limits as reviewed in a recent study [National Academies of Sciences, Engineering, and Medicine 2021], the 771-day mission launch date would be limited to a 6-month period starting in 2034. However, if the mission dose limit is 700 mSv, then the mission would could launch in 2033 or 2034. Earlier or later and the mission dose may exceed the (notionally chosen) 700-mSv limit. Longer missions will naturally have higher doses, approximately scaled by mission duration, as shown in Figure 8.3.6-1. From Figure 8.3.6-2, a 600-day mission launched between mid-2032 through 2034 would be below 600 mSv. It would not exceed 700 mSv for any launch date. Missions longer than 800 days would not be able to meet the 600-mSv dose limit for any launch date.
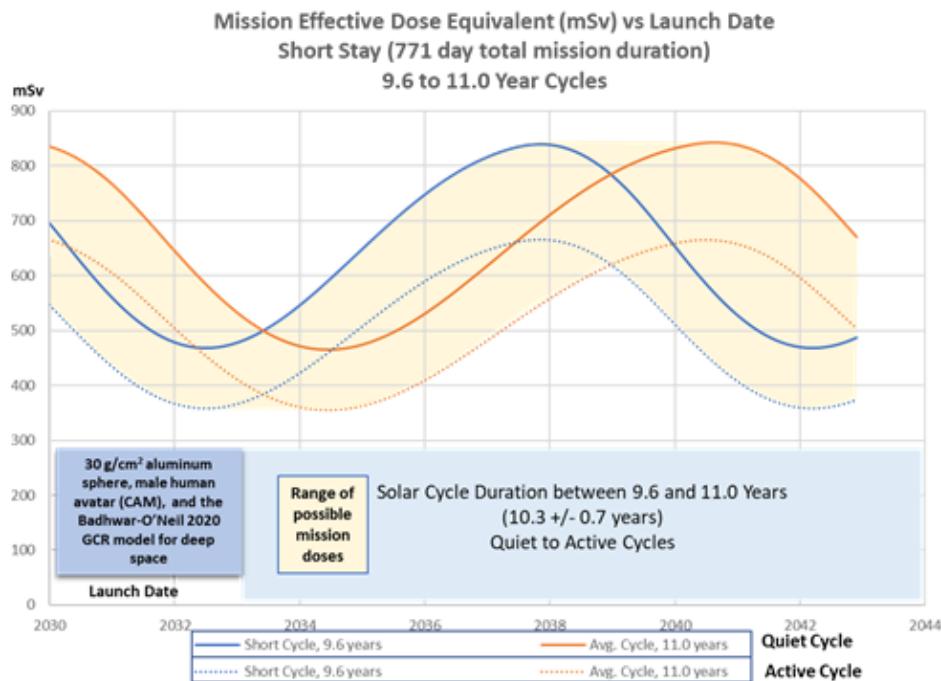
Mission Effective Dose (mSv) Vs Launch Date and Mission Duration

Common to each Panel: Quiet Cycle GCR Effective Dose Equivalent (mSv) under 30 g/cm² Al
Blue line: 9.6 year Solar Cycle
Yellow line: 12.4 year Solar Cycle
Yellow shading: Solar Cycle duration between 9.6 and 12.4 Years
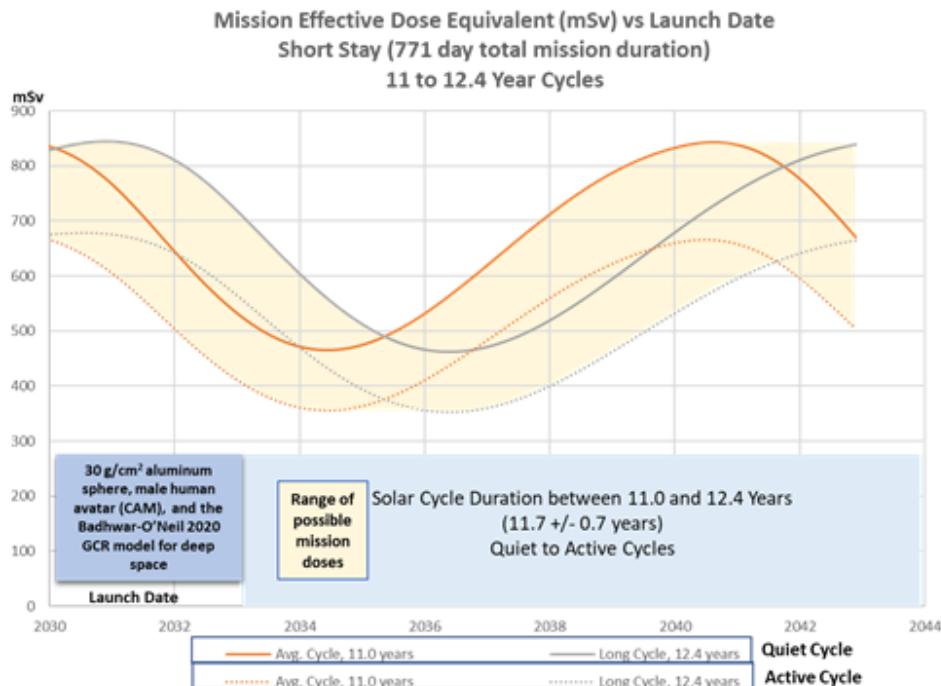
Figure 8.3.6-2. Variation in Mission Dose for 1000-, 900-, 800-, and 600-day Mission Durations

8.3.7 Model Results with Improved Solar Cycle Duration Forecasting

Improvements in forecasting cycle duration could add clarity to expectation of mission doses two or more solar cycles in the future. Figures 8.3.7-1 and 8.3.7-2 are similar to Figure 8.3.6-1, but it is assumed that the durations of the next few solar cycles are known to within a range of 1.4 years (±0.7 years). Figure 8.3.7-1 shows durations from 9.6 to 11 years; Figure 8.3.7-2 shows durations from 11 to 12.4 years.

Figure 8.3.7-1. Variation in Mission Dose for a 771-day, Short-stay Mars Mission, assuming Improved Solar Cycle Duration Forecasting and Cycle Duration between 9.6 and 11 Years

Figure 8.3.7-2. Variation in Mission Dose for a 771-day, Short-stay Mars Mission, assuming Improved Solar Cycle Duration Forecasting and Cycle Duration between 11 and 12.4 Years
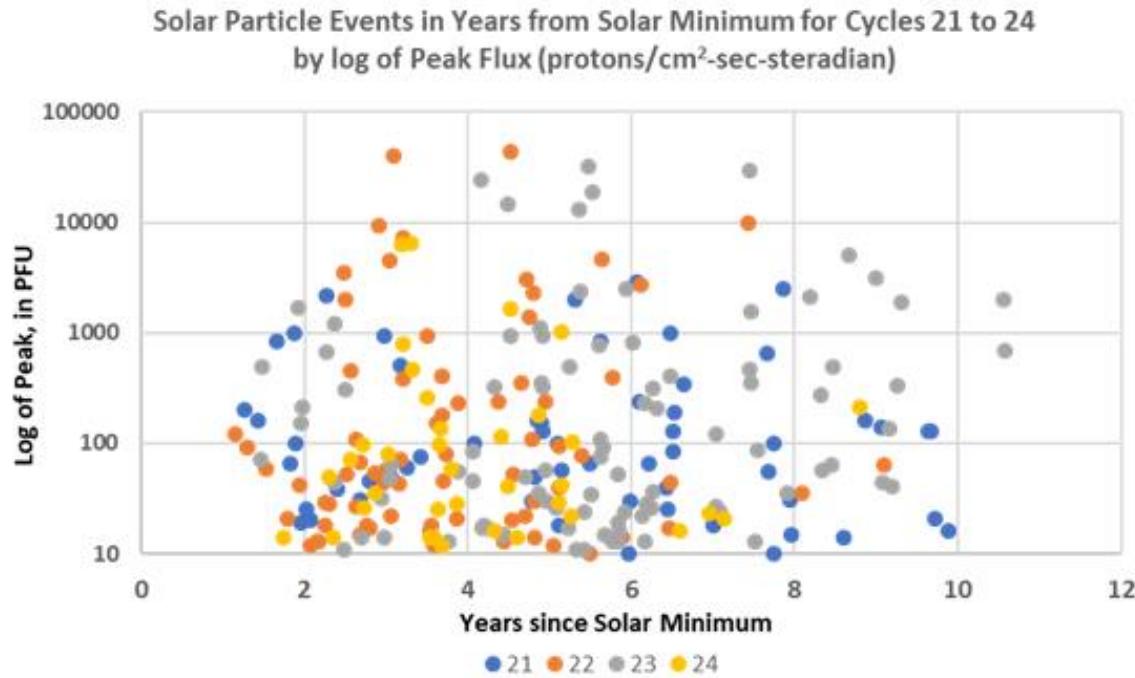
Reducing the uncertainty in solar cycle duration by half (from 2.8 years to 1.4 years) increases the length of the launch window to meet a 600-mSv exposure limit from 6 months to 2 years.

However, the dates of favorable launch depend on the average forecast mean and uncertainty. In Figure 8.3.7-1, where the solar cycle is assumed to be between 9.6 and 11.0 years, a 771-day mission launched between mid-2032 and mid-2034 would meet a 600-mSv limit. However, Figure 8.3.7-1 shows that if the solar cycle is assumed to be between 11 and 12.4 years, then a 771-day mission would have to be launched between the start of 2034 and the end of 2036 to meet the 600-mSv limit.
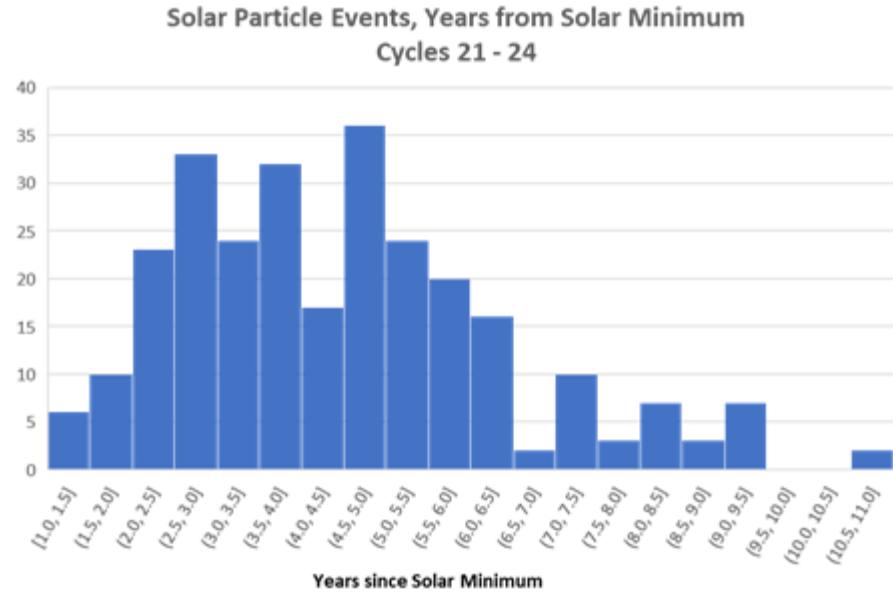
A more complete assessment of GCR impact would be to examine an expanded distribution of solar cycle variability, including both length and intensity (particularly the likelihood of even deeper solar minima observed so far) and a better representation of exposure during the surface phase of the mission. This was beyond the scope of this assessment but would not change the conclusion that the highest doses would be on missions near solar minimum.

8.3.8   SPE Considerations
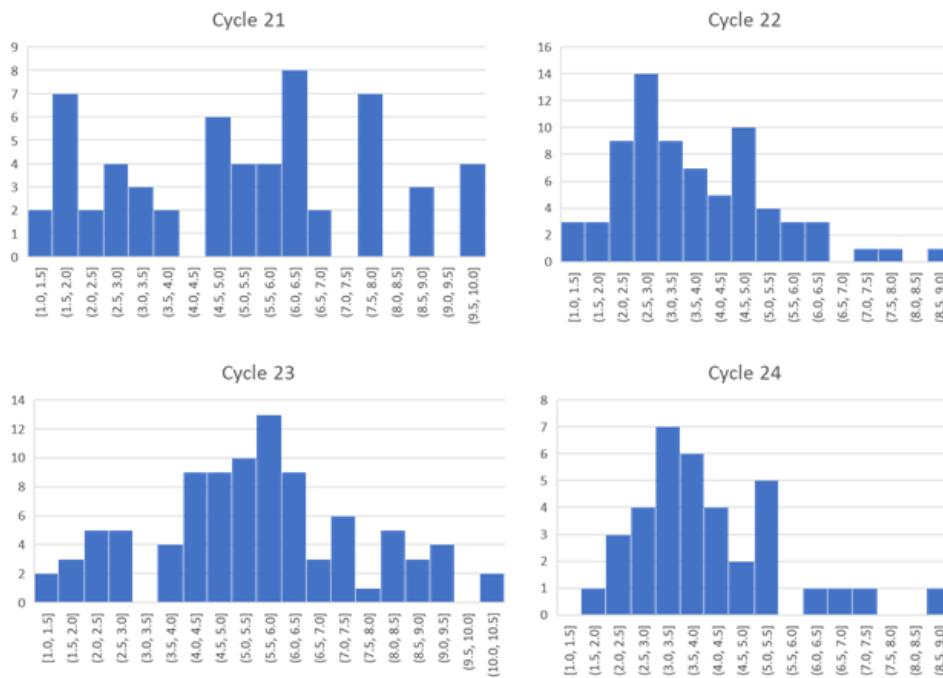
Radiation from SPEs could also contribute to total dose of a future Mars mission. SPEs are produced by solar eruptions, and significant SPEs are generally associated with strong, fast CMEs. In active cycles, SPEs, which last 2 to 5 days, can occur as often as one to three times per month, particularly in the years around solar maximum (nominally years two through seven). Intensities of SPEs vary by orders of magnitude, with only a few per cycle intense enough to contribute significant dose to an astronaut under the nominal shielding expected to be available in a Mars mission. Figure 8.3.8-1 illustrates the distribution of SPEs in the last four cycles. Figure 8.3.8-2 is a histogram of years from solar minimum for all four solar cycles. Figure 8.3.8-3 shows the variability between cycles of the distribution of SPEs.

Figure 8.3.8-1. Distribution of SPEs in Last Four Cycles by Peak Flux

Solar Particle Events, Years from Solar Minimum
Cycles 21 - 24
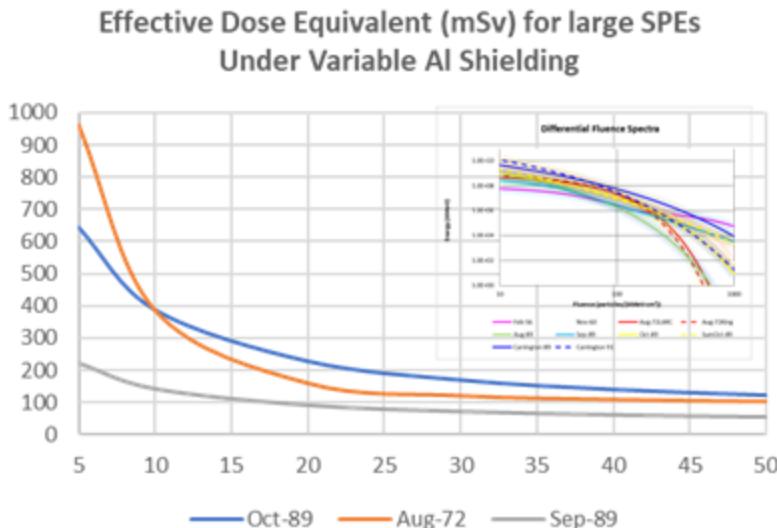
Figure 8.3.8-2. Histogram of Years from Solar Minimum for Combined Last Four Solar Cycles

Figure 8.3.8-3. Histogram of Years from Solar Minimum Separately for Last Four Solar Cycles

Solar energetic particles associated with SPEs vary in energy from tens to hundreds of MeV, compared with GCR energies of hundreds of MeV/nucleon to several tens of GeV/nucleon. While posing a major risk for lunar surface EVA with very thin shielding, this range of energies is relatively easily shielded for the modest habitat and vehicle shielding expected for a Mars mission. Even on the Mars surface, the thin atmosphere provides more than 20 g/cm^2 shielding directly overhead and significantly more from angles greater than overhead (see Figure 8.3.8-4).

Effective Dose Equivalent (mSv) for large SPEs Under Variable Al Shielding
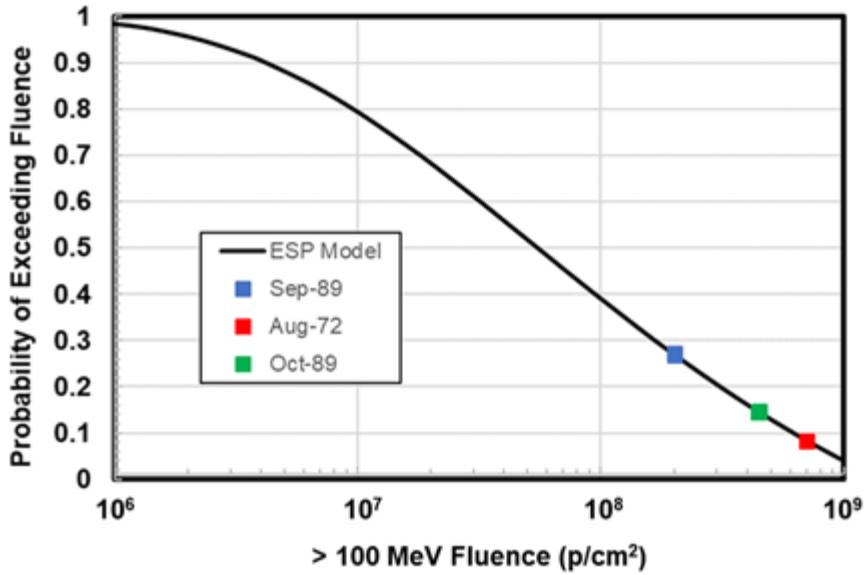
Figure 8.3.8-4. Solar Energetic Particle EDE under Shielding for Major Events, using Historical SPEs in OLTARIS for Same Conditions and Endpoints calculated for GCR Insert shows energy spectrum for large events.

Worst-case solar proton event fluences were calculated for a 2-year period during solar maximum using the ESP model [Xapsos et al. 1999]. This allows energy spectra to be obtained for any specified level of confidence and mission duration. In this case, the fluence greater than 100 MeV during an event was calculated. The probability of exceeding that fluence is 1 minus the confidence level. Results are shown in Figure 8.3.8-5. In addition, fluences for the large events of October 1989, September 1989, and August 1972 are plotted on the line for comparison. The fluence used for the October 1989 event was obtained from the Tylka's Design Reference Spectrum [Tylka et al. 2010]. Fluences for the other two events were taken from Wilson et al. [1999].

An alternative to using a particular event such as the one that occurred in October 1989 for the design reference spectrum that has several advantages is to base the spectrum on a worst-case model, such as that used for Figure 8.3.8-5. Such models give energy spectra that are based on long-term measurements of many events, not a single, arbitrarily chosen event. Furthermore, the model approach accounts for the worst-case energy spectrum dependence on mission duration, which is not the case when using a particular event. In addition, use of a CL- based model opens up additional trade space by allowing variation of the energy spectrum with CL.

If one assumes the unlikely case (less than 1%) of three major SPEs under nominal 30 g/cm^2 aluminum shielding during the deep space mission (summing the October 1989, September 1989, and August 1972 events), then the contribution to mission effective dose would be about 360 mSv.

Providing a storm shelter within the vehicle with thickness greater than 50 g/cm^2, incorporating effective shielding material (i.e., composites, water, or other low-Z material), would further reduce the combined contribution to less than 250 mSv. This increment would occur in the solar active period when the GCR dose is reduced by a comparable amount. So, the impact of assuming three major SPEs during the mission would be to reduce the variability of exposure, moving toward but still below the dose of a mission centered on solar minimum.

Figure 8.3.8-5. Probability of Exceeding >100 MeV fluence for a 2-year Mission (September 1989, August 1972, and October 1989 SPEs are indicated)
Combined probability of all three events is less than 1%.

8.3.9 Summary

This assessment supports the expectation that Mars mission dose varies significantly with assumptions of solar cycle length and intensity. For missions launched prior to 2030, the variation is less than a factor of 1.5; from 2030 to 2040, the range is from 1.5 to 2.25. The variation is dominated by the phasing of the cycles. Under conditions modeled here to estimate the benefit, it was found that reducing the uncertainty in solar cycle duration by half (from 2.8 years to 1.4 years) increases the length of the launch window to meet a 600-mSv exposure limit from 6 months to 2 years. However, the dates of favorable launch depend on the average forecast mean and uncertainty.

F-67.	The previous and current solar cycles 24 and 25 have been a period of historically low solar activity, with a correspondingly high GCR throughout the entire cycle. Continuation of extremely low solar activity could both decrease the probability of solar storms and increase the contribution from GCR.

F-68.	Mars missions during solar maximum could have half the dose of a similar mission at solar minimum.

F-69.	SPEs are likely to contribute to exposure for a mission conducted in solar maximum, but the likelihood is that for reasonable vehicle shielding the total (i.e., GCR plus SPE) exposure will not increase the total effective dose above the levels that would be experienced for a mission conducted during solar minimum.

F-70.	Research into forecasting solar cycles has focused on predicting the amplitude of the next solar maximum, but little has been done to forecast solar cycle duration.

F-71.	Reducing the uncertainties in forecasts of solar cycle duration would enable more informed calculations of GCR exposure.

O-27.	Due to strong effect on radiation exposure, mission timing with respect to the solar cycle should be considered an input factor to Mars mission planning. Additional research in forecasting solar cycle amplitude and duration would be beneficial for Mars mission planning.

O-28.	Use of a CL-based model to determine a worst-case design reference spectrum for solar protons has several advantages over using a particular event such as the one that occurred in October 1989.

These findings are neither surprising or alarming. GCR exposure is nominally twice as high at solar minimum than at solar maximum. Solar cycle length variation will have a significant impact on estimates of mission dose if the projection is for 20 years out: two consecutive short cycles will be at solar minimum in 2039; two nominal solar cycles will be at solar minimum in 2042 and in the declining active phase in 2039; and two long cycles will be at minimum in 2045 and near solar maximum in 2039. Note that this extreme variability is significantly reduced when looking out only 10 years, or one solar cycle. Looking only 5 years out (when some design changes are still possible) reduces the variability even further.

Major SPEs during solar active periods could reduce the variability by increasing mission dose during solar active periods, but the largest exposures would still likely occur on missions occurring over solar minimum. Continuation of extremely low solar activity beyond the historic lows of cycle 24 could both decrease the probability of solar storms and increase the contribution from GCR.

It is important to note, in any case, that the schedule for a Mars mission is likely to be driven by factors other than expectations of solar activity levels. The schedule will be driven by policy considerations, including cost, hardware development, and political considerations. Launch windows constrained by orbital mechanics will be a major design driver. A schedule delay due to hardware delays could force a launch delay by 26 months to the next available launch window.

A Mars campaign of two or more successive human missions would not be able to ensure each mission was able to fit within periods of reduced GCR radiation. It would be prudent to plan shielding to ensure that dose limits are not exceeded if a mission is launched during solar minimum and to ensure there are limited storm shelters within the deep space vehicle that could further reduce exposure to potentially intense solar storms if launched during a return to high solar activity.

8.4   Implications for GCR Standards

It is important to meaningfully reduce crew exposure to GCR regardless of mission architecture or time in the solar cycle. This ensures risks are minimized, while maximizing spaceflight opportunities for astronauts within the limits set forth in Sections 4.8.2 (Career Space Permissible Exposure Limit for Space Flight Radiation) and 4.8.3 (Short Term Radiation Limits-Solar Particle Events) of NASA-STD-3001 Volume 1. During solar minimum in free space (i.e.,

far enough from a celestial body such that the combined effects from terrestrial, atmospheric, and magnetic shielding can be ignored), the GCR effective dose rate can be reduced to approximately 1.0 to 1.3 mSv/day depending on the shielding material used, as shown in Table 8.4-1. These exposures are achieved with shielding thicknesses between 10 and 40 g/cm^2, consistent with extensive verification and validation studies involving thick targets and GCR environments. Further reductions to effective dose are difficult to realize given the fact that shield thicknesses between 40 and 100 g/cm^2 have either a negligible or negative impact on the exposure rate while potentially introducing a significant mass/launch burden.

Table 8.4-1 only provides first-order bounds on the effectiveness of passive shielding strategies, since vehicle and habitat systems will not be constructed of purely aluminum or hydrogeneous materials such as polyethylene. The value of 1.3 mSv/day is near the optimal value for pure aluminum shielding but is also achieved with less than 10 g/cm^2 of polyethylene. Vehicles and habitats should inherently include sufficient mass (with average thickness distributions between 10 and 40 g/cm^2) and a mixture of materials to enable design optimization efforts to satisfy this requirement without the need for additional or significant parasitic shield mass.

Variability in solar minima is another contributing factor that could influence the ability of a shielding concept to meet this requirement. The 2009 solar minimum is used as the representative case for Table 8.4-1. Recent updates to GCR models have yielded more reliable historical reconstructions of solar activity, and it has been found that the 2009 environment is closely related to the upper 85th percentile of all solar minima over the past 270 years. The value of 1.3 mSv/day therefore includes reasonable conservatism to protect against the possibility of intensifying cosmic rays in the future.

During solar maximum, the heliosphere deflects a portion of the lower energy GCR ions observed in the vicinity of the Earth, Moon, and Mars, making shielding strategies appear to be less effective compared with solar minimum. For example, the ambient (no shielding) daily effective dose rate during solar minimum is reduced by 21% from 1.52 mSv/day to 1.21 mSv/day with 20 g/cm2 of aluminum shielding, while this same shielding provides only a 12% reduction during solar maximum. It is important to note, however, that during solar maximum, exposures are naturally ~50% lower than for solar minimum, and the required daily value of 1.3 mSv/day is easily satisfied. Despite the natural reduction in crew exposure during solar maximum, vehicles shall be designed to meet solar minimum conditions and implement the ALARA principle in Section 4.8.1 of the NASA-STD-3001 Volume 1 to pursue further exposure reductions where possible.

On the lunar and Martian surfaces, free-space GCR exposures are also reduced by approximately 50% due to planetary blockage, while additional exposure (10 to 20% of the total surface effective dose) is introduced by albedo, or backscattered, radiation. Effective dose estimates for the lunar surface as a function of shield thickness are provided in Table 8.4-2. The impacts of shielding material and solar activity are similar to those previously discussed for free space. As a result, 0.8 mSv/day is a reasonable limiting value for surface habitats and vehicles. It is important to note that shielding strategies on the Martian surface may be unable to appreciably reduce crew exposure without parasitic hydrogenous shielding or excavation and construction of massive regolith structures. Mars mission architectures necessitate further analysis to determine a more precise GCR daily exposure limit.

Based on this rationale, a new standard for GCR shielding for human exploration missions beyond LEO is needed. It is recommended that for missions beyond LEO, vehicles and habitat systems should provide sufficient protection to reduce exposure from GCR by 15 to 20% compared with free space such that the effective dose (Career Space Permissible Exposure Limit for Space Flight Radiation, as defined in Section 4.8.2 of NASA-STD-3001 Volume 1) from GCR remains below 1.3 mSv/day for systems in free space and below 0.8 mSv/day for systems on planetary surfaces. The exposure shall be verified as a percent of estimated crew time spent at locations within the vehicle and/or habitat system. Further measures shall be taken to reduce crew exposure in accordance with the ALARA principle.

Table 8.4-1.[*] NASA Effective Dose (mSv/day) for Female Astronaut as Function of Shield Thickness during Solar Minimum and Maximum Conditions in Free Space

	No Shielding	Aluminum Shield Thickness (g/cm^2)				Polyethylene Shield Thickness (g/cm^2)			
		10	20	40	60	10	20	40	60
Solar minimum**	1.52	1.28	1.21	1.23	1.34	1.14	1.04	1.03	1.07
Solar maximum***	0.63	0.57	0.55	0.60	0.68	0.50	0.48	0.51	0.56

[*] The NASA effective dose is calculated using the NASA radiation quality factor and GCR tissue weights for a female astronaut (never smoker) [Cucinotta et al. 2013].

** The 2009 solar minimum was calculated with the BON2020 model.

*** The 2001 solar maximum was calculated with the BON2020 model.

Table 8.4-2. NASA Effective Dose (mSv/day) for Female Astronaut as Function of Shield Thickness during Solar Minimum and Maximum Conditions on Lunar Surface

	No Shielding	Aluminum Shield Thickness (g/cm^2)				Polyethylene Shield Thickness (g/cm^2)			
		10	20	40	60	10	20	40	60
Solar minimum**	0.90	0.78	0.73	0.73	0.78	0.66	0.58	0.56	0.57
Solar maximum***	0.40	0.36	0.35	0.37	0.41	0.30	0.28	0.28	0.31

[*] The NASA effective dose is calculated using the NASA radiation quality factor and GCR tissue weights for a female astronaut (never smoker) [Cucinotta et al. 2013].

** The 2009 solar minimum was calculated with the BON2020 model.

*** The 2001 solar maximum was calculated with the BON2020 model.

S-4.	A standard for GCR shielding for human exploration missions beyond LEO is needed. It is recommended that vehicles and habitat systems provide sufficient protection to reduce exposure from GCR by 15% compared with free space, such that the effective dose from GCR remains below 1.3 millisieverts per day (mSv/day) for systems in space and below 0.8 mSv/day for systems on planetary surfaces. This standard is based on missions during solar minimum (the worst-case scenario). It can be achieved with current aluminum spacecraft structures. For Mars missions *longer than 600 days*, additional GCR mitigation strategies will be required to meet the newly approved 600-mSv crew lifetime exposure limit (except for potentially limited opportunities for missions during solar maximum, when the overall GCR exposure is the lowest).

8.5 HSIA - Approaches to Mitigate the Risk of Inadequate HSIA for LDEMs

For exploration beyond LEO, intermittent and delayed communication with the ground necessitates greater crew autonomy in many aspects of the mission. Two categories of activities currently require substantial ground involvement: 1) troubleshooting unanticipated safety-critical anomalies and 2) executing complex procedures. Unanticipated safety-critical anomalies share three characteristics that make them particularly dangerous during LDEMs and make troubleshooting them difficult. They are *unanticipated*, meaning there is no set procedure in place for anomaly response; they are *unknown,* meaning the source of the anomaly is not initially understood and requires causal analysis; and they are *urgent*, meaning they have short times to effect for unwanted outcomes and must be triaged immediately. Events with this combination of factors (i.e., unanticipated, unknown, and urgent) are met with labor-intensive, ground-heavy anomaly response and often have the potential for LOC/LOM. Executing complex procedures, often involved in maintenance and repair tasks, while typically less urgent, currently requires the crew to be overseen by the ground team. Here, the ground also acts as decision maker when a conditional step is encountered. Data from anomalies analyzed does not indicate that there is an excess in capability on the ground. On the contrary, it is frequent that more capability is pulled in.

For LDEMs, crew members will need to independently respond to urgent, unanticipated anomalies that have potential LOC/LOM consequences. Mission Control flight controllers will still be available, but in the case of a Mars mission, they will only receive notice of an anomalous event after some time has passed, and they will constantly be working from stale data. Any messages they send to the crew will be further delayed. Therefore, the crew will make up the front-line team of anomaly resolution, responding immediately to diagnose time-critical issues, determine time-to-effect for unwanted consequences, and execute any system commands from onboard the vehicle. In addition to limited communication, deep space missions will experience limited sparing, resupply, and evacuation opportunities, further complicating vehicle repair and maintenance.

This paradigm shift in mission operations requires fundamental changes in NASA's current HSIA. Because HSIA spans the whole system (i.e., the crew, all engineered systems supporting the mission, human experts on the ground, data systems, screens, communication devices and schema, and physical spaces), these changes must be made at the systems level, encompassing all aspects of communication, coordination, and collaboration among the crew, vehicle, and ground.

Further, where the other sections of this report are likely to see significant improvement from certain technical and engineering solutions, these solutions are likely to increase system complexity. The future HSIA solution must adequately address increasing system complexity; if done poorly, the future HSIA may cause more problems than it solves.

Enabling a small crew to venture deeper into space for much longer missions without real-time communications will require significant advances across many engineering and technology applications. At this point, NASA does not have integrated data systems, but they will likely be needed onboard to make access to the right data at the right time possible with greatly reduced expertise. Similarly, for telemetry, a significant number of data streams are currently monitored in real time by many ground controllers, 24 hours per day. Some form of monitoring will likely

need to be done onboard to catch problems in a timely manner. It will likely also be necessary to provide some onboard analytical support for the crew to identify adverse trends to manage workload. Human-centered design and new tools and processes also must be brought to bear, in particular to ensure maintainable and diagnosable vehicle systems.

Many current technologies may provide solutions, as these are increasingly designed to provide diagnostic support. Cars, computers, phones, home internet, thermostats, and so on are presently able to provide information about their own state-based sensor and reporting capabilities. Similarly, digital transformation across industries (e.g., the financial sector) have dramatically increased the speed and quality of response to rapidly changing situations. In other areas, simplification of design has evolved. Ikea, for example, became one of the largest furniture makers in the world by working out the details of flat packing and easy home assembly with minimal tools, as well as standardization across the product line. In maintenance and repair, additive manufacturing may also help with certain parts. Each of these examples represents relevant aspects of the state of knowledge relative to enabling crew to manage vehicle malfunctions, although none has had to be adopted by NASA so far because risk has been mitigated through real-time communication with the ground.

8.5.1   LDEM HSIA Risk Drivers

A first step toward characterizing the requirement for an HSIA for missions beyond LEO is investigating the onboard capabilities needed for crew-driven anomaly resolution during LDEMs.

To further assess where current capabilities may need to evolve, the detailed timelines reconstructed for past ISS anomaly resolution processes (see Section 6.5.2.2) were mapped onto Mars transit conditions that shift immediate response, time-critical task execution, and vehicle commanding to the crew. Hypothetical Mars timelines were created for the 2013 Cooling Loop and 2010 Oxygen Generation Assembly (OGA) anomalies, detailing how on-orbit events, ground actions, and the asynchronous communication between the crew and the ground team may take place. Only the 2013 Cooling Loop Mars timeline is included in this version of this report due to OGA anomaly data sensitivity.

In creating these timelines, several assumptions were made. The timelines assume a 20-minute communication delay for uplink and downlink, meaning the ground does not become aware of an anomalous event until 20 minutes after the event occurs. Any subsequent instruction from the ground is at least 40 minutes outdated, but the ground is receiving a constant stream of system telemetry on a 20-minute delay. These communication conditions actually represent a "best-case scenario" for communications during Mars transit (see Section 6.5.2.3); therefore, a conservative approach was taken by assuming these conditions. While the ISS is almost entirely commanded from the ground, the Mars transit timelines assume the communication delay will preclude the ground from commanding the vehicle and shifts command execution to the crew. Importantly, the timelines also assume successful resolution of the anomalies, requiring the crew to take many of the steps performed by the ground during the actual anomaly. In detailing successful anomaly resolution in transit to Mars, the timelines highlight where effective resolution requires drastically evolved onboard capabilities.

The timelines also seek to demonstrate the iterative nature of the diagnostic process, with ground teams and crew members constantly developing and testing hypotheses to further anomaly resolution efforts. On a mission to Mars, ground teams will not simply provide one solution for

the crew to work after they are notified of the anomaly 20 minutes after the fact; anomaly resolution is iterative and requires a continuous back and forth. Every time a hypothesis is tested, new information is gathered that influences the next steps taken. Crew members will frequently be waiting up to an hour for ground team instruction after hypothesis testing, but when the situation unfolds unexpectedly and demands an immediate response, crew members will need to act without any ground involvement or instruction.

The details of these timelines were operationally realistic, and the way events had been reimagined for Mars transit conditions was assessed as plausible based on interviews with flight controllers. One flight controller involved in response to the Cooling Loop A anomaly and one flight controller involved in response to the OGA anomaly were interviewed, as well as multiple subject matter experts in mission operations. When reflecting on their first-hand experience with these anomalies, flight controllers shared lessons learned, key challenges and pain points, and opportunities for improvement, all of which are reflected in the observations and findings for this section.

8.5.1.1   Cooling Loop Anomaly (2013) Reimagined in Mars Transit

Recreating the Cooling Loop A timeline with Mars transit conditions shifts a large portion of the initial troubleshooting work to the crew (see Figure 8.5.1.1-1). Given the communication delay, the crew detects the anomaly, determines a course of action, and begins time-critical pump recovery procedure execution without ground confirmation. As procedures are currently written, it is not uncommon for crew members to pause activity and seek ground guidance when a conditional step is met. If the crew needed ground input at any point during the pump recovery procedure, procedure execution would be on hold for *at least* 40 minutes while the ground determined a course of action. Despite the likelihood of needing ground guidance, the timeline presented here assumes a "best case scenario" in which the crew can complete the procedure without ground intervention.

Even when made aware of the anomaly 20 minutes after its occurrence, the ground cannot send commands to the vehicle, as the ground is "blind" to the current vehicle status. The crew executes all vehicle commands and reports troubleshooting results to the ground. After initial stabilization and procedure execution, the ground investigates relevant troubleshooting activities and continuously communicates actions to the crew. Throughout the timeline, the crew and ground are communicating asynchronously, with testing instructions and results sent between the two groups. Given the time critical nature of some parts of the anomaly response, the operations concept will need to enable the crew to perform some level of diagnosis, testing, and simulation without help from the ground.
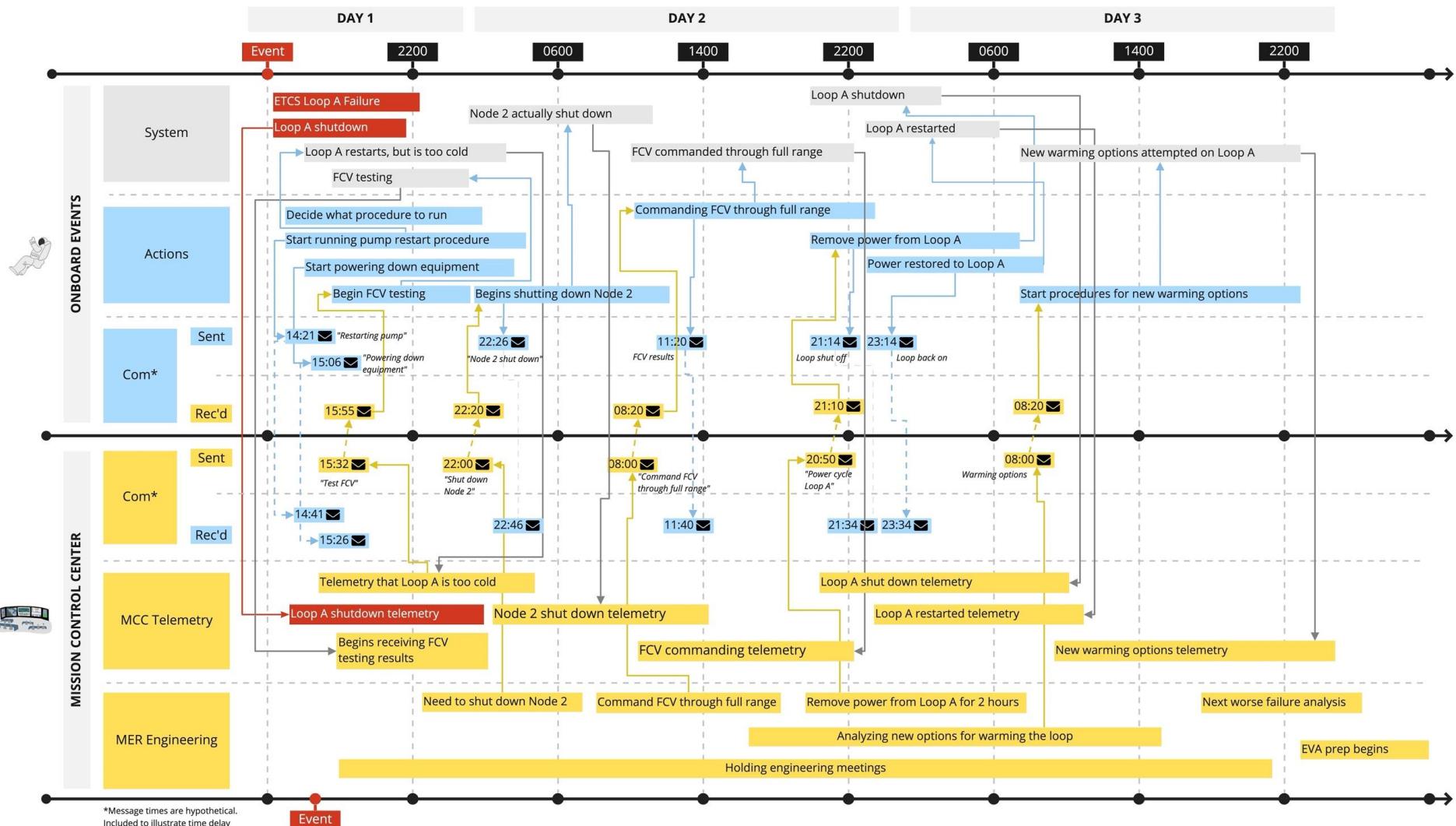
Figure 8.5.1.1-1. First 3 days: Cooling Loop Anomaly Scenario Reimagined in Mars Transit

8.5.1.2 OGA Anomaly (2010) Reimagined in Mars Transit

Recreating the OGA Anomaly event with Mars transit conditions accelerates the timeline, given the inability to resupply oxygen. While it is assumed that the crew will have access to backup oxygen when the OGA initially fails, the repair preparation cadence increases in an effort to waste as little backup oxygen as possible. The crew must perform the entirety of the necessary procedures on-orbit without real-time support from ground. The time it takes to complete the procedures is increased given that the crew must perform and oversee the activity.

8.5.1.3 Mars Transit Findings

The notional Mars timelines were analyzed for key decision points, challenges, and close calls, and insights were extracted regarding the onboard capabilities, data, and tools that are needed for enhanced crew autonomy. It became evident that crew members will be required to recognize, evaluate, and respond to time-critical anomalies and execute vehicle and troubleshooting commands that have historically been controlled from the ground. Therefore, onboard procedures and tools must be designed with autonomous operations in mind. Crew members must have a deep understanding of vehicle systems, flight rules, and data to make informed decisions. Even with all this, it is not clear that the onboard capability will even approximate a fraction of what is on the ground. Effective human-machine teaming onboard and asynchronous communication with the ground will both be critical to mission success.

Mission Control has an army of flight controllers dedicated to monitoring massive amounts of telemetry data across each major vehicle system in real time. During the first hour of the Cooling Loop incident, the ground used telemetry, as well as engineering data to prioritize troubleshooting actions. All of Mission Control and their support teams immediately got to work triaging onboard equipment based on cooling needs and simultaneously preparing for the "next worst failure," while the SPARTAN (i.e., Station Power, Articulation, Thermal Analysis console) controllers executed the important pump recovery procedure. After the onboard crew completed their regularly scheduled workday activities, they assisted the ground in performing some of the steps to power down equipment.

In a deep space scenario, monitoring data, detecting anomalies, and distributing and prioritizing the immediate response will need to be performed onboard by a combination of the crew and vehicle systems. In this case, all four crew members would likely work the anomaly together, with one person executing the pump recovery procedure, a second person assisting them, and the other two monitoring equipment temperatures. Adequate human/machine and human/human teaming will be critical for detecting and rapidly assessing failures. Machine intelligence may be advantageous for augmenting human ability to monitor complex systems like the thermal control system, where pattern recognition is key.

Adding to crew workload, long communication delays in deep space will prevent flight controllers from being able to execute commands on the vehicle from the ground as they do today with the ISS; "commanding in the blind" with a significant delay would be dangerous. When diagnosing anomalies (and during many other tasks) crew members will need to independently execute complex procedures that have historically been handled remotely.

Procedures are not written with autonomous crews in mind. Flight controllers and MER engineers sometimes pause at points in a procedure to consult their investigative fault trees, review data and resources, and debate amongst the team on how to proceed. In deep space

operations, crews will need access to such resources to alleviate this ambiguity. Overall, future spacecraft systems will need to be designed for reliability, simplicity, and ease of maintenance.

Deep space missions may also experience unanticipated anomalies that are not well understood and have no set procedure in place. In these cases, crew members may need flexibility in pulling from and combining multiple procedures, as well as quick access to resources like system documentation and schematics.

O-29.	Autonomous operations require different onboard procedures and tools than those currently used.

F-72.	With a significant light-time delay, ground controllers would be commanding in the blind.

In addition to monitoring the constant stream of telemetry in real time, MCC and MER engineers employ historical/trending data, engineering data, and manufacturing data to make decisions and prioritize activities. System experts have the ability to pinpoint the information needed to answer a given question and understand what they are looking at in the context of a diagnostic goal.

Unlike system experts, crew members are typically generalists who have been trained across a wide range of systems. They work with a smaller and more high-level data set on board. Flight controller interview participants emphasized that *telemetry only tells part of the story.* Understanding how the system is put together and how it functions is crucial. Crew members will need a combination of preflight training and continuous training and scenario exercises to achieve the necessary level of systems understanding.

Onboard data systems need to be designed to enable the crew to find, comprehend, and work with a vast amount of data, some of which are typically only accessible on the ground. The data systems must strike a balance between providing raw data versus contextualized and/or visualized data; interfaces should be designed to aid the crew's understanding and highlight notable patterns but must not oversimplify to the point of introducing unintended biases. Providing the crew with *the right data at the right time to make the right decision* is a fundamental challenge of crew autonomy. Data systems must be designed and tested iteratively using discovery and HITL simulation to assess human/machine performance.

O-30.	Current onboard systems do not support sufficient crew situation awareness for diagnostic processes. Crew also need to understand the context for telemetry, engineering, and safety data to effectively diagnose.

The MCC is designed with a goal of funneling information succinctly to a single decision maker, who is skilled in rapid risk assessment: the Flight Director. In future situations when there is not time to consult Mission Control before making a decision, the Commander's authority becomes absolute. It becomes necessary for the crew to have a deep understanding of the rationale behind flight rules, to make sound decisions, and then understand the downstream consequences of their actions. For experienced design engineers, it can be easy to think that every possible eventuality has been anticipated, with concomitant procedures developed should they arise. However, complex interactions or other unanticipated problems do often arise.

> **O-31.** Based on extensive discussions with astronauts and FOD, deep space crews will need an understanding of how systems work, an understanding of the rationale behind flight rules, and critical thinking skills to make informed decisions when responding to urgent, unanticipated anomalies.

On the ISS today, the availability of real-time ground support, resupply, and sparing has led to a vehicle that is not specifically designed for repairability, maintainability, and diagnosability. Instead, the ground uses their expertise and resupply abilities to address issues with the vehicle as they occur.

When the OGA unexpectedly failed, ground support knew they could rely on backup oxygen that could later be resupplied. Both the OGA and Cooling Loop anomalies used spare units on board the vehicle to repair broken parts, with the knowledge that these spares could be replaced by later missions. During the Cooling Loop anomaly, the broken part was not accessible to the crew without an EVA, hampering diagnosis capabilities. Because the part was not visible to the crew, the ground had to execute a variety of troubleshooting vehicle commands to diagnose the anomaly from afar. When things went wrong during repair, the ground investigated and addressed the issue in real time, advising the crew on how to proceed.

On a deep space mission, the crew will not be afforded real-time ground support or resupply opportunities. Given the inability to resupply, crew members will need to focus on maintaining the vehicle to avoid draining backup resources due to system failure. A vehicle designed for maintainability can also mitigate the lack of real-time ground support, assisting in avoiding situations when time-critical repair typically relies on ground expertise. Making vehicle parts accessible to crew members allows crew members to perform more frequent maintenance while also providing greater diagnosability. When a system does fail, focusing on repair, not replacement, will help preserve spare parts. 3D printing may also contribute to preserving spares but will require bringing the right proportion of raw materials. During the OGA anomaly, the crew replaced the entire Hydrogen Dome ORU for a failure in the cell stack, a suboptimal solution when limited spares exist. Designing systems with maintenance, repair, and diagnosis in mind can help avoid resource draining and mitigate the consequences of time-critical system failures.

> **O-32.** A high level of systems expertise and many hours are required by the crew and ground team to perform system maintenance, diagnosis, and repair tasks, as demonstrated by current and past crewed missions.

Despite the necessary increase in crew autonomy on deep space missions, MCC and MER experts will still be indispensable. In both anomalies the team investigated, the MER held recurring anomaly resolution team meetings, which resulted in investigative fault trees and recommendations for troubleshooting activities and workarounds. For future deep space missions, it will likely still be necessary for the MER to operate in much the same way but with delayed implementation of their contributions. Efficient asynchronous communication will be valuable for consultation throughout all stages of anomaly resolution, but it will perhaps be especially important during time-consuming repair and maintenance activities during which the crew may pause for input, such as choosing whether to replace or repair the unit during the OGA anomaly.

When time-critical circumstances preclude waiting for ground input, crew members must rely on their own capabilities combined with the capabilities of the machines onboard. Machine intelligence may be useful for tasks such as monitoring telemetry; recognizing data patterns; and searching to provide the relevant manuals, schematics, and other resources for a given situation. To work with crew members, onboard systems must possess teaming capabilities, including observability, predictability, and directability [Johnson and Vera 2019]. Onboard systems and tools designed to support the crew in anomaly resolution must be designed and tested iteratively using HITL simulations.

> **O-33.** Efficient asynchronous collaboration with the ground and effective human/machine teaming onboard are the cornerstones of successful anomaly resolution in deep space.

8.5.2 Engineering and Technology Mitigations for HSIA Risk

The reason for the inattention to the HSIA risk is fourfold. First, there is the aspiration to better engineer mission systems to be more reliable and robust, so that no unanticipated anomalies or failures occur. Unfortunately, history has shown, across many high-consequence complex systems, that this cannot be achieved. A second oft-stated approach is to employ next-generation AI and autonomous systems to anticipate, diagnose, and repair such anomalies; all projections indicate this cannot be achieved by extrapolating current AI methods. Third, some believe that different selection and training processes will sufficiently amplify the capabilities of each crew member so that the crew can cover what is now done by the ground. This would require that each crew member take on the monitoring and time-critical response work of between 8 and 21 people on the ground at any given time (estimated based on MCC-H staffing for an Orbit 2 shift in nominal circumstances and during anomaly resolution, respectively)—an unlikely amplification even before accounting for the need to work 24 hours a day. The fourth approach relies on the promise of continuous communication flow and sufficient bandwidth that will allow the ground team to continue to manage mission operations in the way it has for the past decades. While improved communication systems will allow ground teams to continue to support operations to some degree, light-time delays and increased distances will significantly reduce the timeliness and effectiveness of this assistance.

While none of the above approaches can be the single-point solutions, per the findings discussed in Section 6.5, each will be a contributor to the solution. Ground control will continue to provide a great deal of support, even if asynchronously, and without commanding in the blind. Section 8.5.2.1 discusses the advances in communications necessary to enable the ground to be of maximal help to the crew and vehicle. Section 8.5.2.2 discusses what will be needed in terms of onboard data systems, both for telemetry monitoring and systems analysis/diagnostics. Section 8.5.2.3 discusses how next-generation vehicles can be engineered to be more resilient, especially in the context of where crew will need to be much more independent when executing complex procedures and diagnosing problems. Section 8.5.2.4 discusses where intelligent systems might be able to help with increasingly autonomous crewed missions beyond LEO. Note that the evidence base is minimal for how to enable a small number of humans to safely manage complex engineered systems at greater distances from Earth. As such, the final section discusses the critical need for NASA to develop mission analogues and simulation technologies aimed at informing investment decisions with respect to mitigation of this risk.

8.5.2.1   Communications Requirements (Transit and Surface Operations)
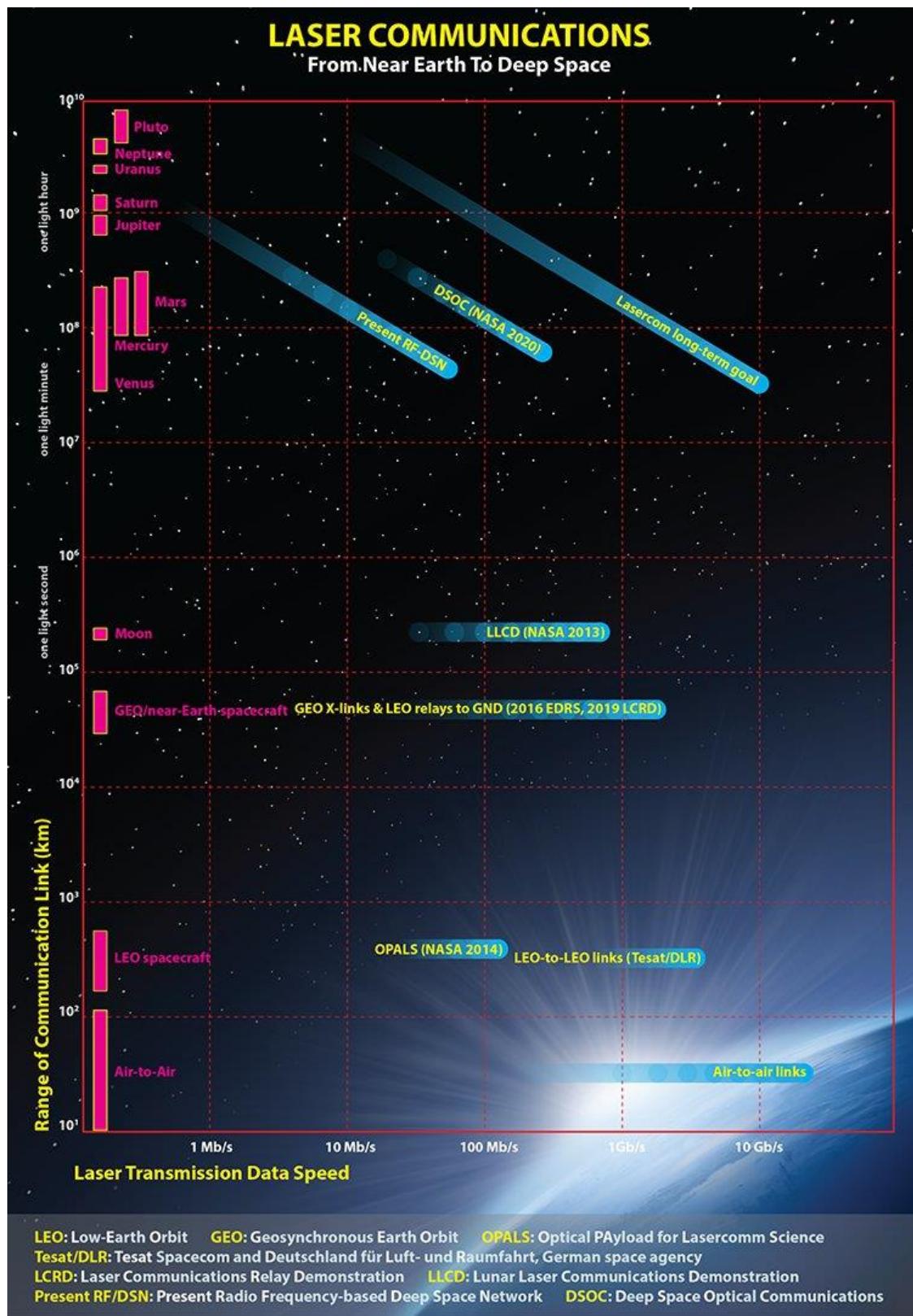
As described above, current communications capabilities to and from Mars are far from those utilized by ISS crewed missions. The current Mars forward/uplink capability is *three orders of magnitude less* than the uplink from MCC to the ISS. The current Mars downlink capability is *50 times less* than the downlink rate from the ISS. Based on discussions with the SCaN team, the ISS downlink rate is likely the minimum required for human Mars missions.

While future optical (laser) communication systems can meet the data rate requirements, these systems will have to use high-orbit relays at Mars to meet link availability needs for crewed missions. Earth-based optical systems will need to provide concurrent visibility to the spacecraft/relays from multiple sites to address weather and other reliability issues. Even so, the communications delay will range from 4 to 24 minutes one way during the mission, including transit there, orbital/surface operations, and transit back. Research on the effects of delayed communication on the performance of distributed teamwork suggests that even at 50 seconds of one-way delay, collaboration is substantially impacted, especially for tasks that are complex and intensive (i.e., have a high tempo) [Fischer and Mosier 2014; Fischer, Mosier, and Orasanu 2013].

The current operational approach of 24/7, real-time communications will have to adjust to accommodate light-time delays and link availability constraints, especially during transit to Mars (see Figure 8.5.2.1-1). A steady delivery of data to the ground requires continuous pointing of the vehicle (through relay satellites) to ground stations on Earth. This approach is not only inefficient from a network standpoint, it also requires considerable ground infrastructure and onboard resources; typically, for missions today, data are saved and scheduled to be sent at maximum data rates once a buffer is full so that assets are not overused. However, it is difficult to support off-nominal operations and anomaly resolutions with such intermittent communications [Rader et al. 2012].

F-73.	Technology solutions exist to meet data rate and link availability needs (e.g., optical communication, relays, etc.) for crewed Mars missions. However, light-time delays, as well as reliability concerns, will still affect Earth/Mars communications.

F-74.	Communication becomes difficult with a 5-second delay and is substantially impacted when the delay is greater than 50 seconds.

Figure 8.5.2.1-1. Laser Communications from Near Earth to Deep Space
[Illustration by Phil Saunders/Source: Don Boroson, Massachusetts Institute of Technology Lincoln Laboratory]

8.5.2.2 Onboard versus Ground Trend Analysis and Knowledge Base Access

The CAIB's report pointed at "dysfunctional" databases as a contributing cause of the accident. There were 50 separate PRACA systems for the Space Shuttle Program, 18 at JSC alone, each with different terminologies, taxonomies, and processes. It was therefore difficult to see patterns of problems and failures. In fact, most of NASA's incidents and accidents have been caused, not by unknown unknowns, but rather by unknown knowns (i.e., the pattern is in our data but we cannot see it). The Constellation Program brought with it managers with Shuttle and ISS experience who knew that change was needed in terms of how mission data are managed.

It was clear even 15 years ago that data systems integration was not just possible but also a good investment. The financial sector of the economy saw the value of rapid, informed decision making and invested strongly in data integration capabilities. Over the past decade, similar efforts can be seen in other sectors (e.g., medical services and even the United States Postal Service). Nevertheless, much of the engineering data integration effort that started with the Constellation Program was rolled back because of the removal of Level 1 program structure with the establishment of the Human Exploration Program. The good news is that the rollback was not due to technology challenges. Data integration itself is not technologically challenging at this point.

Nevertheless, even if the organizational and procurement challenges were to be surmounted, such that all the engineering analysis could be well integrated and available onboard for the crew to work with, the expertise required to understand and work with that data remains an enormous hurdle. In addition to the technical complexity of engineering data (e.g., Problem Reports, Hazard Analyses, etc.), the volume of telemetry data that needs to be monitored and analyzed in the context of the engineering data is enormous. Over a 24-hour period, there are over 60 flight controllers monitoring telemetry: about 1,440 expert hours per day. If crew were to do nothing but monitor telemetry and sleep, it would amount to about 64 hours per day. Obviously, crew cannot be monitoring telemetry 16 hours per day. The technological challenges for deep space exploration with respect to onboard data systems are therefore about monitoring and analyzing very large data sets and making that analysis useful to humans working to anticipate and troubleshoot problems.

Onboard data systems will need to bring together telemetry from sensors with engineering data to help support troubleshooting of malfunctions, making complex technical content comprehensible and useful to the crew. It is easy to underestimate the challenge of this effort. As discussed in Section 6.5.2.1, the breadth and depth of expertise on the ground that has provided the system resilience until now is vast. Tying data together (e.g., parts with their problem histories, associated hazards, and failure modes), most likely in manipulable visualizations that also capture current and recent state from telemetry, may help. This is a critical challenge for deep space exploration, and there are few analogs on Earth that provide a relevant evidence base.

Given that NASA has not focused on quantitatively capturing the time and expertise associated with data retrieval, analysis, and integration for anomaly resolution processes, it is difficult to quantify just how far we are from being able to have a crew of four perform these functions at least partially independently from Earth. Shuttle missions after the *Columbia* accident had a standing team of 30 or so experts working across three shifts focused exclusively on working problems. The night shift of the Shuttle Problem Investigation Team (SPIT) was responsible for retrieving information on the problems being worked [Johnson 2011].

For example, during the STS-117 Shuttle mission, a small corner of thermal blanket over one of the Orbital Maneuvering System pods was found, by robotic arm inspection, to be lifted a couple of inches [Chen 2007]. It would not be an easy on-orbit repair, so the questions quickly became about what would happen with air rushing past it during reentry. It took nearly 24 hours to determine what was under that specific, potentially exposed corner of blanket. It is not difficult to imagine having sensors in that area detecting the lifting of the blanket and then using that telemetry data along with hazards analyses and system drawings to present the crew with a much more integrated picture of the problem. Rather than having to find and align each piece of the puzzle, crew can be provided with pre-integrated data to inform decision making. The data and data integration does not need to be perfect, it just needs to reduce the workload sufficiently to allow crew to troubleshoot without immediate ground support.

> **F-75.** A critical challenge for deep space exploration is developing onboard data systems that will integrate sensor telemetry and engineering data to support anomaly resolution by the crew.

8.5.2.3 Maintainability, Diagnosability, Repairability: Technological Improvements

As discussed earlier, maintainability generally refers to the ease with which hardware and software functions can be preserved against failure or decline. Performing maintenance can include the act of diagnosis and repair, thus maintainability also includes attributes of diagnosability and repairability. Bongarra et al., in human factors design guidelines written for maintainability of Department of Energy nuclear facilities, further clarify *ease* to mean "the amount of time necessary to repair, test, calibrate, or adjust an item to a specified condition, when using defined procedures and resources" [Bongarra et al. 1985]. Bongarra et al. note that maintainability depends just as much on the characteristics of the maintainer-user (i.e., existing knowledge, practices, skills, facilities, environment, and supplies) as on the design of the equipment. Echoing Bongarra et al. in his definition of maintainability, Dhillon [1999] emphasizes measures taken during the development, design, and installation of a manufactured product to reduce required maintenance, manhours, tools, logistic cost, skill levels, and facilities.

Therefore, maintainability (and, by association, diagnosability and repairability) is achieved through design considerations for hardware and software (e.g., standardization, interchangeability, modularization, simplification, accessibility, and identification) as well as human factors (e.g., human body measurement, human sensory capacities) [Dhillon 1999]. Maintainability can also be improved by technological solutions that help reduce the costs associated with performing maintenance duties. Simplification of maintenance procedures and built-in execution guidance for maintenance procedures has become increasingly common in industrial and end-user applications.

Diagnosability is an area of technology that has advanced quickly over the past decade. More and more systems come with built-in sensors that provide diagnostic information. In some cases, these codes are for use by experts (e.g., where the diagnostics system in a car generates specific problem/failure codes to be read by a mechanic). Increasingly, however, diagnostic systems are being built into end-user technologies (e.g., thermostats, computers, refrigerators, etc.). Perhaps the most significant advances are coming from the combination of sensor data with machine learning (ML) algorithms. With help from new sensor technologies, predictive maintenance with ML is seen in applications like vibration-based condition monitoring for gas turbine engine health [Matthaiou et al. 2017], oil analysis (i.e., degradation, oxidation, contamination) for

machine health [Keartland and Van Zyl 2020], and thermal imaging for detecting flaws on metal surfaces [Atwya and Panoutsos 2020].

Advances in ML and deep learning (DL) allow AI-based techniques to go beyond total reliance on older, brittle AI methods (e.g., expert systems). In ML, a set of algorithms is trained to detect patterns in data first by being explicitly taught examples identified by subject matter experts (thus also referred to as supervised learning). Once sufficiently trained, the set of algorithms can then be deployed to monitor and detect learned patterns. DL is a subfield of ML that trains layered algorithms (called an artificial neural network) to ultimately learn to make decisions on its own. ML/DL can be used to automatically detect faults (for diagnosis), off-nominal conditions (for health monitoring), or precursors to failure (for prognostics). This ability enables a shift from a time- or schedule-based and reactive maintenance model to a condition-based predictive maintenance model where maintenance is only performed when needed on the specific component that needs it, thus reducing the need for manpower and corrective actions.

Even though the application of techniques like ML/DL in maintenance, diagnostics, and data monitoring is relatively recent, the desire to automate and improve the maintenance process is by no means new, especially in an industry like aerospace where the cost of safety can be significant. Integrated Vehicle Heath Management (IVHM) was an attempt by NASA to coordinate, integrate, and apply advanced software, sensors, and design technologies to increase the level of intelligence, autonomy, and health state determination and response of future vehicles [Baroth et al. 2001]. It was first identified by the NASA Office of Space Flight in 1992 as the highest priority technology for (then) present and future space transportation systems [General Research Corporation 1992]. The advancement of IVHM has paralleled that of AI technologies, and IVHM is seen applied in the health management of aircraft as well as Mars rovers.

Over the years, NASA has continued to invest at a low level in IVHM, particularly in the development of reasoning systems for monitoring the health of space shuttles, satellites, and aircraft [Ezhilarasu et al. 2019]. Similar applications of ML/DL techniques to extract sensor data for real-time decision-making and system management are seen in other domains as well (e.g., residential building electricity load monitoring) [Berges et al. 2010].The challenge for IVHM approaches has been the same as that for knowledge-based AI: IVHM systems only know what they know and are therefore brittle in the face of conditions not programmed in by the engineers who created the system. They also require significant amounts of test and/or operational data to generate relevant patterns to which to train. Other challenges with IVHM onboard the vehicle include avionics, radiation-hardened components, and computing power. Current processors and networks have nowhere near the computing power afforded on ground for ML/DL applications. It is not currently possible to pump all vehicle data to an AI-enabled computer for analysis, so "filtering" the data to a hierarchy or distribution of systems is used. This filtering masks the ability to actually do the ML/DL needed.

Another NASA effort proposed to address the shortcoming of conventional maintenance approaches was "digital twin." A digital twin is "an integrated multiphysics, multiscale, probabilistic simulation of an as-built vehicle or system that uses the best available physical model, sensor update, fleet history, etc., to mirror the life of its corresponding flying twin" [Glaessgen and Stargel 2012, p. 5]. Conventional approaches, Glaessgen and Stargel argue, rely on probabilistic and reliability methodologies based on assumed similitude between the

circumstances in which the underlying statistics were obtained and the environment in which a vehicle operates.

The same assumptions do not necessarily hold for future vehicles built with new designs that have no clear or well understood legacy. The operating condition of those vehicles may also defy inspection and maintenance in the conventional sense (e.g., on long-duration deep space missions). The digital twin can integrate sensor data from an operating vehicle's onboard IVHM system to forecast the health of the vehicle, predict system response to safety critical events, and uncover previously unknown issues. The combined use of IVHM and digital twin could be made capable of mitigating damage or degradation by activating self-healing mechanisms or by recommending changes in mission profiles to adjust loading in ways to increase component and system lifespan. The key challenges for digital twin approaches are simulation fidelity (e.g., down to the chemistry and physics) and engineering assumptions regarding as-designed, as-build, and as-flown. The digital twin is only as effective as the level of resolution of the digital simulation and the correct engineering representation of the actual vehicle. Importantly, neither IVHM nor digital twin efforts have focused on integration with human problem-solving and reasoning.

Logistics is another area that has greatly benefited from recent technological advances (e.g., Li and Liu [2016]). Computer vision can be used to survey inventory and, with the help of ML, determine damage on items. Radio frequency identification (RFID) combined with Internet of Things (IoT) is used to support automatic identification and tracking of inventory items [NASA 2014]. If every tool and part onboard were fitted with sensors that could transmit information about themselves (e.g., location or whether it is being used, etc.), then this would address many aspects of current onboard logistics and support procedure execution by the crew, especially if combined with a technology such as augmented reality. Sensor technology is advancing quickly, and it may be that power and mass issues are sufficiently reduced over the next decade to make this approach viable. Another challenge of IoT and of highly integrated sensor networks with edge computing is the potentially negative impact to having hundreds of thousands of wireless signals.

In-space manufacturing technology capabilities (including three-dimensional printing of spares and recycling of materials) are potentially valuable for space logistics if the technology can be developed to a point where the capability is reliable and efficient in terms of managing cost, onboard mass, quality control, and complexity. To take advantage of these capabilities, vehicle systems would need to be designed from the outset to account for the constraints and opportunities associated with three-dimensional printing. NASA's In-Space Manufacturing (ISM) project seeks to develop the materials, processes, and manufacturing technologies needed to provide an on-demand manufacturing capability for deep space exploration missions, using the ISS' Additive Manufacturing Facility (AMF) as a testbed. [Prater et al. 2019] This emerging technology should continue to be investigated and assessed for feasibility of use on LDEMs.

> **F-76.** In-space manufacturing technology capabilities (including 3D printing of spares and recycling of materials) are potentially valuable for space logistics.

8.5.2.4 AI and Autonomous Systems

AI and autonomous systems have advanced quickly over the past decade, largely due to the availability of very large data sets and the capability for rapid pattern analysis. New technologies in areas such as natural language processing and facial recognition have quickly emerged and

become useful in everyday life. There was also a strong push over the last decade in the area known as discovery systems, with IBM's Watson system as the most well-known exemplar [Lohr 2021]. These systems can consume enormous volumes of textual information and then search them very quickly looking for matching syntactic patterns, yielding extremely accurate answers to questions that have been asked before. Much of this progress is now evident in current search engines. Robotics has advanced quickly as well, with companies such as Boston Dynamics building systems that can perform remarkable physical feats [Ng 2021].

In parallel with the rapid advances of the past decade, it has become clear that these new technologies are not replacing human capability for adaptive problem-solving and developing workaround solutions to unforeseen problems, but instead are adding new types of capabilities to the mix, especially in areas where powerful raw pattern recognition is relevant. Leading AI researchers conclude that AI is not presently on a convergent path with human intelligence [Davis et al. 2021]. This is not inherently a problem; AI is already superior to humans in many domains, and this will continue to improve, perhaps especially with the ability to quickly find patterns in massive data sets [Memarzadeh et al. 2021]. However, hallmarks of human problem-solving (e.g., causal reasoning) currently remain distinctly human capabilities, and a primary goal for AI becomes to support and enable human performance rather than replace it [Woods 2021; Mindell 2015].

Humans, because of their causal, inductive, adaptive problem-solving skills, provide much of the resilience in complex engineered safety-critical systems. The view that humans will remain essential to systems safety is accepted by operations experts across domains such as air traffic control and the nuclear power industry. It is also shared by researchers in the field of AI, who see machine intelligence evolving in a different direction than human intelligence. In fact, a recent study by the National Academies of Sciences, Engineering, and Medicine [2021] concluded that AI will remain unable to independently respond to complex and novel situations for the foreseeable future and emphasized the need for human oversight and management of future human-AI teams.

In a prescient paper titled "The Autonomy Paradox," Blackhurst, Gresham, and Stone [2011], then with the Air Force's 711th Human Performance Wing, argued that new intelligent technologies were increasing rather than decreasing operational costs. This was due to the fact that, although the new capabilities did what they were supposed to do, they did so in a way that was incomprehensible to the humans remaining in the mix such that, when things went in unexpected ways as they tended to do, more staffing was required than had been needed previously. Two new Defense Advanced Research Projects Agency (DARPA) initiatives, for example, are focused on developing ways to make new AI technologies team better with human operators. The Competency-Aware Machine Learning initiative focuses on developing pattern recognition systems for graphic images, for example, that have some awareness of their own competency and that can therefore interact better with the human imagery analysts. The Collaborative Human and Machine Planning initiative similarly focuses on developing AI planning systems that work more interactively and collaboratively with humans in the operational loop.

These new DARPA programs have emerged because, a decade after the start of this third AI "summer," the autonomy paradox remains. There are exceptions (e.g., Apple) where a very significant investment in human-computer interactions has resulted in natural language and face recognition capabilities that work seamlessly in daily use. For NASA, advances in AI have also

come in areas where there are large-scale data sets, such as space science in analyzing telescope and satellite imagery of the cosmos. It has also been used on the Mars rover missions over the past 20 years to enable the rovers to autonomously navigate distances from several meters to tens of meters on the Martian surface.

Next-generation human exploration missions to the Moon and beyond may be able to use advanced AI systems, especially in areas with big data (e.g., telemetry). Pattern analysis over telemetry may help with early detection of anomalous system states, tracking not only subtle, unanticipated shifts over time but also the interactions between sensors. This is possible based on today's technology, although the engineering impacts to processing and data architectures and implementations must be addressed through spaceflight avionics, software, robotics, and human element trades. The most significant challenge, however, will be determining how to have such systems work with crew to increase their onboard problem-solving capabilities without increasing workload. It is critical to note that because these are evolving technologies, NASA does not have standards in place that can guide the implementation. Developing the standards and requirements that appropriately integrate these new technologies in the context of human spaceflight needs is an engineering research challenge.

F-77.	Current autonomous system capabilities are not capable of managing unanticipated vehicle malfunctions, and although AI will continue to make progress in this direction, it is not expected that machine intelligence will be able to supervene human problem-solving capabilities within NASA's mission timeframes.

F-78.	Research has shown that autonomous and automated systems can increase workload and complexity of tasks for humans, especially in off-nominal situations when human-systems integration was not considered.

8.5.2.5 NASA Analog and Simulation Capability Requirements

The successful integration of humans and systems is paramount to crew performance in anomaly response during LDEMs. Researchers working to assess this risk and engineers working to develop technology solutions do not currently have a method to systematically study anomaly response in high-fidelity analog environments. Several such environments exist but do not yet have the capability to inject realistic faults and allow testing of technological solutions and their integration with crew.

Prior research provides insights into the types of data, models, and procedures needed for onboard problem detection, diagnosis, resolution, and contingency management [Panontin et al. 2021; Frank et al. 2013; Siebert et al. 2019; Beaton et al. 2019; Abercromby et al. 2013; Lim et al. 2019]. These have been gained through systematic analyses of ISS system malfunctions and off-nominal operations; remote observations of MER investigations and deliberations; interviews of astronauts, flight controllers, and instructors; reviews of flight and operation logs; and studies of troubleshooting approaches in analogous domains. The research to date is based solely on past and current operations—any insights, new approaches, and new solutions must be vetted, refined, and most importantly, tested for the LDEM environment.

To meet the challenge of developing a fundamentally new HSIA for LDEMs, NASA requires simulation capabilities to help develop and verify requirements. HITL simulation-based assessments in analogous operational environments provide the best route to understanding

effective human/system teaming designs that accommodate communications limitations expected in a Mars mission. These assessments will allow NASA to iteratively develop and assess onboard tools that increase human/systems resilience, as measured by the proportion of events that are addressable by the crew without ground team support.

The cornerstone of the simulation capability is a platform integrating the information, models, procedural support, etc., that are needed for anomaly resolution by the crew. The platform should provide data structures that enable access, management, and organization of data across interconnected subsystems of a vehicle. It should accommodate and test crew interfaces, ideally through a medium that is portable and can be used across a range of analog platforms at NASA.

Through HITL simulation and iterative design and development, NASA will investigate the architectures and technologies needed to support Earth-independent anomaly response and other safety-critical operations.

F-79.	An HITL simulation and iterative design capability does not currently exist and is needed to investigate the architectures and technologies required to support Earth-independent anomaly response and other safety-critical operations and to validate subsequent design solutions.

O-34.	Researchers should consider the impact of human space-adapted functional/performance capabilities in simulation design.

8.5.2.6 Summary: Systems Engineering for Earth-Independent Operations

The engineering implementation of any space system design provides the realization of a solution bound by technical, cost, schedule, personnel, and political constraints. For current human spaceflight missions, the crew are invaluable to the achievement of the mission objectives, but keeping the vehicle functioning is largely done by human experts on the ground. As discussed throughout this report, the engineering implementation for exploration beyond LEO must therefore support the crew's performance and accommodate their constraints throughout the mission. The HSIA risk described in this report focuses on engineering solutions to enable effective anomaly management and complex procedure execution as the need for Earth-independent operations increases.

While it is possible to reduce anomaly rates through improved reliability analysis and testing, and anomaly impacts though added robustness, such mitigations address only known failure modes and known uncertainties. The historical ISS failure rate noted in Section 6.5.1 is the trend for significant, *unanticipated* anomalies—those that are unknown or even unknowable prior to operations. To address the risk of unanticipated anomalies requires increasing *resilience,* the adaptive capacity and extensibility of the integrated human-system to respond to surprises. Resilience in complex systems is largely dependent on human invention and intervention; this is repeatedly demonstrated by the success of Earth-dependent space missions (e.g., MCC managing ISS) and of other high-consequence operations (e.g., pilots commanding aircraft). Supporting and amplifying crew capabilities to problem solve and manage complex operations will be vital to the success of future, Earth-independent mission operations—hence, the emphasis on *human/systems* integration and the architecture that enables it.
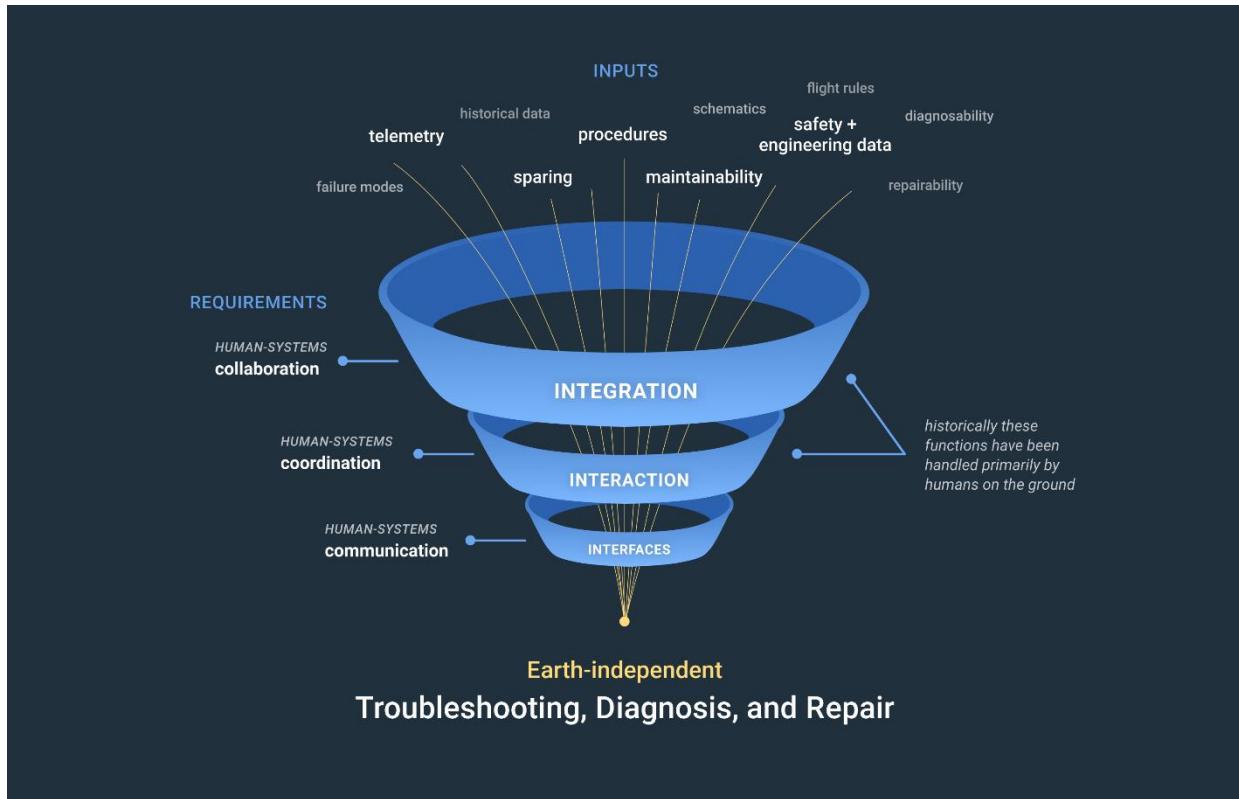
As described above, an HSIA requires communication, coordination, and collaboration between humans and systems. Table 8.5.2.6-1 shows the elements comprising such an architecture and

maps these elements to the current capabilities used for LEO missions and potential future capabilities needed for LDEMs. These capabilities are dependent on the technologies described above (e.g., data systems, ML).

Table 8.5.2.6-1. HSIA Elements and Corresponding Capabilities

Requirement	Architectural Element	Function	Example Current Capability	Example Future Capability
Collaboration	Integration	Anomaly detection	Human monitored telemetered data	System self-monitored, onboard data
		Problem solving	Procedure based, ground driven	Model based, crew driven
		Planning	Asynchronous, ground-optimized timelines	Real-time, constraint-based timeline options
Coordination	Interaction	Procedure execution	Digital checklist, monitored from ground	Embodied AI agent, real-time on board assistance
		Caution and warning	Diffuse alarms, broad system and time criticality cues	Focused alarms, specific system and time criticality cues
		Training	Practice, memorization	Real-time refresh or emergency guidance
Communication	Interfaces	Information gathering	Typed queries	Voiced queries
		Information presentation	2-D screen views	3-D immersive
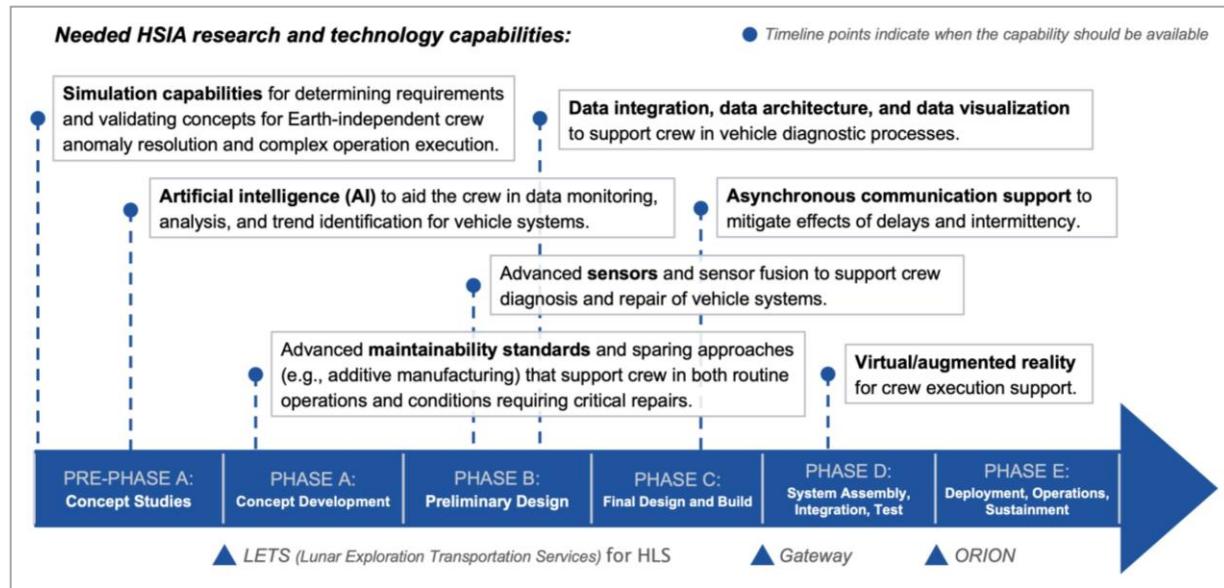
It is also important to note that the capabilities and their overarching architectural elements and requirements rely on each other for an effective HSIA for LDEMs. As represented in Figure 8.5.2.6-1, collaboration between crew and onboard systems enables coordination between system and crew actions, which allows for the appropriate communication of meaningful content (through interfaces). Systems engineering processes must ensure the necessary capabilities are there for collaboration between crew and systems, providing the foundation for the design of interaction and interfaces. Improvement in interfaces only, for example, does not provide the crew with the interactive and integrated content required for Earth-independent activities. Capabilities for all three architectural elements—interfaces, interaction, and integration—need to be in place to enable high-criticality mission functions (e.g., anomaly resolution). Table 8.5.2.6-1 captures the current and potential future technological and engineering capabilities needed to enable critical mission functions for increasingly Earth-independent operations.

Figure 8.5.2.6-1. Overview of HSIA Elements

Aided by HITL simulation and iterative design and development, NASA must take an architecture-level approach to the technologies needed to support Earth-independent anomaly response and other safety-critical operations (pictured in Figure 8.5.2.6-2).

There is an historical organizational and cultural challenge to address for the necessary onboard crew performance support to materialize. Past engineering development programs have had the opportunity to trade within programmatic (e.g., cost and schedule) and technical constraints to prioritize flight vehicle challenges over those associated with in-mission crew performance and operations. This valid prioritization approach allowed for some challenges to be addressed by ground operators and augmented capabilities flown at a later time. By not prioritizing performance support capabilities, ownership of performance challenges is not explicitly taken by the engineering community and is, by default, passed along to the operations community. To date, keeping the vehicle alive has been a function of good up-front systems engineering and a major operational ground support effort. Going beyond LEO, the need to keep the vehicle alive will remain same, but the ground support component will be increasingly reduced.

Figure 8.5.2.6-2. Research and Technology Capabilities must be matured to Support Earth-Independent Anomaly Response and Other Safety-Critical Operations
An architecture-level approach to human-systems integration for planned future Earth-independent missions requires that this work start immediately to impact upcoming contracts.

To compound this ownership ambiguity, the human research community may characterize crew performance support capabilities as an engineering issue outside the scope of more health-centric research (e.g., HRP). This has historically left crew performance support solutions in the hands of the operations community. For missions requiring more Earth-independence, as discussed throughout this report, development of the solutions apart from the flight vehicle development is not possible because more capabilities will need to be onboard. This convergence of challenges leads to the finding that there is not clear organizational ownership of research and engineering implementation, within and across programs, that enables Earth-independent performance.

F-80.	It is possible to reduce anomaly rates through improved reliability analysis and testing, and anomaly impacts through added robustness, but such mitigations address only known failure modes and known uncertainties.

F-81.	Systems engineering solutions and/or technology advances that are needed to improve the onboard HSIA for LDEMs fall outside the scope of existing human health and performance research programs and are missing from many technology maturation roadmaps.

F-82.	Programmatic and mission-level elements supporting increasingly Earth-independent missions are not currently explicit in architecture and design development processes. This increases the risk of ineffective implementation.

F-83.	There is no clear organizational ownership of research and engineering implementation, within and across programs, that enables Earth-independent performance.

S-5.	NASA engineering and human health and medical communities should collaborate to develop a strategic plan to address the paradigm shift needed for the operation of long-duration missions beyond LEO. HSIA requirements must be levied at the onset of the design and development cycle for increasingly Earth-independent missions. Research and technology capabilities to focus on include but are not limited to: • AI to aid the crew in data monitoring, analysis, and trend identification for vehicle systems. • Advanced sensors and sensor fusion to support crew diagnosis and repair of vehicle systems. • Virtual/augmented reality for crew execution support. • Data integration, data architecture, and data visualization to support crew vehicle diagnostic processes. • Asynchronous communication support to mitigate effects of delays and intermittency. • Development of simulation capabilities for determining requirements and validating concepts for Earth-independent crew anomaly resolution and complex operation execution. • Advanced maintainability standards and sparing approaches (e.g., additive manufacturing) that support crew in both routine operations and conditions requiring critical repairs.

9.0   Findings, Observations, and Suggestions for Future Research

9.1   Findings

Space Radiation Environment Characterization: Galactic Cosmic Rays (Section 6.1.1)

F-1.   During solar minimum, the magnetic field is at its weakest point, and the GCR intensity is maximized.

F-2.   Although overall exposures are reduced by about a factor of two during solar maximum compared with solar minimum, it is important to recognize that the GCR remain highly penetrating at all points in the solar cycle.

F-3.   GCR models are sufficiently advanced that they can be reliably (within ±15%) used to specify the flux of protons and heavier ions of importance to crew health and single event effects (SEEs) if the solar cycle activity is known.

F-4.   The ability to predict future GCR environments is limited by the ability to predict future solar activity, including parameters such as sunspot number and the F10.7 cm radio flux index, particularly for periods of time beyond the minima in activity between two cycles.

Space Radiation Environment Characterization: Solar Particle Events (Section 6.1.2)

F-5. A mission that is launched during solar maximum will be subject to a higher frequency of SPEs. One that is launched during solar minimum will experience higher intensities of GCRs.

F-6. The capability to nowcast (monitor) solar energetic particle events is sufficient to support crew warnings for onset of radiation events in time to implement radiation mitigation strategies.

F-7. The capability to *predict* the onset of solar energetic particle events in advance is limited.

Space Radiation Environment Characterization: Near Earth (Section 6.1.3)

F-8. Knowledge of long-term mean and statistical variations in the trapped radiation belt environments is sufficiently advanced to support design of crewed spacecraft that transit the belts on trajectories between LEO and the Moon and Mars, as long as the time spent in the belts is <24 hours.

F-9. Knowledge of long-term mean and statistical variations in the trapped radiation belt environments is sufficiently advanced to support design and operations of robotic missions that spend long periods of time in the radiation belts, such as the Gateway Power and Propulsion Element (PPE) and future uncrewed logistics vehicles using solar electric power to operate ion engines for gradual orbit raising through the belts.

F-10. The ability to forecast the state of the radiation belts for specific short periods of time (i.e., on the order of several weeks) is currently limited due to the lack of nowcast data and predictive models.

Planetary Surface Radiation Environments: Moon (Section 6.1.4)

F-11. Past efforts to measure lunar albedo neutrons have only extended to energies of 15 or 20 MeV. In-situ measurements of the secondary neutron environment on the lunar surface extending beyond tens to hundreds of MeV and GeV energies are needed to support dose estimates for long-term lunar exploration.

Radiation from Onboard Sources (Section 6.1.5)

F-12. The use of nuclear fission reactors for future crewed missions to Mars has been and continues to be examined by NASA as a potential power source for propulsion (NTP or NEP) or for surface operation. Shielding the reactor radiation is a key challenge for NTP or NEP concepts. The crew dose limit will drive the reactor shield design and mass.

F-13. Nuclear reactors operated in the Earth's radiation belts have interfered with gamma ray astronomical observations in the past. It seems likely that a NEP system on the Mars transit vehicle operated within the Earth's magnetosphere will interfere with future gamma ray astronomy missions.

Mission Radiation Exposure Summary (Section 6.1.6)

F-14. Radiation exposure on the lunar surface is about twice that of ISS. Lunar surface exposures depend more heavily on the exposure quantity (dose equivalent versus effective dose) and shielding. Taking these factors into account, Table 6.1.6-2 shows that the exposures range from 1.56 mSv/day (dose equivalent with no shielding at solar minimum) to 0.31 mSv/day (effective dose with 20 g/cm^2 shielding at solar maximum).

F-15. Exposures during solar minimum are higher by roughly a factor of two than during solar maximum, depending on shielding.

F-16. Mitigating the exposure from a reactor can be achieved by employing combinations of passive material shielding and distance. However, such mitigation strategies may lead to challenging and possibly unrealistic launch and in-flight requirements.

F-17. During solar minimum, astronauts' radiation exposure during Mars DRMs will exceed lifetime allowed radiation exposure limits even if that limit is raised to 600 mSv as recommended by the National Academies study.

Passive Shielding for Electronics/Materials from GCR and SPE (Section 6.2.1)

F-18. Only limited work has been done on innovative electronics radiation shielding for human exploration vehicles for solar protons for TID and DDD outcomes.

F-19. For human-rated vehicles and habitats, the mass required to significantly reduce SEEs in electronics is typically unfeasibly large.

F-20. SEE mitigations for human-rated missions are typically accomplished through means other than shielding, including but not limited to part selection and part design to improve hardness.

Crew Radiation Shielding from SPE (Section 6.2.2.1)

F-21. SPEs are considered mitigated as a health risk with adequate shielding.

F-22. Zero additional mass solutions are possible for SPE storm shelters within a vehicle or habitat.

F-23. While shielding mass and geometrical distribution are the primary drivers of protection, preferential use of hydrogen-rich, low-atomic-charge materials in the design of storm shelters improves shielding properties.

Crew Radiation Shielding from GCR (Section 6.2.2.2)

F-24. For a real vehicle, taking into account all the mass and varied materials, improvements in human exposure within the vehicle are typically in the region of diminishing returns where very large additional thickness of shielding are needed to make moderate improvements in reducing exposure.

F-25. Hydrogen-rich, low-atomic-charge materials are the shielding material of choice to reduce crew exposure to GCRs to manageable levels.

F-26. The amount of shielding mass required to provide a given benefit in exposure reduction is highly dependent on assumed spacecraft and shield architecture.

Active Shielding (Section 6.2.3)

F-27. In principle, sufficiently intense magnetic shielding or electrostatic shielding concepts could reduce radiation exposure on long-duration missions by deflecting high-energy GCR particles away from a crewed vehicle.

F-28. Active shielding concepts studied to date within the limits of current technology do not offer dramatic improvement over passive shielding in terms of mass and power requirements and bring new risks in the case of system failure.

F-29. There is no mature electrostatic shielding design available to estimate even a rough comparison with passive shielding.

Forecast Models (Section 6.3.2.2)

F-30. The HESPERIA REleASE model will benefit from an instrument that will provide real-time electron fluxes 24/7 in the energy range of 1 to a few MeV.

AG Research (Section 6.4.1)

F-31. Altered gravity is a significant cross-cutting hazard for human system risks when considering factors for safe exploration beyond LEO, especially for Mars missions where long-duration exposure to microgravity significantly exceeds our current baseline experiences and possible countermeasure applicability.

F-32. Upon return to Earth, the effects of altered gravity recover over periods approaching 1 week, depending on specific actions. Current altered gravity hazard mitigations appear to work for times up to ~1 year, but more data are required to build trends for longer duration uses or applications.

F-33. AG has the unique feature of potentially protecting all physiological systems in all individuals against the effects of an altered gravity hazard, because throughout evolution all creatures on the surface of the Earth adapted to the same 1-g level.

AG Research (Section 6.4.1)

State of AG Technology (Section 6.4.2)

F-34. There are several ways to generate a force that simulates gravity (e.g., linear acceleration or centripetal acceleration), although all but centripetal acceleration appear to be impractical for orbital or interplanetary transit implementations, leading to a focus on short- and large-radius centrifugation systems.

F-35. In recent studies, intermittent ground-based short-radius centrifugation AG appeared to have a positive effect on deconditioning responses induced by strict HDBR, suggesting that future efforts target longer duration and/or greater magnitudes of exposure to iAG.

F-36. The engineering trade space for in-space options to produce continuous and iAG exposure (e.g., internal short-arm centrifuges, tethers, and other rotating systems) contains several point designs with various levels of detail but is not as sophisticated as the current state of the art for ground-based AG investigations. This is largely driven by the lack of a consensus dose-response model for an AG countermeasure.

Human-Systems Integration Architecture (Section 6.5)

F-37. The likelihood of high-consequence problems of uncertain origin occurring during spaceflight is high (conservatively, exceeding 50% during Mars transit) based on historical trends.

HSIA: Team Expertise (Section 6.5.2.1)

F-38. For human spaceflight missions, monitoring of mission system data and diagnosis/mitigation of unanticipated critical malfunctions have been done from the ground by 80+ highly experienced engineers with deep systems expertise. Some of

this data monitoring and problem-solving capability will need to be on board to support the crew when ground intervention is unavailable or delayed.

Crewed Space Communication: ISS (Section 6.5.2.3.1)

F-39. Every 10 seconds, ISS generates 300,000 individual pieces of data but only sends 30,000 to the ground. The rest are pulled down by the ground as needed to solve problems.

Mars Deep Space Communications (Section 6.5.2.3.3)

F-40. Currently, Earth/Mars communications have far lower data rates and link availability than those used to support crewed missions in LEO.

Onboard versus Ground Trend Analysis And Knowledge Base Access (Section 6.5.2.4)

F-41. Current databases supporting ISS operations are not well integrated on the ground nor are they accessible to the crew.

Spaceflight Maintainability Standards (6.5.2.5.2)

F-42. NASA STD 8729.1A and NASA-STD-3001 are based on evidence that comes primarily from LEO and could be incomplete for the full suite of beyond Earth orbit mission objectives (e.g., human lunar return segment, sustained lunar presence segment, and humans to Mars segment).

Integrated Human Health Risk Assessment for Missions to Mars (Section 7)

F-43. As mission duration increases, crew capability is expected to degrade and the likelihood of LTH impacts is expected to increase. Estimates of expected crew capability degradation are limited.

F-44. A radical shift in operational paradigm, systems design, and human/system integration approaches is the only viable approach to improve the risk posture.

F-45. Reductions in the radiation-associated LTH risk can be achieved through decreasing exposure time (fast transit) and/or decreasing exposure magnitude (shielding improvements).

F-46. Increased duration of exposure to altered gravity worsens multiple human system risks and contributes to degradation of crew capability in mission and for LTH outcomes.

F-47. Improvements in fast transit or AG can serve to improve risk by reducing exposure time or reducing exposure magnitude.

F-48. Attempting to use the LEO operational paradigm (the current HSIA) with communication and resupply delays is high risk.

F-49. A trade space exists between the benefits and increased complexity of new engineering solutions (e.g., fast transit, AG, active shielding, and advanced AI) which affects the HSIA risk.

F-50. The risks of microgravity exposure, radiation exposure, and reduced ground support (inadequate HSIA) increase with Mars mission duration/distance from Earth such that there is a high likelihood of serious adverse outcomes (e.g., LOC/LOM) for 3-year missions (if unmitigated).

F-51. A 1-year Mars mission duration significantly reduces the risks of microgravity exposure and radiation exposure. Some benefits would be gained for the risk associated with reduced ground support (inadequate HSIA), but these may be offset by the increased system complexity needed to shorten mission duration.

F-52. Significant investments in research and technology advancement are needed to reduce the risks of microgravity exposure, radiation exposure, and reduced ground support (inadequate HSIA) to acceptable levels for long Mars mission durations.

Fast Transit to Mars Feasibility Study (Section 8.1)

F-53. For the scenario and launch period analyzed in this study, minimum roundtrip Earth-Mars-Earth Δv requirements are found to be approximately 14 km/s when a VGA is used during the Mars-to-Earth journey and approximately 15 km/s when no VGA is used.

F-54. During the 2035 to 2037 launch period analyzed in this study, a VGA during the Mars-to-Earth journey is found to reduce Δv requirements by more than 1 km/s. A VGA requires the geometry of Earth, Mars, and Venus to align properly, so the geometry for a beneficial VGA does not repeat as frequently as the geometry for an Earth-Mars-Earth trajectory without a VGA.

F-55. For the scenario analyzed in this study, placing the spacecraft in a 2.5-sol Mars parking orbit increases Δv requirements by approximately 200 m/s compared with placing the spacecraft in a 5-sol orbit.

F-56. For the scenario analyzed in this study, increasing the Mars orbit stay time from 10 sols to 15 sols increases Δv requirements by 300 to 600 m/s. Increasing the Mars orbit stay time from 15 to 20 sols increases Δv requirements by a further 300 to 600 m/s.

F-57. The minimum-Δv trajectories without a VGA use a >2km/s DSM during the Earth-to-Mars journey.

F-58. The minimum-Δv trajectories found in this study result in minimum solar distances approximately equal to Venus's orbital distance, regardless of whether a VGA is used. Solar distances less than Earth's orbital distance are driven by the short flight-time requirement.

F-59. The minimum-Δv trajectories found in this study result in maximum solar distances approximately equal to Mars's orbital distance. Solar distances greater than Mars' orbit distance are generally incompatible with the short flight-time requirement.

F-60. If the total mission duration for a crewed mission to Mars is allowed to be significantly greater than 400 days, then the crew time in interplanetary cruise can be significantly reduced compared with the case in which the total mission duration is limited to 400 days. The additional total mission duration is spent at Mars.

F-61. The minimum-Δv trajectories found in this study have Earth-to-Mars flight times of approximately 130 days. Restricting the Earth-to-Mars flight time to 90 days or fewer results in a Δv increase of more than 2 km/s.

Passive Shielding for Mars Mission GCR Protection (Section 8.2)

F-62. Human exposures during solar maximum can be as much as 50% lower than during solar minimum when all other variables are constant.

F-63. The increased probability of an SPE during solar maximum may not result in an increase in radiation risk since the SPE exposure can be minimized with reasonable design of a storm shelter.

F-64. Large values of additional water mass for shielding, on the order of 1000 cm, may be needed to reduce the exposure of solar minimum GCR environment to the exposure level for solar maximum GCR.

F-65. The uncertainty in transport codes used to study the shielding efficacy is largely unquantified at material thicknesses greater than 100 g/cm^2.

F-66. Adding shielding to the interior of a vehicle, as opposed to the outside of the vehicle, creates a more optimal solution because less mass is required to optimize shield thickness and mass located closer to the astronaut is a more efficient shield.

Timing of Mars Missions as a Radiation Mitigation Strategy (Section 8.3)

F-67. The previous and current solar cycles 24 and 25 have been a period of historically low solar activity, with a correspondingly high GCR throughout the entire cycle. Continuation of extremely low solar activity could both decrease the probability of solar storms and increase the contribution from GCR.

F-68. Mars missions during solar maximum could have half the dose of a similar mission at solar minimum.

F-69. SPEs are likely to contribute to exposure for a mission conducted in solar maximum, but the likelihood is that for reasonable vehicle shielding the total (i.e., GCR plus SPE) exposure will not increase the total effective dose above the levels that would be experienced for a mission conducted during solar minimum.

F-70. Research into forecasting solar cycles has focused on predicting the amplitude of the next solar maximum, but little has been done to forecast solar cycle duration.

F-71. Reducing the uncertainties in forecasts of solar cycle duration would enable more informed calculations of GCR exposure.

Approaches to Mitigating Risk of Inadequate HSIA on Missions to Mars (Section 8.5)

F-72. With a significant light-time delay, ground controllers would be commanding in the blind.

F-73. Technology solutions exist to meet data rate and link availability needs (e.g., optical communication, relays, etc.) for crewed Mars missions. However, light-time delays, as well as reliability concerns, will still affect Earth/Mars communications.

F-74. Communication becomes difficult with a 5-second delay and is substantially impacted when the delay is greater than 50 seconds.

F-75. A critical challenge for deep space exploration is developing onboard data systems that will integrate sensor telemetry and engineering data to support anomaly resolution by the crew.

F-76. In-space manufacturing technology capabilities (including 3D printing of spares and recycling of materials) are potentially valuable for space logistics.

F-77. Current autonomous system capabilities are not capable of managing unanticipated vehicle malfunctions, and although AI will continue to make progress in this direction, it is not expected that machine intelligence will be able to supervene human problem-solving capabilities within NASA's mission timeframes.

F-78. Research has shown that autonomous and automated systems can increase workload and complexity of tasks for humans, especially in off-nominal situations when human-systems integration was not considered.

F-79. An HITL simulation and iterative design capability does not currently exist and is needed to investigate the architectures and technologies required to support Earth-independent anomaly response and other safety-critical operations and to validate subsequent design solutions.

F-80. It is possible to reduce anomaly rates through improved reliability analysis and testing, and anomaly impacts through added robustness, but such mitigations address only known failure modes and known uncertainties.

F-81. Systems engineering solutions and/or technology advances that are needed to improve the onboard HSIA for LDEMs fall outside the scope of existing human health and performance research programs and are missing from many technology maturation roadmaps.

F-82. Programmatic and mission-level elements supporting increasingly Earth-independent missions are not currently explicit in architecture and design development processes. This increases the risk of ineffective implementation.

F-83. There is no clear organizational ownership of research and engineering implementation, within and across programs, that enables Earth-independent performance.

9.2 Observations

Active Shielding (Section 6.2.3)

O-1. With the present-day HTSC technology, dose reduction from magnetic shielding can be up to ~45% with 23 Tm (field on versus field off). The total shield mass in the simulation is 137 metric tons, and the stored energy in the shield exceeds 15 GJ. The actual engineering design mass can be (much) larger.

O-2. Magnetic shielding concepts encounter many operational, technical, and design challenges, to include managing the thermal energy release of potential quenching of the superconducting coils and restoring the magnetic fields after a shutdown of the current (planned or otherwise).

Forecast Models (Section 6.3.2.2)

O-3. There are at least 40 short-term forecast models (new models under development and currently available models), many of which are being refined.

O-4. To protect crews in deep space (and at Mars) when near real-time communciations with Earth is not feasible, increased on-location capability to generate timely and actionable space weather forecasts is required. Development of an Earth-independent space weather forecasting capability (i.e., onboard transit vehicles or on site at Mars) is needed such that the system collects and processes data and generates space weather forecasts

autonomously. This will require on-site computational and modeling capabilities, as well as retrieval and processing of data from solar observatories at various locations in the solar system.

AG Research (Section 6.4.1)

O-5. Some altered gravity human health and performance risks, like SANS, are unique and currently lack broadly accepted countermeasures.

State of AG Technology (Section 6.4.2)

O-6. To date, there have only been four documented instances of in-space human-based AG research: 1) during Gemini XI in 1966, 2) on Spacelab-1 in 1985, 3) on IML-1 in 1992, and 4) during the Neurolab mission on STS-90 in 1998.

Spaceflight Maintainability Standards (6.5.2.5.2)

O-7. Current approaches to system robustness (e.g., carrying and/or upmassing many ORUs) may not be feasible for extended missions beyond LEO.

O-8. Safe and cost-effective beyond-LEO operations will require a new approach to flight-like systems testing and HITL simulation during development.

Integrated Human Health Risk Assessment for Missions to Mars (Section 7)

O-9. Interventions such as fast transit, AG, and radiation mitigations are intended to limit the extent of crew capability degradation and LTH impacts.

O-10. Improving the knowledge base that frames our understanding of mechanisms and consequences of radiation carcinogenesis, CVD, and CNS impacts may serve to decrease our estimate of risk associated with a Mars mission.

O-11. Implementation of fast transit faces engineering hurdles, some outside the scope of this report. These include increases in system complexity that can worsen HSIA risk. In the case of NTP or NEP, risks include development uncertainty and additional radiation considerations for astronauts.

O-12. Implementation of AG solutions faces developmental hurdles and increases to system complexity that can worsen HSIA risk.

O-13. Status quo approaches rely on adequate exercise capability to be accepted and fielded by programs during the systems trades and design phases. Historically, this has been a challenge for NASA programs.

O-14. NASA has not adequately characterized the magnitude of the HSIA risk and the set of countermeasures needed to ensure mission success.

O-15. Apart from AG, Newton-level breakthroughs needed for radiation protection and HSI are unlikely to move a Mars mission toward LEO-like risk levels.

Fast Transit to Mars Feasibility Study (Section 8.1)

O-16. The analyses described in this assessment report are based on assumptions and constraints developed after consultation with the MAT.

O-17. The trajectory characteristics, including Δv requirements, described in this assessment report represent values obtained for the specific set of assumptions and constraints

described in the Fast Mars Transfer study document. Additional analysis would be required to draw conclusions for different sets of assumptions and constraints.

O-18. The analyses described in this assessment report focus on overall Δv minimization. However, further study of the Fast Mars Transfer scenario will necessarily take into account additional, possibly competing, objectives. Additionally, Δv requirements must also be translated into fuel requirements based on architectural development (e.g., propulsion system selection, staging selection, etc.).

O-19. For a Mars orbit stay time of 20 sols or less, a 5-sol Mars parking orbit may be too large to allow for an acceptable amount of time for the crew on the Martian surface.

O-20. The analyses described in this feasibility study provide only a cursory overview of possible operational concepts for a crewed Mars mission with a total duration of less than 400 days.

O-21. Further work is needed to develop additional mission architecture elements of a fast crewed Mars mission to provide context for the described Δv trade study.

O-22. Further work is needed to investigate the implications of current technology and near-term technology development on the feasibility of a fast crewed Mars mission architecture based on the described trajectories.

O-23. Further analysis on Mars parking orbits smaller than 5 sols (e.g., 2.5 sols) is needed because the benefits of a smaller orbit are likely to outweigh the Δv penalty for a Mars orbit stay time of 20 sols or less.

O-24. Additional trade studies are needed to further understand specific elements of the fast Mars trajectory trade space, such as the >2 km/s DSM during the Earth-to-Mars journey for the minimum-Δv trajectory without a VGA.

O-25. It would be beneficial to examine in more depth the implication of trajectory options that produce short total cruise times (less than 300 days) but long Mars stay times (greater than 600 days).

Passive Shielding for Mars Mission GCR Protection (Section 8.2)

O-26. Additional work needs to be done to quantify the uncertainty in radiation transport codes at large material thicknesses (greater than 100 g/cm^2).

Timing of Mars Missions as a Radiation Mitigation Strategy (Section 8.3)

O-27. Due to strong effect on radiation exposure, mission timing with respect to the solar cycle should be considered an input factor to Mars mission planning. Additional research in forecasting solar cycle amplitude and duration would be beneficial for Mars mission planning.

O-28. Use of a CL-based model to determine a worst-case design reference spectrum for solar protons has several advantages over using a particular event such as the one that occurred in October 1989.

Approaches to Mitigating Risk of Inadequate HSIA on Missions to Mars (Section 8.5)

O-29. Autonomous operations require different onboard procedures and tools than those currently used.

O-30. Current onboard systems do not support sufficient crew situation awareness for diagnostic processes. Crew also need to understand the context for telemetry, engineering, and safety data to effectively diagnose.

O-31. Based on extensive discussions with astronauts and FOD, deep space crews will need an understanding of how systems work, an understanding of the rationale behind flight rules, and critical thinking skills to make informed decisions when responding to urgent, unanticipated anomalies.

O-32. A high level of systems expertise and many hours are required by the crew and ground team to perform system maintenance, diagnosis, and repair tasks, as demonstrated by current and past crewed missions.

O-33. Efficient asynchronous collaboration with the ground and effective human/machine teaming onboard are the cornerstones of successful anomaly resolution in deep space.

O-34. Researchers should consider the impact of human space-adapted functional/performance capabilities in simulation design.

9.3 Suggestions for Future Research

In this report, the assessment team discussed a number of recommendations based on the gap analysis and case studies that were performed for long-term expeditions to Mars. In principle, these recommendations fall into two categories: recommendations that can be potentially instrumental in reducing the risks to crew health on expeditions to Mars, and recommendations that enhance our knowledge base and understandings of the risks involved. *Only recommendations that can potentially impact risk reduction for a first human expedition to Mars are listed here*. Additionally, because of the interdisciplinary nature of these recommendations, they are put forward as suggestions to the science, technology, engineering, and operations communities to collaborate and explore the optimum solution space further.

S-1. Additional space weather monitoring assets (i.e., solar coronagraph and particle detector suites) at Sun-Earth Lagrange point L4 and Sun-Mars L1 and L4/L5 can enable sufficient early warnings for Mars missions during transit and stay. The Sun-Mars L4/L5 assets would also provide a communications relay solution for when the Earth line of sight to Mars is behind or close to the Sun, leading to a 2-week blackout period every 2 years.

S-2. Human research investigations should be pursued to evaluate more fully the safety and efficacy of an iAG countermeasure for exposure durations (doses) greater than 30 minutes per day, in combination with strict long-duration head-down bed rest deconditioning. Future AG investigations should be supported by current human research efforts to assess lower body negative pressure, as well as plans to use Gateway in combination with surface lunar gravity exposure and explore commercial partnership opportunities to understand in-space centrifugation.

S-3. Fast Mars transit approaches (i.e., round-trip duration of approximately one year) using on-orbit staging with chemical propulsion, or nuclear thermal or electric propulsion (NTP or NEP) technologies should be studied further as a possible baseline mission approach to reduce the integrated risks.

S-4. A standard for GCR shielding for human exploration missions beyond LEO is needed. It is recommended that vehicles and habitat systems provide sufficient protection to reduce

exposure from GCR by 15% compared with free space, such that the effective dose from GCR remains below 1.3 millisieverts per day (mSv/day) for systems in space and below 0.8 mSv/day for systems on planetary surfaces. This standard is based on missions during solar minimum (the worst-case scenario). It can be achieved with current aluminum spacecraft structures. For Mars missions *longer than 600 days*, additional GCR mitigation strategies will be required to meet the newly approved 600-mSv crew lifetime exposure limit (except for potentially limited opportunities for missions during solar maximum, when the overall GCR exposure is the lowest).

S-5. NASA engineering and human health and medical communities should collaborate to develop a strategic plan to address the paradigm shift needed for the operation of long-duration missions beyond LEO. HSIA requirements must be levied at the onset of the design and development cycle for increasingly Earth-independent missions. Research and technology capabilities to focus on include but are not limited to:

- AI to aid the crew in data monitoring, analysis, and trend identification for vehicle systems.
- Advanced sensors and sensor fusion to support crew diagnosis and repair of vehicle systems.
- Virtual/augmented reality for crew execution support.
- Data integration, data architecture, and data visualization to support crew vehicle diagnostic processes.
- Asynchronous communication support to mitigate effects of delays and intermittency.
- Development of simulation capabilities for determining requirements and validating concepts for Earth-independent crew anomaly resolution and complex operation execution.
- Advanced maintainability standards and sparing approaches (e.g., additive manufacturing) that support crew in both routine operations and conditions requiring critical repairs.

10.0   Alternate Technical Opinion(s)

No alternate technical opinions were identified during the course of this assessment by the NESC assessment team or the NESC Review Board (NRB).

11.0   Other Deliverables

No unique hardware, software, or data packages, other than those contained in this report, were disseminated to other parties outside this assessment.*]*

12.0   Recommendations for the NASA Lessons Learned Database

No recommendations for NASA lessons learned were identified as a result of this assessment.

13.0   Recommendations for NASA Standards, Specifications, Handbooks, and Procedures

This assessment contains a suggestion for updating NASA STD-3001 (Vol. 1, "Crew Health") standards on GCR shielding for human-carrying spacecraft beyond LEO (see suggestion 4 (S-4)).

14.0 Definition of Terms

Absorbed Dose	Energy deposited per unit mass (Gy).
Dose Equivalent (Sv)	Absorbed dose multiplied by a radiation quality factor for cancer endpoints accounting for the increased biological effectiveness of high-LET ions compared with gamma rays.
Effective Dose (Sv)	The weighted sum of organ dose equivalents, where the weights sum to unity and quantify the relative radio sensitivity of all tissues included in the calculation.
Finding	A relevant factual conclusion and/or issue that is within the assessment scope and that the team has rigorously based on data from their independent analyses, tests, inspections, and/or reviews of technical documentation.
Lesson Learned	Knowledge, understanding, or conclusive insight gained by experience that may benefit other current or future NASA programs and projects. The experience may be positive, such as a successful test or mission, or negative, as in a mishap or failure.
Linear Energy Transfer (LET)	Energy deposited per unit path length (keV/um) .
Mean Organ Absorbed Dose (Gy)	The mass-averaged dose for a given tissue.
Observation	A noteworthy fact, issue, and/or risk, which is not directly within the assessment scope, but could generate a separate issue or concern if not addressed. Alternatively, an observation can be a positive acknowledgement of a Center/Program/Project/Organization's operational structure, tools, and/or support.
Organ Dose Equivalent (Sv)	The mean absorbed dose in an organ or tissue weighted with the radiation quality factor for cancer endpoints.
Problem	The subject of the independent technical assessment.
Recommendation	A proposed measurable stakeholder action directly supported by specific finding(s) and/or observation(s) that will correct or mitigate an identified issue or risk.
Supporting Narrative	A paragraph, or section, in an NESC final report that provides a detailed explanation of a succinctly worded finding or observation. For example, the logical deduction that led to a finding or observation; descriptions of assumptions, exceptions, clarifications, and boundary conditions.

15.0   Acronyms and Nomenclature List

ACE	Advanced Composition Explorer
AES	Advanced Exploration Systems
AG	Artificial Gravity
AGBRESA	Artificial Gravity Bed Rest – European Space Agency Study, 2019
AGREE	Artificial Gravity with Ergometric Exercise
AI	Artificial Intelligence
ALARA	As Low as Reasonably Achievable
AMF	Additive Manufacturing Facility
ARC	Ames Research Center
ARD	Active Radiation Detector
ARES	Active Radiation Environment Sensor
ARRT	Acute Radiation Risk Tool
ARS	Acute Radiation Syndrome
ART	Anomaly Resolution Team
ASCAN	Astronaut Candidate
ASTRO	Active Station Thermal Resources and Operations
ATCS	Active Thermal Control System
AU	Astronomical Unit (= 1.495978707×1011 m)
BFO	Blood Forming Organ
BoC	Basis of Comparison 2019 (mission concept)
BON2020	Badhwar-O'Neil 2020 GCR model
BR-AG1	Bed Rest Antigravity Study, 2010
CAIB	Columbia Accident Investigation Board
CAM	Computerized Anatomical Male
CBEF	Centrifuge-equipped Biological Experiment Facility
CCMC	Community Coordinated Modeling Center
CCOR	Compact Coronagraph
CELIAS	Charge, Element, and Isotope Analysis System
CHI	Crew Health Index
CHIT	Mission Action Request
CHP	Crew Health and Performance
CI	Confidence Interval
CL	Confidence Level
cm	centimeter
CME	Coronal Mass Ejection
CMILP	Consolidated Maintenance Inventory Logistics Planning

CNS	Central Nervous System
COB	Connection to Observer
CONOPS	Concept of Operations
COSTEP	Comprehensive Suprathermal and Energetic Particle Analyzer
CHP	Crew Health and Performance
CVD	Cardiovascular Disease
C&W	Caution and Warning
DAP	Digital Autopilot
DARPA	Defense Advanced Research Projects Agency
DDCU	Direct Current to Direct Current Converter Unit
DDD	Displacement Damage Dose
deg	degree
DL	Deep Learning
DMI	Deferred Maintenance Item
DRM	Design Reference Mission
DSCOVER	Deep Space Climate Observatory
DSM	Deep Space Maneuver
DSN	Deep Space Network
ECLSS	Environmental Control and Life Support System
EDE	Effective Dose Equivalent
EHIS	Energetic Heavy Ion Sensor
EIT	Extreme Ultraviolet Imaging Telescope (SOHO)
ELFIN	Electron, Proton, and Helium Instrument
EMTG	Evolutionary Mission Trajectory Generator
EPAM	Electron Proton Alpha Monitor (ACE)
EPHIN	Electron Proton Helium Instrument
ERNE	Energetic and Relativistic Nuclei and Electron
ERSA	European Radiation Sensor Array
ESA	European Space Agency
ESP	Energetic Storm-time Particle
ESPE	Energetic Solar Particle Event
ETCS	External Thermal Control System
ETHOS	Environmental and Thermal Operating Systems
EUV	Extreme Ultraviolet
eV	electron volt
EVA	Extravehicular Activity
EVAC	Probability of Evacuation

EXIS	Extreme Ultraviolet and X-ray Irradiance Sensor (GOES)
FCR	Flight Control Room
FCT	Flight Control Team
FDIR	Fault Detection, Isolation, and Recovery
FIT	Flight Investigation Team
FN	Flight Note
FT 2021	Fast Transit (mission concept)
FUV	Far Ultraviolet
GA	Gravity Assist
GCR	Galactic Cosmic Radiation
Geant3/Geant4	GEometry ANd Tracking (toolkit for simulating the passage of particles through matter)
GHz	gigahertz
GOES	Geostationary Operational Environmental Satellite
GeV	gigaelectronvolt
GeV/n	gigaelectronvolt
GONG	Global Oscillations Network Group
GRS	Gamma Ray Spectrometer
GSFC	Goddard Space Flight Center
g/cm^2	grams per square centimeter
HCZ	Hub Control Zone
HDBR	Head-down Bed Rest
HEOMD	Human Exploration and Operations Mission Directorate
HEPS	High-energy Particle Spectrometer
HERA	Hybrid Electronic Radiation Assessor
HERMES	Heliophysics Environmental and Radiation Measurement Experiment Suite
HI	Heliospheric Imager
HITL	Human-in-the-Loop
HLS	Human Landing System
HMF	Heliospheric Magnetic Field
HMI	Helioseismic and Magnetic Imager
HPU	HERA Processing Unit
HQ	Headquarters
HRP	Human Research Program
HSIA	Human Systems Integration Architecture
HSIR	Human Systems Integration Requirements
HSR	Human System Requirements

HSRB	Human System Risk Board
HSU	HERA Sensor Unit
HTSC	High-temperature Superconductor
HZE	high atomic number, high energy
HZETRN	space radiation transport code
HZETRN2020	space radiation transport code 2020
H/W	hours per week
iAG	Intermittent Artificial Gravity
ICME	Interplanetary Coronal Mass Ejection
IDRD	Interface Definition & Requirements Document
IFHX	Interface Heat Exchanger
IFI	Item for Investigation
IMAG	International Multidisciplinary Artificial Gravity
IMAP	Interstellar Mapping and Acceleration Probe
IML	International Microgravity Laboratory
IMM	Integrated Medical Model
IMP-8	Interplanetary Monitoring Platform 8
IoT	Internet of Things
ISEP	Integrated Solar Energetic Particle (Alert/Warning System Scoreboard)
ISM	In-Space Manufacturing
ISRO	Indian Space Research Organization
ISS	International Space Station
iSWA	Integrated Space Weather Analysis System
ITCS	Internal Thermal Control System
IVA	Intravehicular Activity
IVHM	Integrated Vehicle Health Management
JAXA	Japan Aerospace Exploration Agency
JPL	Jet Propulsion Laboratory
JSC	Johnson Space Center
kbps	kilobits per second
km	kilometer
km/s	kilometers per second
KSC	Kennedy Space Center
kWe	1,000 watts of electrical power
LaRC	Langley Research Center
LASCO	Large Angle and Spectrometric Coronagraph

LBNP	Lower-body Negative Pressure
LDEM	Long-duration Exploration Mission
LEO	Low Earth Orbit
LET	Linear Energy Transfer
LNDE	Lunar Neutron Density Experiment (Apollo 17)
LOC	Loss of Crew
LOCL	Loss of Crew Life
LOM	Loss of Mission
LOMO	Loss of Mission Objectives
LRU	Line Replaceable Unit
LSAH	Lifetime Surveillance of Astronaut Health
LSPE	Low-energy Solar Particle Event
LTH	Long-term Health (post-mission)
LTL	Low Temperature Loop
L×C	Likelihood × Consequence
m	meter
MAG4	Magnetogram Forecast System
MARS	Multiple Artificial-gravity Research System
Mars-GRAM	Mars Global Reference Atmospheric Model
MART	Multilateral Anomaly Resolution Team
MAT	Mars Architecture Team
Mbps	Megabits per second
MBSU	Main Bus Switching Unit
MCC	Mission Control Center
MCC-COL	Mission Control Center Cologne
MCC-H	Mission Control Center Houston
MCD	Mars Climate Database
MCNPX	Monte Carlo N–Particle Transport Code System, Extended
MDM	Multiplexer/Demultiplexer
MER	Mission Evaluation Room
MeV	megaelectronvolt
mGy	milligray
MHz	megahertz
ML	Machine Learning
MPCV	Multi-Purpose Crew Vehicle
m/s	meters per second
MPSR	Multi-Purpose Support Room

MSFC	Marshall Space Flight Center
MSLRAD	Mars Science Laboratory Radiation Assessment Detector
mSv	millisievert
MTL	Moderate Temperature Loop
MW	megawatt
NCEI	National Centers for Environmental Information
NEP	Nuclear Electric Propulsion
NESC	NASA Engineering and Safety Center
NIAC	NASA Institute for Advanced Concepts
NOAA	National Oceanic and Atmospheric Administration
NSRC	NASA Space Cancer Risk (model)
NTP	Nuclear Thermal Propulsion
OCHMO	Office of the Chief Health and Medical Officer
OGA	Oxygen Generation Assembly
OLTARIS	NASA tool for quantifying radiation exposure
OMS	Orbital Maneuvering System
ORU	Orbital Replacement Unit
PC	Personal Computer
PCVP	Pump & Control Valve Package
PD	Performance Decrement
PEL	Permissible Exposure Limit
PFU	Particle Flux Unit
pH	Potential of Hydrogen
PlasMag	Plasma Magnetometer
PoD 2020	Point of Departure (mission concept)
PRACA	Problem Reporting and Corrective Action System
PSRD	Program System Requirements Document
PTCS	Passive Thermal Control System
PUNCH	Polarimeter to Unify the Corona and Heliosphere
QD	Quick Disconnect
R&M	Reliability and Maintainability
R&R	Removal and Replacement
RBVM	Radiator Beam Valve Module
REID	Risk of Exposure-induced Death
REM2	Radiation Environment Monitor 2
RF	Radio Frequency
RFID	Radio Frequency Identification

RHA	Radiation Hardness Assurance
RPC	Remote Power Controller
RPCM	Remote Power Controller Module
RTSW	Real-time Solar Wind
Sv	sievert
SAA	South Atlantic Anomaly
SANS	Spaceflight Associated Neuro-ocular Syndrome
SCaN	Space Communication and Navigation
SCLT	Systems Capability Leadership Team
SDO	Solar Dynamic Observatory
sec	second
SECS	Sequential Events Control System
SEE	Single Event Effect
SEPMOD	Solar Energetic Particle MODel
SGPS	Solar and Galactic Proton Sensor
SIS	Solar Isotope Spectrometer (ACE)
SMD	Science Mission Directorate
SMM	Solar Maximum Mission
SOHO	Solar and Heliospheric Observatory
SOI	Sphere of Influence
SPARTAN	Station Power, Articulation, Thermal, and Analysis
SPD-1	Space Policy Directive-1
SPE	Solar Particle Event
SPIT	Shuttle Problem Investigation Team
SRAG	Space Radiation Analysis Group
SR2S	Space Radiation Superconducting Shield
SSA	Space Situational Awareness
STAT	SPE Threat Assessment Tool
STEREO	Solar Terrestrial Relations Observatory
STMD	Space Technology Mission Directorate
SUVI	Solar Ultraviolet Imager (GOES)
Sv	sievert
SWFO-L1	Space Weather Follow-on - Lagrange 1
SWiPS	Solar Wind Plasma Sensor
SWPC	Space Weather Prediction Center
TDRS	Tracking and Data Relay Satellite
TID	Total Ionizing Dose

Tm	Tesla-meter
TREAT Astronauts Act	To Research, Evaluate, Assess, and Treat Astronauts Act
UMASEP	University of Malaga Solar Energetic Particles
UV	Ultraviolet
UVCS	Ultraviolet Coronograph Spectrometer
VGA	Venus Gravity Assist
WOOV	Water On/Off Valve
xEMU	Exploration Extravehicular Mobility Unit
ZSOI	Zero Sphere of Influence

16.0   References

"Apollo Lunar Surface Journal," (E. M. Jones and K. Glover, Eds.). Last revised June 5, 2018. URL: https://www.hq.nasa.gov/alsj/, last accessed on January 13, 2022.

Abercromby, A. F. J., Chappell, S. P., and Gernhardt, M. L., (2013) "Desert RATS 2011: Human and Robotic Exploration of Near-Earth Asteroids," *Acta Astronautica* (91): 34-48, October-November 2013. URL: https://www.sciencedirect.com/science/article/pii/S0094576513001525

Adams, J. H., Bhattacharya, M, Lin, Z. W., Pendleton, G, and Watts J. W. (2007) "The Ionizing Radiation Environment on the Moon," *Adv. Space Res.* 40: 338-341.

Ambroglini, F., Battiston, R., and Burger, W. J. (2016) "Evaluation of Superconducting Magnet Shield Configurations for Long Duration Manned Space Missions" *Front. Oncol.* 6. https://doi.org/10.3389/fonc.2016.00097

American Cancer Society (2022) "Lifetime Risk of Developing or Dying from Cancer." URL: https://www.cancer.org/cancer/cancer-basics/lifetime-probability-of-developing-or-dying-from-cancer.html, last accessed January 14, 2022.

Antonsen, E. L. and Van Baalen, M. (2021) "Comparison of Health and Performance Risk for Accelerated Mars Mission Scenarios," NASA Technical Memorandum NASA/TM-20210009779, February 2021.

Antonsen, E. L., Myers, J. G., Boley, L. A., Arellano, J. D., Kerstman, E. L., Kadwa, B. K., Buckland, D. M., and Van Baalen, M. (2021) "Estimating Medical Risk for Human Spaceflight," Accepted for publication to *NPJ Microgravity,* October 2021.

Antonsen, E., Hansen, A., Shah, R., Reed, R., and Canga, M. (2016) "Conceptual Drivers for an Exploration Medical System," in proceeding from 67th International Astronautical Congress, Guadalajara, Mexico, September 2016, vol. IAC-16,A1,3,9,x35689, p. 10.

Arbeille, P., Gauquelin, G., Pottier, J. M., Pourcelot, L., Güell, A., and Gharib, C. (1992) "Results of a 4-week Head-Down Tilt with and without LBNP Countermeasure: II. Cardiac and Peripheral Hemodynamics—Comparison with a 25-day Spaceflight," *Aviat Space Environ Med* 63(1): 9-13.

Artificial Gravity, G. Clément and A. P. Bukley, Eds., Springer, Hawthorne, CA, 2007.

Atwell, W., Rojdev, K., Aghara, S., and Sriprisan, S. (2013) "Mitigating the Effects of the Space Radiation Environment: A Novel Approach of Using Graded-Z Materials," AIAA Space 2013 Conference and Exposition. doi: 10.2514/6.2013-5385

Atwya, M., and Panoutsos, G. (2020) "Transient Thermography for Flaw Detection in Friction Stir Welding: A Machine Learning Approach," *IEEE Transactions on Industrial Informatics* 16(7), 4423–4435. https://doi.org/10.1109/TII.2019.2948023

Augustine, N. R., Auston, W. M., Chyba, C., Kennel, C. F., Bejmuk B. I., Crawley, E. F., Lyles, L. L., Chiao, L., Greason, J., and Ride, S. K. (2009) "Review of U.S. Human Spaceflight Plans Committee – Seeking a Human Spaceflight Program Worthy of a Great Nation," Washington, DC.

Badavi, F. F. (2012) A Dynamic Model for Validation of Cosmic Rays Anisotropy at Low Earth Orbit," *IEEE Trans. Nucl. Sci.* 59: 447-455.

Bailey, L. J., Folta, D., Barbee, B. W., Vaughn, F., Campbell, B., Thronson, H. A., . . . Lin, T. Y. (2013) "A Lean, Fast Mars Round-trip Mission Architecture: Using Current Technologies for a Human Mission in the 2030s," *AIAA SPACE Conference and Exposition.* San Diego, CA. (NTRS-20180006138/GSFC-E-DAA-TN8715)

Ball, R. and Evans, C. H., Eds., (2001) *Safe Passage: Astronaut Care for Exploration Missions*, National Academies Press. URL: https://www.nap.edu/catalog/10218/safe-passage-astronaut-care-for-exploration-missions

Baroth, E., Powers, W., Fox, J., Prosser, B., Pallix, J., Schweikard, K., and Zakrajsek, J. (2001) "IVHM (Integrated Vehicle Health Management) Techniques for Future Space Vehicles," *37th Joint Propulsion Conference and Exhibit*. 37th Joint Propulsion Conference and Exhibit, Salt Lake City, UT, July 8, 2001. URL: https://doi.org/10.2514/6.2001-3523

Battiston, R., Burger, W. J., Calvelli, V., Musenich, R., Choutko, V., Datskov, V. I., Della Torre, A., Venditti, F., Gargiulo, C., Laurenti, G., Lucidi, S., Harrison S., and Meinke, R. (2011) "Active Radiation Shield for Space Exploration Missions," Final Report ESTEC Contract No. 4200023087/10/NL/AF, "Superconductive Magnet for Radiation Shielding of Human Spacecraft," November 2011.

Beaton, K. H., Chappell, S. P., Abercromby, A. F. J., Miller, M. J., et al. (2019) "Using Science-Driven Analog Research to Investigate Extravehicular Activity Science Operations Concepts and Capabilities for Human Planetary Exploration," *Astrobiology*, March 6, 2019. URL: https://www.liebertpub.com/doi/full/10.1089/ast.2018.1861

Berges, M. E., Goldman, E., Matthews, H. S., and Soibelman, L. (2010) "Enhancing Electricity Audits in Residential Buildings with Nonintrusive Load Monitoring," *Journal of Industrial Ecology* 14(5): 844–858. https://doi.org/10.1111/j.1530-9290.2010.00280.x

Biesecker, D. (2008) "Predictions of the Solar Cycle, Past and Present," Presentation at Space Weather Week, Boulder, CO.

Biesecker, D., "The Solar Cycle 24 Consensus Prediction," National Oceanographic and Atmospheric Administration (NOAA), URL: https://www.swpc.noaa.gov/sites/default/files/images/u2/Solar%20Cycle%20Progression%20and%20Prediction.pdf, last accessed January 14, 2022.

Blackhurst, J., Gresham, J., and Stone, M., (2011) "The Autonomy Paradox: Why 'Unmanned Systems' don't Shrink Manpower Needs," 2011, Air Force 711th Human Performance Wing, *Armed Forces Journal*. URL: http://www.armedforcesjournal.com/2011/10/7604038

Blue, R. S., Chancellor, J. C., Antonsen, E. L., Bayuse, T. M., Daniels, V. R., and Wotring, V. E. (2019b) "Limitations in Predicting Radiation-Induced Pharmaceutical Instability during Long-Duration Spaceflight," *NPJ Microgravity* 5(1): 15, 2019. doi: 10.1038/s41526-019-0076-1

Blue, R. S., Chancellor, J. C., Suresh, R., Carnell L. S., Reyes, D. P., Nowadly C. D., and Antonsen, E. L. (2019c) "Challenges in Clinical Management of Radiation Induced Illnesses in Exploration Spaceflight," *Aerosp Med Hum Perform,* Vol. 90(11): 966–977, November 2019. PMID 31666159

Blue, R. S., et al., (2019a) "Supplying a Pharmacy for NASA Exploration Spaceflight: Challenges and Current Understanding," *NPJ Microgravity* 5(1): 14, December 2019. doi: 10.1038/s41526-019-0075-2

Bongarra, J. P. Jr., VanCott, H. P., Pain, R. F., Peterson, L. R., and Wallace, R. I. (1985) *Human Factors Design Guidelines for Maintainability of Department of Energy Nuclear Facilities,* UCRL-15673, 6341066, Lawrence Livermore National Laboratory. URL: https://doi.org/10.2172/6341066

Braun, M. (2019) "AGBRESA – Strict Bed-Rest for 60 Days,". Retrieved from https://www.dlr.de/blogs/en/desktopdefault.aspx/tabid-5893/9577_read-1096/, last accessed January 12, 2022.

Buckley, A., Paloski, W., and Clement, G. (2007) "Physics of Artificial Gravity," In G. Clement and A. Buckley (Eds.), *Artificial Gravity,* Hawthorne, CA: Springer, pp. 33-58.

Chamberlain, N., Gladden, R., Barela, P., Epp, L., and Bruvold, K. (2015) "MAVEN Relay Operations," 2015 IEEE Aerospace Conference, March 7–14, 2015. doi: 10.1109/AERO.2015.7119237

Chancellor, J. C., Blue, R. S., Cengel, K. A., Aunon-Chancellor, S. M., Rubins, K. H., Katzgraber, H. G., and Kennedy, A. R. (2018) "Limitations in Predicting the Space Radiation Health Risk for Exploration Astronauts," *NPJ Microgravity* 4(8): 1–11, April 3, 2018. doi: 10.1038/s41526-018-0043-2

Chen, A. (2007) "STS-117 Atlantis Thermal Protection Blanket Repair [Video]," June 15, 2007. YouTube. URL: https://www.youtube.com/watch?v=71kInEU5jg8

Clément, G. R., Bukley, A. P., and Paloski, W. H. (2015) "Artificial Gravity as a Countermeasure for Mitigating Physiological Deconditioning during Long-Duration Space Missions," *Frontiers in Systems Neuroscience* 9(92). doi:10.3389/fnsys.2015.00092

Clément, G. (2015) "Human Health Countermeasures Element Evidence Report on Artificial Gravity," NASA Johnson Space Center.

Clément, G., (2017) "International Roadmap for Artificial Gravity Research," *NPJ Microgravity* 3, article 29, November 24, 2017. https://doi.org/10.1038/s41526-017-0034-8

Clément, G., and Bukley, A. (2008) "Research Recommendations of the ESA Topical Team on Artificial Gravity," *Acta Astronautica* 63(7): 783-790. https://doi.org/10.1016/j.actaastro.2007.11.008

Clette, F., Svalgaard, L., Vaquero, J. M., and Cliver, E. W., (2014) "Revisiting the Sunspot Number A 400-year Perspective on the Solar Cycle," arXiv:1407.3231 (astro-ph.SR), submitted on July 11, 2014.

Columbia Accident Investigation Board (2003) "Columbia Accident Investigation Board Report: Volume 1," August 2003. URL: https://www.nasa.gov/columbia/home/CAIB_Vol1.html

Cooper, M., Douglas, G., and Perchonok, M. (2011) "Developing the NASA Food System for Long-Duration Missions," *Journal of Food Science* 76(2): R40–R48. doi: 10.1111/j.1750-3841.2010.01982.x

Cucinotta, F. A. and Cacao, E. (2020) "Predictions of Cognitive Detriments from Galactic Cosmit Ray Exposure to Astronauts on Exploration Missions," *Life Sciences in Space Research* 25: 129–135.

Cucinotta, F. A., Kim, M. Y., and Chappell, L. J. (2013) "Space Radiation Cancer Risk Projections and Uncertainties - 2012," NASA/TP-2013-217375, January 2013. URL: https://spaceradiation.jsc.nasa.gov/irModels/TP-2013-217375.pdf

Cucinotta, F. A., Kim, M. Y., and Ren, L. (2006) "Evaluating Shielding Effectiveness for Reducing Space Radiation Cancer Risks," *Radiation Measurements* 41: 1173-1185. https://doi.org/10.1016/j.radmeas.2006.03.011

Davis, J. R., Stepanek, J., Fogarty, J. A., and Blue, R. S., Eds. (2021) *Fundamentals of Aerospace Medicine*, 5th ed., Philadelphia, PA: Wolters Kluwer.

Davis, R., LeCun, Y., Mitchell, T., Rogers, T., and Riecken, D., (2021) "What's the Next Big Question? Leaders in A.I. Discuss the Science of the Future," U.S. Air Force Office of Scientific Research, A.I. 2040 and Beyond Series, Speaker Discussion, Virtual Event. URL: https://community.apan.org/wg/afosr/w/researchareas/31842/a-i-2040-and-beyond-20211027/

De Angelis, G, Badavi, F. F., Clem, J. M., Blattnig, S. R., Clowdsley, M. S., Nealy, J. E., Tripathi, R. K., and Wilson, J. W. (2007) "Modeling of the Lunar Radiation Environment," *Nucl. Phys. B* 166: 169-183.

Dempsey, R. (Ed.), (2013) "The International Space Station: Operating an Outpost in the New Frontier," April 13, 2018. URL: https://www.nasa.gov/connect/ebooks/the-international-space-station-operating-an-outpost

Denisov, A. N., Kuznetsov, N. V., Nymmik, R. A., Panasyuk, M. I., and Sobolevsky, N. M. (2010) "Assessment of the Radiation Environment on the Moon," *Acta Astronaut* 68: 1440-1447.

Dhillon, B. S. (1999) *Engineering Maintainability: How to Design for Reliability and Easy Maintenance*. Gulf Publishing Company.

Douglas, G. L., Zwart, S. R., and Smith, S. M. (2020) "Space Food for Thought: Challenges and Considerations for Food and Nutrition on Exploration Missions," *J Nutr* 150(9): 2242–2244, September 2020. doi: 10.1093/jn/nxaa188

Drake, B. G. and Watts, K. D., eds. (2009) "Human Exploration of Mars Design Reference Architecture 5.0: Addendum #2," NASA SP–2009-566-ADD2.

Drake, B. G., ed. (2009a) "Human Exploration of Mars Design Reference Architecture 5.0," Mars Architecture Steering Group, NASA SP–2009-566, July 2009.

Drake, B. G., ed. (2009b) "Human Exploration of Mars Design Reference Architecture 5.0: Addendum #1," Mars Architecture Steering Group, NASA SP–2009-566-ADD, July 2009.

Edwards, C. D., Jr., Arnold, B., DePaula, R., Kazz, G., Lee, C., and Noreen, G. (2006) "Relay Communications Strategies for Mars Exploration through 2020," *Acta Astronautica* 59:310–318.

Elgart, R., et al. (2018) "Radiation Exposure and Mortality from Cardiovascular Disease and Cancer in Early NASA Astronauts," *Nature Scientific Reports* 8:8480, May 2018.

Ellison, D. H., Conway, B. A., Englander, J. A., and Ozimek, M. T. (2018) "Analytic Gradient Computation for Bounded-Impulse Trajectory Models Using Two-Sided Shooting," *Journal of Guidance, Control, and Dynamics* 41(7): 1449-1462. doi:10.2514/1.G003077

Englander, J. A. and Conway, B. A. (2017) "An Automated Solution of the Low-Thrust Interplanetary Trajectory Problem," *Journal of Guidance, Control, and Dynamics,* 40(1):15-27. doi:10.2514/1.G002124

Evans, W. A., de Weck, O., Laufer, D., and Shull, S. (2006) "Logistics Lessons Learned in NASA Spaceflight," NASA/TP-2006-214203, May 2006.

Ewert, M. K., Broyan, J. L., Semones, E. J., Goodliff, K. E., Chai, P. R., Singleterry, R. C., Abston, L., Clowdsley, M. S., Wittkopp, C. J., and Vitullo, N. A. (2017) "Comparing Trash Disposal to Use as Radiation Shielding for a Mars Transit Vehicle," 47th International Conference on Environmental Systems, ICES-2017-178.

Ezhilarasu, C. M., Skaf, Z., and Jennions, I. K. (2019) "The Application of Reasoning to Aerospace Integrated Vehicle Health Management (IVHM): Challenges and Opportunities," *Progress in Aerospace Sciences* 105: 60–73. https://doi.org/10.1016/j.paerosci.2019.01.001

Fischer, U. and Mosier, K. (2014) "The Impact of Communication Delay and Medium on Team Performance and Communication in Distributed Teams," *Proceedings of the Human Factors and Ergonomics Society Annual Meeting* 58: 115-119. 10.1177/1541931214581025

Fischer, U., Mosier, K., and Orasanu, J. (2013) "The Impact of Transmission Delays on Mission Control-Space Crew Communication," *Proceedings of the Human Factors and Ergonomics Society Annual Meeting* 57:1372-1376. 10.1177/1541931213571303

Folta, D., Barbee, B. W., Englander, J., Vaughn, F., and Lin, T. Y. (2013) "Optimal Round-trip Trajectories for Short Duration Mars Missions," *AAS/AIAA Astrodynamics Specialists Conference*.

Folta, D., Vaughn, F., Westmeyer, P., Rawitscher, G., and Bordi, F. (2005) "Enabling Exploration Missions Now: Applications of On-Orbit Staging," *AAS/AIAA Astrodynamics Specialists Conference*. Lake Tahoe, CA.

Forget, F., Hourdin, F., Fournier, R., Hourdin, C., Talagrand, O., Collins, M., Lewis, S. R., Read, P. L., and Huot, J. P. (1999) "Improved General Circulation Models of the Martian Atmosphere from the Surface to Above 80 km," *J. Geo. Res.* 104: 24155-24176.

Frank, J. D., Spirkovska, L., McCann, R., Wang, L., Pohlkamp, K., and Morin, L. (2013) "Autonomous Mission Operations," 2013 IEEE Aerospace Conference, pp. 1–20. URL: https://doi.org/10.1109/AERO.2013.6496927

Furukawa, S., Chatani, M., Higashitani, A., Higashibata, A., Kawano, F., Nikawa, T., . . . Watanabe-Takano, H. (2021) "Findings from Recent Studies by the Japan Aerospace Exploration Agency examining Musculoskeletal Atrophy in Space and on Earth," *NPJ Microgravity* 7(1): 18. doi:10.1038/s41526-021-00145-9

Gazenko, O. G., Genin, A. M., and Egorov, A. D. (1981) "Summary of Medical Investigations in the U.S.S.R. Manned Space Missions," *Acta Astronautica,* 8(9): 907-917. doi: https://doi.org/10.1016/0094-5765(81)90061-8

General Research Corporation (1992) "Research and Technology Goals and Objectives for Integrated Vehicle Health Management (IVHM)," Contractor Report NASA-CR-192656). URL: https://ntrs.nasa.gov/citations/19930013844

Gilland, J. H., LaPointe, M., Oleson, S., Mercer, C., Pencil, E., and Mason, L. (2011) "MW-Class Electric Propulsion System Designs for Mars Cargo Transport," *AIAA SPACE 2011 Conference and Exposition*, Long Beach, California, AIAA-2011-7253.

Ginet, G. P., O'Brien, T. P., Huston, S. L., Johnston, W. R., Guild, T. B., Friedel, R., Lindstrom, C. D., Roth, C. J., Whelan, P., Quinn, R. A., Madden, D., Morley, S., and Su, Y. J. (2013) "AE9, AP9, and SPM: New Models for Specifying the Trapped Energetic Particle and Space Plasma Environment," *Space Sci. Rev.* 179: 579-615.

Girbau, C. E. (2020) "Design for Diagnosability: Methodologies and Guidelines for Standardization," Master's Thesis submitted in partial fulfillment of the requirements for the Master's Degree in Electronic Engineering, Universitat Politecnica de Catalunya, June 2020.

Glaessgen, E. and Stargel, D. (2012) "The Digital Twin Paradigm for Future NASA and U.S. Air Force Vehicles," 53rd AIAA/ASME/ASCE/AHS/ASC Structures, Structural Dynamics and Materials Conference; 20th AIAA/ASME/AHS Adaptive Structures Conference, Honolulu, Hawaii, April 23, 2012. URL: https://doi.org/10.2514/6.2012-1818

Goswami, N., Blaber, A. P., Hinghofer-Szalkay, H., and Convertino, V. A. (2019) "Lower Body Negative Pressure: Physiological Effects, Applications, and Implementation," *Physiol Rev,* 99(1): 807-851. doi:10.1152/physrev.00006.2018

Hadfield, C. (2022) "Chris Hadfield Teaches Space Exploration," *MasterClass*, 2018. URL: https://www.masterclass.com/classes/chris-hadfield-teaches-space-exploration, last accessed January 12, 2022.

Hamilton, D., Smart, K., Melton, S., Polk, J. D., and Johnson-Throop, K. (2008) "Autonomous Medical Care for Exploration Class Space Missions," *Journal of Trauma and Acute Care Surgery*, 64(4): S354, April 2008. doi: 10.1097/TA.0b013e31816c005d

Hargens, A. R., Whalen, R. T., Watenpaugh, D. E., Schwandt, D. F., and Krock, L. P. (1991) "Lower Body Negative Pressure to provide Load Bearing in Space," *Aviat Space Environ Med* 62(10): 934-937.

Hathaway, D. (2010) "The Solar Cycle," *Living Rev. Solar Phys.* 7.

Hayatsu, K., Hareyama, M., Kobayashi, S., Yamashita, N., Miyajima, M., Sakurai, K., and Hasebe, N. (2008) "Radiation Doses for Humans Exposed to Galactic Cosmic Rays and Their Secondary Products on the Lunar Surface," *Bio. Sci. Space* 22: 59-66.

Heilbronn, L. H., Borak, T. B., Townsend, L. W., Tsai, P. E., Burnham, C. A., and McBeth, R. A. (2015) "Neutron Yields and Effective Doses Produced by Galactic Cosmic Ray Interactions in Shielded Environments in Space," *Life Sci. Space Res.* 7: 90-99.

Heinbockel, J. H., Slaba, T. C., Tripathi, R. K., Blattnig, S. R., Norbury, J. W., Badavi, F. F., Townsend, L. W., Handler, T., Gabriel, T. A., Pinsky, L. S., Reddell, B., and Aumann, A. R. (2011) "Comparison of the Transport Codes HZETRN, HETC, and FLUKA for Galactic Cosmic Rays," *Advances in Space Research* 47: 1089-1105. https://doi.org/10.1016/j.asr.2010.11.013.

HEO-DM-1002, "Mars Mission Duration Guidance for Human Risk Assessment and Research Planning Purposes," Human Exploration and Operations (HEO) Systems Engineering and Integration (SE&I) Decision Memorandum, September 28, 2020.

Hiraiso Solar Terrestrial Research Center (1997) "Solar-terrestrial Predictions V, STPW'96," Heckman, G. R., Marubashi, K., Shea, M. A., RWC Tokyo, Communications Research Laboratory, 1997.

Hones E. W. and Higbee, P. R. (1989) "Distribution and Detection of Positrons from an Orbiting Nuclear Reactor," *Science* 44: 448.

Huff, J., et al. (2016) "Evidence Report: Risk of Radiation Carcinogenesis," Human Research Program, NASA, April 7, 2016.

Hughlett, J. L., Turner, E. T., Slack, K. J., and Sipes, W. E. (2020) "Spaceflight Operational Psychological Support for Astronauts and their Families," in *Psychology and Human Performance in Space Programs: Extreme Application*, Vol. 2, L. B. Landon, K. J. Slack, and E. Salas, Eds., CRC Press: Abingdon, UK, pp. 133–154.

Human Research Program (2021) "Human Research Roadmap," National Aeronautics and Space Administration Human Health and Performance Directorate. URL: https://humanresearchroadmap.nasa.gov/

International Commission on Radiological Protection (ICRP) (1991) "1990 Recommendations of the International Commission on Radiological Protection," ICRP Publication 60, *Ann. ICRP* 21: 1-3, Pergamon Press.

International Commission on Radiological Protection (ICRP) (2007) "2007 Recommendations of the International Commission on Radiological Protection," ICRP Publication 103, Pergamon Press, 2007.

Jia, Y. and Lin, Z. W. (2010) "The Radiation Environment on the Moon from Galactic Cosmic Rays in a Lunar Habitat," *Rad. Res.* 173: 238-244, 2010.

Johnson Space Center (JSC) Safety & Mission Assurance (S&MA) Flight Safety Office (2014) "Internal Thermal Control System Heat Exchanger Close Call Study," JSC-2014-025.

Johnson, M. and Vera, A. (2019) "No AI Is an Island: The Case for Teaming Intelligence," *AI Magazine* 40(1): 16-28. https://doi.org/10.1609/aimag.v40i1.2842

Johnson, S. J. (2011) "NASA Johnson Space Center Oral History Project Transcript," Bryan D. O'Connor, ed., August 3, 2011. URL: https://historycollection.jsc.nasa.gov/JSCHistoryPortal/history/oral_histories/OConnorBD/OConnorBD_8-3-11.htm

Jones, H. W. (2016) "Using the International Space Station (ISS) Oxygen Generation Assembly (OGA) is not Feasible for Mars Transit," 46th International Conference on Environmental Systems.

Joosten, B. K. (2007) "Preliminary Assessment of Artificial Gravity Impacts to Deep-Space Vehicle Design," NASA Johnson Space Center, JSC-63743, February 1, 2007. URL: https://ntrs.nasa.gov/citations/20070023306

Joselyn, J. A., Anderson, J. B., Coffey, H., Harvey, K., Hathaway, D., Heckman, G., Hildner, E., Mende, W., Schatten, K., Thompson, R., Thomson, A. W. P., and White, O. R. (1997) "Panel Achieves Consensus Prediction of Solar Cycle 23," *Eos* 78(20), May 20, 1997.

Justh, H. L., Dwyer, A. M., Burns, K. L., Hoffman, J., and Powell, R. W. (2019) "Mars Global Reference Atmospheric Model (MARS-GRAM) Upgrades" 9th International Conference on Mars.

Kahn, J., Liverman, C. T., and McCoy, M. A., Eds. (2014) *Health Standards for Long Duration and Exploration Spaceflight: Ethics Principles, Responsibilities, and Decision Framework*, Institute of Medicine of the National Academies, The National Academies Press.

Keartland, S. and Van Zyl, T. L. (2020) "Automating Predictive Maintenance using Oil Analysis and Machine Learning," *2020 International SAUPEC/RobMech/PRASA Conference*, 1–6. https://doi.org/10.1109/SAUPEC/RobMech/PRASA48453.2020.9041003

Landon, L. B., Slack, K. J., and Barrett, J. D. (2018) "Teamwork and Collaboration in Long-Duration Space Missions: Going to Extremes," *Am Psychol* 73(4): 563–575, June 2018. doi: 10.1037/amp0000260.

Landon, L.B., et al. (2017) "Selecting Astronauts for Long Duration Space Exploration: Considerations for Team Performance and Functioning," *REACH - Reviews in Human Space Exploration 5*, 33–5.

Laurie, S. S., Greenwald, S. H., Marshall-Goebel, K., Pardon, L. P., Gupta, A., Lee, S. M. C., . . . Bershad, E. M. (2021) "Optic Disc Edema and Chorioretinal Folds Develop during Strict 6° Head-Down Tilt Bed Rest with or without Artificial Gravity," *Physiological Reports* 9(15): e14977. doi: https://doi.org/10.14814/phy2.14977

Laurie, S. S., Lee, S. M. C., Macias, B. R., Patel, N., Stern, C., Young, M., and Stenger, M. B. (2020) "Optic Disc Edema and Choroidal Engorgement in Astronauts During Spaceflight and Individuals Exposed to Bed Rest," *JAMA Ophthalmology* 138(2): 165-172. doi:10.1001/jamaophthalmol.2019.5261

Lee, S. M. C., Schneider, S. M., Boda, W. L., Watenpaugh, D. E., Macias, B. R., Meyer, R. S., and Hargens, A. R. (2007) "Supine LBNP Exercise Maintains Exercise Capacity in Male Twins during 30-d Bed Rest," *Medicine & Science in Sports & Exercise,* 39(8): 1315-1326. doi:10.1249/mss.0b013e31806463d9

Li, J. and Liu, H. (2016) "Design Optimization of Amazon Robotics," *Automation, Control and Intelligent Systems 4*(2): 48–52. URL: https://doi.org/10.11648/j.acis.20160402.17

Lim, D. S. S., Abercromby, A. F. J., Kobs-Nawotniak, S. E., et al. (2019) "The BASALT Research Program: Designing and Developing Mission Elements in Support of Human Scientific Exploration of Mars," *Astrobiology* 19(3), March 6, 2019. URL: https://doi.org/10.1089/ast.2018.1869

Linnarsson, D., Hughson, R. L., Fraser, K. S., Clément, G., Karlsson, L. L., Mulder, E., . . . Zange, J. (2015) "Effects of an Artificial Gravity Countermeasure on Orthostatic Tolerance, Blood Volumes and Aerobic Power after Short-term Bed Rest (BR-AG1)," *J. Appl. Physiol. (1985),* 118(1), 29-35. doi:10.1152/japplphysiol.00061.2014

Lock, R. E., Edwards, C. D., Nicholas, A. K., Woolley, R., and Bell, D.J. (2016) "Small Aerostationary Telecommunications Orbiter Concepts for Mars in the 2020s," In Proceedings of the 2016 IEEE Aerospace Conference, pp. 1–12.

Lohr, S. (2021) "What Ever Happened to IBM's Watson?" *The New York Times*, New York, NY, July 16, 2021. URL: https://www.nytimes.com/2021/07/16/technology/what-happened-ibm-watson.html.

Mader, T. H., Gibson, C. R., Pass, A. F., Kramer, L. A., Lee, A. G., Fogarty, J., . . . Polk, J. D. (2011) "Optic Disc Edema, Globe Flattening, Choroidal Folds, and Hyperopic Shifts Observed in Astronauts after Long-duration Space Flight," *Ophthalmology* 118(10): 2058-2069. https://doi.org/10.1016/j.ophtha.2011.06.021

Mader, T. H., Gibson, C. R., Pass, A. F., Lee, A. G., Killer, H. E., Hansen, H.-C., . . . Pettit, D. R. (2013) "Optic Disc Edema in an Astronaut After Repeat Long-Duration Space Flight" *Journal of Neuro-Ophthalmology* 33(3): 249-255. doi:10.1097/WNO.0b013e31829b41a6

Mason, L., Oleson, S., Schmitz, P., Qualls, L., Smith, M., Ade, B., and Navarro, J. (2021) "Nuclear Power Concepts for High-Power Electrical Propulsion Missions to Mars," *Nuclear and Emerging Technologies for Space*, ORNL.

Matthaiou, I., Khandelwal, B., and Antoniadou, I. (2017) "Vibration Monitoring of Gas Turbine Engines: Machine-Learning Approaches and Their Challenges," *Frontiers in Built Environment* 3. https://doi.org/10.3389/fbuil.2017.00054

Matthia, D., Berger, T., Mrigakshi, A.I., and Reitz, G. (2013) "A Ready-to-Use Galactic Cosmic Ray Model," *Adv. Space Res.* 51: 329-338.

Matthia, D., Ehresmann, B., Lohf, H., Kohler, J., Zeitlin, C., Appel, J., Sato, T., Slaba, T. C., Martin, C., Berger, T., Boehm, E., Boettcher, S., Brinza, D. E., Burmeister, S., Guo, J., Hassler, D. M., Posner, A., Rafkin, S. C. R., Reitz, G., Wilson, J. W., and Wimmer-Schweingruber, R. F. (2016) "The Martian Surface Radiation Environment – A Comparison of Models and MSL/RAD Measurements," *J. Space Weather Space Clim.* 6: A13.

Matthia, D., Hassler, D. M., de Wet, W., Ehresmann, B., Firan, A., Flores-McLaughlin, J., Guo, J., Heilbronn, L. H., Lee, K., Ratliff, H., Rios, R. R., Slaba, T. C., Smith, M., Stoffle, N. N., Townsend, L. W., Berger, T., Reitz, G., Wimmer-Schweingruber, R. F., and Zeitlin, C. (2017) "The Radiation Environment on the Surface of Mars – Summary of Model Calculations and Comparison to RAD Data," *Life Sci. Space Res.* 14: 18-28.

McGuire, K., Easter, B., Mindock, J., Hanson, A., Hailey, M., Vega, L., Antonsen, E., and Lehnhardt, K. (2021) "Using Systems Engineering to Develop an Integrated Crew Health and Performance System to Mitigate Risk for Human Exploration Missions," 50th International Conference on Environmental Systems. July 2021.

McKinney, G. W., Lawrence D. J., Prettyman T. H., Elphic R. C., Feldman W. C., Hagerty J. J. (2006) "MCNPX Benchmark for Cosmic Ray Interactions with the Moon," *J. Geophys. Res.* 111:E06004.

McTigue, K. R., Parisi, M. E., Panontin, T. L., Wu., S.., and Vera, A. H. (2021) "Extreme Problem Solving: The New Challenges of Deep Space Exploration," In *Proceedings of SpaceCHI: Human-Computer Interaction for Space Exploration (CHI '21)*, May 2021.

Memarzadeh, M., Matthews, B., and Templin, T., (2021) "Multiclass Anomaly Detection in Flight Data Using Semi-Supervised Explainable Deep Learning Model," NASA Ames Research Center, September 28, 2021. URL: https://arc.aiaa.org/doi/full/10.2514/1.I010959

Miller, J., Reitz, G., Norbury, J., eds. (2017) "Radiation on the Martian Surface: Model Comparisons with Data from the Radiation Assessment Detector on the Mars Science Laboratory (MSL/RAD): Results from the 1st Mars Space Radiation Modeling Workshop," *Life Sci. Space Res.* 14: 1-74.

Millour, E., Forget, F., Spiga, A., Vals, M., Zakharov, V., Montabone, L., Lefevre, F., Montmessin, F., Chaufray, J. Y., Lopez-Valverde, M. A., Gonzalez-Galindo, F., Lewis, S. R., Read, P. L., Desjean, M. C., and Cipriani, F. (2018) "The Mars Climate Database (Version 5.3)," from the Mars Express to ExoMars Scientific Workshop. Madrid, Spain.

Mindell, D., (2015) *Our Robots, Ourselves: Robotics and the Myths of Autonomy*. Print. ISBN: 9780525426974 0525426973

Minow, J. I., Mertens, C. J., Parker, L. N., Allen, J. R., Fry, D. J., Semones, E. J., Hock, R. A., Jun, I., Onsager, T. G., Pulkkinen, A. A., and St. Cyr, C. (2020) "Space Weather Architecture Options to Support Human and Robotic Deep Space Exploration," NASA TM 20205000837.

Moore, S. T., MacDougall, H. G., and Paloski, W. H. (2010) "Effects of Head-Down Bed Rest and Artificial Gravity on Spatial Orientation," *Experimental Brain Research* 204(4): 617-622. doi:10.1007/s00221-010-2317-0

Nandy, D. (2020) "Progress in Solar Cycle Predictions: Sunspot Cycles 24–25 in Perspective," *Solar Physics*, to be published, 2020.

NASA (1995) "Man-System Integration Standards," NASA-STD-3000, Revision B, July 1995 (has been superceded and is no longer being maintained).

NASA (2014) "RFID Tag for Long Range and Wide Coverage Capabilities," (MSC-TOPS-51). Patents 9715609, 9977121, 10243412. URL: https://technology.nasa.gov/patent/MSC-TOPS-51

NASA (2017) "NASA Reliability and Maintainability (R&M) Standard for Spaceflight and Support Systems," NASA-STD-8729.1, Revision A, June 13, 2017.

NASA-STD-3001 (2015) "NASA Space Flight Human-System Standard, Volume 1: Crew Health," NASA-STD-3001, Revision A w/change 1, February 12, 2015.

NASA-STD-3001 (2019) "NASA Space Flight Human-System Standard, Volume 2: "Human Factors, Habitability, and Environmental Health," NASA-STD-3001, Revision B, September 9, 2019.

National Academies of Sciences, Engineering, and Medicine (2021) "Human-AI Teaming: State of the Art and Research Needs," Washington, D.C.: The National Academies Press. URL: https://doi.org/10.17226/26355

National Academies of Sciences, Engineering, and Medicine (2021) "Space Nuclear Propulsion for Human Mars Exploration," Washington, D.C.: The National Academies Press. URL: https://doi.org/10.17226/25977; http://nap.edu/25977

National Aeronautics and Space Administration (NASA) (2020) "Human System Risk Management Plan," NASA Johnson Space Center, JSC 66705, Revision A.

National Aeronautics and Space Administration (NASA) (2021) "Imagine the Universe," May 2021. URL: https://imagine.gsfc.nasa.gov, accessed May 2021.

National Council on Radiation Protection and Measurements (NCRP) (2000) "Radiation Protection Guidance for Activities in Low-Earth Orbit," NCRP Report No. 132.

National Oceanic and Atmospheric Administration (NOAA) (1986) "Solar-terrestrial Predictions: Proceedings of a Workshop at Meudon, France: June 18-22, 1984," Simon, P. A., Heckman, G. R., and Shea, M. A., eds., January 1, 1986.

National Oceanic and Atmospheric Administration (NOAA) (1990) "Solar-terrestrial Predictions: Proceedings of a Workshop at Leura, Australia: October 16-20, 1989," Thompson, R. J., ed., Environmental Research Laboratories.

National Research Council (2012) "Technical Evaluation of the NASA Model for Cancer Risk to Astronauts Due to Space Radiation," Washington, DC, The National Academies Press. URL: https://doi.org/10.17226/13343, https://www.nap.edu/download/13343

Nelson, G. A., Simonsen, L., and Huff, J. L. (2016) "Evidence Report: Risk of Acute and Late Central Nervous System Effects from Radiation Exposure," Human Research Program Space Radiation Program Element, January 1, 2016.

Ng, B. (2021) "Could Robots from Boston Dynamics Beat Me in a Fight?" *The New York Times*, New York, NY, September 8, 2021. At: https://www.nytimes.com/2021/09/08/magazine/boston-dynamics-robots.html

Norbury, J. W., Miller, J., Adamczyk, A. M., Heilbronn, L. H., Townsend, L. W., Blattnig, S. R., Normany, R. B., Guetersloh, S. B., and Zeitlin, C. J. (2012) "Nuclear Data for Space Radiation," *Rad. Meas.* 47: 315-363.

Norman, R. B., Slaba, T. C., Blattnig, S. R. (2013) "An Extension of HZETRN for Cosmic Ray Initiated Electromagnetic Cascades," *Adv. Space Res.* 51: 2251-2260.

Oleson, S., Burke, L., Chaiken, M., Klefman, B., Tian, L., Martini, M., Faller, B., Turnbull, B., Hartwig, J., Simon, P., Dosa, B., Mason, L., Dudzinski, L., Smith, D., Packard, T., Colozza, A., Gyekenyesi, J., Fittje, J., and Schmitz, P. (2020) "Mars Opposition Piloted Nuclear Electric Propulsion (NEP)-Chem Vehicle," ASCEND 2020 Virtual Event.

OLTARIS, "On-Line Tool for the Assessment of Radiation in Space." URL: https://oltaris.nasa.gov/

Palinkas, L. A., Gunderson, E. K., Holland, A. W., Miller, C., and Johnson, J. C. (2020) "Predictors of Behavior and Performance in Extreme Environments: the Antarctic Space Analogue Program," *Aviat Space Environ Med* 71(6): 619–625, June 2000.

Paloski, W. and Charles, J. B. (2014) "Artificial Gravity Workshop White Paper," NASA Ames Research Center.

Paloski, W. and Young, L. (1999) "Proceedings and Recommendations from the Artificial Gravity Workshop," Johnson Space Center: NASA & NSBRI

Panontin, T. L., Wu, S., Parisi, M. E., McTigue, K. R., and Vera, A. H. (2021) "Human-Systems Integration Architecture Needs Analysis: On-board Anomaly Resolution During Autonomous Operations," Human Research Program Technical Report.

Patel, Z., Huff, J., Saha, J., Wang, M., Blattnig, S., and Wu, H. (2016) "Evidence Report: Risk of Cardiovascular Disease and Other Degenerative Tissue Effects from Radiation Exposure," Human Research Program Space Radiation Program Element, April 6, 2016.

Pavy-Le Traon, A., Heer, M., Narici, M. V., Rittweger, J., and Vernikos, J. (2007) "From Space to Earth: Advances in Human Physiology from 20 Years of Bed Rest Studies (1986–2006)," *European Journal of Applied Physiology* 101(2): 143-194. doi:10.1007/s00421-007-0474-z

Pesnell, W. D. (2016) "Predictions of Solar Cycle 24: How are We Doing?" *Space Weather* 14:10–21. doi:10.1002/2015SW001304

Pham, T. T. and El-Genk, M. S. (2009) "Dose Estimates in a Lunar Shelter with Regolith Shielding," *Acta Astronaut* 64: 697-713.

Posner, A. (2021) "Earth/Sun L4: Covering the Solar Radiation Hemisphere for Human Exploration," presented at European Space Weather Week 17, Session cd01, Glasgow, Scotland, October 25, 2021.

Posner, A., Agre, C. N., Staub, J., St Cyr, O. C., Folta, D., Solanki, S. K., Strauss, R. D. T., Effenberger, F., Gandorfer, A., Heber, B., Henney, C. J., Hirzberger, J., Jones, S. I., Kuhel, P., Malandraki, O., and Sterken, V. J. (2021) "A Multi-Purpose Heliophysics L4 Mission, *Space Weather* 19. doi: 10.1029/2021SW002777.

Posner, A. and Strauss, R. D. (2020) "Warning Time Analysis From SEP Simulations of a Two-Tier REleASE System Applied to Mars Exploration," *Space Weather* 18(4); April 2020. https://doi.org/10.1029/2019SW002354

Prater et al. (2019) "NASA's In-Space Manufacturing Project: Update on Manufacturing Technologies and Materials to Enable More Sustainable and Safer Exploration." URL: https://ntrs.nasa.gov/citations/20190033333

Rader, S., Reagan, M., Janoiko, B., and Johnson, J. (2012) "Human-in-the-Loop Operations over Time Delay: NASA Analog Missions Lessons Learned," NASA Johnson Space Center. URL: https://www.nasa.gov/sites/default/files/atoms/files/missionops_human_in_the_loop_over_time_delay_ops_lessons.pdf

Reames, D. V. (2021) *Solar Energetic Particles: A Modern Primer on Understanding Sources, Acceleration and Propagation*, Second Edition, Springer.

Rowe, J. (2020) "Artificial Gravity in Mars Orbit for Crew Acclimation," Paper presented at the IEEE Aerospace Conference, Big Sky, MT.

Seaton, K. A., Slack, K. J., Sipes, W., and Bowie, K. (2007) "Artificial Gravity as a Multi-System Countermeasure: Effects on Cognitive Function," *J. Gravit. Physiol.* 14(1): 27-30.

Share, G. H. et al., (1989) "Geomagnetic Origin for Transient Particle Events from Nuclear-Reactor-Powered Satellites," Science 44: 444.

Sheeley, N. R., Jr., Howard, R. A., Koomen, M. J., and Michels, D. J. (1983) "Associations between Coronal Mass Ejections and Soft X-ray Events," *Astrophys. J.* 272: 349.

Shiba, D., Mizuno, H., Yumoto, A., Shimomura, M., Kobayashi, H., Morita, H., . . . Takahashi, S. (2017) "Development of New Experimental Platform 'MARS'—Multiple Artificial-gravity Research System—to Elucidate the Impacts of Micro/Partial Gravity on Mice," *Scientific Reports* 7(1): 10837. doi:10.1038/s41598-017-10998-4

Siebert, M. A., Lim, D. S., Miller, M. J., et al. (2019) "Developing Future Deep-Space Telecommunication Architectures: A Historical Look at the Benefits of Analog Research on the Development of Solar System Internetworking for Future Human Spaceflight," *Astrobiology*.

Simon, M. A., Cerro, J., Clowdsley, M., Latorella, K, Watson, J., Albertson, C., Le Bouffe, V., and Walker, S. (2014) "Design of Two RadWorks Storm Shelters for Solar Particle Event Shielding," AIAA Space 2014 Conference and Exposition. doi:10.2514/6.2014-4473

Simonsen, L., Nealy, J., Townsend, L., and Wilson, J. (1990) "Space Radiation Shielding for a Martian Habitat," *SAE Transactions* 99: 972-979. URL: http://www.jstor.org/stable/44472557, last accessed July 9, 2021.

Simonsen, L.C. and Slaba, T.C. (2021) "Improving Astronaut Cancer Risk Assessment from Space Radiation with an Ensemble Model Framework," *Life Sci. Space Res.* 31: 14-28.

Simonsen, L.C., Slaba, T.C., Guida, P., and Rusek, A., (2020) "NASA's First Ground-based Galactic Cosmic Ray Simulator: Enabling a New Era in Space Radiobiology Research," *Plos Biolog*y 18: e3000669.

Slaba, T. C. and Whitman, K. (2020) "The Badhwar-O'Neill 2020 GCR Model," *Space Weather* 18.

Slaba, T. C., Bahadori, A. A., Reddell, B. D., Singleterry, R. C., Clowdsley, M. S., and Blattnig, S. R. (2017) "Optimal Shielding Thickness for Galactic Cosmic Ray Environments," *Life Sciences in Space Research* 12: 1-15. https://doi.org/10.1016/j.lssr.2016.12.003

Slaba, T. C., Blattnig, S. R., and Badavi, F. F. (2010) "Faster and More Accurate Transport Procedures for HZETRN," *J. Comp. Phys.* 229: 9397-9417.

Slaba, T. C., Blattnig, S. R., and Clowdsley, M. S. (2011) "Variations in Lunar Neutron Dose Estimates," *Rad. Res.* 176: 827-841.

Slaba, T. C., Blattnig, S. R., Badavi, F. F., Stoffle, N. N., Rutledge, R. D., Lee, K. T., Zapp, E. N., Dachev, T. P., and Tomov, B. T. (2011) "Statistical Validation of HZETRN as a Function of Vertical Cutoff Rigidity using ISS Measurements," *Advances in Space Res.* 47: 600-610. https://doi.org/10.1016/j.asr.2010.10.021

Slaba, T. C., Blattnig, S. R., Reddell, B., Bahadori, A., Norman, R. B., and Badavi, F. F. (2013) "Pion and Electromagnetic Contribution to Dose: Comparisons of HZETRN to Monte Carlo Results and ISS Data," *Advances in Space Research* 52a: 62-78. https://doi.org/10.1016/j.asr.2013.02.015

Slaba, T. C., Qualls, G. D., Clowdsley, M. S., Blattnig, S. R., Walker, S. A., and Simonsen, L. C. (2010) "Utilization of CAM, CAF, MAX, and FAX for Space Radiation Analyses using HZETRN," *Adv. Space Res.* 45: 866-883.

Slaba, T. C., Wilson, J. W., Werneth, C. M., and Whitman, K. (2020) "Updated Deterministic Radiation Transport for Future Deep Space Missions," *Life Sci. Space Res.* 27: 6-18.

Slack, K. J., Williams, T. J., Schneiderman, J., Whitmire, A. M., and Picano, J. J. (2016) "Evidence Report: Risk of Adverse Cognitive or Behavioral Conditions and Psychiatric Disorders," NASA Johnson Space Center, April 11, 2016.

Space Nuclear Propulsion Technologies Committee, Aeronautics and Space Engineering Board, and Division on Engineering and Physical Sciences (2021) "Space Nuclear Propulsion for Human Mars Exploration," National Academies Press: Washington, D.C. doi: 10.17226/25977

Takada, K. C., Ghariani, A. E., and Van Keuren, S. (2015) "Advancing the Oxygen Generation Assembly Design to Increase Reliability and Reduce Costs for a Future Long Duration Mission," 45th International Conference on Environmental Systems.

Townsend, L. W. (2005) "Critical Analysis of Active Shielding Methods for Space Radiation Protection," *Proceedings of the 2005 IEEE Aerospace Conference,* pp. 724-730. doi: 10.1109/AERO.2005.1559364.

Townsend, L. W., Adams, J. H., Blattnig, S. R., Clowdsley, M. S., Fry, D. J., Jun, I., McLeod, C. D., Minow, J. I., Moore, D. F., Norbury, J. W., Norman, R. B., Reames, D. V., Schwadron, N. A., Semones, E. J., Singleterry, R. C., Slaba, T. C., Werneth, C. M., and Xapsos, M. A. (2018) "Solar Particle Event Storm Shelter Requirements for Missions Beyond Low Earth Orbit," *Life Sci. Space Res.* 17: 32-39. doi: 10.1016/j.lssr.2018.02.002

Townsend, L. W., Wilson, J. W., and Nealy, J. E. (1989) "Space Radiation Shielding Strategies and Requirements for Deep Space Missions," *SAE Transactions* 98: 326-35. URL: http://www.jstor.org/stable/44471636

Tylka, A. J., Dietrich, W. F., and Atwell, W. A. (2010) "Band Function Representations of Solar Proton Spectra in Ground-Level Events," In 38th Scientific Assembly of the Committee on Space Research (COSPAR), Bremen, Germany, July 18–25, 2010.

University of Wisconsin, "History of Soviet Topaz Reactors," URL: https://fti.neep.wisc.edu/fti.neep.wisc.edu/neep602/SPRING00/lecture35.pdf

Upton, L. (2020) "The Solar Cycle," presented at the Space Weather Operations and Research Infrastructure Workshop, The National Academies, June 17, 2020. URL: https://www.nationalacademies.org/event/06-16-2020/docs/DECE4A50B10B53D62FDABAF9C8FAFB6

Valinia, A., Minow, J., Pellish, J., Vera, A., Allen, J., White, N., Antonsen, E. et al. (2022) "Safe Human Expeditions Beyond Low Earth Orbit (LEO)," NESC-RP-20-01589, January 20, 2022.

Van Driel-Gesztelyi, L. and Owens, M. J. (2020) "Solar Cycle," Space & Climate Physics, Oxford University Press and The American Institute of Physics, July 30, 2020. https://doi.org/10.1093/acrefore/9780190871994.013.9

Vavrina, M. A., Englander, J. A., and Ellison, P. H. (2016) "Global Optimization of N-Maneuver High-Thrust Trajectories using Direct Multiple Shooting," Proceedings of the AAS/AIAA Space Flight Mechanics Meeting, NAPA, CA.

von Braun, W. (1952) "Man Will Conquer Space Soon: Crossing the Last Frontier," *Collier's Weekly,* March 1952, pp. 24-29.

Vuong, X. T. and Vuong, S. T. (1997) "Satellite Link Margin and Availability Issues," *IEEE Trans Broadcast* 43:213–220.

Warner, J. E., Norman, R. B., and Blattnig, S. R. (2018) "HZETRN Radiation Transport Validation using Balloon-Based Experimental Data," *Life Sciences in Space Research* 17: 23-31, 2018. https://doi.org/10.1016/j.lssr.2018.02.003

Westover, S., Meinke, R., Nerolich, S. M., Washburn, S., Battison, R., Burger, W., Kasaboski, D., and Davies, F. (2020) "Magnet Architectures and Active Radiation Shielding Study (MAARSS)," No. ASPP-TP-2020-5002408-revised.

Wikipedia, "BES-5," page last updated September 10, 2021. URL: https://en.wikipedia.org/wiki/BES-5, last accessed January 11, 2022.

Wilson, J. W., Badavi, F. F. Cucinotta, F. A., Shinn, J. L., Badhwar, G. D., Silberberg, R., Tsao, C. H., Townsend, L. W., and Tripathi, R. K. (1995) "HZETRN: Description of a Free-Space Ion and Nucleon Transport and Shielding Program," NASA Technical Paper 3495.

Wilson, J. W., Clowdsley, M. S., Cucinotta, F. A., Tripathi, R. K., Nealy, J. E., and De Angelis, G. (2004) "Deep Space Environments for Human Exploration," *Adv. Space Res.* 34: 1281-1287.

Wilson, J. W., Cucinotta, F.A., Kim, M.-H.Y., Schimmerling, W. (2001) "Optimized Shielding for Space Radiation Protection," *Physica Medica* 17.

Wilson, J. W., et al. (1999) "Shielding from Solar Particle Event Exposures in Deep Space," *Radiat. Meas.* 30: 361-382.

Wilson, J. W., Slaba, T. C., Badavi, F. F., Reddell, B. D., and Bahadori, A. A., (2014) "Advances in NASA Radiation Transport Research: 3DHZETRN," *Life Sci. Space Res.* 2: 6-22.

Wilson, J. W., Townsend, L. W., Schimmerling, W., Khadelwal, G. S., Khan, F., Nealy, J. E., Cucinotta, F. A., Simonsen, L. C., Shinn, J. L., and Norbury, J. W. (1991) "Transport Methods and Interactions for Space Radiations," NASA-RP-1257.

Woods, D. (2021) "How to Kill Zombie Ideas: Why do People Tenaciously Believe Myths about the Relationship between People and Technology?" Georgia Institute of Technology, School of Psychology, Psychology Colloquium, Virtual Event. URL: http://hdl.handle.net/1853/65411

Woolum, D. S., Burnett, D. S., Furst, M., and Weiss, J. R. (1975) "Measurement of the Lunar Neutron Density Profile," *Moon* 12: 231-250.

Wu, S. T. (1989) "Coordination of Advanced Solar Observatory (ASO) Science Working Group (SWG) for the Study of Instrument Accommodation and Operational Requirements on Space Station," Contract No. NAG8-682 Final Report.

Xapsos, M. A. (2019) "A Brief History of Space Climatology: from the Big Bang to the Present," *IEEE Trans. Nucl. Sci.* 66: 17-37.

Xapsos, M. A., Summers, G. P., Barth, J. L., Stassinopoulos, E. G., and Burke, E. A. (1999) "Probability Model for Worst Case Solar Proton Event Fluences," *IEEE Trans. Nucl. Sci.* 46(6): 1481-1485, December 1999.

Yamashita, N., Hasebe, N., Miyachi, T., Kobayahsi, M., Okudaira, O., Kabayashi, S., Ishizaki, T., Sakurai, K., Miyajima, M., Reedy, R., d'Uston, C., Maurice, S., and Gasnault, O., (2008) "Complexities of Gamma-ray Line Intensities from the Lunar Surface," *Earth Planets Space* 60: 313-319.

Zak, A. (2021) "US-A and US-P Military Satellites," November 29, 2021. URL: http://www.russianspaceweb.com/us.html, last accessed January 11, 2022.

Appendix A. Attendees of the NESC/OCHMO Safe Human Expedition Workshop, September 14–16, 2021

Participants in the NASA Engineering and Safety Center (NESC)/Office of the Chief Health and Medical Officer (OCHMO) "Safe Human Expedition" Workshop, held in Houston, Texas, on September 14–16, 2021, are shown in Table A-1.

Table A-1. NESC/OCHMO Safe Human Expedition Workshop Participants

Jim Adams, University of Alabama at Huntsville
John Allen, NASA
Erik Antonsen, Baylor University
Maneesh Arya, NASA
Brad Bailey, NASA
Hazel Bain, NOAA
Robert Beil, NASA
Mario Berges, Carnegie Mellon University
Patrick Chai, NASA
Hector Chavez, NASA
Andrew Choate, ESSCA
Steven Christe, NASA
William Cirillo, NASA
James Clawson, Stellar Solutions, Inc.
Yaireska Collado-Vega, NASA
Michelle Courtney, Wyle Laboratories
Claudio Corti, University of Hawaii at Manoa
Vincent Cross, TACLABS, Inc.
Nancy Currie-Gregg, Texas A&M University
Steven Davison, NASA
Patrick Dees, NASA
Donna Dempsey, NASA
Charles Dischinger, NASA
Stephen Edwards, NASA
Brian Evans, ESSCA
James Favors, NASA
Dave Folta, NASA
David Francisco, NASA
Razvan Gaza, NASA
Brian Gore, NASA
Matthew Guibert, NASA
Alexa Halford, NASA
Noble Hatten, NASA
Michael Hess, NASA
Robert Hodson, NASA
Jon Holladay, NASA
Bryce Horvath, NASA

Robert Howard, NASA
Kyle Hughes, NASA
Kauser Imtiaz, NASA
Matt Johnson, Institute for Human and Machine Cognition
Insoo Jun, JPL
Paul Kessler, NASA
Michael Kirsch, NASA
Irina Kitiashvili, NASA
John Karasinski, NASA
Maria Kuznetsova, NASA
Kara Latorella, NASA
Ruthan Lewis, NASA
Douglas Litteken, NASA
Leila Mays, NASA
Torin McCoy, NASA
Kaitlin McTigue, NASA
Jim Meehan, NASA
Joseph Minow, NASA
Jeff Morrill, NASA
Tiffany Nickens, NASA
Ryan Norman, NASA
Cynthia Null, NASA
Andrew Owens, NASA
Tina Panontin, San Jose State University
Megan Parisi, NASA
Donald Parker, NASA
Jonathan Pellish, NASA
Arik Posner, NASA
James Polk, NASA
Tracie Prater, NASA
Antti Pulkkinen, NASA
Philip Quinn, Wyle Laboratories
Julie Robinson, NASA
Peter Robinson, NASA
Justin Rowe, ESSCA
Michelle Rucker, NASA
Janapriya Saha, Wyle Laboratories
Kevin Sato, NASA
Sabrina Savage, NASA
Victor Schneider, NASA
Richard Schunk, NASA
Edward Semones, NASA
Marc Shepanek, NASA
Lisa Simonsen, NASA
Upendra Singh, NASA

Brock Sishc, Wyle Laboratories
Tony Slaba, NASA
James Spann, NASA
Mike Stenger, NASA
Leland Stone, NASA
Scott Tingle, NASA
Ronald Turner, Analytic Services Incorporated
Walter Twetten, Booz, Allen, and Hamilton
Azita Valinia, NASA
Alonso Vera, NASA
Nicholas White, Space Science Solutions LLC
Tim Wilson, NASA
Edward Wollack, NASA
Shu-Chieh Wu, San Jose State University
Michael Xapsos, NASA
Janice Zawaski, NASA

Appendix B. Ionizing Radiation Human System Requirements for NASA Exploration Programs

B.1 Orion MPCV

- **MPCV 70024, Rev. D "ORION MULTI-PURPOSE CREW VEHICLE (MPCV) PROGRAM: HUMAN-SYSTEMS INTEGRATION REQUIREMENTS (HSIR)" - Released 11/18/2020**

  - [HS3085] Radiation Design Requirements

    The system shall provide protection from radiation exposure consistent with ALARA principles to ensure that effective dose (tissue averaged) to any crewmember does not exceed the relevant value given in HS3085, Table 3.2.7.1-1, System-Specific Radiation Design Requirements, for the design SPE, as specified in SLS-SPEC-159 Cross-Program Design Specification for Natural Environments (DSNE) [reprinted here as Table B-1].

    Table B-1. System-specific Radiation Design Requirements

System	Radiation Design Requirement (mSv)
Orion	150
Lunar Lander	150

  - [HS11038] Crew Personal Radiation Dosimeter

    The system shall provide wearable active dosimetry per crew member per mission.

  - [HS3086] Charged Particle Monitoring

    The system shall continuously measure and record the external fluence of particles of $Z < 3$, in the energy range 30 to 300 MeV/nucleon and particles of $3 \leq Z \leq 26$, in the energy range 100 to 400 MeV/nucleon and integral fluence measurement at higher energies, as a function of energy and time, from a monitoring location that ensures an unobstructed free space full-angle field-of-view 1.1345 radians (65 degrees) or greater.

  - [HS3088] Flux Monitoring

    The system shall provide an omnidirectional system that can continuously measure and record the flux from charged particles with Linear Energy Transfer (LET) 0.2 to 1,000 keV/μm, as a function of time, at an average tissue depth of at least 2 mm.

  - [HS3089] Absorbed Dose Monitoring

    The system shall provide an omnidirectional system that can continuously measure and record the absorbed dose from charged particles with Linear Energy Transfer 0.2 to 1,000 keV/micrometer, as a function of time, at an average tissue depth of at least 2 mm.

  - [HS3090] Area Radiation Monitoring

    The system shall provide dosimetry capable of measuring time integrated absorbed dose and estimating Linear Energy Transfer based quality factors, at a minimum number of four locations as acceptable to the Radiation Health Officer (SRAG) within each pressurized vehicle/element.

- [HS3091] Radiation Data Reporting to the Crew - Absorbed Dose

  The system shall display the measured cumulative absorbed dose/minute averaged dose rate to the crew once per minute, with latency less than five minutes.

- [HS3112] Radiation Data Reporting to Mission Systems - Absorbed Dose

  The system shall provide the measured cumulative absorbed dose/minute averaged dose rate to Mission Systems once per minute during periods when communication is available, with latency less than 5 minutes.

- [HS3113] Particle Archive Data

  The system shall provide the archive of all recorded charged particle measurement data to Mission Systems by the completion of the mission.

- [HS3120] Radiation Data Reporting to Mission Systems – Flux

  The system shall provide the measured flux to Mission Systems once per minute during periods when communication is available, with latency less than 5 minutes.

- [HS3092] Alerting for Radiation Data

  The system shall alert the crew whenever the absorbed dose rate exceeds a preflight programmable threshold in the range 0.02 mGy/min to 10 mGy/min for three consecutive readings.

- [HS11004] Stowage for Suit Dosimeters

  The system shall provide a stowage location on the exterior of the suit for a wearable active personal dosimeter (excluding helmet, gloves, and boots).

- [HS11023] Suited Radiation Flux Monitoring

  The system shall provide an omnidirectional detector that can continuously measure and record the flux from charged particles with Linear Energy Transfer (LET) 0.2 to 300 keV/micrometer, as a function of time, at two shielding depths: 0.5 g cm^{-2} water equivalent and 3.0 g cm^{-2} water equivalent.

- [HS11024] Suited Radiation Absorbed Dose Monitoring

  The system shall provide an omnidirectional detector that can continuously measure and record the absorbed dose from charged particles with Linear Energy Transfer (LET) 0.2 to 300 keV/micrometer, as a function of time, at two shielding depths: 0.5 g cm^{-2} water equivalent and 3.0 g cm^{-2} water equivalent.

B.2   Gateway

- **GP 10017, Rev. A "GATEWAY PROGRAM HUMAN SYSTEM REQUIREMENTS (HSR)" - Released 01/28/2021**
  - L2-HSR-6058 Radiation Exposure Limit for Design Reference Solar Particle Event

    The Gateway shall provide protection to ensure that gray equivalent to astronaut Blood Forming Organs (BFOs) does not exceed 250 mGy-Eq. for the October 1989 design reference solar particle event, specified in Table 3.2.5-3, Design Reference SPE Environment Proton Energy Spectrum [reprinted here as Table B-2].

Table B-2. Design Reference SPE Environment Proton Energy Spectrum

Energy (MeV)	Proton Fluence (#/cm²-MeV)	Energy (MeV)	Proton Fluence (#/cm²-MeV)	Energy (MeV)	Proton Fluence (#/cm²-MeV)	Energy (MeV)	Proton Fluence (#/cm²-MeV)	Energy (MeV)	Proton Fluence (#/cm²-MeV)
1.000E-02	7.761E+14	5.770E-01	3.651E+11	4.810E+00	9.004E+09	3.426E+01	1.641E+08	2.484E+02	5.714E+05
1.338E-02	4.329E+14	6.480E-01	2.979E+11	5.317E+00	7.510E+09	3.775E+01	1.298E+08	2.756E+02	4.006E+05
1.790E-02	2.424E+14	7.263E-01	2.442E+11	5.875E+00	6.257E+09	4.160E+01	1.022E+08	3.060E+02	2.773E+05
2.391E-02	1.369E+14	8.129E-01	2.008E+11	6.490E+00	5.208E+09	4.584E+01	8.008E+07	3.407E+02	1.862E+05
3.183E-02	7.805E+13	9.086E-01	1.655E+11	7.168E+00	4.330E+09	5.052E+01	6.136E+07	3.794E+02	1.230E+05
4.210E-02	4.531E+13	1.014E+00	1.368E+11	7.914E+00	3.594E+09	5.568E+01	4.700E+07	4.232E+02	8.060E+04
5.511E-02	2.697E+13	1.130E+00	1.135E+11	8.736E+00	2.979E+09	6.137E+01	3.600E+07	4.728E+02	5.236E+04
7.112E-02	1.657E+13	1.258E+00	9.421E+10	9.641E+00	2.465E+09	6.765E+01	2.754E+07	5.291E+02	3.367E+04
9.027E-02	1.055E+13	1.400E+00	7.839E+10	1.064E+01	2.035E+09	7.460E+01	2.103E+07	5.930E+02	2.141E+04
1.125E-01	6.989E+12	1.556E+00	6.527E+10	1.174E+01	1.677E+09	8.226E+01	1.603E+07	6.665E+02	1.337E+04
1.375E-01	4.810E+12	1.729E+00	5.441E+10	1.294E+01	1.379E+09	9.074E+01	1.219E+07	7.505E+02	8.141E+03
1.657E-01	3.411E+12	1.919E+00	4.541E+10	1.427E+01	1.131E+09	1.001E+02	9.237E+06	8.471E+02	4.859E+03
1.968E-01	2.489E+12	2.129E+00	3.792E+10	1.574E+01	9.248E+08	1.105E+02	6.966E+06	9.588E+02	2.856E+03
2.303E-01	1.872E+12	2.361E+00	3.168E+10	1.735E+01	7.542E+08	1.220E+02	5.234E+06	1.091E+03	1.633E+03
2.675E-01	1.428E+12	2.617E+00	2.647E+10	1.913E+01	6.132E+08	1.348E+02	3.908E+06	1.244E+03	9.199E+02
3.082E-01	1.108E+12	2.900E+00	2.213E+10	2.108E+01	4.969E+08	1.490E+02	2.902E+06	1.418E+03	5.152E+02
3.525E-01	8.711E+11	3.211E+00	1.850E+10	2.323E+01	4.013E+08	1.648E+02	2.134E+06	1.625E+03	2.802E+02
4.010E-01	6.929E+11	3.555E+00	1.546E+10	2.561E+01	3.229E+08	1.824E+02	1.560E+06	1.869E+03	1.486E+02
4.542E-01	5.560E+11	3.933E+00	1.292E+10	2.822E+01	2.588E+08	2.018E+02	1.131E+06	2.158E+03	7.696E+01
5.126E-01	4.493E+11	4.350E+00	1.079E+10	3.109E+01	2.065E+08	2.239E+02	8.074E+05	2.500E+03	3.891E+01

- L2-HSR-6085 Ionizing Radiation Protection System

  The Gateway shall provide an ionizing Radiation Protection System.

- L2-HSR-6090 Ionizing Radiation Protection System Setup Time

  Configuration of the ionizing Radiation Protection System shall not take more than 30 minutes if assembly and installation is required.

- L2-HSR-6086 Implementation of ALARA Principle

  The Gateway shall design the Spacecraft Protection Systems to ensure that astronaut radiation exposure is kept as low as reasonably achievable (ALARA).

- **GP 10016, Baseline "GATEWAY PROGRAM SUBSYSTEM SPECIFICATION FOR CREW HEALTH AND PERFORMANCE (CHP)" - Released 09/17/2020**

  - L2-CHP-0200 Flux Monitoring – Charged Particles

    The Gateway CHP Radiation Subsystem shall monitor flux from charged particles as a function of time, particle energy and charge, for energies between 50 MeV/n and 2 GeV/n and charges up to Z = 14 during crewed periods [HSR 6060].

  - L2-CHP-0201 Flux Monitoring – Neutrons [TBR-CHP-016]

    The Gateway CHP Radiation Subsystem shall monitor flux from neutrons as a function of time and neutron energy, for energies between 0.1 and 15 MeV during crewed periods [HSR 6087].

  - L2-CHP-0202 Absorbed Dose Monitoring Capability - IVA

    The Gateway CHP Radiation Subsystem shall monitor absorbed dose from charged particles with Linear Energy Transfer 0.1 to 150 keV/micrometer in water, as a function of time for each crewmember [HSR 6061].

  - L2-CHP-0202 Absorbed Dose Monitoring Capability - IVA

    The Gateway CHP Radiation Subsystem shall monitor absorbed dose from charged particles with Linear Energy Transfer 0.1 to 150 keV/micrometer in water, as a function of time for each crewmember [HSR 6061].

- L2-CHP-0207 Report to Crew – Absorbed Dose - IVA

  The Gateway CHP Radiation Subsystem shall display the measured cumulative absorbed dose/minute averaged dose rate to the crew through the vehicle systems once per minute, with latency less than five minutes [HSR 6062].

- L2-CHP-0208 Report to Ground Team – Absorbed Dose and Proton Flux - IVA

  The Gateway CHP Radiation Subsystem shall report the measured cumulative absorbed dose/minute averaged dose rate and proton flux versus energy to the Ground Team once per minute during periods when communication is available, with latency less than 5 minutes [HSR 6063].

- L2-CHP-0209 Report to Ground Team – Neutron Flux

  The Gateway CHP Radiation Subsystem shall provide the measured neutron flux versus energy to the Ground Team once per day during periods when communication is available [HSR 6065].

- L2-CHP-0210 Particle Archive Data – Ground Team

  The Gateway CHP Radiation Subsystem shall provide an archive of all recorded neutron and charged particle measurement data to the Ground Team at the completion of each crewed mission [HSR 6064].

- L2-CHP-0211 Personal Dosimeter Data Transfer

  The Gateway CHP Radiation Subsystem shall facilitate nominal operations of the crew personal dosimeters including transmission of data to the ground as required [HSR 6088].

- L2-CHP-0212 Radiation Subsystem On-Orbit Performance Validation

  The Gateway CHP Radiation Subsystem fixed-location device shall be capable of having its performance validated on-orbit during crewed periods.

B.3   Human Landing System (HLS)

- **HLS-RQMT-001, Rev. D "HUMAN LANDING SYSTEM (HLS) PROGRAM SYSTEM REQUIREMENTS DOCUMENT (PSRD)" - Released 11/30/2020**

  - HLS-HMTA-0088 Radiation Protection, Limitations, and Monitoring

    The system should protect, limit and monitor crew exposure to radiation.

  - HLS-HMTA-0089 Crew Radiation Exposure Limits

    The program shall design systems using the ALARA principle to limit crew radiation exposure.

  - HLS-HMTA-0090 Ionizing Radiation Alerting

    The system shall include a method to alert all crewmembers when radiation levels are expected to exceed acceptable levels.

  - HLS-HMTA-0097 Solar Particle Event (SPE) Protection

    The HLS shall limit crew radiation exposure due to Solar Particle Events using the ALARA principle.

- **HLS-RQMT-002-ANX-01, Baseline "PaSRD TECHNICAL AUTHORITY AGREEMENTS SpaceX - CONTAINS SBU DATA - Released 11/9/2020**

  - HLS-SpaceX-HMTA-0088 Radiation protection, limitations, and monitoring-SpaceX

    The SpaceX system should protect, limit, and monitor crew exposure to radiation.

  - HLS-SpaceX-HMTA-0089 Crew Radiation Exposure Limits-SpaceX

    The program should design systems using the ALARA principle to limit crew radiation exposure.

  - HLS-SpaceX-HMTA-0090 Ionizing Radiation Alerting-SpaceX

    The SpaceX system shall alert all crewmembers when the NASA GFP area radiation monitor indicates radiation levels are expected to exceed acceptable levels.

  - HLS-SpaceX-HMTA-0097 Solar Particle Event (SPE) protection-SpaceX

    The SpaceX system shall limit exposure to solar particle events so that astronaut mGy equivalent to blood forming organs does not exceed 250 mGy-Eq for a design reference SPE spectrum equivalent to the sum of the events that occurred in October 1989 as modeled by Tylka. Design iterations, meaning interior mass, are complete when calculated improvement in Gy-Eq to BFO is less than 3% from the previous iteration of the highest crew member's calculated exposure. The Gy-Eq to BFO is to be calculated using RBE factors recommended by the NCRP.

- **HLS-RQMT-006 HLS PROGRAM SUSTAINED SYSTEM REQUIREMENTS – Draft (5/11/2021) (Appendix C) – in work**

  - HLS-HMTA-0090 Ionizing Radiation Alerting (Approved - HLS HMTA PreCR TCM)

    The system shall include a method to issue a caution and warning (C&W) alert to all crewmembers when notified by the NASA GFE radiation area monitor.

  - HLS-HMTA-0097 Solar Particle Event (SPE) protection (Approved - HLS HMTA PreCR TCM)

    Consistent with ALARA, the HLS shall limit crew radiation exposure due to Solar Particle Events (SPEs) to ensure that astronaut effective dose does not exceed 250 mSv for the design SPE specified in Table C.1-13: Design Reference SPE Environment Proton Energy Spectrum [reproduced here as Table B-3].

Table B-3. Design Reference SPE Environment Proton Energy Spectrum (sum of the proton spectra for the events that occurred during October 1989, as modeled by Tylka)

Energy (MeV)	Proton Fluence (#/cm^2-MeV)	Energy (MeV)	Proton Fluence (#/cm^2-MeV)	Energy (MeV)	Proton Fluence (#/cm^2-MeV)	Energy (MeV)	Proton Fluence (#/cm^2-MeV)	Energy (MeV)	Proton Fluence (#/cm^2-MeV)
1.000E-02	7.761E+14	5.770E-01	3.651E+11	4.810E+00	9.004E+09	3.426E+01	1.641E+08	2.484E+02	5.714E+05
1.338E-02	4.329E+14	6.480E-01	2.979E+11	5.317E+00	7.510E+09	3.775E+01	1.298E+08	2.756E+02	4.006E+05
1.790E-02	2.424E+14	7.263E-01	2.442E+11	5.875E+00	6.257E+09	4.160E+01	1.022E+08	3.060E+02	2.773E+05
2.391E-02	1.369E+14	8.129E-01	2.008E+11	6.490E+00	5.208E+09	4.584E+01	8.008E+07	3.407E+02	1.862E+05
3.183E-02	7.805E+13	9.086E-01	1.655E+11	7.168E+00	4.330E+09	5.052E+01	6.136E+07	3.794E+02	1.230E+05
4.210E-02	4.531E+13	1.014E+00	1.368E+11	7.914E+00	3.594E+09	5.568E+01	4.700E+07	4.232E+02	8.060E+04
5.511E-02	2.697E+13	1.130E+00	1.135E+11	8.736E+00	2.979E+09	6.137E+01	3.600E+07	4.728E+02	5.236E+04
7.112E-02	1.657E+13	1.258E+00	9.421E+10	9.641E+00	2.465E+09	6.765E+01	2.754E+07	5.291E+02	3.367E+04
9.027E-02	1.055E+13	1.400E+00	7.839E+10	1.064E+01	2.035E+09	7.460E+01	2.103E+07	5.930E+02	2.141E+04
1.125E-01	6.989E+12	1.556E+00	6.527E+10	1.174E+01	1.677E+09	8.226E+01	1.603E+07	6.665E+02	1.337E+04
1.375E-01	4.810E+12	1.729E+00	5.441E+10	1.294E+01	1.379E+09	9.074E+01	1.219E+07	7.505E+02	8.141E+03
1.657E-01	3.411E+12	1.919E+00	4.541E+10	1.427E+01	1.131E+09	1.001E+02	9.237E+06	8.471E+02	4.859E+03
1.968E-01	2.489E+12	2.129E+00	3.792E+10	1.574E+01	9.248E+08	1.105E+02	6.966E+06	9.588E+02	2.856E+03
2.303E-01	1.872E+12	2.361E+00	3.168E+10	1.735E+01	7.542E+08	1.220E+02	5.234E+06	1.091E+03	1.633E+03
2.675E-01	1.428E+12	2.617E+00	2.647E+10	1.913E+01	6.132E+08	1.348E+02	3.908E+06	1.244E+03	9.199E+02
3.082E-01	1.108E+12	2.900E+00	2.213E+10	2.108E+01	4.969E+08	1.490E+02	2.902E+06	1.418E+03	5.152E+02
3.525E-01	8.711E+11	3.211E+00	1.850E+10	2.323E+01	4.013E+08	1.648E+02	2.134E+06	1.625E+03	2.802E+02
4.010E-01	6.929E+11	3.555E+00	1.546E+10	2.561E+01	3.229E+08	1.824E+02	1.560E+06	1.869E+03	1.486E+02
4.542E-01	5.560E+11	3.933E+00	1.292E+10	2.822E+01	2.588E+08	2.018E+02	1.131E+06	2.158E+03	7.696E+01
5.126E-01	4.493E+11	4.350E+00	1.079E+10	3.109E+01	2.065E+08	2.239E+02	8.074E+05	2.500E+03	3.891E+01

- HLS-HMTA-0483 Report to Crew – Absorbed Dose – IVA (under review)

  The HLS shall display the radiation reports as specified in Table B-4 Radiation Data Reports and archive all recorded absorbed dose, proton flux, and neutron flux measurements for reporting to the Crew and Ground Team at the completion of each crewed mission.

Table B-4. Radiation Data Reports

Radiation Instrument	Radiation Report type	Radiation Report Time	Latency
Active Radiation Environment Sensor (ARES)	Absorbed Dose Display to Crew	Once/minute	< 5 minutes
Active Radiation Environment Sensor (ARES)	Absorbed Dose to Ground Team	Once/minute, when communication is available	< 5 minutes
Active Radiation Environment Sensor (ARES)	Proton Flux to Ground Team	Once/minute, when communication is available	< 5 minutes
Neutron Detector (TBD)	Neutron Flux to Ground Team	Once/day, when communication is available	N/A
Crew Active Dosimeter (CAD)	Absorbed Dose Ground Team	As required, when communication is available	N/A
Crew Active Dosimeter (CAD)	Absorbed Dose to Crew	R+21 days, Post-mission	N/A
Notes: Absorbed dose includes measured cumulative absorbed dose/minute averaged dose rate data; Proton and Neutron flux include flux vs. energy data.			

Appendix C. Artemis Concept of Operations for Mitigation of an Enhanced Space Radiation Environment and Impacts to Crew Operations

C.1   Executive Summary

As space exploration goals transition from the International Space Station (ISS) to the lunar and Mars surfaces, the operational paradigm must also transition to meet the needs of crew health and safety. In the case of the space radiation environment, the impact of both background galactic cosmic radiation (GCR) and episodic solar particle events (SPEs) must be monitored to effectively maintain the crew radiation exposure to levels as low as reasonably achievable (i.e., ALARA). The long history of the space program has been a benefit to mission planning, influencing advancements in space weather modeling methods, monitoring capabilities, and vehicle shielding concepts. These technologies have been applied to the next generation of space travel through the development of new instrumentation, updated vehicle design, and innovative tools for console operations. The application of these combined assets has resulted in an updated radiation concept of operations for the beyond low Earth orbit (LEO) mission era, summarized herein. The resulting mitigation and impacts to operations are summarized.

C.2   Scope

C.2.1   Description

The Artemis Concept of Operations for Mitigation of an Enhanced Space Radiation Environment outlines the roles and responsibilities of the radiation console from vehicle launch through vehicle landing. The document is intended to cover operations for all anticipated design reference missions (DRMs); extravehicular activity (EVA) operations from both the vehicle and the lunar surface will be considered, as will the operations for the individual mission segments. During the mission, the Space Radiation Analysis Group (SRAG) is tasked with maintaining radiation exposures as low as reasonably achievable (ALARA).

Space radiation sources are divided into three types, each with its own characteristics. *Trapped radiation* refers to that experienced by the vehicle due to passes through the Van Allen belts. During ISS missions, these passes are predictable and brief in duration but result in a greater dose rate than the remainder of the nominal ISS trajectory. In missions beyond LEO, the vehicle passes through the Van Allen belt during the ascent and descent phase, contributing to the crew cumulative radiation exposure. The dose rate of the trapped radiation exposure is not great enough to require crew to shelter. *Galactic cosmic radiation* (GCR) comprises mostly high-Z and high-energy particles and is difficult to shield effectively. While the rate of GCR exposure is not great enough for acute radiation syndrome (ARS) to be a concern, it is monitored to mitigate the risk of long-term health effects. During LEO missions, including ISS, the Earth's geomagnetic field protection results in only a periodic exposure to GCR throughout the vehicle trajectory. During beyond LEO (free space) missions, the vehicle is under constant GCR exposure; therefore, it is important to consider cumulative GCR exposure in an overall radiation mitigation strategy. Conversely, radiation exposure from *solar particle events* (SPEs) is sporadic, resulting in higher dose rates that may require operational mitigation steps including a request that the crew shelter in a higher shielded location. As with GCR exposure, the Earth's geomagnetic field results in only a periodic crew exposure for the duration of the SPE. During

missions beyond LEO, the vehicle will be in free space and therefore exposed to the full effect of the SPE.

Much of the effort in planning for missions beyond LEO involves improving both the vehicle shielding and the ability of the SRAG console to understand and predict temporary enhancements to the space environment. Mitigation of radiation hazards is achieved through a multi-pronged approach:

- **Vehicle design:** The Multi-Purpose Crew Vehicle (MPCV), also designated *Orion*, has been designed to maximize overall mission shielding. This includes the design of a short-term radiation shelter for protection during SPEs. Vehicle design details and shielding analyses are available for reference during mission planning. Note that the Human Landing System (HLS) is in development; information on shielding will be available at a future date.

- **Real-time dosimetry:** Both active and passive radiation detectors are planned to be available for use in area (vehicle) and individual crew monitoring.

- Satellite assets: While SRAG is aware of the current suite of satellites available for use, this status does not represent the entirety of what may be available in the future. This document will therefore list monitoring requirements and examples of available satellite data.

- **Console support:** SRAG currently provides 24/7 mission support for the ISS, with a combination of in-person and on-call availability. The current document outlines additional support for missions beyond-LEO.

- **Modeling capabilities:** The Acute Radiation Risk Tool (ARRT) and Integrated Solar Energetic Particle Alert/Warning System (ISEP) scoreboards have been developed to augment the current tool suite available to the Space Environment Officers (SEOs).

C.2.2   Assumptions and Definitions

The following section represents assumptions used in the development the current concept of operations. While the details of the DRMs are not indicated below, the assumptions of the general mission stages are included.

- 24/7 SRAG console support is expected during all missions beyond LEO. This may overlap with current ISS mission support.

- All lunar or planetary surface missions will be planned as a direct HLS mission and/or transit to Gateway, with no early return to Gateway from the surface.

- The most conservative case is assumed, with no lunar/planetary or geomagnetic shielding.

- Radiation shelter:
  - Available in Orion, with 30 minutes required for assembly.
  - HLS is in development, shelter assembly operations and shielding efficacy will be provided once available.
  - Shelter cannot be deployed or ingressed prior to (outbound) or following (inbound) TLI burn.
  - Essential operational tasks take precedence over shelter tasks.

- Operational Limits:
  - Short-term (mission) dose limit is the permissible exposure limit (PEL): 250 mGy-Eq per 30 days.

- Hybrid Electronic Radiation Assessor (HERA) caution and warning (acute dose limit) will be set at 50 µGy/min.
- Event Definitions:
  - SPE: >10MeV > 10 pfu
  - Low-Energy SPE (LSPE): SPE, SPE only with minimal increase in >30 MeV protons
  - Energetic SPE (ESPE): >100 MeV > 1 pfu
- EVA duration is limited to 8 hours due to consumables usage. During an EVA, crew can return to the vehicle in less than 1 hour in response to a contingency.

C.3   Background

C.3.1   Current (ISS) Operations

All solar energetic particle event forecasting/nowcasting is based on direct communications between SRAG and the National Oceanic and Atmospheric Administration (NOAA)/Space Weather Prediction Center (SWPC). SRAG flight controllers monitor console during enhanced solar activity, particularly predicted or observed SPE or ESPE. At event onset and throughout the duration of the event, the SRAG console distributes Alert/Warning messages to JSC management and the Flight Control Team (FCT) and ensures ISS radiation monitoring system availability, in addition to making any recommendations for crew activity in coordination with the FCT.

If the projection of additional exposure due to the event is determined to be negligible, no action will be recommended. If energetic particle flux has increased above event threshold or a radiation detector alarm activation is confirmed, the crew is directed to remain in higher shielded areas (including the service module aft of the treadmill, Node 2 Crew Quarters, and the US Lab) during intervals of high-risk orbital alignments. This response evolves over several hours with international coordination. Beyond-LEO missions will require this process to be much faster, as solar energetic particles can reach peak flux levels in less than 5 hours. The overall impact to ISS crew is a periodic short-term (10- to 15-minute) relocation to shielded locations, with dose on the order of quiet days of extra exposure.
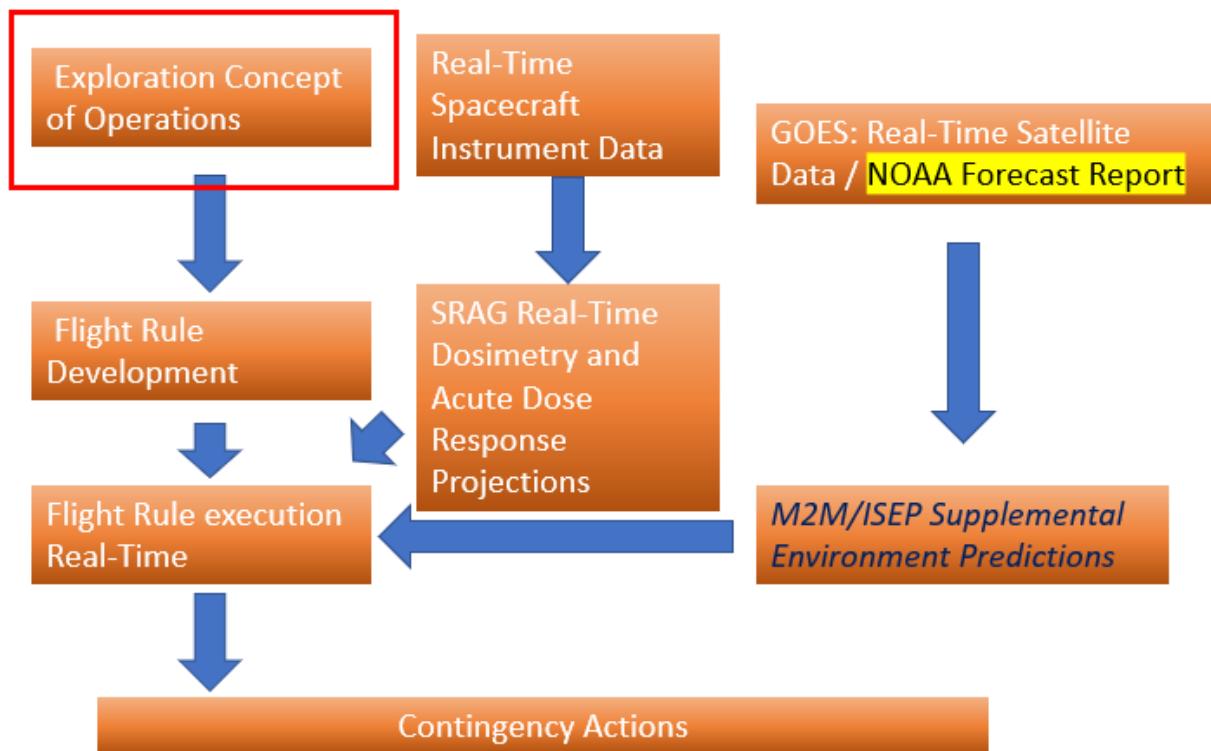
C.3.2   Operational Schema for Artemis Missions

The planned schema for Artemis Mission support is shown in Figure C-1. Both internal NASA and external Agency support are represented to describe the full radiation mitigation concept for these free space missions. The schema considers the concept of operations, real-time radiation monitoring instrumentation, and real-time satellite data.

The baseline version of the "Artemis Concept of Operations for Mitigation of an Enhanced Space Radiation Environment" was published in February 2021. The current document represents an overview of the more detailed concept of operations. In addition to directing SRAG's operational philosophy and training, the concept of operations will also be used to develop the flight rules that are referenced during contingency console support.

Real-time spacecraft instrument data, both vehicle and personal monitors, are used to gain insight into the real-time environment, which is used as an input for ARRT. The measurements can indicate when crew should build, ingress, and egress shelter. Finally, the instrumentation can be linked to a caution and warning alarm to alert the crew to the need to shelter.

Real-time satellite data are monitored by SRAG console operators and are the basis for the current forecast reports provided by NOAA/SWPC for ISS mission operations, which are expected to continue into the Artemis era. These data also act as input for many of the models supported by the ISEP scoreboards and the corresponding M2M (i.e., Moon to Mars (Space Weather Office) support.

Figure C-1. Interconnection of Internal NASA Products and External Agency Support for Mitigation of Solar Energetic Particle Exposure during Artemis Missions

C.3.3 Artemis Mission Segments

This concept of operations is structured to emphasize the anticipated mission stages as opposed to any single DRM in order to provide flexibility. The location of the vehicle is considered the prime indicator of required radiation mitigation operations. This approach is intended to apply to a range of free space missions, whether the vehicle docks at an intermediate location or travels directly to a lunar/planetary surface. In the context of a space environments document, the following mission stages are considered:

- **Earth to/from translunar injection (TLI):** Launch commit criteria (LCC) shall be defined such that the exposure due to a large event will surpass a defined threshold, causing SRAG to be No-Go for launch. Regardless of the final DRM, it is assumed that crew cannot build shelter prior to TLI burn (outbound) or following TLI burn (inbound).

- **TLI to/from Gateway cruise segment:** This phase represents the vehicle in free space. All radiation mitigations operations assume the most conservative case (no lunar/planetary or geomagnetic field shielding). A shelter can be constructed if needed.

- **Moon/Mars Orbit:** This phase represents the vehicle in lunar or planetary orbit. All radiation mitigations operations assume the most conservative case (no lunar/planetary shielding). A shelter can be constructed if needed.
- **Orbit to/from surface (HLS):** No early return from the surface is possible, and shelter capability of the HLS is unknown.
- **Surface/EVA operations:** At this stage, no shelter activity is possible. The crew shall wear an active dosimeter, such as the active radiation dosimeter (ARD). During an ESPE, if the active dosimetry in conjunction with vehicle shielding analyses indicates a marked reduction in exposure inside the vehicle, the decision shall be made with the FCT as to whether to continue with EVA.

C.4   Space Weather Operations Definitions

Environment condition definitions for both ISS and Artemis operations are defined in this section. Table C-1 summarized these definitions for Artemis operations and shows the applicable console tools for each observable condition.

Table C-1. Environment Condition Definitions for Artemis Missions (available assets and tools for guiding console operations are also indicated)

	Definition	**Applicable Tools**
All Clear	Space weather models are forecasting that an ESPE is unlikely to occur in the next 24 hours	All-Clear Scoreboard
Event Watch	Space weather models are forecasting that an ESPE is likely to occur in the next 24 hours	All-Clear Scoreboard Event Probability Scoreboard NOAA/M2M Support
Event Warning	Enhanced space radiation environment has been observed but does not satisfy the ESPE condition	Event Probability Scoreboard Event Intensity Scoreboard NOAA/M2M Support Satellite Assets
Event Contingency	ESPE conditions has been confirmed and crew action may be required to minimize increase in radiation exposure	Event Intensity Scoreboard NOAA/M2M Support Satellite Assets
Projected Dose Surpasses Threshold	Radiation exposure has been predicted or confirmed to surpass threshold (250mGy-Eq per 30 days OR 50 µGy/min)	Active Instrumentation ARRT

C.4.1   Space Weather Console Status Definitions

C.4.1.1   Nominal Conditions

The term *nominal* denotes the typical background space environment, absent of any adverse space environment conditions. This definition is common to ISS and beyond LEO mission support.

C.4.1.2 Off-nominal Conditions

The term *off-nominal* denotes a disturbance or increase in the space environment that could impact operations. This definition is common to ISS and beyond LEO mission support.

C.4.1.3 Alert-level Definitions

C.4.1.3.1 All-Clear

The term *all-clear* denotes nominal conditions where space weather models are forecasting that no ESPE will occur in the next 24 hours.

C.4.1.3.2 Watch

The term *watch* denotes nominal conditions where space weather models are forecasting that an ESPE is likely to occur in the next 24 hours.

C.4.1.3.3 Warning

For beyond-LEO mission support, the term *warning* denotes off-nominal conditions where an enhanced space radiation environment has been observed but does not satisfy the ESPE condition. *Warning* has also been used in the ISS Space Environment Flight Rules to indicate a warning generated by NOAA/ SWPC.

C.4.1.3.4 Contingency

The term *contingency* was used in the ISS Space Environment Flight Rules to denote off-nominal conditions where ESPE conditions are confirmed and crew action may be required to minimize an anticipated or confirmed increase in radiation exposure. Use of this term will continue into beyond-LEO mission support. A radiation contingency is initiated when any of the following events occur:

- (IVA) >100 MeV proton flux > 50 pfu
- (IVA) dose rate
- (EVA) dose rate

A contingency is downgraded to a warning when flux levels have been reduced below ESPE threshold criteria for three consecutive readings and show a clear trend down. Termination of active event support is at the discretion of the SRAG SEO.

C.4.1.3.5 Alert
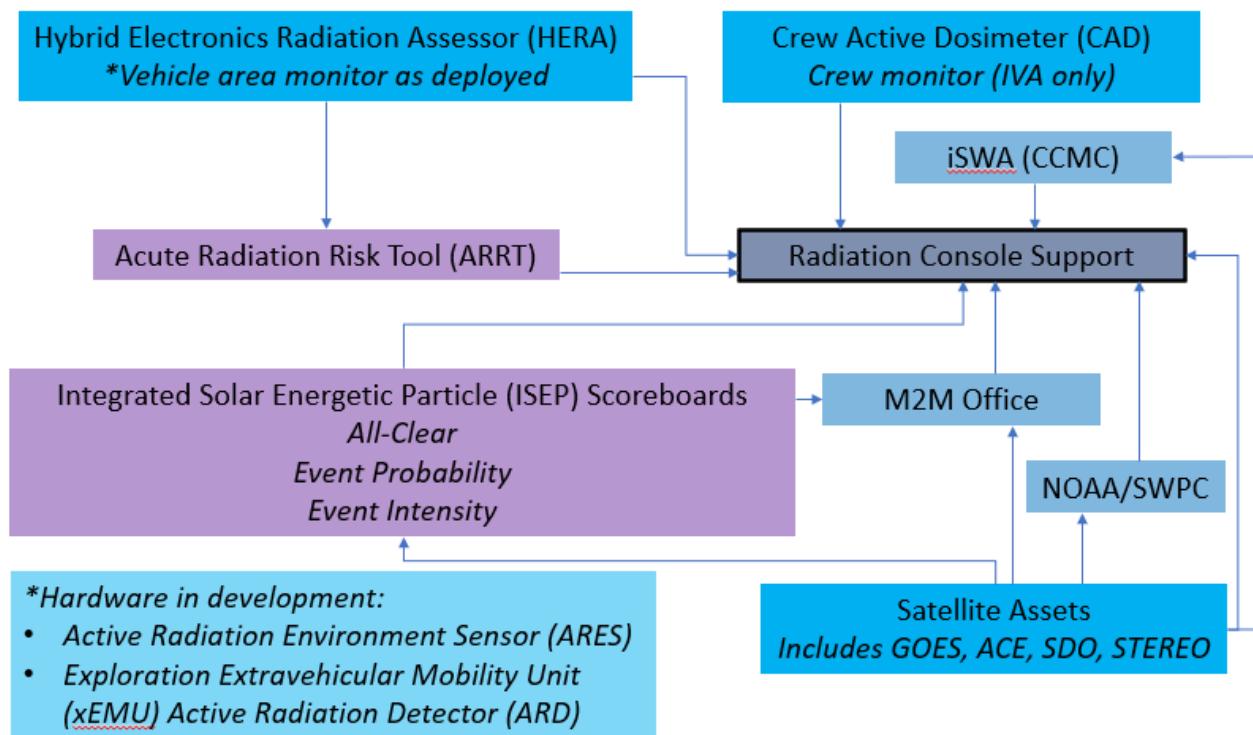
The term *alert* is used in the ISS Space Environment Flight Rules to denote a condition where an increase in crew radiation exposure is either imminent or observed but not yet at a level requiring crew intervention. For missions beyond LEO, *alert* has been superseded by the use of *warning* and *contingency*. An alert may be initiated by any of the following events:

- SPE warning issued by NOAA/SWPC
- SPE
- High-quality/high-confidence forecasts
- X-ray event >M5
- CME warning w/expected significant impact (possible ESP, EVA concern)
- LSEP (EVA only)

An alert is downgraded to nominal when (1) time projected by NOAA/SWPC for a generated SPE warning has expired OR (2) flux levels for an SPE in progress have been reduced below event threshold criteria for three consecutive readings and show a clear trend down. Termination of active event support is at the discretion of the SRAG SEO.

C.5   Available Hardware

Figure C-2 shows the relationship between the tangible assets (i.e., monitoring hardware, satellite assets), console tools (i.e., ARRT, ISEP scoreboards) and organizations (i.e., M2M Office, Community Coordinated Modeling Center (CCMC), SWPC) supporting Artemis radiation console operations.

Figure C-2. Interaction of all Artemis Operational Assets described in Upcoming Sections

C.5.1   Radiation Monitoring

Passive and/or active area and crew monitoring shall be available throughout all possible DRM. In the initial Artemis I/II missions, passive monitoring will be performed using the Radiation Area Monitor (RAM), while active monitoring will be performed by the HERA (area monitoring) and the Crew Active Dosimeter (CAD) (crew monitoring).

The following measurements will be performed to characterize and manage radiation exposures:

- **Measured radiation quantities:** Absorbed dose, dose equivalent, and flux energy spectra (as a function of direction, energy, and charge).
- **Measured locations:** Intravehicular area monitoring, intravehicular and EVA crew personal monitoring.

Radiation monitoring instrumentation on spacecraft is required for routine mission insight of the current radiation environment, risk analysis exposure documentation, and crew-independent contingency actions. Crew-independent contingency action capability may be required for planetary excursions, where communications may be intermittent.

C.5.2 Internal Radiation Monitoring Hardware

C.5.2.1 Hybrid Electronic Radiation Assessor (HERA)

The HERA System consists of several self-contained components, each including a HERA processing unit (HPU) and one to three HERA sensor units (HSUs). Each HPU has one internal sensor and supports up to three external HSUs. HSUs are powered via the HPU and can be controlled independently. There are two HERA systems installed in the MPCV; the uncrewed Artemis I mission will only manifest one HERA system. Each system contains one HPU and two HSUs.

Each HSU contains a Timepix pixelated radiation detector, which provides energy deposition and spatial pattern information for tracks resulting from the passage of ionizing radiation through the sensor. The energy and pattern information can be analyzed to provide dose rates as well as spectral information for the incident radiation field.

Each HPU provides current and recent dose rates and cumulative mission doses for onboard display. The collected radiation data are also packaged and relayed to the ground for more detailed analysis, which would be too computationally intense to be performed by the HPU. All the information passed to the Orion systems for display is directly prepared by the HPU.

The HERA system is connected to the onboard C&W system and provides a C&W signal when the defined threshold is exceeded.

C.5.2.2 Crew Active Dosimeter (CAD)

CADs will be used for measuring absorbed dose in the space radiation environment for bBeyond-LEO missions inside the Orion vehicle. The dosimeters are worn by the crew and of active nature (i.e., absorbed dose data are autonomously measured and stored in time segments continuously over the course of the mission without the need for ground communication or crew interaction).

Crew will transfer the CAD upon garment changes into the currently worn garments (e.g., garment changes for exercise). No other interaction is required. The display will provide cumulative mission dose and dose rate for crew information.

The CAD has no internal alarm capabilities. During an SPE where the vehicle C&W system indicates elevated radiation levels, crew shall seek shelter according to FCT/SRAG recommendation. The display on the CADs allows the crew to monitor changes in the dose rate throughout the event, complementing information from the ground and the onboard system.

C.5.3 External Radiation Monitoring Hardware

No external charged particle monitoring is currently planned for the initial Artemis I/II missions.

C.5.4 Hardware Development

- **Active radiation environment sensor (ARES):** ARES is a charged particle detector planned for use in later beyond-LEO missions, including Gateway and HLS. More information will be provided as the hardware development progresses.

- **ARD:** CAD is not rated for use on EVA due to the battery and the lack of vacuum capability. ARD is planned for use as an active personal dosimeter for EVA. More information will be provided as the hardware development progresses.

- **Neutron dosimeter:** A neutron detector has not been funded at this time. If/when an instrument is funded, more information will be provided about its operational use.

C.6 Available Tools

C.6.1 Space Weather Monitoring Asset Needs

Multiple space weather parameters are monitored and used for analysis and assessment supporting the manned spaceflight program. The sources of these measurements are satellites characterizing different elements of the environment from many different locations. Current measurement locations include Earth orbit, the Sun-Earth Lagrangian point (L1), and remote locations along the Earth orbital track. It is presumed that measurements from similar assets will continue to be available for mission support during beyond-LEO missions. This section will identify satellite resources required by SRAG to perform space weather monitoring and suggest potential resources for future programs.

C.6.1.1 Energetic Proton Flux

Measurements of integral and differential particles fluxes are required for dose projections through the spacecraft shield. Energy ranges from 10 through 100 MeV are currently of interest. Additionally, energies up to 500 MeV are of practical utility. Currently, proton flux levels are supplied from the Geostationary Operational Environmental Satellite (GOES) and the Advanced Composition Explorer (ACE) Solar Isotope Spectrometer (SIS).

C.6.1.2 Energetic Electron Flux

Energetic electron fluxes are not considered a hazard at this time.

C.6.1.3 X-ray Flux

This primary parameter is used to flag the initiation of a solar transient. Currently, X-ray information is supplied from GOES ("1.0-8.0A" channel). According to NOAA, moderate (R2) solar activity is defined with the observation of an M5 flare (5×10^{-5} W/m^2) and strong (R3) solar activity is defined with the observation of an X1 flare (1×10^{-4} W/m^2). Attainment of these thresholds, although they do not directly impact crew radiation exposure, indicate a possible increase in solar particle fluence.

C.6.1.4 Radio Frequency (RF) Emissions

A wide range of radio frequency (RF) emissions are released during the course of solar transients. Several emission types are characteristic of different processes that are of interest. Type II, Type IV, and tenflares are the most useful parameters in evaluating a solar energetic proton-producing transient. Some emissions provide a glimpse of how energetic the release is, and the simultaneous emission of all three is almost a guarantee of the onset of a SPE and CME.

C.6.1.5 Solar Imaging

Solar imaging is essential to assess solar conditions, including:

- Characteristics and trends of active sunspot regions.
- Determination of X-ray source location.

- Vector magnetographs to assess the magnetic energy bound above an active region.
- Coronal imagers for CME analysis.
- Ultraviolet wavelengths, which reflect a different aspect of coronal activity. The image cadence available with the Solar Dynamic Observatory (SDO) is more than adequate for operational support requirements.

C.6.1.6 Low Energy Electrons (still relativistic)

Low energy electrons, such as those in the energy ranges measured by the ACE Electron Proton Alpha Monitor (EPAM), provide an indicator of connectivity between the transient location and the spacecraft, which is useful for providing an early warning monitoring energetic events. Relativistic electrons measurements as a driver to support proton event forecasting is recognized as a critical need. Protons released during ground-level events will arrive rapidly, making the connectivity assessment using electrons ineffective.

C.6.1.7 Low Energy Protons

Low energy protons, such as those measured by the ACE/EPAM, provide an indicator of connectivity to an in-bound CME. The proton flux slowly rises as a CME approaches, peaking at the onset of the CME shock arrival. This measurement provides confirmation of an approaching CME.

C.6.1.8 IP Solar Wind

Solar wind parameters include wind speed, density, and temperature, along with local solar magnetic field line direction and magnitude. Many of these parameters are collectively analyzed to characterize transients observed at the satellite, including ACE and the Solar Terrestrial Relations Observatory (STEREO). This suite of measurements is most useful in defining the interplanetary environment's influence on the Earth's magnetic field and resulting magnetic storm intensity.

C.6.2 ISEP Scoreboards

As NASA plans for missions outside LEO, the need for improvements in space weather environment modeling capability has been strongly emphasized. SRAG and CCMC began a three-year project, sponsored by the Advanced Exploration Systems (AES) program and the Crew Health and Performance/Systems Capability Leadership Team (CHP/SCLT), in Summer 2018 to focus on the transition of space weather models from research to operational use. At the end of the initial project, ISEP will deliver a series of scoreboards, each one featuring an ensemble of models focused on a specific event characteristic, to aid the operator in future short-term mission planning and operations. As ISEP continues beyond the original 3-year plan, it is expected that the work will continue through the initial Artemis missions, evolving to meet the needs of the mission support team.

The transition of these space weather models from research to operations has been, and continues to be, the result of multiple iterative steps between SRAG, CCMC, and the individual model developers. The ISEP team first identified the space weather models that best combined utility to beyond-LEO console operations and the ability to be easily transitioned to operations. Next, the ISEP team worked with the model developers to host their work at CCMC and fully understand the underlying theory and application of the model results. This step will continue through the life of the project, allowing for improvement of predictive capability as available research

matures. Finally, the use of the ISEP scoreboards must be smoothly integrated into both the nominal and off-nominal operations through training and simulations.

C.6.2.1 Scoreboard Descriptions

The three Scoreboards are hosted at GSFC/CCMC. The M2M Office will work with CCMC and SRAG to bring these model results to operations use. The three scoreboard types are:

1. Probability: The likelihood of an event represented on a continuous scale. Examples of this include the Magnetogram Forecast (MAG4, University of Alabama at Huntsville) and the PROTONS model used by SWPC, with a human factor, for their daily flare/SPE predictions.

2. Intensity: This is a single scoreboard with the following two functions represented:

   - Peak proton flux: Heat map representing the projected maximum proton flux. An example of this includes the University of Malaga Solar Energetic Particles (UMASEP) model family, named UMASEP-10/-30/-50/-100/-500 based on the proton energy modeled.

   - Time series: The predicted time course of an event. These are frequently provided by physics-based rather than empirical models, such as Solar Energetic Particle MODel (SEPMOD) and SPE Threat Assessment Tool (STAT). The physics-based models generally require more computing time, and an effective method of transitioning to real-time operations is in work.

3. All-Clear: The likelihood of an event represented on a binary scale, or on a probabilistic scale upon which a threshold has been established to create a "Yes/No" prediction. This scoreboard, rather than providing feedback to the FCT on the need to implement mitigation tasks, can give the FCT confidence that an event will not occur in the next given span of time (e.g., 24 hours). This knowledge is useful in planning crew tasks such as EVAs.

C.6.2.2 Scoreboard Use in Operations

As the scoreboards have been designed to model the characteristic space environment as opposed to the impact on a vehicle, transition to operations has started to allow SEOs to become familiar with the tool. The SEOs can use the time prior to the launch of Exploration missions to identify any issues and provide additional feedback to CCMC.

During the first uncrewed mission (currently Artemis I), the SRAG console will be used as a testbed for the use of the scoreboards in nominal operations and the prediction of any changes to the space environment. As the need for crew protection is negated during this testbed mission, the following priorities are established:

- Continuous function of the ISEP scoreboards.

- Continuous access to the ISEP scoreboards at CCMC, through the M2M group as required.

- Smooth integration of the scoreboard into console operations.

- Recommendations for updates to the scoreboard for utility.

- Validation of any model predictions.

Use of the ISEP scoreboards as part of an overall radiation exposure mitigation strategy is addressed later in this section, as it requires a thoughtful inclusion of multiple partners.

C.6.3 Acute Radiation Risk Tool (ARRT)

The MPCV will feature shelter configurations, and crew may need to shelter for an extended period of time. The ARRT uses work performed for the Defense Threat Reduction Agency to predict the likelihood and severity of specific ARS symptoms due to radiation exposure.

The ARRT uses real-time telemetry from the intravehicular area monitoring system, currently the HERA, as well as data from historic SPEs and previous free space missions to determine blood-forming organ (BFO) dose in several vehicle locations.

The ARRT predicts the incidence and the severity of two of the six symptoms of ARS: upper gastrointestinal distress (UG) and fatigability and weakness (FW); not predicted are lower gastrointestinal distress (LG), hypotension (HY), infection and bleeding (IB), and fluid loss/electrolyte imbalance (FL). In addition to these symptoms, the ARRT also calculates the performance decrement (PD), a factor that indicates the extent to which a crew member is limited in performing a set of mission-critical tasks.

C.6.4 Support Organizations

SRAG is supported by NOAA/SWPC and GSFC/CCMC. The SWPC, which currently supports ISS operations, is expected to provide situational awareness of the space environment, while CCMC provides scientific expertise.

C.6.4.1 Space Weather Prediction Center (SWPC)

The role of the NOAA/SWPC team is to provide a daily status of the current space environment and a projection of any changes over the next 72 hours. The role of SWPC in SRAG console operations is not expected to change for beyond-LEO missions.

C.6.4.2 Goddard Space Flight Center (GSFC)

C.6.4.2.1 CCMC Role

The GSFC/CCMC group has worked with SRAG through the ISEP collaboration to develop the scoreboards described above. Prior to the first uncrewed mission, CCMC will continue to work with SRAG console operators to integrate these scoreboards into the operational concept, incorporate any new model outputs, and validate the model results. Following the first uncrewed mission, CCMC will use feedback provided by the SRAG SEO group to make any additional improvements to the ISEP scoreboards. CCMC will not perform a forecast. The forecast will be delivered by the M2M Office to the SRAG console operators. M2M will work with CCMC to develop any improvements that may be needed to perform a space weather analysis.

CCMC will maintain the scoreboards. The M2M Office will provide troubleshooting capability after hours and 24/7 access (will have installation on cloud servers for SRAG use), with a goal to transition all responsibility at a future date.

C.6.4.2.2 Moon to Mars (M2M) Space Weather Office

The M2M Office at GSFC was established at the end of FY20 to act as a SRAG "back room" and provide a link between the science support provided by CCMC and the real-time operational needs of SRAG. As the M2M Office becomes more established, the day-to-day operations will be better known. As with NOAA/SWPC, it is expected that the M2M Office will participate in a daily brief of the outputs of the space environment models represented by the ISEP scoreboards.

It is expected that SRAG will be able to access the ISEP scoreboards 24/7. In the event of an issue with connectivity to the ISEP scoreboards from Johnson Space Center (JSC), the M2M Office will identify a reliable backup mechanism for a subset of the models, working in collaboration with CCMC. Issues with availability of individual model inputs or outputs will be worked between CCMC, SRAG, and M2M as a part of the initial transition to operations and as part of a lesson learned following the initial uncrewed mission.

C.6.4.2.3 Integrated Space Weather Analysis System (iSWA)

The iSWA is a public-facing model repository hosted by CCMC. Most models hosted on the ISEP scoreboards have an associate iSWA cygnet, as does the comparison of multiple connectivity models displaying the footprint of the Earth on the solar surface. The user can customize iSWA as desired.

C.6.4.2.4 Interaction of Support Organizations – Crewed Missions

As with the uncrewed missions, radiation console support for the initial crewed Exploration missions are expected to be conducted alongside (but separate from) the ISS radiation console support. This section lists the anticipated coordination of inputs from the available satellite assets, NOAA/SWPC, GSFC/M2M Office, ISEP scoreboards, and ARRT for both nominal and off-nominal/contingency support to the FCT. It is important to note here that these inputs all are provided in support of the SRAG console; a successful implementation of a space weather mitigation strategy requires a highly skilled and well-trained SRAG SEO group, and console expertise also must play a role in interactions with the FCT.

C.7 Radiation Mitigation for Enhanced Environments

As noted above, the Exploration concept of operations considers the location of the vehicle rather than the DRM, as the mitigation steps to be recommended rely upon the space environment. This section lists the steps taken for each environmental condition listed in Table C-1 based on the mission segment.

C.7.1 Segment: Earth to/from TLI

This segment represents the initial and final mission segments. All recommendations listed in Table C-2 are driven by the assumption that crew cannot take shelter between Earth and TLI burn.

Table C-2. Recommendations for Missions Between Earth and TLI

Condition	Recommendation/Impacts
All-Clear	GO for launch/landing
Event Watch	GO for launch/landing
Event Warning	GO for launch if LSPE in progress, assuming no EVA planned (next 72 hr) GO for landing
Event Contingency	Potential NO-GO for launch GO for landing
Projected Dose Surpasses Threshold	Potential NO-GO for launch if projected mission dose will exceed any PEL GO for landing

C.7.2 Segment: Free Space

This segment represents mission segments in free space. All recommendations listed in Table C-3 are driven by the assumption that crew is able to shelter per the vehicle design.

Table C-3. Recommendations for Free Space Missions

Condition	Recommendation/Impacts
All-Clear	Nominal operations
Event Watch	Nominal operations
Event Warning	Deploy shelter (Orion) Nominal operations
Event Contingency	Deploy shelter (Orion) Crew will be recommended to take shelter when: > 100 MeV proton flux > 50 pfu OR if the >100 MeV flux has not yet peaked at 2 hours following onset and the >100 MeV flux is expected to exceed 50 pfu. An ESP onset (CME arrival) occurs during the event and P >100 MeV flux is >50 pfu. A second ESPE occurs during a mission.
Projected Dose Surpasses Threshold	Deploy and ingress shelter (Orion) (Note: HERA C&W is generated at 50 µGy/min. Crew can permanently egress the radiation shelter once HERA units display a dose rate of 2.5µGy/min. Dose rates 2.5 through 50 µGy/min are subject to ALARA and further flight rule development.)

C.7.3 Segment: Moon/Mars Orbit

This segment represents mission segments in lunar or planetary orbit. All recommendations listed in Table C-4 are driven by the assumption that crew is able to shelter per the vehicle design. The most conservative case (no lunar/planetary shielding) is assumed.

Table C-4. Recommendations for Moon/Mars Orbit

Condition	Recommendation/Impacts
All-Clear	Nominal operations
Event Watch	Nominal operations
Event Warning	Deploy shelter (Orion/Gateway/HLS) GO for nominal operations NO-GO for surface transit
Event Contingency	Deploy and ingress shelter (Orion/Gateway/HLS) Same ingress/egress conditions as free space NO-GO for surface transit
Projected Dose Surpasses Threshold	Deploy and ingress shelter (Orion/Gateway/HLS) Same ingress/egress conditions as free space NO-GO for surface transit

C.7.4 Segment: Orbit to/from Surface (HLS)

This segment represents mission segments from lunar or planetary orbit to the surface. All recommendations listed in Table C-5 are driven by the current unknown surrounding the HLS vehicle design; these impacts may change as the design matures. The most conservative case (i.e., no lunar/planetary shielding) is assumed.

Table C-5. Recommendations for Lunar/Planetary Orbit to Surface

Condition	Recommendation/Impacts
All-Clear	Nominal operations
Event Watch	Nominal operations
Event Warning	NO-GO (orbit to surface) GO (surface to orbit)
Event Contingency	NO-GO (orbit to surface) NO-GO (surface to orbit)
Projected Dose Surpasses Threshold	NO-GO (orbit to surface) NO-GO (surface to orbit)

C.7.5 Segment: Surface/EVA

This segment represents mission segments on the lunar/planetary surface, including EVA. All recommendations listed in Table C-6 assume an 8-hour duration EVA and a maximum dose rate less than 10.0 µGy/min, implying a possible total 5 mGy exposure for the EVA.

Table C-6. Recommendations for Surface/EVA Operations

Condition	Recommendation/Impacts
All-Clear	Nominal operations GO for EVA
Event Watch	GO for EVA
Event Warning	NO-GO for EVA unless event has peaked and measured dose rates are < 10.0 µGy/min EVA in progress will be terminated as quickly and as safely as possible during LSPE if the dose rates exceeds 10.0µGy/min as measured at the EVA suit (Exploration Extravehicular Mobility Unit (xEMU) ARD)
Event Contingency	NO-GO for EVA unless event has peaked and measured dose rates are estimated to be <10.0 µGy/min, based on ARES Terminate EVA in progress, crew recommendations based on comparison between ARES (IVA) and xEMU ARD (EVA)
Projected Dose Surpasses Threshold	NO-GO for EVA Terminate EVA in progress

Appendix D. Health and Medical Approach Analogous to Human Systems Integration Architecture (HSIA)
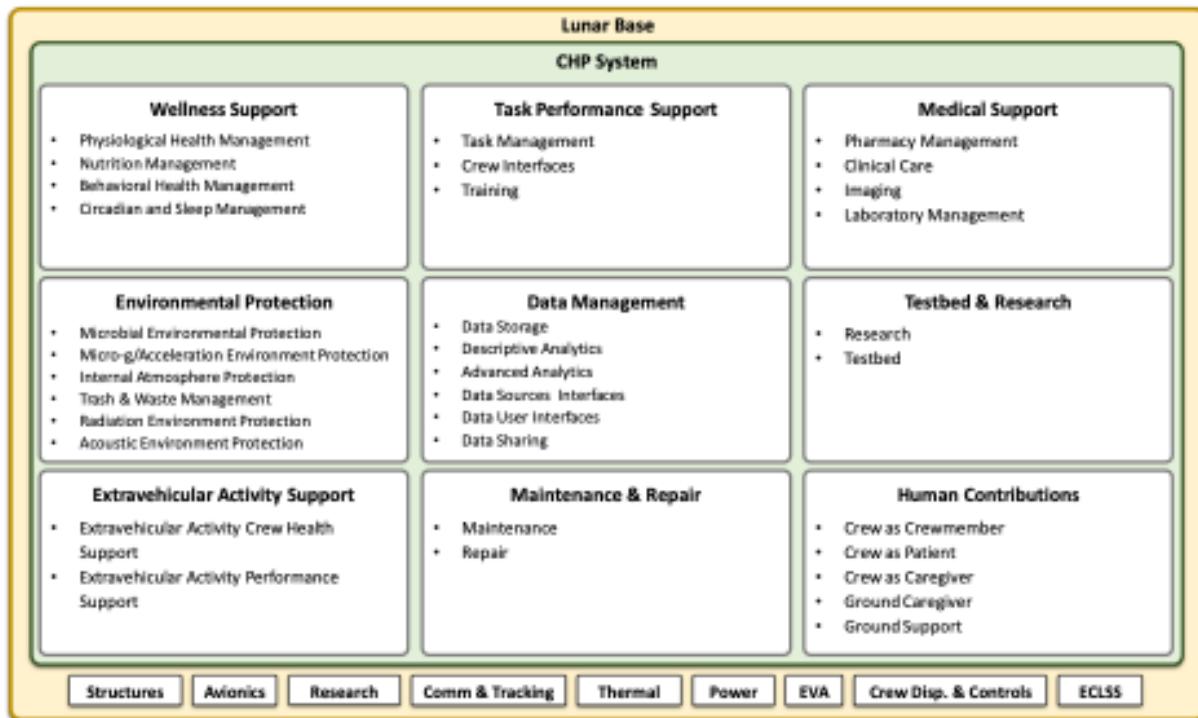
D.1   Onboard CHP System

Onboard knowledge base, artificial intelligence (AI), and autonomous systems capabilities must be complemented by the vehicle's ability to include and accommodate the crew's capabilities. The crew capabilities at any given time, or "state" of the crew, is influenced by the various spaceflight hazards, including radiation exposure and altered gravity exposure as discussed in this NESC final report. Going beyond the clinical health of the crew, a more comprehensive state of the crew must be monitored and supported to enable the crew to accomplish mission-scientific and exploration objectives and execute anomaly resolution and prevention.

An integrated crew health and performance (CHP) system is an engineering approach to bring together the various functions required to monitor and support both crew health and crew task performance. A CHP system concept is complementary to an environmental control and life support system (ECLSS), whose function traditionally focuses on keeping the crew alive with the necessary air and water resources and removing products such as carbon dioxide.

Figure D-1 represents a broad set of functions that enable monitoring and support of crew state by a notional CHP system for a lunar base [McGuire et al. 2021], but the functions remain the same for a long-duration Mars mission. The high-level functions shown are:

- Wellness support
- Environmental protection
- Extravehicular activity support
- Task performance support
- Data management
- Maintenance and repair
- Medical support
- Testbed and research
- Human contributions

Figure D-1. CHP System-centric Function Diagram

As detailed mission architectures and solutions are developed and trades performed, some of these functions may indeed be allocated to systems outside what is shown here as CHP. In addition, broader implementations to meet these needs will likely be managed in other vehicle systems. For example, under Environmental Protection, decomposed functions are shown to include protection from the altered gravity exposure and radiation exposure hazards discussed in this report. This does not mean vehicle-level solutions (e.g., AG and vehicle shielding) would be managed under a CHP system. The functions serve as a reminder for these needs and as a placeholder for potential additional solutions, such as crewmember-specific compression garments (in the case of the altered gravity hazard to address the potential for orthostatic intolerance) and crewmember-specific radiation protection.

The health and performance impacts of a cohesively developed CHP system may be obvious, but it is worth noting explicitly that engineering solutions addressing a more holistic view of crew needs are expected to have a more impactful health and performance result as compared with those developed in an independent manner.

The engineering impacts of a conceptually (although not necessarily strict physically) integrated CHP system are expected to be beneficial from a spacecraft resources perspective as compared with the largely separate and distinct solutions on the International Space Station (ISS) today. For example, medical resources for crew care would be expected to also meet research needs. Exercise systems would be expected to explicitly support behavioral health as well. Data collection, storage, analysis, and display would be expected to be compatible and consistent CHP system-wide, and ideally throughout the entire vehicle. A cohesively developed CHP system is expected to provide mass, power, and volume savings versus independently developed solutions. Compatible and consistent data would provide more effective and efficient crew state monitoring

and support capabilities that will, in turn, enable crew execution of mission objectives and anomaly resolution and prevention.

While the CHP system in part compensates for crew functional deterioration, it also monitors the state of the crew in a data-intensive process. Part of effective HSIA is matching all vehicle and system support to the expected state of the crew throughout the mission. Whether engineering solutions include onboard knowledge base, AI, or autonomous systems, these solutions must be integrated with the other vehicle systems. A human centered-design approach that ensures that the data architecture for the mission is sufficiently integrated and wrapped around the crew is a different design paradigm than has been used in the past.

D.2 Effective Communication Among Exploration Programs and Health and Performance Personnel

In the context of spacecraft design, there is a natural tension between the engineering and science communities. The science objectives of a mission often drive the highest-level capabilities and constraints of a mission. The engineering implementation provides the realization of a solution bound by scientific, technical, cost, schedule, personnel, and political constraints. Both NASA's engineering and health and performance communities have challenges to overcome to achieve successful long-duration exploration missions. The following are broad generalizations and observations discussed for the purposes of identifying recommendations and certainly have counterexamples not discussed here.

Within the engineering community, there may be a tendency to assume an understanding of the needs of a human crew because the engineers themselves are human. This assumption, however, does not give proper value to disciplines supporting successful human spaceflight (e.g., physiology, space medicine, behavioral health, and human factors). Engineers are not typically trained in these areas and can lack an awareness of the constraints in human capabilities. Resources such as NASA-STD-3001 set the stage for ensuring crew needs are met; however, there may be a temptation to "check the boxes" of this lengthy set of standards and derived requirements without truly addressing the intent of the content. This may happen, especially when spaceflight resources (e.g., mass, power, and volume) are constrained heavily and data to support defense of human accommodation do not yet exist or are exptrapolated from other contexts (e.g., Earth analogs or shorter mission durations). An underlying approach of designing to the "harder" engineering physics constraints and that later humans will just "make it work" through operations and compromises in efficiency, ease of use, and even risk of injury may be a bias not fully acknowledged. This bias may be compounded by the engineering community typically being driven more by the engineering challenge itself—the development, launch, and operation of a successful vehicle—than the science objectives and knowledge to be gained. This is not a judgment but a recognition of valid differences in team member motivations.

The health and performance community has its own challenges. There is a strong cultural legacy of scientific research-driven product priorities focused on publications. A focus on the integrated development of an actual (i.e., not paper) exploration spaceflight system and the associated engineering realities is still evolving. Much of the recent historical cultural viewpoint is that the spacecraft is the "platform" for performing research. This ISS-centric model will not hold true as easily for deep space, due to spaceflight resource constraints, as the mission CHP needs, along with research objectives, will need to be integrated with the vehicle more intimately for deep space. The community is often missing the connection between daily work deliverables and the

specific spaceflight system development products—standards, requirements, designs, verifications and validations, protocols—those products will inform. There is also a challenge for the community to clearly communicate to engineers the problem to be solved, why it is important, and the impacts of health and performance solutions from an engineering perspective. Engineering talent certainly exists within the health and performance community, although it has largely provided more standalone products and therefore generally has less experience participating as an equal player in the development of large-scale spaceflight systems.

These challenges illuminate the following recommendations:

- Raise awareness through training and other communication methods regarding each community.

- For the engineering community, raise awareness throughout the program team regarding human capabilities and constraints in spaceflight and the limits of current knowledge.

- For the health and performance community, raise awareness of spacecraft design principles, constraints, and processes.

- Programs view a CHP system at the same conceptual level as other traditional spacecraft systems (e.g., structures, avionics, software, ECLSS). This is especially important during early development phases when concepts and requirements that drive key resource allocations such as mass, power, and volume are maturing.

- Include in program teams technical systems engineers (going beyond less technical "integrators") working both with and from within the health and performance community that are well versed in both spacecraft development and human systems to serve as effective bi-directional translators. This may require additional workforce development.

- Continue an emerging pivot of the health and performance community to succinctly connect work deliverables with spaceflight program development products.

- Continue to train the health and performance community on communicating problems, their importance, and solution impacts in engineering terms.

Appendix E. Summary of Previous Space Weather Mission and Instrumentation Studies

E.1 Existing Missions and Instruments that will Contribute to Protection of Space Crews on Missions beyond LEO

NOAA's Geostationary Operational Environmental Satellites (GOES) in geosynchronous orbit: The currently operational GOES satellite is from the GOES-R series. GOES-16 (launched November 19, 2016) and GOES-17 (launched March 1, 2018) are currently in orbit and operational. GOES-T is to be launched in March 2022. These satellites host a suite of instruments including a solar UV imager, extreme UV and X-ray irradiance sensors, and instruments that monitors proton, electron, alpha particle, and heavy ion fluxes (see https://www.goes-r.gov/education/docs/Spaceweather.pdf and links therein for details). GOES-U, to be launched in 2024, will include these instruments plus a white light coronagraph. These satellites detect the solar eruptions that can cause SPEs. Together, observations from these instruments are intended to enable NOAA's SWPC to provide the space weather forecasts and nowcasts that NASA's SRAG will use to manage the radiation exposure of space crews on deep space missions. Currently, only the SGPS instruments (i.e., to monitor proton, electron, and heavy ion fluxes) on GOES-16 have a final validation. There are still may issues with these instruments that remain to be corrected. Comparisons between the instrument suites on GOES-16 and GOES-17, as well as between these suites and the earlier instruments on GOES-13 and GOES-15, show significant discrepancies.

Solar and Heliospheric Observatory (SOHO) at L1: The ESA SOHO mission has been at L1 since December 2, 1995. It carries the LASCO and two solar energetic particle detectors. The Energetic and Relativistic Nuclei and Electron (ERNE) instrument measures protons and helium from 1.4 to 540 MeV/n and electrons from 5 to 60 MeV. The EPHIN measures electrons from 250keV to >8.7 MeV and protons and helium from 4 MeV/n to >53 MeV/n. SOHO is nearing the end of its mission life and must be replaced. The pointing mechanism of SOHO's high-gain antenna malfunctioned on June 27, 2003. This has resulted in the loss of some real-time data from LASCO since the failure.

Advanced Composition Explorer (ACE) at L1: NASA's ACE mission has been at L1 since December 13, 1997. ACE's Real Time Solar Wind (RTSW) system provides solar wind and energetic electron flux data to the SWPC. The fuel for station-keeping is expected to last until at least 2026.

Deep Space Climate Observatory (DSCOVR) at L1: NOAA's DSCOVR mission reached L1 on May 22, 2015. It provides real-time solar wind measurements to SWPC. It is now the primary source of solar wind data, replacing ACE. From July 2019 until March 2, 2020, DSCOVR was offline because of a problem with its pointing system. ACE remains the backup for solar wind data.

Solar Dynamic Observatory (SDO) satellite in geosynchronous orbit: NASA's SDO was launched February 11, 2010. The Helioseismic and Magnetic Imager (HMI) on SDO provides real-time data that are used by the Magnetogram Forecast (MAG4) system to provide all-clear forecasts for SPEs. SDO is expected to remain operational until 2030.

E.2   Space Weather Architecture Options to Support Human and Robotic Deep Space Exploration

This study found that no fundamentally new instrumentation needs to be developed to provide the basic level of space radiation monitoring to protect crew from enhanced radiation environments during SPEs. The study provides a set of recommendations for measurements of important space weather parameters at three levels: baseline, enhanced, and comprehensive for both lunar and Mars missions.

For the lunar missions, the baseline recommendation is to make the measurements needed to create magnetic field maps of the solar photosphere; measure solar energetic ions, electrons, and soft X-rays; and locate the flare responsible for elevated X-ray emission. The magnetic field maps are needed for all-clear forecasts that provide warnings of possible SPEs in the next 24 to 48 hours. The energetic ion measurements indicate the onset of an SPE and provide the basis for forecasting crew dose. The electron measurements are needed to create a prediction of the ion fluxes to be expected. The detection of X-ray flares, together with their location, helps predict SPEs before their onset in cislunar space.

These measurements could be enhanced by adding white-light coronagraph measurements, in-situ magnetic field measurements, and solar wind plasma measurements. The coronagraph measurements permit the detection of CMEs. If the coronagraph images can be transmitted promptly, they can be used to predict SPEs at the crewed vehicle before the onset occurs. The in-situ magnetic field and solar wind measurements can detect the onset of energetic storm-time particle (ESP) enhancements in the solar energetic particle flux.

Finally, a comprehensive set of measurements should include the enhanced measurements plus measurements of Type II and Type III radio noise. These radio noise signals indicate that electrons are being accelerated by the solar activity, implying that protons and other ions are also being accelerated. The recommended measurements could be made from L1, Gateway, and, in some cases, geosynchronous orbit.

In support of lunar missions, this study recommended a mission to the L4 Lagrange point (located at 1 AU from the Sun and leading Earth by 60 degrees). This mission should carry the instrumentation to make the baseline set of measurements described here. The data from this mission would give warnings of SPEs originating from a site in the photosphere that has rotated off the solar disk (as visible from Earth) by passing around the west limb.

For Mars missions, this study recommends that measurements be made on the Mars transit vehicle carrying the crew. The baseline measurements should include the magnetograph measurements needed to make photospheric magnetic field maps and soft X-ray measurements, along with measurements that locate the flare that is the source of the X-rays.

These baseline measurements can be enhanced by adding a white light coronagraph, in-situ magnetic field, solar wind properties, and space-based radio measurements. These additional measurements would enable the prediction of SPEs before their onset at the transit vehicle and identify the arrival of an ICME at the vehicle that may be accompanied by a storm-time increase in the solar energetic particle flux.

A comprehensive set of measurements would add an EUV imager, a heliospheric imager, EUV/far ultraviolet (FUV) irradiance measurements covering both EUV and FUV wavelengths, and an intravehicle dosimeter. The EUV/FUV images would better characterize active regions

that could be the sources of SPEs. Heliopheric images would make it possible to identify approaching ICMEs and enable an understanding of the magnetic connectivity between active regions on the Sun and the transit vehicle.

It was also suggested that solar monitoring missions could be placed at L3, L4, and L5 to monitor the Sun on all sides in support of Mars missions. L3 is the third Sun-Earth Lagrange point located 1 AU on the opposite side of the Sun from the Earth. This would provide the data that would enable for the transit vehicle the same types of forecasts currently being developed for cislunar space. It should be noted that data from these monitors would have to be collected by receivers on Earth, processed, and then transmitted to the transit vehicle. The data reaching the transit vehicle could have significant latency. If Mars is in superior conjunction, then the data latency from the signal transit time alone is 38 minutes.

It was further suggested that the ISS and Gateway be used as developmental testbeds for the instruments that would fly on the transit vehicle to Mars.

E.3 Planning the Future Space Weather Operations and Research Infrastructure: Proceedings of a Workshop

This workshop considered many adverse effects of space weather, in addition to the radiation hazard to space crews. Some of the recommendations included in the workshop report are repeats of recommendations described in Section E.1 and are not repeated here. Only new recommendations for measurements, instruments, and missions relevant to crewed missions beyond LEO are described here.

The workshop noted the "need for spacecraft to monitor the Sun from more distributed vantage points, including L4 and L5." A monitor at L5 will improve forecasting lead time. A monitor at L4 can monitor active regions that pose an immediate threat of producing disruptive and hazardous SPEs in cislunar space even after rotation around the west limb of the Sun. In the long term, observations at high solar inclinations to monitor the solar polar magnetic fields that affect forecast models would be helpful. The combined data from these vantage points would contribute to better prediction of the probability of occurrence and timing of CMEs that affect crewed spacecraft in cislunar space. It was noted that a similar monitor spacecraft at L3 would provide far-side observations of the solar magnetic field and EUV in active regions that will rotate onto the solar disk (as seen from Earth) over the next 2 weeks, allowing global model-based forecasting. It would also support forecasts for locations between the Earth and Mars. As mentioned, there could be significant data latency.

The 2-week advanced warning of active regions on the Sun that could impact missions near the Earth-Sun line is an average because the rotation rate of the Sun depends on solar latitude. The sidereal rotation period of the Sun at the equator is 24.47 days at the equator and ~38 days at the poles. Viewed from Earth, the solar photosphere at ±26 degrees solar latitude (where sunspots usually appear) is 27.3 days.

The value of an out-of-the-ecliptic monitor was also discussed. It was pointed out that "the Sun's polar magnetic fields also figure prominently in the boundary conditions for coronal and solar wind modeling used in forecasting." It was noted that NASA's Solar Obiter mission can serve as a pathfinder for a future out-of-the-ecliptic monitor constellation that would continuously monitor the polar regions of the Sun.

The importance of the Global Oscillations Network Group (GONG) was also emphasized; it provides 24-7 coverage of the Sun's magnetic field state and is therefore a backup for the SDO when generating all-clear forecasts.

The workshop pointed out the value in a heliospheric imager that could image an ICME as it passed from the Sun into the inner heliosphere. It would monitor how the ICME changes due to its interactions with the ambient solar wind. This would greatly improve forecast arrival time of an ICME at any point between cislunar space and Mars (current forecasts for ICME arrivals at Earth are uncertain by 12 hours). The arrival of an ICME can be accompanied by an increase in the ESP flux.

This workshop included several poster presentations of mission concepts worth noting. The "pearl necklace" concept can achieve a 360°view of the Sun from the ecliptic plane by distributing monitor spacecraft around the Sun in the ecliptic plane at ~1 AU. The idea is to co-manifest these monitor spacecraft with launches that replace SWFO-L1 every 5 years. The decommissioned SWFO-L1 spacecraft could also be used as "pearls" in this necklace.

An alternate approach is to repurpose spacecraft that deliver payloads to the lunar Gateway. They would be put into orbit of the Sun close to 1 AU to drift around the Sun, eventually monitoring the Sun on all sides. The necklace would support Mars missions by providing all-clear forecasts for the Mars transit vehicle as it makes its way to and from Mars. It would also provide the data for all-clear forecasts by following active regions over all solar longitudes that can give rise to large SPEs at the Mars transit vehicle. It would also provide the data needed to forecast head-on ICMEs that can produce large ESP enhancements at the transit vehicle. In addition, it would provide the information to forecast all but a very prompt SPE onset, albeit with communication delays due to the distances involved.

Two out-of-the-ecliptic mission concepts were presented. Solaris, proposed by the Southwest Research Institute, and the High Inclination Solar Mission, proposed by NASA Marshall Space Flight Center (MSFC). These are exploratory missions that could lead to a concept for a constellation of monitors that would give 24-7 coverage of the solar polar regions.

E.4   Space Weather Science and Observation Gaps Analysis for NASA

This was a comprehensive analysis covering all space weather research and applications. Some of the recommendations that are relevant to missions beyond LEO were the same as those already mentioned in this report. The relevant new recommendations from this analysis are given below:

- Solar energetic particle and in-situ magnetic field measurements at multiple points at less than 0.9 AU, combined with stereoscopic coronagraphic imaging out to 80 solar radii and photospheric magnetic field measurements, would provide ~2 hour warning of an ICME arrival.
- Modeling should be investigated to determine whether it can provide a sufficient substitute for missing/incomplete data.
- A space weather beacon capability to make data available in near real time should be a requirement for all NASA missions that make relevant space weather observations.
- Innovative solutions for strategic agreements and partnerships could be established to benefit from available rideshare and hosted-payload opportunities to help fill critical space weather observational gaps.

- Relevant measurements (or derived data products) should be standardized to benefit data assimilation and model development.
- All space weather data should be made openly available in near real time to encourage researchers to improve model development.

This analysis also produced some relevant lessons and findings. It was pointed out that most of the observational gaps can be addressed with current technology and capabilities. These gaps most often arise from sparse spatial/temporal/spectral coverage rather than lack of measurement capability. Advances in forecasting can be made if a systematic approach is taken to measurements (i.e., making them in different locations, at multiple points, and in combinations that are complementary). This requires a long-term strategy with an implementation plan.

E.5   Avionics Radiation Hardness Assurance (RHA) Guidelines

This document is a final report from an NESC assessment that primarily deals with radiation effects on electronics. It does, however, contain some findings, observations, and NESC recommendations that are relevant to crewed missions beyond LEO because it bears on the hazards of avionics failures that could cause the degradation or loss of a crewed mission. The most important findings, observations, and NESC recommendations from this document include:

- NASA lacks an enterprise-level RHA standard that can be readily adopted by flight programs and projects. The NASA Office of Safety and Mission Assurance, with support from the Office of the Chief Engineer, should begin near-term development of an Agency-level technical standard for RHA.

- The NASA Office of Safety and Mission Assurance, with support from the Office of the Chief Engineer, should develop a NASA handbook that would provide reference material on radiation assurance for engineering professionals. This handbook should be a companion to the Agency-level technical standard for RHA.

- RHA depends on parts testing at heavy ion radiation test facilities that are already straining to meet the demand. The NASA Space Environments Testing Management Office, working with the Office of the Chief Engineer and the Office of Safety and Mission Assurance, should engage mission directorate stakeholders to support an expanded domestic SEE test facility capacity and capability investments, direct or in kind, in cooperation with relevant external organizations such as the Department of Defense and the Department of Energy.

Appendix F. Studies and Roadmaps Consulted during Preparation of Report

- Planning the Future Space Weather Operations and Research Infrastructure, National Academies Press, 2021, URL: https://www.nap.edu/catalog/26128/planning-the-future-space-weather-operations-and-research-infrastructure-proceedings.

- Space Weather Architecture Options to Support Human and Robotic Deep Space Exploration, J. I. Minow et al., NASA/TM−20205000837 and NESC-RP-17-01215 (2021), URL: https://ntrs.nasa.gov/citations/20205000837.

- Space Weather Phase 1 Benchmarks, A Report by the Space Weather Operations, Research, and Mitigation Subcommittee of the Committee on Homeland and National Security of the National Science & Technology Council, 2018, URL: https://trumpwhitehouse.archives.gov/wp-content/uploads/2018/06/Space-Weather-Phase-1-Benchmarks-Report.pdf.

- Heliophysics Space Weather Strategy, NASA Heliophysics Division, 2020.

- National Space Weather Strategic Action Plan, A product of the Space Weather Operations, Research and Mitigation Working Group of the Space Weather, Security and Hazards Subcommittee of the Committee on Homeland and National Security of the National Science and Technology Council of the National Science and Technology Council, 2019, URL: https://trumpwhitehouse.archives.gov/wp-content/uploads/2019/03/National-Space-Weather-Strategy-and-Action-Plan-2019.pdf.

- Global Roadmap for Better Understanding of Space Weather, released, July 6, 2015, retrieved January 29, 2021, URL: https://phys.org/news/2015-07-global-roadmap-space-weather.html.

- Understanding Space Weather to Shield Society: A Global Road Map for 2015–2025, commissioned by COSPAR and ILWS, Advances in Space Research 55, 2015, pp. 2745–2807.

- Current State and Perspectives of Space Weather Science in Italy, *Journal of Space Weather and Space Climate*, Vol. 10, No. 6, 2020, URL: https://doi.org/10.1051/swsc/2020003.

- Assessment and Recommendations for a Consolidated European Approach to Space Weather – as Part of a Global Space Weather Effort, *Journal of Space Weather and Space Climate*, Vol. 9, A37, 2019, URL: https://doi.org/10.1051/swsc/2019033.

- Space Weather Science and Observation Gap Analysis for NASA, April 2021, URL: https://science.nasa.gov/science-pink/s3fs-public/atoms/files/GapAnalysisReport_full_final.pdf.

- Avionics Radiation Hardness Assurance (RHA) Guidelines, April 1, 2021, URL: https://ntrs.nasa.gov/citations/20210018053.

- Space Radiation and Astronaut Health – Managing and Communicating Cancer Risks, June 24, 2021, URL: https://www.nap.edu/catalog/26155/space-radiation-and-astronaut-health-managing-and-communicating-cancer-risks.

NASA developed a set of ionizing radiation human system requirements for the elements of the ARTEMIS Mission" (based on NASA-STD-3001, Space Flight Human System Standards, Vol. 1, "Crew Health," and Vol. 2, "Human Factors, Habitability, and Environmental Health"). These requirements are contained in the documents:

- MPCV 70024, Rev. D, Orion Multi-Purpose Crew Vehicle (MPCV) Program: Human-Systems Integration Requirements (HSIR) - Released 11/18/2020; GP 10017 Rev. A.

- Gateway Program Human System Requirements (HSR) - Released 01/28/2021.

- HLS-RQMT-001, Rev. D "Human Landing System (HLS) Program System Requirements Document (PSRD)" - Released 11/30/2020.

REPORT DOCUMENTATION PAGE		*Form Approved* *OMB No. 0704-0188*

1. REPORT DATE *(DD-MM-YYYY)*	**2. REPORT TYPE**		**3. DATES COVERED** *(From - To)*
02/18/2022	Technical Memorandum		

4. TITLE AND SUBTITLE	**5a. CONTRACT NUMBER**
Safe Human Expeditions Beyond Low Earth Orbit (LEO)	
	5b. GRANT NUMBER
	5c. PROGRAM ELEMENT NUMBER

6. AUTHOR(S)	**5d. PROJECT NUMBER**
Valinia, Azita; Allen, John R.; Francisco, David R.; Minow, Joseph I.; Pellish, Jonathan A.; Vera, Alonso H.	
	5e. TASK NUMBER
	5f. WORK UNIT NUMBER
	869021.01.23.01.01

7. PERFORMING ORGANIZATION NAME(S) AND ADDRESS(ES)	**8. PERFORMING ORGANIZATION REPORT NUMBER**
NASA Langley Research Center Hampton, VA 23681-2199	NESC-RP-20-01589

9. SPONSORING/MONITORING AGENCY NAME(S) AND ADDRESS(ES)	**10. SPONSOR/MONITOR'S ACRONYM(S)**
National Aeronautics and Space Administration Washington, DC 20546-0001	NASA
	11. SPONSOR/MONITOR'S REPORT NUMBER(S)
	NASA/TM-20220002905

12. DISTRIBUTION/AVAILABILITY STATEMENT
Unclassified - Unlimited Subject Category Man/System Technology and Life Support Availability: NASA STI Program (757) 864-9658

13. SUPPLEMENTARY NOTES

14. ABSTRACT

The NASA Engineering and Safety Center (NESC) conducted an interdisciplinary study and workshop focusing on capabilities needed for crew health and safety on long-duration deep space expeditions in support of the Artemis Program and missions to Mars. The study focused on integration among four disciplines: 1) space weather monitoring and forecasting, 2) shielding technologies, 3) human health research, and 4) human factors engineering tools. An integrated risk assessment was performed to inform characteristics of mission architecture and capabilities needed for safe, long-duration human expeditions beyond low Earth orbit. This report contains the outcome of the NESC assessment.

15. SUBJECT TERMS

Low Earth Orbit; NASA Engineering and Safety Center; Human Expedition; Galactic Cosmic Rays; Space Weather; Shielding Technologies; Artificial Gravity; Human Systems Integration Architecture

16. SECURITY CLASSIFICATION OF:			**17. LIMITATION OF ABSTRACT**	**18. NUMBER OF PAGES**	**19a. NAME OF RESPONSIBLE PERSON**
a. REPORT	**b. ABSTRACT**	**c. THIS PAGE**			STI Help Desk (email: help@sti.nasa.gov)
					19b. TELEPHONE NUMBER *(Include area code)*
U	U	U	UU	238	(443) 757-5802